ISTANBUL TECHNICAL UNIVERSITY ★ GRADUATE SCHOOL

CONCENTRATE TREATMENT VIA MEMBRANE DISTILLATION/CRYSTALLIZATION METHOD

Ph.D. THESIS

Öykü MUTLU SALMANLI

Department of Environmental Engineering

Environmental Sciences and Engineering

AUGUST 2023

ISTANBUL TECHNICAL UNIVERSITY ★ GRADUATE SCHOOL

CONCENTRATE TREATMENT VIA MEMBRANE DISTILLATION/CRYSTALLIZATION METHOD

Ph.D. THESIS

Öykü MUTLU SALMANLI
(501152708)

Department of Environmental Engineering

Environmental Sciences and Engineering

Thesis Advisor: Prof. Dr. İsmail KOYUNCU
Co-Advisor: Prof. Dr. Mark R. WIESNER

AUGUST 2023

İSTANBUL TEKNİK ÜNİVERSİTESİ ★ LİSANSÜSTÜ EĞİTİM ENSTİTÜSÜ

MEMBRAN DİSTİLASYON/KRİSTALİZASYON YÖNTEMİ İLE KONSANTRE ARITIMI

DOKTORA TEZİ

Öykü MUTLU SALMANLI
(501152708)

Çevre Mühendisliği Anabilim Dalı

Çevre Bilimleri ve Mühendisliği

Tez Danışmanı: Prof. Dr. İsmail KOYUNCU
Eş Danışman: Prof. Dr. Mark R. WIESNER

AĞUSTOS 2023

Öykü MUTLU SALMANLI, a Ph.D. student of İTU Graduate School student ID 501152708 successfully defended the thesis/dissertation entitled "CONCENTRATE TREATMENT VIA MEMBRANE DISTILLATION/CRYSTALLIZATION METHOD", which she prepared after fulfilling the requirements specified in the associated legislations, before the jury whose signatures are below.

Thesis Advisor :	**Prof. Dr. İsmail KOYUNCU** Istanbul Technical University	.....
Co-advisor :	**Prof. Dr. Mark R. WIESNER** Duke University	.....
Jury Members :	**Prof. Dr. Halil HASAR** Fırat University	.....
	Prof. Dr. Vedat UYAK İstanbul Technical University	.....
	Prof. Dr. Vahid VATANPOUR Kharazmi University	.....
	Assist.Prof. Dr. Mehmet Emin PAŞAOĞLU İstanbul Technical University	.....
	Assist.Prof. Dr. Türker TÜRKEN İstanbul Technical University	.....

Date of Submission : 25 May 2023
Date of Defense : 28 August 2023

To my angel dad and my son,

FOREWORD

Firstly I would like to express my profound gratitude to my advisor Prof.Dr. Ismail KOYUNCU for his support, knowledge and guidance during my thesis study and enlightened my path and gave me the opportunity to work and be a member of MEMTEK (National Research Center on Membrane Technologies) family. Without his support and encouragement, the completion of this work would not have been possible.

I would like to express my deepest gratitude to Prof. Dr. Mark WIESNER for his valuable input on my research as co-advisor. I thank him for his support, hospitality and I am so pleasure to giving me the opportunity to work with him and his group at Duke University.

I would also like to thank TUBITAK-BIDEB 2211-C PhD Scholarship Program Intended for Priority Areas and TUBITAK-BIDEB 2214-A International Doctoral Research Fellowship Programme for their financial supports throughout my PhD studies.

A special thanks to Anıl KAZAK who helped me on toilsome pilot scale studies. I would like to thank MEM-TEK where I had experience and good times for the last seven years and in this sense I also would like to thank each and every MEM-TEK member for their friendship, support and helps. Especially Assoc. Prof. Bihter ZEYTUNCU-GÖKOĞLU, Assoc. Prof. Börte KÖSE MUTLU, Assist. Prof. Ayşe YÜKSEKDAĞ, Assist. Prof. Türker TÜRKEN, Assist. Prof. Recep KAYA, Assist. Prof. Mehmet Emin PAŞAOĞLU, Assist. Prof. Bahar YAVUZTÜRK-GÜL, Academic Ayşegül Derya ALTINAY, and rest of all MEMTEK members.

I would also like to express my thanks to my researcher friends in Wiesner Group at Duke University. In particular, I would like to thank Dr. Amalia TURNER for her hospitality, her support during my study at Duke University and for being my sister.

Most importantly I would like to thanks my mother Yasemen MUTLU and my father Ihsan MUTLU for always being proud of me, encourage me especially in my academic career, support me in every step of my life and giving me all opportunities whatever they could do even in hard times of their life . All opportunities and accomplishments I owe to my family. I could not be the person who am I now without you. My dear father left me a lot of precious traces and memories, tought me honesty, kindness, goodness, generosity, thinking logically, thoughtfullness and very important things that I can not enumerate here. And also he left the deepest and biggest heartbreak in my life by leaving us to start his journey in eternity. I know you are in the heaven and wish to meet you in there, until then you will always be in my heart and my dreams, I love and miss you so much. I also would like to thanks to my all family members who offers me a warm family atmosphere and love and for being proud of me. I also would like to thanks my deceased beloved bird Sushi for being the most intelligent and sweetest bird in the world and for this love you make us feel. I also would like to thanks my pawed and furry baby Mia for reducing my stress and relieving me.

I also would like to specially thank to my beloved husband Ramazan SALMANLI for his support, help and encouragements. A very special thanks to my beloved, precious little son Atlas Ihsan SALMANLI for have made me a mother and have made my world much more beautiful and meaningful, I am feeling so lucky and happy to have you.

May 2023

Öykü MUTLU SALMANLI
(M.Sc. Environmental Engineer)

TABLE OF CONTENTS

Page

ABBREVIATIONS

AEMs : Anion Exchange Membranes
AGMD : Air Gap Membrane Distillation
BisF-Bz : Fluoro Containing Benzoxazine Monomer
BMED : Bipolar Membrane Electrodialysis
BPMs : Bipolar Membranes
BSRs : Boron Selective Resins
BWRO : Brackish Water Reverse Osmosis
Bz : Benzoxazine Monomer
CEMs : Cation Exchange Membranes
CNTs : Carbon Nanotubes
DCMD : Direct Contact Membrane Distillation
DD : Donnan Dialysis
EC : Electrocoagulation
ED : Electrodialysis
FO : Forward Osmosis
FT-IR : Fourier-Transform Infrared Spectroscopy
FSSLM : Flat Sheet Supported Liquid Membrane
FA : Fly Ash
FSSLM : Flat Sheet Supported Liquid Membrane
GAC : Granular Activated Carbon
GOR : Gained Output Ratio
ICP-OES : Inductively Coupled Plasma-Optical Spectrometer
LEP : Liquid Entry Pressure
LM : Liquid Membrane
MD : Membrane Distillation
MF : Microfiltration
MFC : Microbial Fuel Cells
NF : Nanofiltration
NMDG : N-methyl-D-glucamine
PA : Polyamide

PBz : Polybenzoxazine

PP : Polypropylene

PTFE : Polytetrafluoroethylene

PVDF : Polyvinylidene Fluoride

RO : Reverse Osmosis

SEC : Specific Energy Consumption

SEM-EDS : Scanning Electron Microscopy-Energy Dispersive X-Ray Spectroscopy

SGMD : Sweeping Gas Membrane Distillation

SLM : Supported Liquid Membrane

SWRO : Sea Water Reverse Osmosis

TFC : Thin-film Composite

UF : Ultrafiltration

VMD : Vacuum Membrane Distillation

VAGMD : Vacuum Assisted Air Gap Membrane Distillation

VAGMDC : Vacuum Assisted Air Gap Membrane Distillation Crystallization

WCA : Water Contact Angle

WHO : World Health Organization

XRD : X-Ray Diffraction

XRF : X-Ray Fluorescence

SYMBOLS

$B(OH)_4^-$	: Borat anion
C_f	: Concentration of Feed
C_p	: Concentration of Permeate
C_m	: Permeability coefficient
EC	: Energy Consumption
Fe^{3+}	: Iron oxide
H_2SO_4	: Sulfuric acid
H_3BO_3	: Boric acid
HNO_3	: Nitric acid
M_d	: Dry weight of the membrane
M_w	: Weight of membrane
$NaHCO_3$	: Sodium Bicarbonate
NaOH	: Sodium hydroxide
P	: Vapor Pressure
P_i	: Density of isopropanol
P_m	: Vapor Pressure Difference
P_p	: Density of polymer
P_i	: Density of isopropanol
R	: Recovery rate
ε	: Porosity

LIST OF TABLES

Page

LIST OF FIGURES

Page

CONCENTRATE TREATMENT VIA MEMBRANE DISTILLATION/CRYSTALLIZATION METHOD

SUMMARY

Boron is an important semimetal element that is found in water, soil and rocks. Boron is widely used in a variety of industries such as glass, semi-conductors, detergents, cosmetics, drugs and fertilizer. Boron is also an essential nutrient for animals, plants and humans that needs to be found in dietary intake. Although it is beneficial the excessive amount of boron can lead to some health problems for humans and growth problems or death for plants. The boron content in wastewater is increasing due to the increasing industrial activities. Boron can also be found naturally from rocks, salt deposits or rainfalls and approximately 75% of the boron reserves of the world are found in Turkey.

In the second chapter of this thesis study a literature review was prepared comprehensively. Boron removal and recovery techniques were reviewed. The increasing demand for clean water resources makes boron removal from water resources much more important. However, the removal is not enough alone in the aspect of sustainability. The removal and recovery techniques both conventional methods like precipitation, adsorption, coagulation, ion exchange and membrane processes are examined to juxtapose the states of the science in these two related—and increasingly important—processes.

In the third chapter, the optimization studies of the membrane distillation process used in the thesis study were conducted. 2 different MD configurations, 3 different vacuum pressures, 6 different membranes and 3 different feed water were used to determine the optimum conditions. VAGMD had the higher fluxes since vacuum assistance enhanced fluxes while decreasing specific energy consumption. The boron content in permeate waters was lower than the 0.5 mg/L.

In the fourth chapter hydrophobic and superhydrophobic membrane production methods were investigated. Different fabrication techniques as phase inversion and electrospinning were utilized while coating was applied to modify commercial and fabricated membranes. Different coagulation bath mediums for phase inversion method, nanoparticle additives and different coating solutions were compared. It was possible to obtain a superhydrophobic membrane that has a contact angle of 153°.

A novel hydrophobic blend membrane was fabricated to use in VAGMD within the scope of the fifth chapter. NaCl, synthetic boron solution and real RO concentrate supplied from the boron mining area were tested. A fluoro-containing benzoxazine monomer (Bz) was blended with our base polymer PVDF. The cross-linking of Bz is provided by thermal curing. According to the results, the BisF-Bz membrane showed higher hydrophobicity, more durability and physical stability compared to the pristine membrane. Boron rejection was highest for the BisF-Bz blended and two times thermally cured nanofiber membrane.

In chapter six VAGMDC system was utilized to remove and recover boron from the concentrate stream. The concentrate problem is the main drawback of membrane processes so needs additional treatment and management. To address this problem VAGMDC system was tested. Synthetic boron solution was used to optimize process conditions such as concentration, pH and membrane type. Real RO concentrate was tested in the following experiments. Flux values, boron concentration and boron rejections, SEM-EDS analysis and XRF analysis for obtained crystals were conducted. The results showed that VGMDC could be successfully used for the removal and recovery of boron.

The pilot scale VAGMDC system was tested in the scope of chapter seven. Different recovery ratios and operating modes were tested. Highly boron-contented raw river water and RO concentrate of that water were fed to the pilot scale MD system. Conductivity, flow rate and vacuum pressure were observed during the experiments. Boron, arsenic, hardness and conductivity removals were analyzed and determined. After VAGMD operation crystallization was applied to the obtained concentrate. 43.9% B_2O_3 contented crystals could be obtained. In conclusion, the relatively new VAGMDC process is an effective method for boron removal and recovery.

MEMBRAN DİSTİLASYON/KRİSTALİZASYON YÖNTEMİ İLE KONSANTRE ARITIMI

ÖZET

Bor, suda, toprakta ve kayaçlarda bulunan önemli bir yarı metal elementtir. Cam, yarı iletkenler, deri, deterjan, kozmetik, ilaç, pestisit ve gübre gibi çeşitli endüstrilerde yaygın olarak kullanılmaktadır. Endüstriyel kullanımının yanı sıra bor ayrıca hayvanlar, bitkiler ve insanlar için önemli bir nütrienttir, bazı metabolik fonksiyonlar borun varlığına ihtiyaç duyar ve bu nedenle günlük olarak belirli miktarlarda alınması gerekir. Bor faydalı olmakla birlikte fazlası insanlarda kusma, ishal, cilt döküntüsü ve hatta hamile kadınlarda düşüğe sebep olabilirken uzun süreli maruz kalımlarda ise kardiyovasküler sistem, sinir sistemi ve üreme sistemlerinde hasara yol açabilir. Bitkilerde tolere edilebilir miktarın aşılması durumunda büyümenin baskılanması, verimin azalması, yaprak ucu sararması ve hatta bitkinin ölümüne neden olabilir.

Bor deniz suyu, içme suyu ve yeraltı sularında hem doğal hem de antropojenik kaynaklara bağlı olarak bulunabilmektedir. Artan endüstriyel faaliyetlere bağlı olarak atıksudaki bor içeriği her geçen gün artmaktadır. Sularda bulunan borun en önemli antropojenik kaynağı ise madencilik faaliyetleridir. Ayrıca bor, doğal olarak kayalardan, tuz yataklarından veya yağışlardan kaynaklanmaktadır. Tuz birikintisi sızıntı suyu, kaya ayrışması ve okyanus spreyinden gelen deniz tuzu içeren yağmurlar borun doğal sularada bulunmasına etken birincil doğal kaynaklarıdır. Dünyadaki bor rezervlerinin yaklaşık %53 ü ise Türkiye'de bulunmaktadır.

Bu tez çalışmasının kapsamında öncelikli olarak kapsamlı bir literatür taraması hazırlanmıştır. Bor giderimi ve ayrıca geri kazanım teknikleri gözden geçirilmiştir. Bu kapsamda çöktürme, adsorpsiyon, koagülasyon, iyon değişimi gibi geleneksel yöntemler ile membran prosesleri gibi ayırma ve geri kazanma teknikleri, bu iki ilgili -ve giderek daha önemli hale gelen– süreç bakımından bilimin durumunu karşılaştırmak için incelenmiştir. Artan nüfus ve azalan kaynaklar sebebi ile temiz su kaynaklarına olan talebin artması, su kaynaklarından bor giderimini çok daha önemli hale getirmektedir. Ancak sürdürülebilirlik açısından giderim tek başına yeterli değildir. Bu önemli kaynağın geri kazanılması ve yeniden kullanılabilmesi önem arz etmektedir. Literatürde bor geri kazanımı ile bor giderimi terimleri arasında net bir ayrım yapılmamakla birlikte kullanılabilir nitelikte ürün eldesine dayanan çalışma sayısı oldukça azdır. Bu bölümde giderim ve geri kazanım kavramları açıklanmaya çalışılmış giderim ve geri kazanım yöntemleri ayrı olarak incelenmiştir. Konvansiyonel yöntemlerin bazı kısıtlarından ötürü son yıllarda membran prosesler daha çok dikkat çekmeye ve araştırılmaya başlanmıştır.

Membran distilasyonu (MD) konvansiyonel distilasyon ile membran prosesi birleştiren termal sürücülü bir ayırma prosesidir. Temel prensip membran gözeneklerinden su yerine su buharının geçişini sağlamaktır. Bu prensip ile yüksek kalitede su eldesine imkan veren bir saflaştırma prosesi olarak konvansiyonel distilasyondan daha düşük sıcaklıklar gerektirirken ters osmoz (TO) prosesine göre

daha düşük enerji sarfiyatına sahiptir. Aynı zamanda giriş suyu kirletici konsantrasyonlarından çok fazla etkilenen bir proses olmaması ile de öne çıkmaktadır.

Tezin üçüncü bölümünde bu tez çalışması kapsamında kullanılmasına karar verilen membran distilasyon prosesinin optimizasyon çalışmaları yapılmıştır. Optimum koşulları belirlemek için hava boşluklu ve vakum destekli hava boşluklu olmak üzere 2 farklı MD konfigürasyonu, 3 farklı vakum basıncı, 3 farklı polimer türünde ve 2 farklı por çapına sahip olmak üzere 6 farklı membran ve 3 farklı besleme suyu kullanılmıştır. Vakum destekli hava başluklu membran distilasyon (VAGMD) sisteminde, vakum desteği akıları artırırken kullanılan vakum enerjisine rağmen spesifik enerji tüketimini azaltmıştır. Gerek tuzluluk gerekse bor giderim verimleri oldukça yüksek sonuçlar vermiştir. 0,5 mg/L'den daha düşük bor içeriğine sahip süzüntü suları elde edilmiştir.

Dördüncü bölümde MD prosesinde kullanılan hidrofobik ve süperhidrofobik membran üretimi üzerine çalışmalar gerçekleştirilmiştir. Ticari ve üretilen membranları modifiye etmek için kaplama yöntemi uygulanırken, faz inversiyon ve elektrospinleme gibi farklı üretim teknikleri de kullanılmıştır. Faz inversiyon yöntemi için farklı içeriklerdeki koagülasyon banyosunun hidrofobisiteye etkisinin yanı sıra, nanoparçacık katkıların ve farklı kaplama çözeltilerinin etkileri karşılaştırılmıştır. Bu çalışma ile temas açısı 153° olan süperhidrofobik membran elde etmek mümkün olmuştur. Yüksek hidrofobisite değerine sahip membranlar ile yapılan arıtılabilirlik çalışmalarının sonucuna göre ise süzüntü suyu akıları ve bor giderim verimleri belirlenmiştir. %90 üzerinde bor giderim verimlerine ulaşmak mümkün olmuştur. Beşinci bölüm kapsamında ise VAGMD'de kullanılmak üzere benzoksazin monomeri (Bz) katkılı yenilikçi hidrofobik membran üretimi çalışması gerçekleştirilmiştir. NaCl, sentetik bor çözeltisi ve bor madenciliği alanından temin edilen yüksek bor içerikli nehir suyundan elde edilen gerçek ters osmoz (TO) konsantresi test edilmiştir. Bir floro içerikli Bz monomeri baz polimerimiz olan PVDF içerisine eklenerek yenilikçi bir membran üretimi gerçekleştirilmiştir. Termal kürleme uygulanarak Bz'nin çapraz bağlanması sağlanmıştır. Bu amaçla farklı tekrarlarda termal kürleme işlemi uygulanarak hem monomer ilavesinin hem de kürleme işleminin membran distilasyon sistemindeki performansı üzerine etkisi incelenmiştir. Elde edilen sonuçlara göre BisF-Bz membran, saf membrana göre daha yüksek hidrofobiklik, daha fazla dayanıklılık ve fiziksel kararlılık göstermiştir. En yüksek bor giderimine ise, BisF-Bz katkılı ve iki kez termal olarak kürlenmiş nanofiber membran ile ulaşılmıştır.

Altıncı bölümde, borun konsantre akışından giderilmesi ve geri kazanılması için Vakum destekli hava başluklu membran distilasyon kristalizasyon (VAGMDC) sistemi kullanılmıştır. Konsantre sorunu, membran prosesleri için ana dezavantajlardan birisidir, bu nedenle ek arıtma ve yönetime ihtiyaç duyar. Bu sorunu çözmek için VAGMDC sistemi test edilmiştir. Konsantrasyon, pH ve membran tipi gibi proses koşullarını optimize etmek için sentetik bor çözeltisi kullanılmış ardından gerçek TO konsantresi test edilmiştir. Akı değerleri, bor konsantrasyonu ve dolayısıyla bor giderim verimi, SEM-EDS analizi ve elde edilen kristaller için XRF analizi yapılmıştır. Sonuçlar, VAGMDC' nin bor giderimi ve geri kazanımı için başarıyla kullanılabileceğini göstermiştir.

Yedinci bölüm kapsamında pilot ölçekli VAGMDC sistemi test edilmiştir. Farklı geri kazanım oranları ve çalışma modları test edilmiştir. Pilot ölçekteki MD sistemine yüksek bor konsantrasyonuna sahip ham nehir suyu ve bu suyun TO konsantresi beslenmiştir. Deneyler sırasında iletkenlik, akış hızı ve vakum basıncı takip edilmiştir.

Bor, arsenik, sertlik ve iletkenlik giderimleri analiz edilerek giderim verimleri belirlenmiştir. VAGMD işleminden sonra elde edilen konsantreye kristalizasyon işlemi uygulanmıştır. %43,9 B_2O_3 içerikli kristallerin elde edilmesi mümkün olmuştur. Sonuç olarak borun giderimi ve geri kazanımı için nispeten yeni bir yöntem olan VAGMDC prosesinin başarılı bir şekilde kullanılabileceği görülmüştür.

1. INTRODUCTION

This thesis study, which consists of eight chapters, is a comprehensive research on the removal and recovery of boron by using the VAGMDC method from RO concentrate. The purpose of the thesis, unique aspect, impact and organization of the thesis are given below.

1.1 Purpose of Thesis

The purpose of this thesis is to develop a new and effective method for concentrate treatment in terms of boron removal and recovery. Membrane distillation crystallization was selected for this purpose which is an effective treatment even a purification method. Within the scope of this thesis study, the following objectives were planned:

- Literature review of the boron removal and recovery techniques
- Optimizing the removal process for concentrate treatment,
- Fabrication of novel hydrophobic/superhydrophobic membranes to use in membrane distillation,
- Removal and recovery studies with membrane distillation crystallization process for concentrate treatment which contains a high amount of boron
- Pilot scale study for the proposed treatment option

1.2 Unique Aspect

Membrane processes have gained attention in the last decades due to their several advantages as low footprint, production of high-quality water, low or no chemical loading and ability to apply for a wide variety of mixtures. However, concentrate production in membrane processes is the major drawback of those processes. RO is a desalination method used to purify the water which means a high concentration of

contaminants in concentrate water produced by RO. So the concentrate stream needs to be managed.

A comprehensive review provides a detailed overview of the conventional processes and membrane processes, reviews recovery and clarifies the difference between removal and recovery for the first time in the literature. The novel side of this thesis is the treatment of concentrate water containing high boron by vacuum-assisted air gap membrane distillation crystallization for boron removal and recovery. Another novelty is the fabrication and modification of novel membranes that have never been used in literature for membrane distillation. Also, the pilot scale membrane distillation crystallization process for boron removal and recovery is the only study in the literature. Up to 43.9% B_2O_3 crystals were obtained in this study which reflects the efficiency of the proposed process.

1.3 Organization of Thesis

The thesis contains an introduction followed by a review chapter (Chapter 2) and five data chapters (3-7) and conclusions and thesis conclusions and recommendations (Chapter 8). Chapter 2 represents a comprehensive review of boron removal and recovery techniques. Firstly conventional techniques such as precipitation, adsorption, coagulation and ion exchange and then the membrane processes were reviewed in terms of removal and recovery, and the difference between removal and recovery was clarified in this section. In the third chapter, the optimization study was conducted for the membrane distillation process. A relatively new VAGMD configuration was selected for further studies. In the fourth and fifth sections, novel hydrophobic and superhydrophobic membrane preparation studies were conducted. Boron removal and recovery by using VAGMDC studies on a lab scale were examined in Chapter 6. A pilot scale study was done in the last experimental study part of Chapter 7. Conclusions and recommendations of the thesis were given in the last chapter.

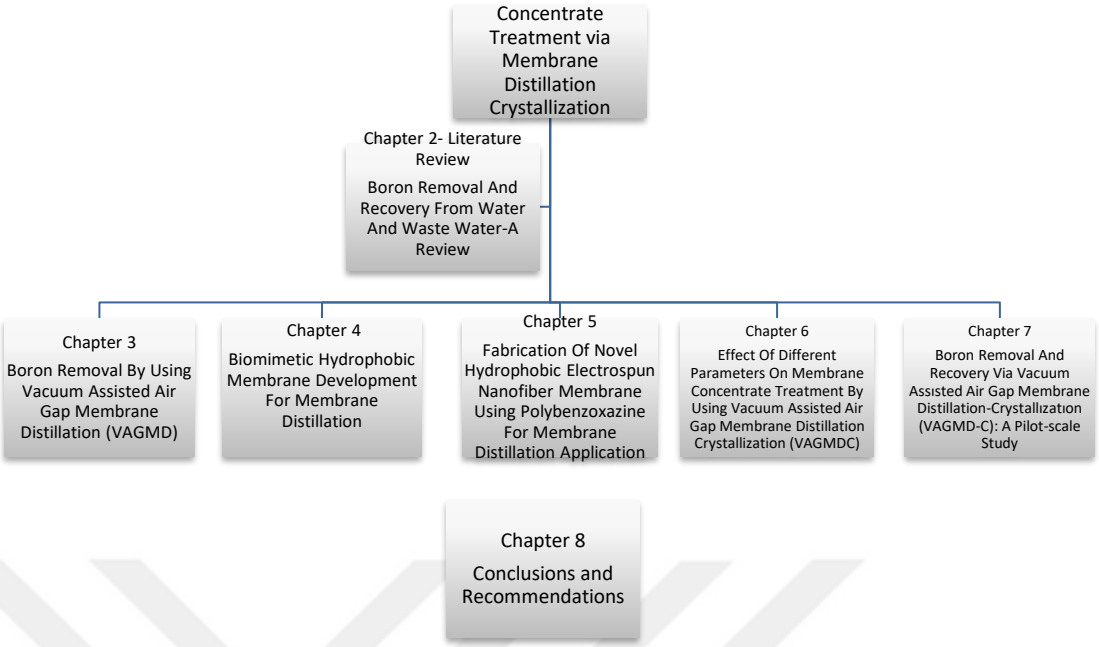

Figure 1.1 : Scheme of thesis outline.

2. BORON REMOVAL AND RECOVERY FROM WATER AND WASTEWATER: A REVIEW[1]

2.1 Introduction

Boron is a crucial element for most organisms and is found in sea water, geothermal water, surface water, and underground water over a range of concentrations. (Hilal et al., 2011). In addition, boron is used in various industrial products, including semi-conductors, leather, glass, detergent, cosmetics, fertilizers, drugs, and insecticides (Özdemir & Kıpçak, 2010; Öztürk et al., 2008; Pearce, 1978). This large-scale industrial use of boron leads to the release of boron compounds to wastewater in substantial quantity. And while boron is beneficial to in limited amounts, excessive boron exposure can be harmful to both plants and humans (Kabay & Bryjak, 2015). As a result, the World Health Organization (WHO) recommends limiting boron concentrations in drinking water to 2.4 mg/L, and boron concentrations in water used for irrigation should not exceed 0.5 mg/L due to lower tolerance levels in plants.

Wastewater containing high levels of boron requires treatment before disposal to remove excessive quantities of this element prior to environmental release (Tagliabue et al., 2014a; Tang et al., 2017). Due to increasing water needs and decreasing availability of clean water resources, the successful treatment of these waters is increasingly important. Many studies in the literature cover methods of boron removal, and in this review we discuss in detail and provide comparisons of the available techniques for removing boron from wastewater, with particular emphasis on the use of membrane processes. But to promote the more sustainable use of this element, recovery and reuse of boron included in these many industrial applications must be explored as a partner to removal, where boron-containing compounds are separated

[1] This chapter is based on 'Oyku Mutlu-Salmanli, Ismail Koyuncu (2022), *Boron removal and recovery from water and wastewater*, Rev Environ Sci Biotechnol, 21, 635–664 https://doi.org/10.1007/s11157-022-09629-w'

from the waters and managed within a circular economy rather than discarded as waste. While, studies on boron recovery from contaminated waters are scarce at this time, we provide in this review a discussion of the available techniques to draw attention to the need for additional work in this area. In addition we have observed that the use of the terms "recovery" and "removal" have sometimes been used interchangeably in the literature, with efforts to remove boron from the water by transport to an alternative medium or through concentration having sometimes been referred to as recovery. In this review, we intentionally classify the existing studies as either removal and recovery studies in hopes that this review will help to more clearly delineate the recovery concept - and its application – from that of removal.

2.2 Boron Chemistry

2.2.1 Boron chemistry

Boron (B) is the sole nonmetal in group IIIA of the periodic table and is most similar to its neighbors carbon, aluminum, and especially silicon. (Kochkodan et al., 2015; Kot, 2015; Tang et al., 2017), The name of this element specifies boron's source and its resemblance to carbon (Greenwood & Earnshaw, 1997). Free elemental boron is solid at room temperature and does not exist in nature (Kochkodan et al., 2015; Kot, 2015; Tagliabue et al., 2014b). It has an atomic mass of 10.81 and a density of 2.84 g/cm^3 (Freger et al., 2015; Kochkodan et al., 2015). The electron structure of boron is a $1s^2 2s^2 2p^1$ configuration expressed in a prevailing tervalence. Because of its electron structure, the bond energies that include boron are such that there is no propensity to form monovalent compounds; boron generally forms three or sometimes four bonds. Boron is in the trivalent oxidation state in its oxides, sulfides, halides, and nitrides compounds. Since its first oxidation potential is high (8.296 eV), electron loss or cation formation does not play a role. However, boron has 3 electrons to promote the covalent bonding of the 4 orbitals (s, px, Py, and pz) giving this element additional features that lead to the behavior of acceptor for an electron-pair with an extremely high oxygen affinity and multicenter bonding (Greenwood & Earnshaw, 1997; Kochkodan et al., 2015; Tagliabue et al., 2014b; Tang et al., 2017).

2.2.2 Boron in the aqueous environment

Boron can be found in brackish waters, seawater, and drinking waters. The largest anthropogenic sources of boron in waters are mining activities and boron-containing fertilizers, cleaning products, and detergents that also contain sodium perborate for bleaching; salt deposit leachate, rock weathering, and rain containing sea salt from ocean spray are the primary natural sources of boron to natural waters (Hilal et al., 2011; Kochkodan et al., 2015; Kot, 2015; Tang et al., 2017). Boron is most naturally abundant in seawater, occurring at an average concentration of 4.6 mg/L and ranging from 0.5 to 9.6 mg/L in the Baltic Sea and Mediterranean sea, respectively. The boron content of surface water and groundwater is typically low compared to seawater. The inherent geochemical conditions, proximity to marine coastal areas, and degree of pollution by contaminated wastewater are the factors that most determine boron concentrations in freshwaters (Freger et al., 2015). Concentrations of boron in surface waters typically range from <0.001 to 2 mg/L in Europe; 0.01 to 7 mg/L in Turkey, Pakistan, and Russia; and 0.02-360 mg/L in North America, but boron concentrations in surface waters can be as high as 100 ppm in certain areas due to anthropogenic activities (Butterwick et al., 1989; Tang et al., 2017). Boron is found naturally in groundwater at concentrations typically lower than 1 mg/L, ranging from 0.5 to 1.5 mg/L in Southern Europe and is present at concentrations around 0.6 mg/L in Northern Europe (Butterwick et al., 1989; Kot, 2015).

Boron is found naturally or anthropogenically in the environment as pH-dependent borate salts of boric acid. Boron is an "electron-deficient element" that acts as a weak Lewis acid in water (boric acid) with a pKa value of around 9.2 at 25 °C. The presence of boric acid or borate in an aqueous solution depends on pH (Figure 2.1), with the nonionized boric acid form occurring at pH < 9.2 and the monovalent borate anion dominating at higher pH, according to Eq. 1 (Guan et al., 2016; Güler et al., 2015; Tagliabue et al., 2014b).

$$B(OH)_3 + H_2O \rightleftharpoons [B(OH)_4]^- + H^+ \quad (2.1)$$

When the concentration is relatively low (<216 mg/L) boric acid and the monoborate anion are found, while at high concentrations (>290 mg/L) boron species such as $B_2O(OH)_6^{2-}$, $B_3O_3(OH)_4^-$, $B_4O_5(OH)_4^{2-}$ and $B_5O_6(OH)_4^-$ can exist (Guan et al., 2016). Boric acid has a water solubility of 55 g/L at 25 °C while the boron salts borax, which

contains the $B_4O_5(OH)_4^{2-}$ ion, and boron trifluoride have water solubilities of 25.2 g/L and 2.4 g/L, respectively. (Dydo & Turek, 2014; Freger et al., 2015; Kochkodan et al., 2015; Özdemir & Kıpçak, 2010; Tagliabue et al., 2014b; Tang et al., 2017; Wolska & Bryjak, 2013).

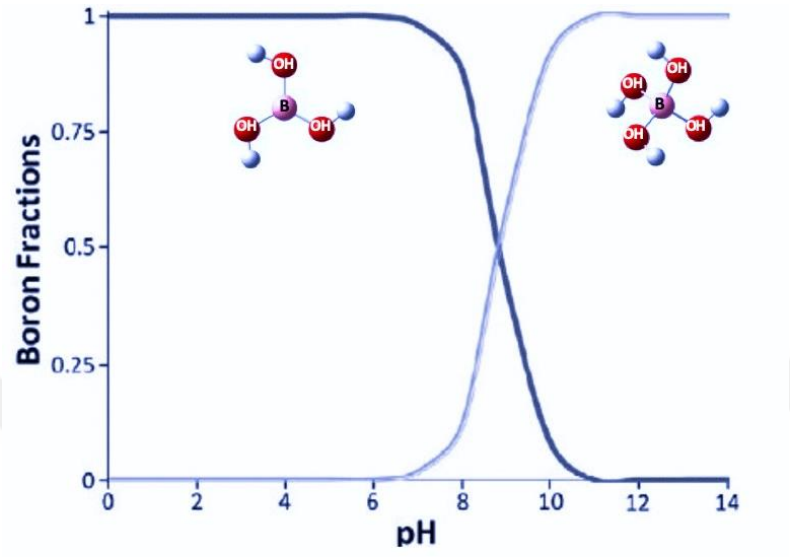

Figure 2.1 : Fraction of $[B(OH)_4]^-$ and H_3BO_3 as a function of pH.

2.2.3 Effect of boron on health in humans and plants

Boron is an essential element for humans, plants, and animals. For the absorption of calcium, magnesium, and phosphorus in human beings, certain metabolic functions require the presence of boron. However, long-term consumption above optimal levels can cause adverse effects in the cardiovascular, nervous, coronary, and reproductive systems. Excessive amounts of boron result in vomiting, diarrhea, anorexia, skin flushing, and even increased risks for pregnant women (Kot, 2015; Wolska & Bryjak, 2013).

Boron is a vital nutrient for the growth of plants, with optimal concentrations depending on the tolerance of the plant. For example, 0.5 ppm in sunflowers promotes growth, while 1 ppm results in a toxic effect. Blackberry and lemon can only tolerate boron concentrations lower than 0.5 ppm, while cotton can tolerate up to 10 ppm. Adverse effects associated with boron levels above the limit of tolerance in plants can include growth inhibition, decreased yield, inhibition of photosynthesis, leaf tips yellowing, edge and tip necrosis, and even the death of the plant (Guan et al., 2016; Hilal et al., 2011; İpekçi et al., 2018).

The WHO recommended a limit of 0.5 mg/L of boron in drinking water between 1998 and 2010, but in 2011 this value was raised to 2.4 mg/L in recognition of the need for dietary intake to promote human health. However, many countries do not comply with this standard as it exceeds the tolerable level of boron in many crops, particularly in countries that obtain irrigation water from desalination plants. In the EU, the upper limit of boron in drinking water is 1 mg/L, 0.6 to 1 mg/L in the United States, 5 mg/L in Canada and Brazil, and 2.4 mg/L in Saudi Arabia, which follows the WHO recommendation. However, boron levels must be lowered to 0.3 mg/L in waters for irrigation due to the higher sensitivity of plants (Freger et al., 2015; Guan et al., 2016; Hilal et al., 2011; Tagliabue et al., 2014b).

2.3 Boron Removal Techniques

Removal of boron from natural waters and wastewater has been the focus of most studies investigating strategies for reducing boron concentrations in these systems to date. The following section decribes both the conventional and advanced methods for boron removal from water, including those of chemical precipitation, coagulation, ion exchange, adsorption, and membrane processes (Wolska & Bryjak, 2013).

2.3.1 Precipitation

Chemical precipitation is a well known conventional technique for boron removal due to its adaptability systems with high boron content. A number of different chemicals can be used for the precipitation of boron. For example, lime (or calcium hydroxide, $Ca(OH)_2$) added to contaminated waters at 50 g/L and held at 90 °C for 2 h was shown to facilitate a precipitation reaction that reduced boron levels from 700 to 50 mg/L (Remy et al. 2005). When held at 150 °C for 14 h, the reaction between boron and lime causes the formation of recyclable $Ca_2B_2O_5.H_2O$ precipitate according to Eq. 2 (Itakura et al. 2005; Irawan et al. 2011).

$$2Ca(OH)_2 + 2H_3BO_3 \rightarrow Ca_2B_2O_5 \cdot H_2O \downarrow + 4H_2O \qquad (2.2)$$

Irawan et al. (2011) reported that pH affects the removal of boron by using $Ca(OH)_2$. At 60 ºC with a $Ca(OH)_2$ dose of 10g/L, 87% boron was removed from concentrated wastewater (Irawan et al., 2011).

Magnesium borate salt solubility is lower than that of calcium borate salts, according to Linke and Seidell (1958) (Atherton Seidell & William F Linke, 1958). Other borate salts are more soluble than calcium or magnesium salts. Additionally, some cations can cause the formation of secondary pollutants such as barium (Remy et al., 2005). Shih et al. (2014) used H_2O_2 as an oxidant in the chemical oxo-precipitation process along with calcium chloride and barium chloride as metal salts in a reaction at room temperature and pH 10. Addition of the oxidant enhanced boron removal from 5% to 80%. And with the use of $BaCl_2$ to treat H_2O_2 treated boron compound 98.5% boron removal efficiency was achieved (Shih et al., 2014). Magnesium salts are non-toxic, inexpensive, and easy to obtain(Fukuda et al., 2020). Boron removal by the generation of hydroxyapatite (HAp) was also investigated by researchers. Ammonia was used to accelerate the reaction between boron and calcium hydroxide by dehydration with ammonia by Yoshikawa et al.(Yoshikawa et al., 2012). Against the re-dissolution of boron precipitate adding phosphoric acid improves boron removal and formed HAp film prevents re-dissolution. Also hydrothermal and microwave techniques for HAp formation are used for boron removal. However hydrothermal treatment is effective for boron removal at high concentrations, and the high energy demand for heating makes microwaves more attractive (Irawan et al., 2011; Itakura et al., 2005; H.-C. Tsai & Lo, 2011; Yoshikawa et al., 2012).

2.3.2 Chemical coagulation and electrocoagulation

Coagulation is a treatment/pretreatment method for the removal of color and suspended matter that also works for boron removal. The most frequent chemical coagulants used to generate settleable flocs formed of hydrous metal oxide precipitates and impurities are aluminum and iron salts. Electrocoagulation (EC) can remove numerous contaminants and does not require the use of additional chemicals. Moreover, lower sludge production, simple equipment needs, and ease of operation make electrocoagulation an accessible option for boron removal (Isa et al. 2014; da Silva Ribeiro et al. 2019; Mollah et al. 2001; Wolska and Bryjak 2013; Chorghe et al. 2017).

Alum and ferric chloride were tested for efficacy of boron removal by Chorghe et al. (2017), who found that waters with high boron concentrations required high doses of iron and aluminum coagulants, resulting in higher sludge production (Chorghe et al. 2017). Chemical coagulation and electrochemical coagulation for removal of boron

from seawater were compared by Ofir et al. (2011) as an alternative to an expensive, multi-stage reverse osmosis (RO) process (Ofir et al. 2011). Yılmaz et al. (2007) compared the boron removal efficiency of chemical coagulation and EC and found that boron removal efficiency with EC topped 94% versus a 24% removal efficiency when chemical coagulation was employed (Yilmaz et al. 2007). Three studies have used EC setups with aluminum electrodes, which achieved 98%, 70%, and 70% boron removal efficiency, respectively (Isa et al. 2014; da Silva Ribeiro et al. 2019; Dolati et al. 2017); other studies have investigated the efficacy iron and zinc electrodes for boron removal (Wolska and Bryjak 2013).

2.3.3 Ion exchange

Ion exchange is a boron removal method that is smost suitable for removing low concentrations of boron from water (del Mar de la Fuente García-Soto and Muñoz Camacho 2005; Yan et al. 2008). Like electrocoagulation approaches, ion exchange pro- cesses result in lower levels of sludge production as compared to chemical coagulation processes (Çermikli et al. 2020). The retention order of some of the most common anions on ion exchange resin is $SO_4^{2-} > NO_3^- > PO_4^{3-} > C_2O_4^{2-} > Cl^- > B(OH)_4^-$; given the poor affinity of borate for commonly used resin, a more specific resin needed to increase retention of this ion (del Mar de la Fuente García-Soto and Muñoz Camacho 2005; Güler et al. 2015). Boron-specific resins(s) were developed in the 1970s with the aim of borate removal from magnesium brine (Hilal et al. 2011; Tagliabue et al. 2014). They are not reactive to other elements but are very selective for boron due to the use of complexion reactions. As shown in Eq. (3), boric acid with hydroxyl-containing organic compounds forms a multitude of borate esters, where the hydrocarbon group is denoted by R.

$$B(OH)_3 + 3ROH \rightleftharpoons B(OR)_3 + 3H_2O \quad (2.3)$$

Hydroxyl groups can form various boric acid esters and quickly dissociate by releasing protons in solution to form complex borate esters. For boron chelation, the presence of the tertiary amine group attached to the polymer matrix is essential. Released protons are caught by tertiary amine sites that act as a proton neutralization agent during hydroxyl functionality complexing of borate, thereby preventing a decrease in pH value. Amine protonation is shown in Eq. (4). Boron absorption on boron selective resins (BSRs) is not due to pure ion exchange, according to this mechanism, so it does

not need boric acid to be completely ionized in water (Hilal et al. 2011; Tagliabue et al. 2014; Güler et al. 2015; Hussain et al. 2019).

$$-CH_2 - N(CH_3) - CH_2 + H^+ \rightleftharpoons -CH_2 - N^+H(CH)_3 - CH_2^- \quad (2.4)$$

BSRs have a macroporous polystyrene backbone that N-methyl-D-glucamine (NMDG) functional groups are attached to, which is the most efficient material for boron removal. The complex between boric acid and methyl glucamine resin is given in Figure 2.2.

Different boron selective resins are commercially available as Amberlite PWA10/IRA743, Diaion CRB03/CRB05, Dowex BSR-1/XUS43594.00, and Purolite S108/S110. These commercially available and newly prepared resins can be used with many water types for the removal of boron as given in Table 2.1.

Commercial Dowex XUS 43594.00 and Diaion CRB02 resins were used by Kabay et al. (2007, 2008) for boron removal from model seawater (5 mgB/L) and seawater RO permeate (1.5–1.6 mgB/L). Accord- ing to their results, both of the resins have very good sorption performance. Diaion reached equilibrium after 120 min and 180 min while Dowex reached equilibrium after 240 min for both model seawater and RO permeate, respectively. Boron removal effi- ciencies of Diaion were 95.6% for model seawater and 93.5% for RO permeate, and removel efficiencies of Dowex were 95.5% for model seawater and 90.8% for RO permeate (Kabay et al. 2007, 2008). Köse and Öztürk successfully used the commercial resin Dowex 2×8 with 600 mgB/L H3BO3 solution for boron removal (Köse and Öztürk 2008). Amberlite IRA743 was used for boron removal from RO perme- ate and geothermal water by Jacob (2007) and Hanay et al. (2003). The boron removal efficiencies of this resin were approximately 99% for both types of feed water (Hanay et al. 2003; Jacob 2007). Besides commercial resins, studies with modified or novel resins are available in the literature. Samatya et al.(2015) and Çermikli et al. (2020) prepared novel resins functionalized with NMDG and reported high boron removal efficiencies comparable with commercial resins (Samatya et al. 2015; Çermikli et al. 2020).

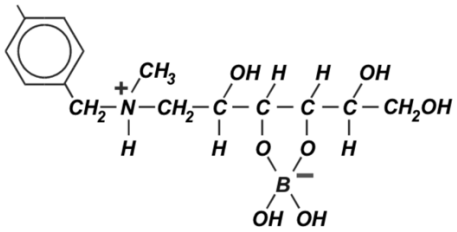

Figure 2.2 : Boric acid-a methyl glucamine resin complex (Jacob 2007).

Table 2.1 : Boron-selective resins for different feed waters.

Resin	Feedwater type	Initial boron concentration	Boron removal	Reference
Amberlite IRA743	RO permeate	1.8 mg/L	>98.8%	(Jacob, 2007)
Dowex-XUS 43594.00	Model seawater	5 mg/L	95.5%	(Kabay et al., 2007)
Dowex XUS 43594.00	SWRO permeate	1.5 mg/L	90.8%	(Kabay et al., 2008)
XSC-800	Refined brine	40 mg/L	97%	(C. Yan et al., 2008)
Amberlite IRA743	Geothermal water	19 mg/L	99%	(Hanay, A. et al., 2003)
Dowex XUS 43594.00	Geothermal water	11 mg/L	95.3%	(Çermikli et al., 2020)
2JW	Geothermal water	10 mg/L	99.7%	
1JW	Geothermal water	10 mg/L	97.4%	
2PTN	Geothermal water	10.31 mg/L	96%	
Poly(VBC-co-DVB)	Geothermal water	11 mg/L	95.9%	(Samatya et al., 2015)
Poly(GMA-co-EDM)	Geothermal water	11 mg/L	96.6%	

2.3.4 Adsorption

Adsorption is a method of isolation in which certain fluid-phase components are transfixed to a solid adsorbent surface. This technique is an effective way to remove boron from waters with low boron concentrations (Ozturk and Kavak 2005; Guan et al. 2016). Treatment of water based on adsorption of pollutants can be helpful and cost-effective in removing boron through drinking water purification, groundwater, and industrial wastewater cleaning. Sorbents such as activated carbon, clays, fly ash, natural mineral products, biological materials, oxides, mesoporous silica, nanoparticles, complexing and selective resins are used in adsorption methods for boron reduction. The most commonly used adsorbent for wastewater treatment is currently activated carbon but due to its higher cost, many researchers have questioned its feasibility as a potential substitute for the more inexpensive, commercially usable

materials (Ozturk and Kavak 2005; Demey et al. 2014a). Iron (Fe^{3+}) oxide/hydroxide-based nanoscale iron, modified silica, fly ash, chitosan, alumina, magnesium oxide, waste sepiolite, natural coal, oxides, and clay minerals are some of the adsorbents investigated in the literature. A novel adsorbent prepared with chitosan and iron (III) hydroxide and named as chiFer(III) by Demey et al. (2014b) for removal of boron from seawater. This mesoporous low-cost material was found to be capable of boron removal efficiencies up to 49.7%. The molar ratio of adsorbed boron and iron(III) hydroxide in the adsorbent was 10.7 mmolB/mol $Fe(OH)_3$ (Demey et al. 2014b). A newly magnetic composite was developed by Pinotti et al. (2022) using $CoFe_2O_4$ and MgO for boron removal. The maximum boron concentration in synthetic effluents was 20 mg/L and the authors reported boron removal up to 92% (Pinotti et al. 2022). Ngwabebhoh et al. (2019) prepared amino-modified nanocellulose (A-NCC) platelet-shaped gels for the removal of boron from aqueous media (Ngwabebhoh et al. 2019). At pH 7, 120.9 mg B/g A-NCC translated to 89.38% boron removal the initial boron concentra- tion of 100 ppm. The authors also reported that the possibility of using the adsorbent for four or more adsorption/desorption cycles in a row with minimal reduction in removal efficiency. Recepoglu et al. (2018) used a novel chelating fiber adsorbent, Che- lest GRY-HW, for boron removal from geothermal brine containing 10.5 mgB/L. The Chelest Fiber GRY-HW has been suggested as a promising adsor-bent with a total ion exchange capacity of 13.47 mg B/g fiber (Recepoğlu et al. 2018). Zhang et al. (2022) designed an organic boron adsorbent (NGN) with NMDG@γ-glycidoxypropyltrimethoxysilane (GPTMS) on nonwoven basalt fibers (NBF). Under pH 9 the optimum adsorption capacity was 1.64 mmol/g. They also reported that NGN was still able to regenerate at a very high rates after eight adsorption–desorption cycles (Zhang et al. 2022). The bio-waste-derived adsorbents were developed by Ahmad et al. (2022) for boron removal from groundwater. At pH 7 boron removal were 44% for roasted date pits (RDPs) and 39% for modified roasted date pits (MDPs) by mercaptoacetic acid (Ahmad et al. 2022).

One of the operational parameters that most affects adsorption of boron is pH, and many different studies have shown the effect of different adsorbents in combination with different pH values on boron removal, as shown in Table 2.2.

Table 2.2 : Summary of select adsorbents and associated boron removal efficiency at certain pH values.

Adsorbent	Initial boron concentration	Sample	Adsorption capacity	pH	Removal efficiency	Reference
Mesoporous silica MCM-41	100mmol/L	Synthetic boron solution	1.799 mmol/g	12		(Y. Chen et al., 2019)
Date seed	5 mg/L	Seawater			71.1%	(Al-Ithari et al., 2011)
Nitrogen-doped GO	5mg/L	Seawater	58.7 mg/g	8.4	77.44%	(F. Chen et al., 2017)
Chitosan-based magnetic nanobeads (CBN)	100 mg/L	Synthetic boron solution	147.6	7	89%	(Oladipo & Gazi, 2017)
$Ni(OH)_2$	300mg/L	Seawater	90g/kg	7.5	70%	(Turek et al., 2007)
Fly ash	600mg/L		20.9 mg/g	2	>60%	(Ozturk & Kavak, 2005)
Fly ash and coal	5.3mg/L	Seawater		>9	>90%	(H. Polat et al., 2004)
Magnesium oxide	500mg/L	Synthetic boron solution		9.5-10.5	95%	(del Mar de la Fuente García-Soto & Camacho, 2006)
Fly ash zeolite (FAZ)	50 mg/L	Aqueous solution	2.3mg/g	7	93%	(Kluczka et al., 2015)
Palm Oil Mill Boiler (POMB) Ash	10 mg/L	Synthetic boron solution	1.796 mg/g	7	65.69%	(Chieng & Chong, 2013)
Calcined alunite	10 mg/L	Synthetic boron solution	3.39 mg/g	10	49%	(Kavak, 2009)
Tartaric acid-modified MWCNTs (TA-MWCNTs)	20 mg/L	Synthetic boron solution	1.97mg/g	6		(Zohdi et al., 2014)
Activated Alumina	50 mg/L	Synthetic boron solution		8-8.5	65%	(H. Liang et al., 2008)
RDPs MDPs	1.502 mg/L	Groundwater	13.34 mg/g 13.42 mg/g	7	44% 39%	

2.3.5 Membrane processes

2.3.5.1 Electrodialysis

Electrodialysis (ED) is an electrically driven process for the removal of boron using ion-exchange membranes. Charged solutes move via selective ion exchange membranes (IEMs) by taking advantage of voltage differences among electrodes (Mezher et al. 2011; Tagliabue et al. 2014; Landsman et al. 2020).

IEMs have synthetically immobilized ion exchangers on membrane material, including cation exchange membranes (CEMs), anion exchange membranes (AEMs), and bipolar membranes (BPMs). CEMs and AEMs in electrodialysis systems are positioned in an alternating configuration and are subject to an external electrical field, as illustrated in Fig. 3 (Dydo and Turek 2013; Tang et al. 2017).

CEMs and AEMs are subject to an outside electri- cal field that causes cations and anions to transition from the dilute chamber to the concentrate chamber (Freger et al. 2015; Tang et al. 2017). Boron-concentration-gradient-driven diffusion, combined with a convective drag of the ion stream, is the key mechanism of boron transport between AEMs and CEMs. In neutral conditions, undissociated boric acid molecules are the dominant species in the boron solution. The majority of boron molecules were discovered to be carried by AEMs rather than CEMs, suggesting that boron is highly influenced by anion and cation form (Goli et al. 2010; Dydo 2012; Tang et al. 2017).

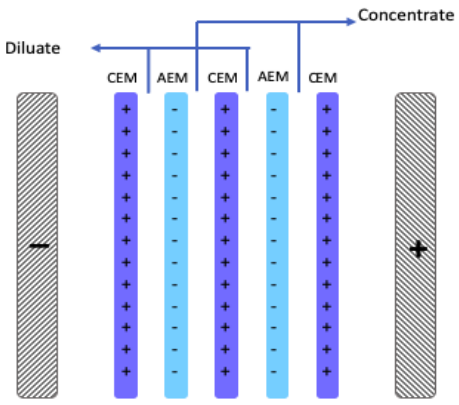

Figure 2.3 : Diagram of the electrodialysis process.

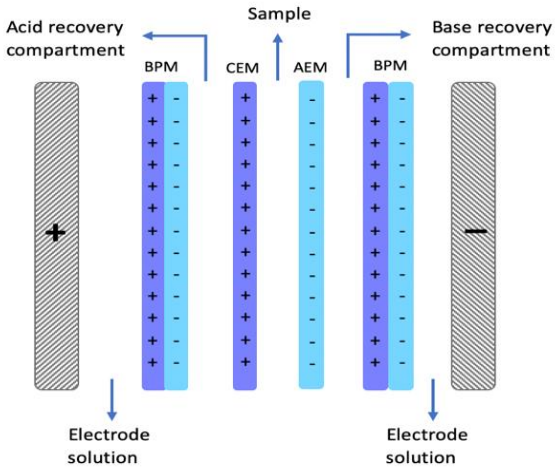

Figure 2.4 : The scheme of BMED process.

AEMs and CEMs in combination with BPMs are used in the bipolar membrane electrodialysis process (BMED) as illustrated in Figure 2.4. When an electrical field is present, a BPM enables water dissociation.

The BPM consists of three major components: the anion exchange layer, the cation-exchange layer, and the hydrophilic interface at the intersection of the anion- and cation-exchange layers. In aqueous solutions, water molecules move to the hydrophilic cavity where they are split into H^+ and OH^- ion ions after a direct current has been applied to a bipolar membrane. The ability of the bipolar membrane to produce proton and hydroxyl ions from water molecules at the hydrophilic interface under direct flow is thus a major factor in the electro membrane separation process. Thus, due to the presence of the bipolar membrane, BMED produces acids and bases as new materials in different chambers. For example, boron has been recovered as H_3BO_3 during the BMED process (Mani 1991; Bunani et al. 2017). Due to the BMED system being intended to separate a saline solution into its acidic and basic components without the need for any chemical additives, it can be considered a relatively "environmentally friendly" technique (Bunani et al. 2017).

In the numerous studies about ED and BMED for the removal of boron from waters, membrane type, ion types that migrate towards the membrane, density of the electric current, and initial boron content of dilute have been shown to be the factors that most strongly affect boron flux at neutral pH. Goli et al. (2010) investigated the effect of acids and salts on boron diffusion via CEMs and found that boron flux reduced with cation type in the following order: $K^+ > Na^+ > H^+ > Ca^{2+} > Mg^{2+} > Al^{3+}$. This order

suggests that boric acid transport occurs more readily in the presence of monovalent cations than with divalent cations. It was further observed that boron was transported more successfully through AEMs when sulfate ions were present than when nitrate and chloride ions were present (i.e., $SO4^{2-}$>Cl^{-}, NO^{3-}). These findings imply that the majority of boron molecules are conveyed by AEMs rather than CEMs and were significantly affected by the anion and cation forms (Goli et al. 2010; Dydo 2012, 2013). Prepared P84 co-polyimide porous membrane modified with quaternized graphene oxide (QGO) were used as an anion exchange membrane for boron removal in the BMED process by Sun et al.(2020). The produced composite membranes were shown to be effective for boron removal, achieving 76.6% boron removal efficiency from a model solution containing 1000 mgB/L (Sun et al. 2020). Dydo and Turek (2013) used various IEMs in pairs to investigate the boron flux obtained from different membranes. The authors found that PC-SA AEMs had the highest flux with an initial boron content of 0.1 M and 100 A m^{-2} electric current density (Dydo 2013). In the study conducted by Nagasawa et al. (2011), 45% boron removal was achieved via ED, whereas < 90% rejection was achieved with BMED (Nagasawa et al. 2011). Similarly, Hung et al. (2022) reported 98.53% boron removal efficiency by using five cycles of sequential feed batch BMED (Hung et al. 2022). İpekçi et al. (2018) investigated the effects of acid and base solution types, concentrations in acid and base compartments, and electrical potential on boron removal. By utilizing HCl and NaOH solutions in acid and base compartments, they obtained 86.9% boron separation (İpekçi et al. 2018).

In ED, organic compounds such as humate can accumulate on ion exchange membranes, which serves to raise the electrical resistance of the membranes (Lee et al. 2003). For instance, humic acid was observed to foul membranes used in ED, impacting salt flux (Lee 2002; Kim et al. 2003; Park et al. 2006). As the majority of organic matter at neutral pH is negatively charged, deposits mostly occur on anion exchange membranes (Banasiak and Schäfer 2009). In addition, the presence of the Mg and Ca ions affects the purity of products treated with BMED. Cations such as Ca^{2+}, Mg^{2+}, and Na^{+} form complexes with boron, which account for 44% of boron in seawater, and so are prevalent in the feed. Removal of such ions is important not only in terms of membrane scaling but also for enhancing the purity of the finished product. As a result, a pretreatment technique is generally suggested prior to the BMED

procedure (Bunani et al. 2017; İpekçi et al. 2018). Transportation of boron in ED increases when the pH of sample water increases higher than 9 (Dydo 2013; Dydo and Turek 2013). However, due to low electrical current performance for boron transport, the ED method for boron removal is comparatively costly; however, it has been proposed that costs can be reduced by improving energy efficiency and using more inexpensive membranes (Tagliabue et al. 2014).

2.3.5.2 Donnan dialysis

Unlike ED, no external electrical field exists in a Donnan Dialysis (DD) operation; only one kind of membrane (CEMs or AEMs) is often used. During DD, borate is transported via AEM in the receiving solution from the so-called feed solution. However, an equivalent amount of another anion—called as driver anion—must be transferred from the receiving solution to the feed solution to satisfy electroneutrality requirements. Chloride, sulfate, or even hydroxyl ions may take the role of the driver ion. The entire procedure takes place before some relationships are reached in obtaining and feeding solutions between borate and driver ion concentration. This ratio is established by the equilibrium of Donnan. Due to the process balance, the driver ion is typically required to be in excess of the extracted ion (Dydo and Turek 2013). The feed solution boron content, presence of accompanying ions, membrane type, pH, and the driver anion in the receiving solution can all affect boron removal in the DD process (Ayyildiz and Kara 2005; Kir et al. 2011).

Ayyildiz and Kara (2005) compared different anion exchange membranes in the DD process for boron removal under various conditions. According to their results, the most effective AEM is AFN, which permitted more boron transport than Neosepta-AHA and AMH membranes. In the presence of HCO_3 ions, boron flux reached a maximum, and the accompanying sodium chloride ion resulted in the highest boron transport rate (Ayyildiz and Kara 2005). Kir et al. (2011) used plasma modification to AEM to enhance its transport capacity and efficiency. The authors reported that as the boron concentration was increased in the feed solution, the flux also increased (Kir et al. 2011). They further used an electron cyclotron resonance plasma (ECR) treatment method to enhance anion exchange membrane performance. The optimum pH selected was 9.5, and the plasma- modified AFX membrane was shown to be the most effective AEM for boron transport while boron flux was observed to decrease in the presence of valence anions in the order of $SO_4^{2-} < Cl^-$.

DD was also used for regeneration of BSR (Dowex XUS 43594.00) by Bryjak et al. (2007), who tested three kinds of AEMs for boron removal; 1) an AESD-2 interpenetrating polymer membrane (IPN), a microheterogeneous polyelectrolyte network; 2) a non-porous poly(phenylene oxide) (PPO), a gel-like membrane which is more homogeneous; and 3) a porous PPO membrane (Bryjak et al. 2007). According to their results, NaCl transports boron far more efficiently than Na_2SO_4. They reported that regeneration of boron-loaded resins can be conducted by Donnan Dialysis and the first- stage seawater RO brine can be effectively used for BSR regeneration (Bryjak et al. 2007). Vanoppen et al. (2015) used RO concentrate in DD to increase recovery for drinking and process water treatment but emphasized that the membrane cost of DD needs to decrease to compare economically with other approaches (Vanoppen et al. 2015). Ping et al. used microbial desalination cells (MDC) coupled with a DD system for boron removal (Ping et al. 2015). Without DD, direct cathodic alkalinization of boron was not successful. Additionally, considerable salt accumulation occurred and lower than 2 mg/L boron concentration was obtained via the MDC-DD treatment (Ping et al. 2015). Ping et al. (2015) also equipped microbial fuel cells (MFC) with AEM to remove excessive boron during desalination by electricity generation. They found MFC to successfully remove boron for both pretreatment and post-treatment modes, and the boron concentration decreased in the post-treatment mode to satisfy requirements for irrigation or municipal use (Ping et al. 2016).

2.3.5.3 Forward osmosis

Forward osmosis (FO) has recently been identified in recent years as a high-potential method for water treatment (Chang et al. 2020; Najid et al. 2021). It requires less energy than RO and boasts operational simplicity (Jin et al. 2012), higher water recovery (Jin et al. 2012; Chang et al. 2020), lower membrane fouling (Jin et al. 2012; Liu et al. 2019), higher boron rejection, and higher cleaning efficiency (Kim et al. 2012; Najid et al. 2021). FO is an osmotic process where the driving force is the osmotic pressure difference between feed solution and draw solution. Water flows from a low osmotic solution to a high osmotic draw solution (DS) across the semi-permeable membrane (Figure 2.5). Hence the draw solution is diluted (Cath et al. 2006; Fam et al. 2014; Liu et al. 2019; Chang et al. 2020; Darwish et al. 2020; Najid et al. 2021).

The energy requirement is lower in FO compared to RO due to the of use the osmotic pressure difference but requires a very high hydraulic energy input (Fam et al. 2014). The draw solution as the final product is diluted to some extent and requires further separation after the initial FO treatment (Fam et al. 2014; Liu et al. 2019; Darwish et al. 2020). As a result, FO would likely need to be used in combination with other processes such as nanofiltration (Kim et al. 2018), reverse osmosis (Arjmandi et al. 2020; Lee et al. 2020; D'Haese et al. 2021), or membrane distillation (Lee et al. 2018b; Islam et al. 2019; Li et al. 2020) for to achieve the required separation or recovery.

FO has been investigated in literature for boron removal, as shown in Table 2.3. The membrane active layer may face the feed solution or the draw solution, but boron retention seems to be more efficient in when the active layer is facing the feed solution (AL- FS mode) than when the active layer is facing the draw solution (AL-DS mode). AL-DS mode is likely more successful due to the combined effects of concentration polarization of the internal concentration (ICP) and dilutive outer polarization, which produce conditions for favorable to borate diffusion (Jin et al. 2012; Kim et al. 2012; Liu et al. 2019). In addition, boron removal by FO has been shown to be affected by feed concentration, draw solution type, pH, and membrane orientation (Kim et al. 2012; Fam et al. 2014).

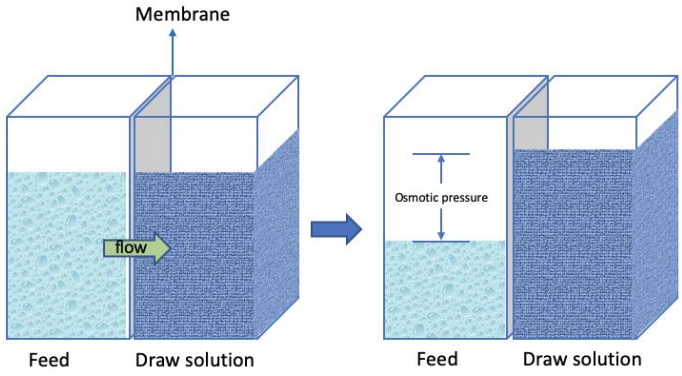

Figure 2.5 : Diagram of forward osmosis process.

Table 2.3 : Summary of select systems for boron removal by forward osmosis.

Operation cond.	Boron removal (%)	Main findings	Draw Solution	Ref
5-10 mg B/L feed solution; AL-FS mode; AL-DS mode; CTA-HW and CTA-W membranes used	29%-62% for CTA-HW membrane for AL-FS	With increased B content in the feed, boron flux increased Higher water flux in AL-DS mode CTA-HW membrane showed higher boron flux	2 M NaCl	(Jin et al., 2011)
pH 7 for feed; pH 5-6.2-9-11 for draw; 80 mg B/L;	ca. 25%-30%	Solute flux did not change with draw solution pH changes; In AL-FS mode water flux and boron flux are lower than in AL-DS mode	2 M NaCl 1.6 M $CaCl_2$ 1.5 M $LaCl_3$	(C. Kim et al., 2012)
5 mg B/L pH 11 for feed solution; TFC membrane	Max. 94% by electrostatic repulsion at pH 11	Water flux for different draw solutions as KCl >$(NH_4)_2SO_4$ > $NH_4H_2PO_4$ Boron rejection rates were KCl > $(NH_4)_2SO_4$ > $NH_4H_2PO_4$ Boron rejection rate increased with increasing KCl draw conc. from 1 mg/L to 3 mg/L; AL-DS mode resulted in higher water flux, boron flux, and lower rejection rates Boron rejection was independent of feed boron conc.	2 M KCl 2 M $(NH_4)_2SO_4$ 2 M $NH_4H_2PO_4$	(Fam et al., 2014)
pH 5.9±0.2, cellulose triacetate FO membrane,	>60% for AL-FS mode	At water fluxes, less than 15.3 L/m^2/h, alginate fouling in the membrane support layer had a negative impact on boron rejection. B rejection was higher in AL-FS mode	NaCl	(Jin et al., 2012)
pH 7-9-11 for TFC-AIM membrane, pH 7 for CTA membrane; 600 mg B/L, 0.5-30 mM CTAB was used in the feed solution, FO-MD hybrid system	Max. 99.9%	CTA membrane achieved 62% boron removal so TFC-AIM membrane was selected; increasing DS conc. resulted in boron conc. decreasing in DS Boron rejection was increased to 99.9% from 98.4% with the addition of CTAB to feed for the TFC-AIM membrane; water flux increased with increasing DS conc.	0.5-2 M $MgCl_2$	(H.-M. Chang et al., 2020)
FTS H2O, PSU, and Aquaporin Inside membranes; feed solution pH 4-10, 10-100 mg B/L	Max 90% for FTS H2O membrane at pH 10	Boron solute flux increased with rising DS and boron conc. however decreased with rising FS pH; boron rejections increased to 90% from 12% for pH 4 and 10 of FS, respectively for FTS H2O membrane, 8% to 84% for PSU, and 8% to 76% for Aquaporin Inside membranes DS conc. raise from 0.5 to 3M resulted in boron rejection rate increment from 20% to 54% for FTS H2O, 14% to 50% for PSU, and 8% to 40% for Aquaporin Inside Boron concentration increment had no significant effect on boron rejection	0.5-3 M $MgCl_2$	(Darwish et al., 2020)

2.3.5.4 Reverse osmosis

One of the most essential technologies for purifying water is reverse osmosis (RO), where pressure is the driving force. Under alkaline conditions (pH>9), boron is mainly found as negatively charged borate ions, which can be removed by RO with very high efficiency due to Donnan repulsion and size exclusion of borate ions. However, RO is incapable of separating the poorly hydrated boron molecules that dominate at acidic and neutral pH, given the lack of electrostatic repulsion (Tang et al. 2017; Najid et al. 2021). When the pH is lower than the pKa value of 9.23 (at atmospheric pressure, 20 °C), boric acid is found as uncharged H_3BO_3 in water, while at pH higher than the pKa, various negatively charged H_3BO_3 compounds dominate in solution and can be rejected by negatively charged membranes. In aqueous solutions, borates are often well hydrated, which increases their molecular sizes on the side of the membrane feed promotes greater retention (Sagiv and Semiat 2004; Hyung and Kim 2006; Oo and Song 2009; Oo and Ong 2010; Tu et al. 2011; Bártová et al. 2016).

Boron rejection by seawater reverse osmosis (SWRO) membranes has been reported as 88–91% and as 30–80% for brackish water reverse osmosis (BWRO) membranes under standard conditions, but shifting the pH to 11 in these systems, resulted in increases of boron rejection to 99.5% for SWRO and 99% for BWRO membranes. However, these high pH values are known to cause scaling layer precipitation; therefore, increased pH is mainly employed in treatment processes utilizing a series of arrays, such as double pass RO (Fig. 6a) or several process configurations (Kabay and Bryjak 2015). For example, pH alteration is generally employed in the second RO stage (BWRO) to prevent scaling (Tang et al. 2017). Farhat et al. (2013) used a two-pass RO system without pH adjustment and achieved boron rejections as high as 96% (Farhat et al. 2013). In a study conducted by Xu et al. (2010), the addition of sodium hydroxide prior to the second stage resulted in boron rejection between 80 and 95%, facilitated by the elevation of pH to 9.5–10.5, the pH regime that favors boron removal (Xu et al. 2010).

A single-stage unit is generally not enough to decrease the boron content to conform to WHO recommended limits, and several more complex designs have been developed to reduce the boron content in RO to meet these guidelines. However, additional steps result in higher energy demands, capital investment, and possibly chemical usage

(Wang et al. 2018). Optimization of eight different design concepts for reducing boron removal costs was conducted by Glueckstern and Priel (2003).

The hybridization of the second pass RO with BSR (Figure 2.6b) was found to reduce cost (Glueckstern and Priel 2003). A study of Taniguchi et al. (2004) confirmed that cost reduction for high boron removal required a two-pass RO and BSR combination (Tani- guchi et al. 2004). Faigon and Hefer (2008) compared a two-pass RO and cascade design (Fig. 6c) and found that the cascade design allows for adjustment of operating conditions based on the temporary demands of the treatment plant, which can lower costs even more than the two-pass system (Faigon and Hefer 2008). Han et al. (2017) investigated a hybrid membrane inter-stage design (HID) with single-pass RO as an alternative to two-stage RO, thus reducing the cost by eliminating the additional pass. They used a 45% recovery rate as the optimal recovery rate and reported that the recovery rate is affected by total dissolved solids (TDS) in the feed, temperature, and the membrane position in the pressure vessel (Han et al. 2017).

The design target should be described by objective functions to evaluate the various configurations: (1) minimizing batch operation; (2) maximizing boron removal; and (3) minimizing the cost of investment. The decision-maker must specify a utility function to enable proper selection (Z_T) (Bick and Oron 2015), as shown in Eq. 2.5.

$$Z_T = (Min\ batch\ operation) + (Max\ boron\ removal) + (Min\ investment\ cost) \quad (2.5)$$

The pH influences the surface characteristics of the membrane, especially membrane charge and zeta potential, as well as the boron speciation. The zeta potential shows that a rise in pH causes membranes to become more negative. An even greater negative charge produces higher rejection as the interactions between membrane and anions are increased by electrostatic forces. Thus, the increase in pH is a proven method to increase boron removal by RO membranes when economically justifiable (Koseoglu et al. 2008, 2010; Oo and Ong 2010; Tu et al. 2013; Freger et al. 2015). In addition to pH, the pressure, temperature, recovery rate, membrane type, and feed solution influence boron separation in RO (Güler et al. 2015; Bártová et al. 2016; Najid et al. 2021). While boron removal through RO can be enhanced by different operational conditions and membrane types, the use of additional processes like ion exchange or second pass means additional operational and capital costs (Han et al. 2017). The membrane is the main component of any RO system. The traditional RO membrane is made of cellulose-based polymers; however, the thin-film (TFC) polyamide (PA)

membranes are now dominating the RO market due to the achievement of 99.8% salt rejection under normal SWRO test conditions (32,000 mg/L NaCl feed solution at 55 bar applied pressure). TFC membranes are also capable of achieving much greater permeability than asymmetric cellulose triacetate-membranes (Lim et al. 2021). The old membrane types (SW-8040) are reported to have a relatively low boron rejection efficiency (75%), particularly after long membrane service. Newer membrane types, such as FilmTec SW 380HR, SW 30HR, and Toray UTC-80-AB, have performed significantly better at removing boron. In seawater desalination, the concentration of boron can be reduced below 1 mg/L in the permeate using these membranes, but this concentration is still higher than the WHO standard (0.5 mg/L) (Glueckstern and Priel 2003; Kabay and Bryjak 2015). At pH 8.2, Kabay and Bryjak (2015) observed boron rejections of 85% and 92% by Toray and Filmtec; however, at pH 10.5, the same membranes were able to achieve higher than 98% rejection and permeate boron concentrations of 0.1 mg/L (Kabay and Bryjak 2015). Four key challenges are still confronting TFC- SWRO membranes: tradeoffs related to permselectivity, poor boron rejection, membrane fouling, and low resistance to chlorine-based oxidizing agents. Therefore, future SWRO membrane research is expected to focus on these four sectors to further enhance the durability and efficiency of SWRO membranes (Lim et al. 2021). Newly developed RO membranes have a tighter selective layer with a greater affinity for water and lower boron affinity (Tang et al. 2017). A recently developed citrate-modified layered double hydroxide (CA-Mg-LDH) TFN membrane was used for boron removal by Zhao et al. (2022) with limited success, For the initial boron concentration of 10 mg/L, these TFN membranes achieved 75% boron rejection (Zhao et al. 2022).

Most manufacturers take the principal approach of producing high-boron refusal grades for RO membranes by "tightening" the membranes and increasing the rejection of boron at the cost of decreased permeability (Freger et al. 2015). Wang et al. (2022) reduced pore size and obtained highly selective SWRO membranes by customizing PA SWRO membranes. The authors achieved 95.34% boron removal efficiency by adjusting the polymeric density and including functional groups of an oligomeric overlay on the PA active layer that were tailored to enhance boron removal (Wang et al. 2022). In a study conducted by Li et al. (2022) on enhancing boron removal by TFC membranes, the authors applied UV irradiation during the interfacial polymerization

(IP) process. With the resulting modified hydroxyl-rich PA TFC membrane, a boron removal efficiency of 92.8% was obtained (Li et al. 2022). Some promising novel materials have also been studied widely by researchers, including carbon-based materials such as graphene, carbon nanotubes (CNTs), and Aquaporin (AQP) proteins (Yang et al. 2018).

Temperature in the RO system has a strong effect on pKa and pKb values of boron, which in turn affects removal. The impact of temperature on the rejection of boron is a tradeoff between increased permeability of boron through the membrane and decreased pKa. Boron rejection will usually decrease at high temperatures because permeability influences recovery more strongly than pKa (Tu et al. 2010). Xu et al. (2010) reported that boron rejection decreased from 85 to 68% with increasing temperatures from 8 to 26 °C. A 46% increase and 3.8% decrease in permeate flux and boron rejection, respectively, resulted from the increase in temperature from 10 to 25 °C (Xu et al. 2010). According to the results of later study by Fujioka et al.(2014), boron rejection decreased from approximately 40% to below 10% with temperature increasing from 10 to 35 °C (Fujioka et al. 2014). Güler et al. (2011a) reported that at 55 bar permeate boron concentration increased from 0.7 to 0.9 mg/L for the temperature values of 9.8 °C and 15.4 °C, respectively (Güler et al. 2011b).

Similar to temperature, higher salinity also lowers pKa and increases borate ions; thus, as salinity increases, boron removal will decrease (Hilal et al. 2011). This phenomenon can be attributed to charge neutralization or obstruction of membrane surface potential. Electrostatic interactions between a membrane surface and a borate ion are reduced, or the membrane charging density is changed, and ions are diffused more rapidly through the membrane due to reduced membrane surface potential at high salinities (Oo and Song 2009; Hilal et al. 2011; Najid et al. 2021).

The rejection of boron increases generally with increasing transmembrane pressure. Concentration polarization increases as a result of increasing applied pressure and the boron concentration at the membrane surface increases, leading to boron diffusion. In general, water flow increases more than boron flow at high applied pressures, which leads to increased boron rejection. Interestingly, pressure affects boron flow considerably if the pH of the feed is low but is negligible if the pH of the feed is high (Kezia et al. 2013; Tang et al. 2017). Koseoglu et al. (2010) investigated the effect of operational parameters on boron removal. They reported that increasing operating

pressure increased boron rejection with BWRO membranes at about 20 bar. The boron rejection was found to be higher than 92% for SWRO membranes operated at about 48 bar (Koseoglu et al. 2010). Boron discharge improved from 82 to 91% at pH 9.5 as the operating pressure was raised from 0.8 to 1.4 MPa during the fixed recovery condition. In addition, the pH of permeate was calculated and the pressure associated with an increasing boron and salt rejection showed a decreasing pattern according to Xu et al. (Xu et al. 2010). Certain chelating agents that have numerous hydroxyl groups and may chelate with boric acid and borate by the addition of glycerol, mannitol, and sorbitol to the feed water, can also have a positive effect on boron removal in nanofiltration and RO processes. Polyols in the retentate are the main problem that needs additional treatment (Dydo et al. 2012; Tu et al. 2013).

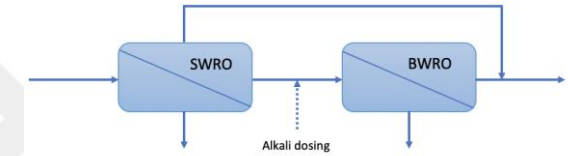

a)

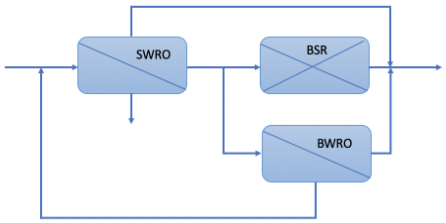

b)

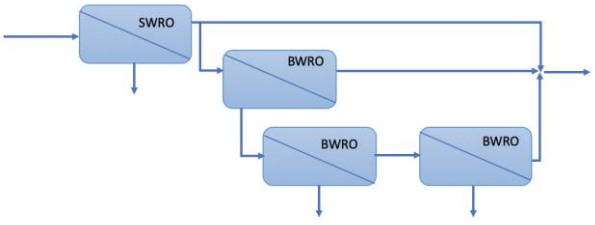

c)

Figure 2.6 : RO system configurations for boron removal by a)Two-stage RO, b)Two-stage with boron selective resins (BSRs), c)Cascade design (modified from Tang et.al. 2017; Butterwick et.al. 1989; Farhat et.al. 2013).

2.3.5.5 Membrane distillation

Membrane distillation (MD) is a relatively new membrane technology that is a thermally driven filtration process. Since changes in boron concentrations in feed water are less critical and require lower temperatures than conventional distillation and lower operating pressure than other membrane processes, MD has gained much attention. Hydrophobic membranes are used for this process to allow only water vapor molecules to transport to the side of the permeate. The schematic of MD is illustrated in Figure 2.7.

Membrane distillation can be found in four main configurations: direct contact membrane distillation (DCMD), air gap membrane distillation (AGMD), sweeping gas membrane distillation (SGMD), and vacuum membrane distillation (VMD). With MD, 100% theoretical rejection for non-volatile solutes is possible (Tang et al. 2017; Najid et al. 2021). Membrane type (Ozbey-Unal et al. 2018); membrane properties such as membrane thickness, hydrophobicity of membranes, and liquid entry pressure (LEP) value (Khayet and Matsuura 2011; Shim et al. 2015; Munirasu et al. 2017); operational parameters (Boubakri et al. 2015; Julian et al. 2016; Kabeel et al. 2017; Eryildiz et al. 2021); and module properties and configurations (Guillén-Burrieza et al. 2012; Abu-Zeid et al. 2015; Mutlu Salmanli et al. 2022) can all affect the flux and removal efficiencies during MD. Hou et al. (2013) used DCMD for the removal of boron from seawater. Starting with a boron concentration of 4.65 mg/L in the feed, the permeate concentration reduced below 20 μg/L and the salt removal efficiency was 99.9% (Hou et al. 2013). Boubakri et al. (2015) conducted a study with a high initial boron concentration of 200 mg/L and achieved 90% rejection via DCMD with a 27 $kgm^{-2}h^{-1}$ flux value. They also treated seawater containing 5.37 mg/L boron and reduced the boron concentration to lower than 0.47 mg/L in the permeate (Boubakri et al. 2015). Vacuum-assisted air gap membrane distillation (VAGMD) was recently used to remove boron from synthetic and geothermal waters (60.84 mgB/L) in our previous study. Boron removal efficiencies were higher than 99%, resulting in permeate boron concentrations below 0.5 mg/L (Mutlu Salmanli et al. 2022). MD is less susceptible to complications from salt in the feed and to pH, which has been proven by the literature. Even up to 750 mg/L initial boron concentration the permeate boron concentration was lower than the max permissible limits and 99.8% removal efficiency was achieved (Hou et al. 2010). However, the feed temperature does affect the flux increment. Due

to the need for energy for heating feed solutions, MD is considered an energy-intensive process. As a result, research on reducing costs have focused on high flux membrane development (Hou et al. 2010, 2013; Xu et al. 2017; Yang et al. 2017, 2019; Duong et al. 2018; Ozbey-Unal et al. 2020) and sustainable energy source usage such as solar energy or waste heat (Suárez et al. 2015; Chafidz et al. 2016; Lee et al. 2018a; Zarzoum et al. 2019; Abdelgaied et al. 2020). Ozbey-Unal et al. (2020) fabricated a high-flux nanofiber-based membrane for boron removal from geothermal water. They used different polymer concentrations (from 10 to 17.5%), different additive concentrations (2.5–10%), and heat treatment to optimize the membranes. They reached a 27.7 kg/ m^2.h flux value and maximum 0.25 mg/L boron in permeate water for the membrane consisting of 15% PVDF + 7.5% PTFE (Ozbey-Unal et al. 2020).

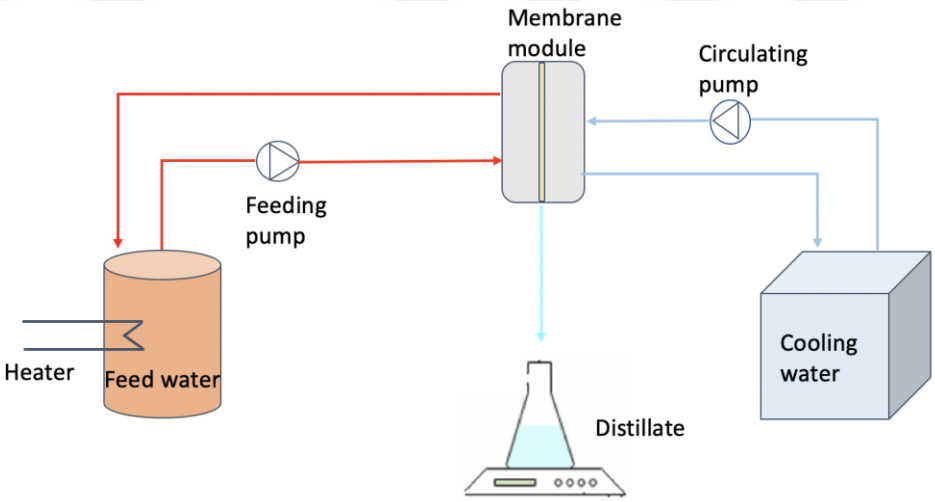

Figure 2.7 : Direct contact membrane distillation (DCMD) setup diagram.

2.3.5.6 Supported liquid membranes

Liquid membranes can selectively complex a single substrate that will be efficiently transported across the membrane via unique carrier molecules, similar to ion-exchange membranes (Abdelgaied et al. 2020). Liquid membranes fundamentally create a double liquid–liquid separation processes in which the amount of organic solvent is reduced. Although liquid membranes have numerous disadvantages, such as instability under long-term operation, they are increasingly being explored for wastewater treatment due to their operational characteristics (Comesaña et al. 2011; Fortuny et al. 2012a). They are commonly classified as bulk liquid membranes, emulsion liquid membranes, and supported liquid membranes (SLM), where capillary forces in a fine, stable, microporous layer immobilize the organic carrier solution, forming a barrier

between two aqueous solutions (the source and receiving phases) (Bachelier et al. 1996). Bulk liquid membranes typically consist of a water- immiscible step in a U-tube of aqueous feeding and stripping phases. BLMs are usually employed to examine the qualities of new carriers; due to the small membrane surfaces of BLMs, these technologies are not broadly applicable (Kocherginsky et al. 2007). Conversely, emulsion liquid membranes have a high surface area and low thickness, which increases the speed of separation and accumulation inside the emulsion tool. The tool has to be stable enough to minimize leakage but not so stable that it cannot be accessed after separation, enabling the removal of the transported substances. Consequently, the process must employ multiple unit operations and becomes technologically unappealing (Kocherginsky et al. 2007). SLMs (Figure 2.8) are an effective way to remove or recover metals at low concentrations (Fortuny et al. 2012a).

The organic liquid is generally embedded in the small pores of a membrane and held there by capillary force. SLM combines the stripping and extraction processes in one step that takes place at the interfaces of the aqueous solution and the organic liquid. A chemical pumping carries the species through the liquid membrane (Güell et al. 2011; Fortuny et al. 2012a). SLMs have high separation factors, low energy requirements, low initial and operational costs, scale-up potential, and can be used with inexpensive carriers, which make them an attractive alternative to conventional methods of treatment and removal (Kocherginsky et al. 2007).

Fortuny et al. (2012b) used triexyl(tetradecyl) phosphonium bis 2,4,4-(trimethylpentyl) phosphinate (Cyphos IL 104) as a carrier in an SLM for boron removal from seawater along with a PVDF 0.45 um membrane as the support (Fortuny et al. 2012b). Trioctyl/decylmethylammonium-bis(2,4,4- trimethilpentyl) phosphinate (ALiCY IL) and the trioctyl/decylmethylammonium decanoate (ALiDEC IL) were used in a study conducted by Coll et al. (2014) for the removal of boron. The authors inves- tigated the dependence of extraction capacity on pH and boron concentrations. About 60% boron extraction was achieved for 0.54 M IL in a wide range of pH according to their results (Coll et al. 2014). The ionic liquids ALiCY and the mixture of Cyphos IL 101 and Cyphos IL 167 with Cyanex 272 were used for the separation of boron via flat sheet SLM in another study by Fortuny et al. (2012a) (Fortuny et al. 2012a). The Cyphos IL 167/Cy272 showed promising results in terms of boron transport. In addition to the flat sheet supported liquid membranes (FSSLM), hollow

fiber supported liquid membranes (HFSLM) offer an additional SLM configuration that balances a higher cost against higher surface area (Kocherginsky et al. 2007). There are very few studies in the literature investigating liquid membrane technology for boron removal.

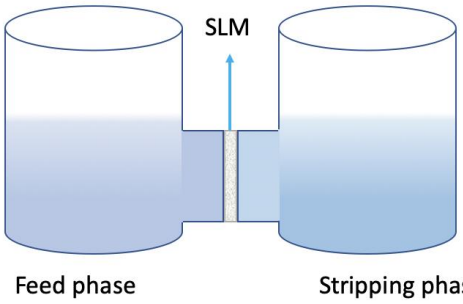

Figure 2.8 : Diagram of supported liquid membrane setup.

2.3.5.7 Hybrid membrane processes

In addition to the conventional and separated membrane processes, hybrid processes have been explored for the removal of boron. Polymer enhanced ultrafiltration (PEUF) is one such process, which uses ultrafiltration together with chelating water-soluble functional polymers. Separation is achieved by ultrafiltration while the role of polymers is complexation with target pollutants. The average size of these complexes is greater than the membrane poresize, resulting in target pollutant retention on the feed side. Chelating polymers should therefore be compatible with the target pollutant type for desired rejection. pH is also an effective parameter for rejection (Zerze et al. 2013; Yürüm et al. 2013). To obtain a stable complex, tetrahedrally coordinated boron should match the chelating polymer, meaning the chelating polymer should contain multi-hydroxyl groups. Commercial polymers such as polyvinyl alcohol and polyethyleneimine could achieve low boron rejections due to the lack of functional groups (Tang et al. 2017).

Different polymers have been synthesized to achieve high boron rejection in various studies. N-methyl-d-glucamine is one of the more commonly used polymers for boron rejection (Yürüm et al. 2013; Sánchez et al. 2013, 2016). Poly(vinyl amino-N,N′- bis-propanediol) (GPVA) was synthesized as a boron removing chelating polymer by Zerze et al. (2013). According to their results, very high boron rejections (96%) at pH 9 were achieved by total recycle PEUF with this newly synthesized polymer and is highly dependent on pH (Zerze et al. 2013). Three different chelating polymers were

synthesized by Yürüm et al. (2013). One of these polymers originated from N-methyl-D-glucamine and others the originated from iminodipropyleneglycol. They reported that increasing the pH value increased the boron retention, with 90.1% retention achieved at pH 10 (Yürüm et al. 2013). Also hyperbranched polyglycidol (HPG) and 2,3-Dihydroxypropyl-hyperbranched polyethyleneimine (Diol-HPEI) were used to test the boron rejection capacity of hyperbranched polymers. A Diol-HPEI polymer achieved 66–91% boron rejection in the pH range between 6.9 and 9.0 (Tang et al. 2016). Hyperbranched polymer solution viscosities are lower than linear polymers, which limits membrane fouling, an important consideration in PEUF (Tang et al. 2017), which could be an effective boron removal technology once optimized.

Another hybrid method that combines BSRs with microfiltration (MF) is adsorption membrane filtration (AMF). The process progresses through the following steps; (1) boron adsorption by BSRs, (2) loaded BSRs separation from treated solution by MF, (3) boron desorption from BSRs with mineral acid, (4) separation of BSRs by MF from brine, (5) BSRs regeneration via mineral base, (6) recovery of BSRs and recycle back to the first step (Hilal et al. 2011; Tagliabue et al. 2014; Tang et al. 2017). The size of BSRs is the primary factor affecting process performance. The adsorption rate of boron tends to increase and pressure decrease with increasing particle size when fine BSRs are used. The pressure drop increment inherent to this process requires higher energy consumption; however, in the AMF, the pressure drop is not dependent on the BSR particle size, but is rather a function of membrane resistance. It follows that BSR size could be reduced to improve process performance and the reduced quantity of BSR would in turn reduce the cost (Koltuniewicz et al. 2004). A challenge is that commercial BSR bead sizes between 300 and 500 μm are too big for use in AMF, so BSR development requires a maximum diameter of 50 μm (Wolska and Bryjak 2013). Thus, newer monodispersed selective ion exchange resins might be regarded as an alternative to commercial resins (Samatya et al. 2012). In addition, the properties of the membrane in the AMF process are important. Membranes should be hydrophilic to reduce fouling while decreasing water transport resistance over the membrane and minimizing any decrease in permeate flow. On the other hand, since acids and bases are used in desorption and regeneration, membranes must be resistant to these harsh conditions. Certain membranes like Teflon, PVDF, and PP are used because of their wide operational pH ranges (Güler et al. 2011a; Darwish et al. 2017; Kabay et al.

2006). Ceramic membranes and submerged hollow fiber membranes can also be considered as alternatives. Ceramic membranes are expensive, but submerged hollow fiber membranes require lower energy inputs (Guo et al. 2005). Yilmaz et al. (2006) used 0.4 μm PP submerged hollow fiber membranes, which require only a low suction pressure, making it less energy demanding than cross-flow microfiltration. The authors also found that CRB02 is more suitable than XUS-43594.00 for the AMF process due to its faster boron sorption kinetics and more rapid establishment of a stable state (Yilmaz et al. 2006). Boron removal from geothermal water by AMF was also tested with submerged MF or UF processes. Different operational conditions were tested, and under optimal conditions, it was possible to reduce boron concentrations to below 1mg/L boron (Kabay et al. 2009, 2013).

2.4 Boron Recovery Techniques

Recovery means obtaining a usable final product, but there has been some confusion in the literature over the meaning of recovery, with certain removal and retention processes being described as recovery processes despite the lack of a (re)usable end product. For example, boron removal from water/wastewater is described by some researchers as recovery, but this separation of the pollutant from the water should instead be considered as removal. To be named recovery, a usable product/raw material must be obtained at the end of the process and the cycle must be closed (Figure 2.9).

As with removal processes, the starting point for recovery is a concentrated stream or source of contaminants that must be purified and/or turned into a usable product. Although it is sometimes referred to as recovery, these purification methods are those of concentration or removal. Chemical methods are mainly used for the recovery of boron that is concentrated or removed with different media. For this reason, when studies in the literature are examined, the number of studies that truly address processes for recovery is quite small. But due to the increasing population and industrial activities requiring resources, which are already finite, the importance of recycling an reuse is becoming correspondingly important and research and development in this area is urgently needed. The remainder of this review is dedicated to the summary of the few available studies on processes for boron recovery.

Figure 2.9 : Schematic of complete wastewater treatment steps for removal, recovery, and reuse.

2.4.1 Adsorption

Adsorption is one of the methods used for boron removal and also recovery. Granular activated carbon (GAC) is a well known and widely used adsorbent for contaminant removal. Zelmanov and Semiat (2014) went a step further than removal and also used GAC for boron recovery by combining the GAC with iron oxide/hydroxide nanoparticles (NanoFe) and NanoFe adsorbent (Zelmanov and Semiat 2014). In the first series of experiments with NanoFe, removal and recovery of 1 and 10 mg/ dm^3 boron were investigated over pH ranging from 6 to 10.5. Concentrations of 30 mg/dm^3 NanoFe and 135 mg/dm^3 NanoFe adsorbent were used for the 1 mg/dm^3 and 10 mg/dm^3 boron concentrations, respectively. A pH 8 range of 8.1–8.3 was selected as optimal for boron adsorption. In the second series of experiments, Fe-impregnated GAC was employed to remove and recover boron at an initial concentration of 10 mg/dm^3 over pH ranging from 7 to 10, with optimal boron adsorption occurring between pH 8.1 and 8.3. Adsorbed boron on NanoFe and Fe-impregnated GAC was then recovered. Increasing pH values to 11–12.5 increased the boron recovery efficiency up to 95–98% while recovering Fe-impregnated GAC particles. By precipitating borates with cations like Ca^{2+}, a concentrated solution with a high pH value may be recovered. The authors indicated that the use of NanoFe and Fe-impregnated GAC allows for recovery efficiencies of 95–98%. Lyu et al. (2017) used pyrocatechol (CL) and nitropyrocatechol (NCL) modified resins, (CL-RESIN and NCL-RESIN) for boron recovery. According to their results, a pH of 9.06 and 6.7 is optimal for boron recovery using CL-RESIN and NCL-RESIN, respectively, resulting in respective adsorption capacities of 0.7886 mmol/g and 0.7931 mmol/g (Lyu et al. 2017).

2.4.2 Boron selective resins

Boron selective resins (BSRs) were previously introduced in the section on boron removal techniques, but BSRs can also be used for recovery of boron. Kabay et al. (2004) used N-glucamine-type resins for boron removal from geothermal wastewater. The boron was then eluted using 5% H_2SO_4. To separate boron from H_2SO_4, Diaion WA30 resin was employed, using various conditioning steps. To see the effect of pH on the separation of boron from H_2SO_4, pH 0.31, 1.0, and 2.0 were tested. The pH of 5% H_2SO_4 was 0.31, and pH was adjusted to 1.0 and 2.0 by $CaSO_4$ precipitating from H_2SO_4 after addition of $Ca(OH)_2$. The authors reported that the ion exchange method for boron separation from H_2SO_4 was not very effective on its own and proposed a subsequent precipitation step followed by further crystallization (Kabay et al. 2004). Diaion CRB05 resin was used by Jung and Kim (2016) for boron recovery from seawater containing 4.43 mg/L boron. In addition, they used H_2SO_4 and HCl for boron desorption. After desorption, a 0.45 μm membrane filter was used, resulting in 89% and 91% boron desorption for 0.05 M H_2SO_4 and 0.25 M HCl, respectively (Jung and Kim 2016). Figueira et al. (2022) used Purolite S108, Diaion CRB03, and CRB05 for boron recovery from seawater desalination plant brine. They reported CRB03 as the best option with a high recovery ratio of 98% (Figueira et al. 2022). Amberlite IRA473 and mixed resin (Dowex 50Wx8 and Ion exchanger II resins) were used to extract and purify the boron by Wang et al. (2010), who reported 102% boron recovery. According to their findings, Amberlite IRA 473 in combination with mixed resin is more effective than Amberlite IRA 473 alone (Wang et al. 2010).

2.4.3 Electrocoagulation and hydrothermal mineralization

Henry Ezechi et al. (2015) used produced water for the recovery of 15 mg/L boron from water treated over a 90 min contact time, at 12.5 mA/cm^2 current density and pH 7, which allowed for 97.6% boron removal by EC. The boron in the flocs obtained from this part of the study was recovered by hydrother- mal mineralization at an 87% boron recovery efficiency (translating to a residual boron concentration of 1.6 mg/L). The recovered hydrated borate compounds can be employed in borax manufacturing as the initial raw material (Henry Ezechi et al. 2015). Isa et al. (2014) also investigated EC and hydrothermal mineralization methods for the removal and recovery of boron from wastewater. The EC process was carried out at pH 7 with a current density of 12.5 mA/ cm^2, over a 90 min contact time; these were reported as optimal conditions

by which 98% of boron was removed. The flocs formed from EC were used for boron recovery by hydrothermal mineralization, achieving recovery of 91.4% boron (Isa et al. 2014).

2.4.4 Hydrothermal treatment

Itakura et al. (2005) investigated the hydrothermal treatment technique for boron recovery as the recyclable precipitate $Ca_2B_2O_5.H_2O$. For synthetic wastewater containing 500 ppm boron, it was possible to reach 99% recovery efficiency under optimal hydrothermal conditions (130 °C, 14 h). The authors indicated that the precipitate can be employed in the manufacturing process of borax as a raw mineral (Itakura et al. 2005). Tsai and Lo (2011) also used $Ca(OH)_2$ and phosphoric acid to remove and recover boron from wastewater. They compared the microwave (MW) hydrothermal method to a conventional heating (CH) method at temperatures between 55 and 130 °C. With increasing reaction temperature, the diffraction peaks of $Ca_2B_2O_5.H_2O$ increased and stabilized after 130 °C, so this was chosen as the reaction tem- perature. Due to the dependance of boron recovery efficiency on pH, they reported results for pH 6–13. pH values higher than 11 raised efficiency, which peaked at 90% for pH 13 and a 10 min reaction time. $Ca(OH)_2$ usage in the MW method resulted in 90% boron recovery efficiency and $Ca_2B_2O_5.H_2O$ crystals were formed. With the addition of phosphoric acid in the MW method, recovery efficiency of boron reached 99% for a 10 min reaction time where $CaHPO_4.H_2O$, $CaHPO_4$, and $Ca_{10}(PO_4)_6(OH)_2$ were formed. Other ions like fluoride, nitrate, and sulfate also affect the recovery efficiency, with high concentrations of these ions retarding the recovery of boron (Tsai and Lo 2011). Pretreated waste oysters and clam shells were used as mineralizers to remove and recover boron in a study conducted by Tsai et al. (2011), and a microwave hydrothermal method was used for mineralization and recovery (Tsai et al. 2011). With a 10 min reaction time, they reached a 95% boron recovery efficiency. Pretreated oyster shells were found as an effective mineralizer for boron recovery from concentrated wastewater.

2.4.5 Solvent extraction

Solvent extraction is a promising method par- ticularly applicable to boron recovery from high boron content liquor. Diols, triols, and polyols with somewhat long aliphatic chains and limited water solubility have often been considered for boron extraction.

This method can be categorized into three classes, (1) physical extraction, (2) non-ionic ester complex extraction, and (3) extraction by borate salts complex. Extractants of groups (2) and (3) are appropriate for the extraction of boron from acidic and alkaline solutions, respectively. Hydroxyl compounds—and particularly 1.3 diols—are believed to be most efficient for boron extraction (Matsumoto et al. 1997). Kwon et al. (2005) used 2-butyl-2-ethyl-1,3-propanediol (BEPD) in 2-ethylhexanol (EHA) as an organic solvent, circulated via an extraction unit to the stripping unit. Boric acid solution was then fed to the extraction unit, and the KOH solution as the stripping phase was circulated in the stripping unit. The pH was maintained at 10.5 and a continuous boron recovery as a crystal was performed successfully at high boron concentration (Kwon et al. 2005). Mohapatra et al. (2008) conducted boron recovery experiments with 2,2,4- trimethyl-1,3-pentanediol ($C_{16}H_{30}O_4$) in carbon tetrachloride as an extractant. The effect of cations/anions, initial boron, extractant concentration, pH, and contact time were investigated. The authors reported 95.6% boron recovery at optimal operational conditions (Debasish Mohapatra et al. 2008). At pH 2, 96.8% boron recovery was achieved for the single extraction stage with 2,2,5-Trimethyl-1,3-hexanediol by Karakaplan et al. Various concentrations of NaOH were also tested, and 96.7% boron recovery was achieved with a single stripping stage using 0.1 M NaOH (Karakaplan et al. 2004). A novel extractant (2-butyl-1-n-octanol dissolved in sulfonated kerosene) was used by Peng et al. (2018) for boric acid recovery from salt lake brines. In the presence of $AlCl_3$, $MgCl_2$, and NaCl, the salting-out effects of the extraction process were examined, and the presence of Na^+, Mg^{2+}, and Al^{3+} cations in the aqueous phase demonstrated a favorable impact on the extraction of boric acid. Salting-out effects on boric acid extraction followed an efficacy gradient of $AlCl_3$ > $MgCl_2$ > NaCl. The authors used water as a stripping agent for boric acid recovery from the loaded organic phase. The total boric acid recovery of over 98% and product purity were achieved after a six-stage counter-current extraction and stripping processes (Peng et al. 2018).

2.4.6 Chemical precipitation

Chemical precipitation is a simple and economical method for boron recovery. The hydrothermal process recovers boron as borate ores but needs high temperature and pH values. With hydrogen peroxide addition, boric acid can be recovered as perborate salts via chemical oxo-precipitation (COP) (Lin et al. 2016). Lin et al. (2016) used

$Ba(OH)_2$ as a precipitant at ratios of 2 and 1 for H_2O_2/B and Ba/B, respectively. The boron was recovered as barium perborate salts with an efficiency of 99.7%. The boron was reduced to 3 ppm from 1000 ppm at pH 10.5 over a 4 h reaction time (Lin et al. 2016). However, precipitation could be unpracticable due to the nonquantitative precipitation of different boron compounds.

2.4.7 Bipolar membrane electrodialysis

The bipolar membrane electrodialysis (BMED) process was developed to divide an aqueous saline solution into its respective acid and base with no external addition of solvent needed. This approach has been documented as a sustainable and clean process (Bunani et al. 2017; İpekçi et al. 2018; Sun et al. 2020). Due to its capacity to generate proton and hydroxyl ions of water molecules at hydrophilic contact under a direct current, a bipolar membrane is particularly important in the process of electro membrane removal. Because of the bipolar membrane, the BMED process provides an acid base for the fresh product in various compartments. During the BMED operation, boron is removed as H_3BO_3, but boron recovery is possible only when boron is found as $B(OH)_4^-$. Bunani et al. (2017) investigated the effects of process conditions like applied potential, sample volume, and pH on the recovery of boron via BMED. They reached 78.8% boron recovery at pH 12.25, which is in contrast to recoveries of 70.9% at pH 10.25 and 63.7% at pH 9.25 (Bunani et al. 2017). İpekçi et al. (2018) investigated the effect of different acid and base solution types, concentrations, and electrical potential on the recovery efficiency of boron by BMED. A maximum of 50% boron recovery was achieved under optimal conditions (30 V, 0.05 M HCl-0.05 M NaOH) (İpekçi et al. 2018). Boron recovery in the acid compartment of BMED system can be repre- sented in Equation 2.6.

$$B(OH)_4^- + H^+ \rightleftharpoons H_3BO_3 + H_2O \text{ (in the acid compartment)} \quad (2.6)$$

The authors observed that the initial electrical conductivities in the acid and base compartments were of more significance than the starting concentrations. Recovery could then be increased by the increased electrical potential and by increased specific power consumption, according to their results (İpekçi et al. 2018). The membrane type and sample solution flowrate are other process parameters that affect the recovery of boron by BMED (İpekçi et al. 2020). A 59% boron recovery efficiency was achieved with heterogeneous ion exchange membranes for an initial boron concentration of 812

mgB/L under optimal conditions (3 mM HCl-3 mM NaOH, 25 V, 50L/h of sample solution flow rate). Simultaneous removal and recovery of boron by multi-step BMED from wastewater was demonstrated by Noguchi et al. (2018) using electrodialysis in a semi-batch mode (Noguchi et al. 2018). The apparatus comprised a stack of five BPM-AEM-BPM, acting to increase boron concentration until sufficient to recover boric acid. Boron concentration in diluate was below 10 mg/L versus 10,000 mg/L in the concentrate solution, thereby allowing for boric acid recovery from effluent. Hung et al. (2022) also studied simultaneous removal and recovery of boron with improved BMED. They used continuous and intermittent BMED modes and indicated that increasing the initial pH decreases the boron removal rate while increasing the mass transfer rate. The boron removal and recovery rates were 98.6% and 86.5%, respectively, for pH 9.5–10.5 and under 12 V (Hung et al. 2022).

2.4.8 Reverse osmosis

RO processes can be used for both boron removal and recovery, but conventional cellulose acetate membranes can achieve only 30% boron rejection. Liang (2005) used a thin-film polyamide RO (tf-PA RO) membrane for boric acid recovery and silica removal. Boron rejection increased up to 60% with the tf-PA RO membranes, and the authors reported that the boron waste quantity after this treatment was expected to be less than 1.5%, the silica concentration less than 1 ppm, and that the boron could be reused (Liang 2005). Bartova et al. (2016) used different commercial PA RO membranes for the recovery of boric acid from a nuclear power plant followed by reuse of the final product at the facility. Feed solution pH, which strongly affects separation efficiency, ranged from 5.2 to 11.2, and H_3BO_3 concentrations ranged from 1 to 20 g/L. They indicated that 40 g/L of H_3BO_3 is needed for reuse at nuclear power plants. It was possible to concentrate H_3BO_3 to a maximum of approximately 93 g/L at high pH, according to their results (Bártová et al. 2016).

Dydo and Turek (2014) investigated the ED-RO integrated system for boron recovery and removal simultaneously. They used ED for the first step to desalinate the boron-containing water, followed by RO for concentration. The wastewater used in this study contained 75 mg/L boron, which was concentrated to more than 10.8 g/L in the retentate during the second stage RO (Dydo and Turek 2014). Before the RO step, diluates were alkalized to pH 10 and mono and dichelate complexes of boron with polyol were formed and the boron-rich alkaline solution was neutralized using strong

mineral acid to form solid boric acid crystals. After the separation of solid and liquid, the supernatant was recirculated back to the ED desalination step, where RO could achieve higher than 80% recovery of boron and lower than 1 mg/L permeate boron.

2.4.9 Membrane distillation

Membrane distillation (MD) uses temperature difference as a driving force, as explained in Section 2.3.5.5 With the help of hydrophobic membranes, which permit volatile materials to pass through and exclude non-volatile materials, MD can be described as a purification process. Depending on feed water characteristics and intended use, it is possible to name this process a recovery. However, if only the boron compound is needed, an additional procedure must be applied to the concentrated feed water, such as crystallization, evaporation, or precipitation. Recovery of certain salts and metals by the additional process following MD has been studied in the literature (Quist- Jensen et al. 2016; Naidu et al. 2018; Choi et al. 2018, 2019; Park et al. 2020).

Jia et al. (2017) applied vacuum membrane distillation crystallization (VMDC) to radioactive wastewater for the recovery of boric acid. The impact of the initial boric acid concentration (0.5–100 g/L) on the rejection ratio was tested. After the concentration of feed water by VMD at 70 °C, the concentrate was collected in the crystallization tank. The feed solution cooled down to 20 °C for the crystallization of boric acid since boric acid solubility decreases as temperature rises. After crystallization was completed, the concentrated solution was filtered to collect the boric acid crystals. At 70 °C, 50% boric acid recovery was achieved using single-stage VMDC, and the purity of the recovered boric acid was found to exceed 99% (Jia et al. 2017).

2.5 Conclusion

Boron is one of the most important elements for humans, plants, and industries. Previous reviews have covered some of the processes for boron removal, but a synthesis of the research on boron recovery was not available at the time this review was prepared. This review is the first to summarize boron recovery techniques and the first to examine processes for boron removal and recovery together. Research in these areas has focused on the effect of operational parameters and on the development and testing of new materials for efficient and cost-effective removal and recovery of boron

from water. Both conventional techniques (e.g., precipitation, coagulation/electrocoagulation, ion exchange, adsorption) and membrane processes (e.g., RO, MD, FO, BMED, SLM, hybrid) were discussed in detail. Conventional processes are better known but sometimes inefficient or ineffective. Membrane processes have gained attention due to advantages such as elimination of chemical addition, little to no sludge production, ease of operation, and lower overall footprint. Studies on boron removal currently vastly outnumber those on boron recovery. More emphasis on recovery is needed in the literature to support efforts to minimize waste and promote sustainability.

3. BORON REMOVAL BY USING VACUUM ASSISTED AIR GAP MEMBRANE DISTILLATION (VAGMD)[2]

3.1 Introduction

Membrane distillation (MD) is an emerging membrane technology that is based on conventional distillation combined with membrane separation. The driving force is the vapor pressure difference between feed and distillate solutions. This vapor pressure difference causes evaporation along the hot side; vapor molecules that passed through membrane pores are condensed when they interact with the cold side. It is possible to obtain highly pure water and highly volatile components from the feed solution in one step. Generally, hydrophobic microfiltration membranes are used for the MD process to let the vapor transport through membrane pores while the water is returned. MD has four basic configurations; 1)Direct Contact Membrane Distillation (DCMD), 2)Air Gap Membrane Distillation (AGMD), 3)Vacuum Membrane Distillation (VMD), 4)Sweep Gas Membrane Distillation (SGMD) (González et al., 2017; Z. Liu et al., 2017; L. Sun et al., 2015).

DCMD is the most commonly used configuration of MD because of its simplicity to operate. Due to the direct contact between the membrane, permeate and feed solutions heat loss is higher than the other configurations (González et al., 2017; Naidu et al., 2017; Puranik et al., 2019). In SGMD configuration a cold sweep gas between the membrane and the cold surface is used. SGMD is more complex and difficult to use so there is limited usage of this configuration (González et al., 2017; Z. Liu et al., 2017). Vacuum pressure is applied to the distillate side in VMD configuration. Because of the mass transfer resistance of the boundary layer and lower heat loss, VMD has higher flux than the other configurations, which makes it an appealing option, especially for use in industry. However, it is more prone to membrane wetting

[2] This chapter is based on 'Oyku Mutlu Salmanli, Ayse Yuksekdag, Ismail Koyuncu (2022), *Boron removal by using vacuum assisted air gap membrane distillation (VAGMD)*, Environmental Technology&Innovation, http://dx.doi.org/10.1016/j.eti.2022.102395'

owing to vacuum conditions and membrane fouling when compared with other configurations (M. A. E.-R. Abu-Zeid et al., 2015; González et al., 2017; L. Sun et al., 2015). AGMD is the air gap added version of DCMD. Due to the lower heat loss than DCMD, AGMD is one of the most preferable and most widely used MD configurations.

AGMD is assumed to be the most promising MD configuration in terms of heat recovery due to the vaporization and recovery of the latent heat of condensation in the module simultaneously. But the air gap causes a higher mass transfer resistance which results in flux decrease. Although AGMD is assumed to be the promising configuration of MD technology, its production per membrane area is lower than the DCMD configuration (Cheng et al., 2009; Z. Liu et al., 2017). Water vapor pressure decreases when the non-volatile concentration increases in the solution fed to the module which causes decreasing in the permeate flux also (Khayet & Matsuura, 2011a). On the contrary, due to the design of the AGMD module, the permeate is condensed on a cold surface instead of on a membrane surface so AGMD can be used in areas that usage of DCMD is limited (Asghari et al., 2015; El-Bourawi et al., 2006).

Non-condensable gases are the gases dissolved in the feed solution such as air, carbon dioxide, and other gases. These gases are absorbed into the membrane pores and pass to the permeate solution as well. Because of the presence of these gases that reduces the condensation in the feed solution, vapor diffusion of water is decreased which results in decreasing permeate flux (Khayet & Matsuura, 2011a; Z. Liu et al., 2017; Naidu et al., 2017). By lowering the air gap pressure until it is equal to the water vapor pressure the permeate flux of AGMD increases. Removal of these non-condensable gases which are responsible for the main mass transfer resistance improves the permeate flux compared to the AGMD at atmospheric pressure (Alsaadi et al., 2015; El Amali et al., 2004; Guijt et al., 2005).

There are studies about boron removal by using MD technology in the literature. Boubakri et.al. studied boron removal with DCMD. They used different boron concentrations from 2 to 200 mg/L. They observed that the permeate boron concentration was below 0.8 mg/L. It was lower than the limit value of 2.4 mg/L imposed by WHO for potable water. They reported the calculated flux value according to the Knudsen-molecular model and experimental flux was stable at 11 kg/m^{2}h. They also used seawater for boron removal by DCMD. The initial boron concentration was

5.37 mg/L and the maximum permeate boron concentration was 0.47 which is below the limit value recommended for drinking water by WHO (Boubakri et al., 2015a). In the study conducted by Wen et.al., the boron removal from highly saline radioactive wastewater by DCMD was investigated. The permeate boron concentration remained below 2 mg/L and the rejection factor was higher than 99.97% (Wen et al., 2016). Hou et. al. used DCMD for desalination and boron removal of 4.65 mg/L boron contained seawater. They reported the boron concentration kept below 20 μg/L and salt rejection over 99.9% (Hou et al., 2013a). There are a few studies about VAGMD in the literature but there is no study about the removal of boron by using VAGMD which encouraged us to make this study. Andrés-Mañas et. al. conducted VAGMD configuration by using pilot-scale modules and reported that they increased permeate flux up to 234% (Andrés-Mañas et al., 2020). Abu-Zeid et al. used different salt concentrations up to 44825 ppm and compare the non-vacuum and vacuum-assisted AGMD. They also reported the vacuum integration to the air gap membrane distillation improves the permeate flux due to the removal of non-condensable gases (Abu-Zeid et al., 2016). Liu et al. also studied VAGMD and investigated the effect of some parameters on optimal vacuum pressure (Liu et al., 2017). Summary of VAGMD studies were listed in Table 3.1.

Table 3.1 : Summary of VAGMD studies from the literature.

Feed water	Membrane Material	Vacuum Pressure	Flux	GOR	SEC	Scale	Reference
Saline solution	PTFE	0 – 0.01 MPa	4.37 – 11.87 kg/(m^2.h)	0.48 – 1.28	NA	Lab scale	(M. A. E.-R. Abu-Zeid et al., 2016)
Tap water	PVDF	0 – 0.1 MPa	3 – 15 kg/(m^2.h)	1 – 6.5	125 – 300 (kWh/m^3) (EE)	Lab scale	(Z. Liu et al., 2017)
Saline solution	NA	150 – 200 mbar	~0 – 8.5 L/m^2.h	1.4 – 13.5	100 – 900 (kWh/m^3) (TE)	Pilot-scale	(Andrés-Mañas et al., 2020)
Synthetic saline wastewater	PVDF (PAC addition)	0 – 0.8 bar	5 – 22 L/m^2.h	NA	NA	Lab-scale	(Y. Kim et al., 2020)

*EE: electrical energy, TE: thermal energy

The AGMD and VAGMD configurations were used in this study to remove boron which is an important element with usage in various fields from various water sources. Different vacuum pressures were compared to observe the effect of pressure on the

VAGMD process. Both NaCl solution and synthetic boron solution were also used to determine the process efficiency in terms of conductivity and boron removal. In this context, six different commercial flat sheet membranes were used. The effect of vacuum pressures was investigated in terms of permeate flux, salt removal efficiency, and boron removal efficiency. According to the results of this study, it is clear that VAGMD could be used successfully for the treatment of waters containing boron by utilization of its higher flux and gained output ratio (GOR) whereas lower energy consumption which reduced the costs.

3.2 Material Methods

3.2.1 Material and equipment

Commercial membranes used in this study were polyvinylidene fluoride (PVDF), polytetrafluoroethylene (PTFE), and polypropylene (PP). PVDF and PTFE were purchased from Sterlitech while PP membranes were supplied from GE Water. Two different pore sizes were selected for each membrane. The properties of membranes was taken from a supplier can be seen in Table 3.2. The contact angle of membranes was measured by using the sessile drop technique with KSV Attension Theta branded contact angle meter. Distilled water was used to determine the contact angles of membranes. Water was dropped onto the straight membrane surface via a microsyringe. At least, five measurements were conducted for each membrane sample and the values were averaged. Liquid entry pressure (LEP) analysis was conducted by using Quantachrome 3G Porometer using DI water similar to the literature. Air pressure was increased gradually till liquid passed through the membrane. At this inlet pressure, the flow rate of the gas is recorded by the sensors, and the corresponding pressure is recorded as the liquid inlet pressure (Ahmed et al., 2017).

Table 3.2 : The properties of commercial membranes.

Membrane Type	Pore size (µm)	Membrane thickness (µm)	IPA Bubble Point (psi)
PTFE	0.22	102-152	>20
PTFE	0.45	76-127	>10
PVDF	0.22	140-250	40-60
PVDF	0.45	140-250	25-40
PP	0.20	110	15.0
PP	0.45	110	11.0

Boron concentration of both feed and permeate water measured via ICP-OES Optima 7000. Five-points, at least, calibration done by using 1000 ppm B (Inorganic Ventures) solution and 3% HNO_3. R^2 coefficient is higher than 0.999. Each sample was measured three times.

3.2.2 Experimental setup

The experimental setup was given in Figure 3.1. Vacuum pressure was applied to the permeate side thereby enabling the convective transport process. Thanks to the hydrophobicity of the membrane liquid transport were not permitted to the membrane pores and a liquid-vapor interface occurred. Vacuum pressure was created by a vacuum pump. Feedwater was heated to 70 °C by using a heating bath and circulated via a peristaltic pump which has a 1.4 L/min flow rate. Cooling water which is 20 °C flowing of 480 mL/min rate from cooling bath was used to cool membrane module which has 7 mm air gap width for fixing the vacuum line and hydrophobic flat sheet membrane that has a 44.18 cm^2 active area located in the middle of the module. Because of the inserting of the vacuum pipeline into the module the air gap width had to be chosen 7 mm the minimum. The membrane module was tested both in the air gap and vacuum-assisted air gap configurations. 5 different vacuum pressures were applied 0 bar (AGMD), 0.02 bar (VAGMD), 0.04 bar (VAGMD), 0.06 bar (VAGMD), and 0.08 bar (VAGMD) and 3 different water samples were tested for both configurations (salty water, synthetic water, and geothermal water). NaCl was used for the preparation of salty water and boric acid (H_3BO_3) and sodium bicarbonate ($NaHCO_3$) purchased from Merck, was used for the preparation of synthetic boron solution. Geothermal water was supplied from a geothermal energy plant from Turkey. The characteristic of geothermal water was shown in Table 3.3 as given in the previous study. The boron content of geothermal water was 60.8 mg/L and conductivity was 5.6 mS/cm. Flux values of membranes were recorded by using a computer connected to a scale through 4 different vacuum pressures. Conductivity meters measured the conductivity of both feed and permeate water for determining the removal efficiencies. The boron content of the samples was analyzed using the ICP-OES.

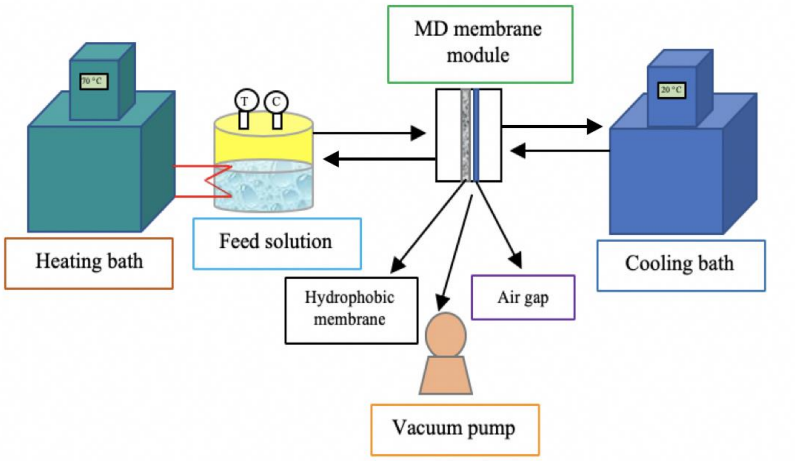

Figure 3.1 : Experimental setup of VAGMD.

Table 3.3 : Characteristic of geothermal water.

Parameter	*Value*	*Parameter*	*Value*
pH	7.67	PO_4^{3-}	41.60 mg/L
Conductivity	5.6 mS/cm	SO_4^{2-}	514.13 mg/L
Na^+	3622.20 mg/L	F^-	9.17 mg/L
K^+	335.95 mg/L	NO_3^-	108.45 mg/L
Ca^{2+}	41.22 mg/L	B	60.84 mg/L
Mg^{2+}	8.32 mg/L	Si	113.7 mg/L
Li^+	6.46 mg/L	Fe	0.096 mg/L
NH_4^+	117.85 mg/L	Mn	-
Cl^-	3297.19 mg/L	As	0.237 mg/L

3.2.3 Theoretical background

Water flux (J) and removal efficiency (R) is mainly used to characterize the performance of VAGMD. J ($Lm^{-2}h^{-1}$) depicts the production capacity of MD and was calculated by the following equation (M. A. E.-R. Abu-Zeid et al., 2016);

$$J=\frac{\Delta m}{A.\Delta t} \quad (3.1)$$

Where Δm is the amount of the permeate water (kg), A is the effective surface area of membrane used in the membrane module (m^2) and Δt is the operating time (h). Permeate flux J is proportional with the vapor pressure difference across the membrane (M. A. E.-R. Abu-Zeid et al., 2016; Alsaadi et al., 2015; Naidu et al., 2017);

$$J_m = C_m . \Delta P_m \quad (3.2)$$

Cm is the permeability coefficient, Pm is the vapor pressure difference across the membrane.

The water vapor pressure (*P*) can be calculated from the Antoine equation for different temperatures (*T*) (Pangarkar et al., n.d.; L. Sun et al., 2015);

$$P = \exp\left(23.1964 - \frac{3816.44}{(T+273.15)-46.13}\right) \quad (3.3)$$

the removal efficiency of both salt and boron are calculated using the following equation;

$$R(\%) = \left(1 - \frac{c_p}{c_f}\right) x100 \quad (3.4)$$

Where the C_f is the concentration of feed solution and C_p is the concentration of permeate solution.

Gained output ratio (GOR) was also used to evaluate the performance the of VAGMD system. GOR is the energy ratio of heat of evaporation to the input thermal energy (H. Lee, 2002; Z. Liu et al., 2017) ;

$$GOR = \frac{J.S.\Delta H}{Q C_{pf}.(T_i - T_o)} \quad (3.5)$$

Where Q is the flow rate(L/h), T_i and T_o are the hot feed inlet temperature and cold feed outlet temperature (°C), C_{pf} is the heat capacity of feed solution (kJ / kg.°C), S is the effective surface area of membrane (m^2), ΔH is the evaporation enthalpy of feed solution (kJ/kg) can be calculated by using the following equation;

$$\Delta H = 2258.4 + 2.47(373 - (T + 273.15)) \quad (3.6)$$

Where T is the mean temperature of the feed solution inside the module (°C).

Specific energy consumption (SEC) could be calculated by dividing the energy consumption for vacuum energy during the operation time by the volume of distillate (kWh/m^3) (M. A. E.-R. Abu-Zeid et al., 2016; Dow et al., 2016; Z. Liu et al., 2017) Since all other parameters are the same for both configurations (AGMD and

VAGMD), constant energy consumption was assumed and calculated only the extra energy required by vacuum for VAGMD;

$$SEC = \frac{EC}{W} \tag{3.7}$$

Where EC represents the vacuum energy consumption, KWh. The vacuum pump's energy consumption remained practically constant, at around 100W.

3.3 Results and Discussion

Commercial membranes were characterized in terms of contact angle, liquid entry pressure (LEP), and scanning electron microscope (SEM) analysis. Contact angle results display the hydrophobicity of the membranes that were used (Table 3.4). Since hydrophobicity increases with increasing contact angle, we can say that the most hydrophobic membrane was PTFE 0.22 membrane. PVDF membranes have the lowest contact angles compared to PP and PTFE membranes. Contact angles decreased with the increasing pore sizes for the same polymer-type membranes. This could be attributed to the membranes are more prone to wetting since larger pore sizes decreased the capillary pressure which prevents the liquid passage from membrane pores (Chamani et al., 2021). LEP values (Table 3.4) decreased while pore size increased and contact angle decreased. For a good performance MD membrane, the LEP value is expected to be as high as possible. Because as this value increases, the vapor passes through the membrane pores instead of water, and when this value decreases, water can escape from the membrane pores without evaporation even at low-pressure values. In general, it is known that smaller pore size, greater contact angle and surface tension increase the LEP value. PP and PTFE membranes have higher contact angle values and therefore have higher LEP values. SEM analysis results of membranes were reported in our previous study (Ozbey-Unal et al., 2018). According to these results, PVDF has a denser top layer which causes lower porosity while PTFE seems more fibrous. As can be seen in the experimental results, these differences directly affected the filtration performances.

Table 3.4 : Contact angle and LEP values of membranes.

Membrane	Contact angle (°)	LEP (kPa)
0.22 PTFE	130.87 ± 0.38	69.5
0.45 PTFE	121.39 ± 0.41	67.2
0.22 PVDF	115.19 ± 0.18	64.2
0.45 PVDF	110.29 ± 0.11	62.6
0.20 PP	127.38 ± 0.31	69.6
0.45 PP	122.13 ± 0.31	64.7

According to FT/IR results given in Figure 3.2, spectra of PP membranes have asymmetric C-H bands of $–CH_3$ (methyl) groups at 2970-2800 cm^{-1} . 1480-1380 cm^{-1} absorption bands are belonging to the C-H groups of CH_2 bonds. 1167, 997, 841, and 809 cm^{-1} signals belong to crystal shape configurations of PP (Tapiero et al., 2017). CF_2 symmetric and asymmetric bonds were observed at 1146 and 1202 cm^{-1} from the results of PTFE membranes (L. Li et al., 2008). When FT/IR spectra of the PVDF membrane were taken into account -OH groups were observed between 3500-3000 cm^{-1} wavelengths, H-O-H bonds were observed between 1629-1381 cm^{-1} wavelengths. Absorption bonds of C-F groups were observed at 1231 cm^{-1} wavelength (Ghasemian et al., 2017).

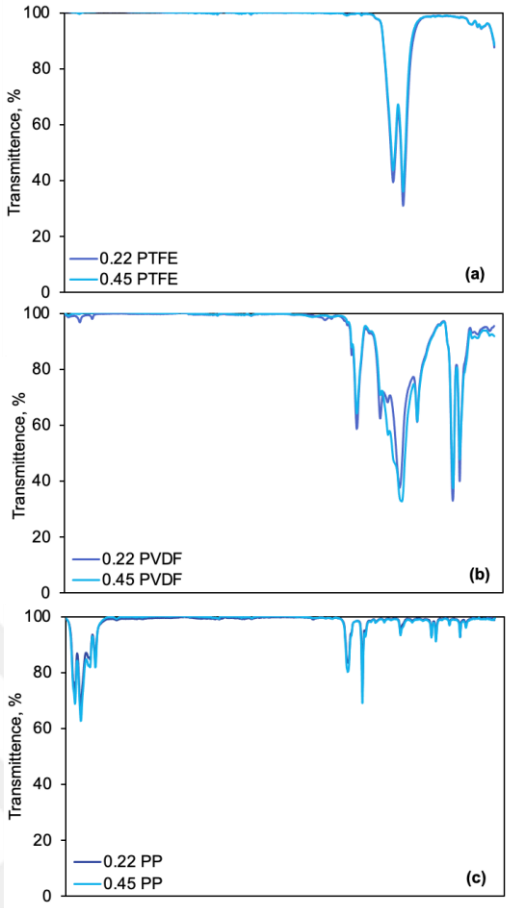

Figure 3.2 : FT/IR results of PP, PVDF, and PTFE membranes.

The NaCl solution was prepared and tested before testing synthetic and geothermal water sources in the AGMD and VAGMD systems to control the vapor transport and efficiency of the membranes. The conductivity of both feed and permeate was measured and removal efficiencies were calculated by using these values. Flux, GOR, and SEC values vs. vacuum pressures and removal efficiency graphs were drawn and given in Figure 3.3 and Table 3.5.

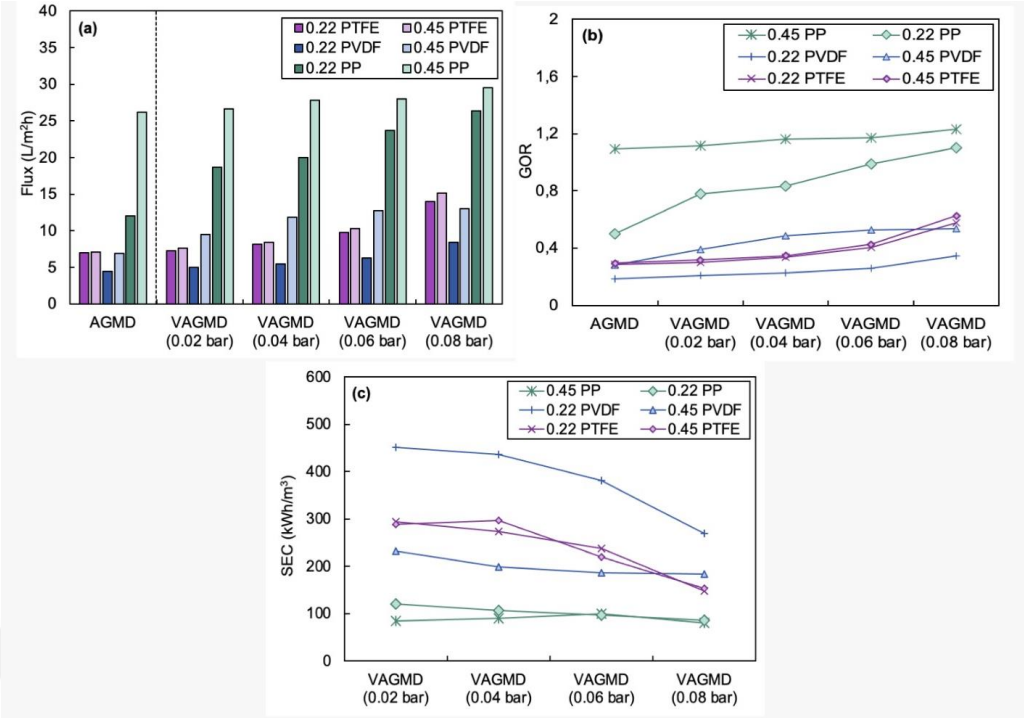

Figure 3.3 : . Flux (a), GOR (b) and SEC values (c) vs. vacuum pressures for NaCl solution.

Fluxes increased with the increasing vacuum pressure. The reason for flux increasing is explained due to the extraction of stagnant air in the pores by vacuum and thus accelerating the vapor transmission by reducing the vapor diffusion resistance across the membrane and enhanced total pressure gradient in the pore that increased convective mass transport (Naidu et al., 2017). Besides that, part of NCGs could be removed by applied vacuum therefore the mass transfer resistance decreased and flux increased. Furthermore, as Liu et al., (Liu et al., 2017) reported, the boiling point of water is precisely proportional to the ambient pressure, according to the Antoine equation. As a result, the vacuum pressure decreased the boiling point and encourages the formation of water vapor. SEC values showed that less energy was consumed for higher vacuum pressures. Due to the increasing amount of permeate water energy consumption decreased with the increasing vacuum pressures. Flux values also increased with the increasing pore sizes through all vacuum pressures. The penetration of vapor across membranes is enhanced by increased pore sizes according to the permeate flux equation by Lawson and Lloyd where the flux is proportional to the average pore radius (X. Chen et al., 2018; Lawson & Lloyd, 1997). Also the high vacuum degree in permeate side causes the increase of vapor pressure difference so it results in higher flux. The findings of previous studies confirmed these results (X.

Chen et al., 2018; F. Jia et al., 2017a; Y. Yang et al., 2017). Furthermore, it can be said that VAGMD fluxes were increased by increasing the vacuum pressure independent from membrane material. Apart from PP 0.45 membrane, flux values were almost 50% increased with 0.08 bar vacuum pressure as against AGMD. As it can be seen in Figure 3.3(b), GOR was lower than 1 for AGMD studies, as expected. Liu et al., (Liu et al., 2017) were also reported that GOR of conventional MD processes was found between 0.2 – 1. However, GOR was slightly increased and exceeded 1 by applying vacuum pressure in our study. Besides, GOR values also increased with the increasing J values. The rise in J means that the hot feed used more heat for evaporation requirement, and the cold feed could utilize the excessive vapor heat and hot feed which is the vapor anymore passing through membranes get lost its heat. As a result, the vapor tends to condense more and the J increment. Consequently, GOR also increased with the increment in J (Liu et al., 2017).

All removal efficiencies are higher than 98.7%. Li and Sirkar also obtained high removal efficiency of 93.2% with PVDF 0.45 μm membrane and 94.3% with PTFE 0.45 μm membrane in their study (Li & Sirkar, 2017). Zhang et al. also used PTFE membranes for desalination experiments via the VMD system. They reported that in all operating conditions the removal efficiencies are higher than 90% (Zhang et al., 2016).

Table 3.5 : Removal efficiency vs. vacuum pressures for NaCl solution.

Membrane	Conductivity removal efficiency (%)				
	VAGMD (0.08 bar)	**VAGMD (0.06 bar)**	**VAGMD (0.04 bar)**	**VAGMD (0.02 bar)**	**AGMD**
0.22 PVDF	99.7	99.8	99.6	99.7	99.7
0.45 PVDF	99.6	99.5	99.4	99.4	99.6
0.22 PP	99.3	99.6	99.3	99.6	99.8
0.45 PP	99.6	99.7	99.9	99.6	99.6
0.22 PTFE	99.5	99.2	99.4	99.0	98.8
0.45 PTFE	99.2	98.7	99.6	99.4	99.3

A synthetic boron solution which is 10 mg B/L was also used in this study to see the effectiveness of the VAGMD system to boron removal from water. Boron content and conductivity values of both feed and permeate water were observed. The flux, GOR, and SEC vs. vacuum pressures as given in Figure 3.4. Similar results with salt solution experiments were obtained in terms of flux and GOR increment with vacuum pressure.

The improved flux was caused by an increase in the pressure difference on the membrane and temperature polarization declining at the membrane surface on the side of the air gap by a vacuum pump (Abu-Zeid et al., 2016). The highest flux value was obtained for PP 0.45 μm membrane which is 29.8 L/m^{2}h. SEC results showed that specific energy consumption decreased with increasing fluxes due to the higher permeate weight.

Conductivity values were measured for both feed and permeate water and from these values, the removal efficiencies were calculated. The general trend for removal efficiency was decreased with the increase in vacuum pressures. We obtained higher than 98.2% removal efficiency for all membranes used in this study. Jia et. al. investigated the effect of boric acid concentration with the prepared synthetic solution on the VMD system at 70 °C temperature. They reported that they reached higher than 90% removal efficiency (Jia et al., 2017a).

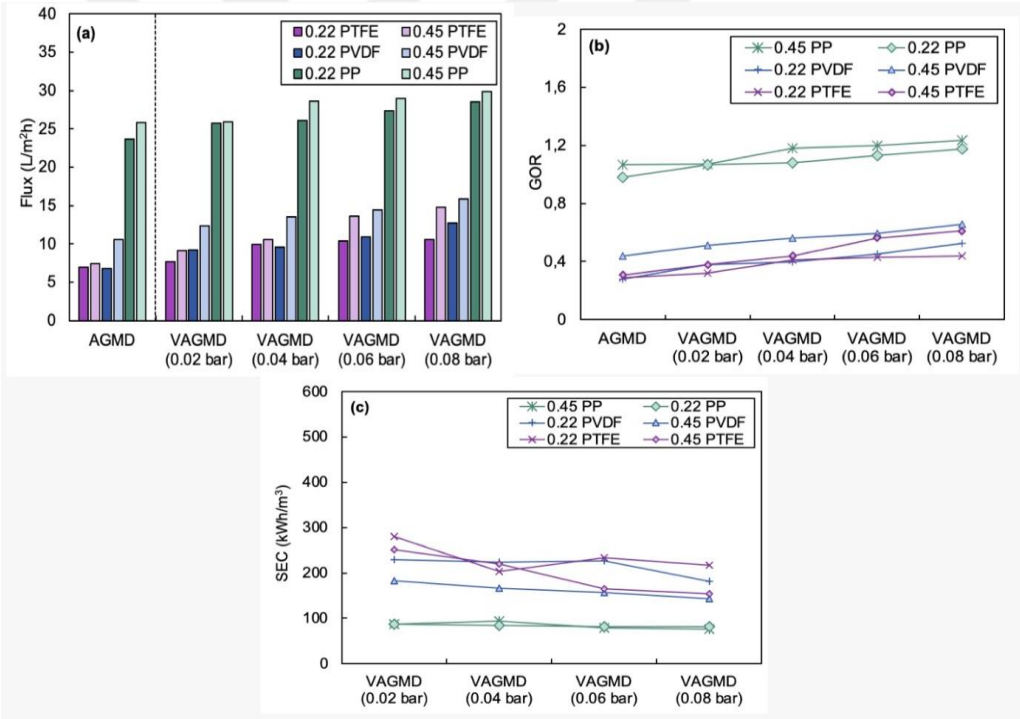

Figure 3.4 : Flux (a), GOR (b), and SEC values (c) vs. vacuum pressures for synthetic boron solution.

Table 3.6 : Removal efficiency vs. vacuum pressures for synthetic boron solution.

Membrane	Conductivity removal efficiency (%)				
	VAGMD (0.08bar)	VAGMD (0.06bar)	VAGMD (0.04bar)	VAGMD (0.02bar)	AGMD
0.22 PVDF	98.7	98.5	99.0	99.2	98.5
0.45 PVDF	98.8	99.5	99.6	99.2	99.2
0.22 PP	99.6	99.7	99.8	99.5	99.8
0.45 PP	99.2	99.1	99.4	99.5	98.2
0.22 PTFE	99.1	98.8	99.8	99.1	99.4
0.45 PTFE	99.2	98.8	99.4	99.5	99.0

Experiments carried out in the MD system using real geothermal water with commercial membranes were carried out with the air gap configuration and under vacuum pressures of 0.02-0.04-0.06 and 0.08 bar. During the experiments, the conductivity and the amount of boron were both monitored in the feed and permeate water. The flux-vacuum pressures graph of the experiments performed with real geothermal water was given in Figure 3.5.

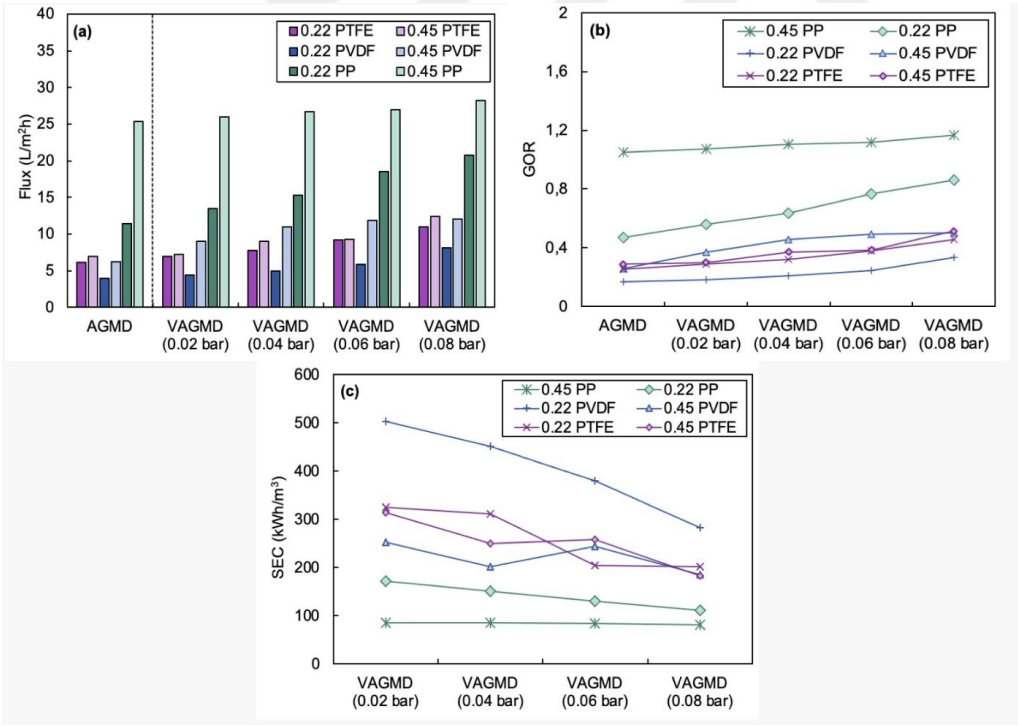

Figure 3.5 : Flux (a), GOR (b), and SEC values (c) vs. vacuum pressures for geothermal water.

Flux values increased with the increasing vacuum pressure from 0 to 0.08 bar for all membranes. Higher flux value obtained from 0.45 µm PP membrane as 28.2 L/m^2.h. When we look at the flux values between the two pore sizes for all membranes, the

flux values of the 0.45 μm pore-sized membranes were higher than the flux values of the 0.22 μm pore-sized membranes. The increasing pore sizes enhance the mass transfer that results in increased water flux (Liu et al., 2017). The flux values were slightly lower than the results of the experiments conducted with synthetic boron solution. The reason for this phenomenon is the water vapor pressure decrease with rising inlet salt concentration. According to Raoult's law increasing the salinity of feedwater reduces the partial vapor pressure and reduces the driving force. An additional boundary layer forms next to the membrane interface which is concentration polarization. When this concentration boundary layer together with the thermal boundary layer (temperature polarization), reduces the driving force which causes the decrease of permeate flux (Alkhudhiri & Hilal, 2017; Qtaishat et al., 2008; Safavi & Mohammadi, 2009a). For PP membranes with higher fluxes than other polymeric membranes, the rate of decrease in flux (PP 0.22 μm) was observed to be higher with the increase in the conductivity of the feed water and the reduction in the pore diameter at the same time. The conductivity removal vs. vacuum pressures graph of membranes was given in Table 3.7. Removal efficiencies were obtained higher than 98.7% for experiments carried out in this study.

Table 3.7 : Removal efficiencies vs. vacuum pressures for geothermal water.

Membrane	**Conductivity removal efficiency (%)**				
	VAGMD (0.08bar)	**VAGMD (0.06bar)**	**VAGMD (0.04bar)**	**VAGMD (0.02bar)**	**AGMD**
0.22 PVDF	99.3	99.2	98.9	99.0	99.2
0.45 PVDF	98.9	98.7	98.9	99.1	99.4
0.22 PP	99.0	99.1	99.1	99.1	99.8
0.45 PP	99.3	99.4	99.4	99.4	99.1
0.22 PTFE	99.5	99.7	99.5	99.3	99.2
0.45 PTFE	99.5	99.6	99.7	99.8	99.3

For geothermal water experiments, the amount of permeate boron was analyzed with ICP-OES. All boron concentrations were below 0.5 mg/L, the limit set by the World Health Organization for boron concentration of drinking water. Boron removal efficiency vs. vacuum pressures was given in Table 3.9. Higher than 99% removal efficiency was obtained for all membranes and configurations used in this study for geothermal water. There are a few studies about geothermal water treatment by using MD in the literature. For example, Sharbatly and Chaim studied geothermal water

treatment by using VMD. They reached a 6.56 kg/m^{2}h flux value with 0.22 µm PVDF membrane which is lower than our results. This difference may be due to the use of different configurations (Sarbatly & Chiam, 2013). Bouguecha and Dhahbi used fluidized bed crystallizer and AGMD for the treatment of geothermal groundwater. They used PP-supported membranes and investigated the effect of operating parameters on flow rate, temperature, and salt concentration. They reached a maximum of 7.5 kg/m^{2}h flux values. Our results are higher probably because of air gap width, membrane type, and MD configuration. El Amali et.al. studied geothermal and seawater desalination via AGMD and DCMD. They investigated the effect of the operating variables: feed temperature, air gap width, and feed flow. Their flux values were 3-5 kg/m^{2}h and salt rejection was 97% which is similar to our results (El Amali et al., 2004). The PP membranes showed higher flux values than PVDF and PTFE membranes for all types of feed waters. membrane thickness is an important parameter for membrane flux in MD since a thicker membrane reduces the heat transfer from the feed side to the permeate side. The membrane structure, on the other hand, lowers the ease of penetration, restricting transmembrane flow. Decreasing membrane thickness enhances the mass and heat transfer through the membrane. So the thicker membranes resulted in lower fluxes which are PVDF and PTFE (Eykens, Hitsov, et al., 2016; Swaminathan et al., 2018a; H. Y. Wu et al., 2014).

Boron contents of permeate water were analyzed using the ICP-OES. As seen in Table 3.8 and Table 3.9, boron removal efficiencies were higher than 99%. All permeate water boron concentrations were below 0.5 mg/L which is the limit value for drinking water accepted by World Health Organization.

Table 3.8 : Boron removal efficiency for synthetic boron solution.

	Boron removal efficiency (%)					
	0.22PP	**0.45PP**	**0.22PTFE**	**0.45PTFE**	**0.45PVDF**	**0.22PVDF**
AGMD	99.97	99.98	99.94	99.98	99.92	99.94
VAGMD(0.02bar)	99.97	99.94	99.97	99.96	99.97	99.97
VAGMD(0.04bar)	99.99	99.98	99.97	99.98	99.94	99.98
VAGMD(0.06bar)	99.98	99.97	99.96	99.97	99.94	99.98
VAGMD(0.08bar)	99.72	99.89	99.23	99.54	99.91	99.95

Table 3.9 : Boron removal efficiencies for geothermal water.

	Boron removal efficiency (%)					
	0.22 PVDF	**0.45 PVDF**	**0.22 PTFE**	**0.45 PTFE**	**0.22 PP**	**0.45 PP**
AGMD	99.79	99.68	99.67	99.24	99.52	99.68
VAGMD(0.02bar)	99.87	99.64	99.75	99.81	99.75	99.80
VAGMD(0.04bar)	99.87	99.45	99.77	99.81	99.75	99.79
VAGMD(0.06bar)	99.88	99.36	99.78	99.82	99.66	99.76
VAGMD(0.08bar)	99.78	99.21	99.72	99.75	99.65	99.73

Table 3.10 : Comparison of boron removal performances of various MD processes.

Feed water	**Process**	**Membrane material**	**Flux**	**Boron rejection**	**GOR**	**SEC**	**Ref.**
Synthetic boron solution	DCMD	PVDF	3 – 35 kg/m^{2}h	> 99.8%	NA	NA	(Hou et al., 2010a)
Seawater	DCMD	PVDF	47.6 kg/m^{2}h	> 99.5%	NA	NA	(Hou et al., 2013a)
Seawater	DCMD	PVDF	27.5 kg/m^{2}h	> 90.52%	NA	NA	(Boubakri et al., 2015a)
Radioactive wastewater	DCMD	PP	~20 L/m^{2}h	> 99.97%	NA	NA	(Wen et al., 2016)
Radioactive wastewater	VMDC	PP	2.98 – 6.90 L/m^{2}h	> 99.9%	NA	NA	(F. Jia et al., 2017a)
Synthetic surface water, RO brine	DCMD	PVDF	5 – 25 kg/m^{2}h	> 99.9%	NA	NA	(D. Han et al., 2017)
Synthetic and real geothermal water	AGMD	PVDF PP PTFE	5 – 30 kg/m^{2}h	> 99.5 %	NA	NA	(Ozbey-Unal et al., 2018)
Synthetic radioactive wastewater	VMD	Ceramic hydrophobic membrane	15 – 25 L/m^{2}h	~ 99.9%	NA	NA	(X. Chen et al., 2019)
Geothermal water	AGMD	PVDF - PTFE mixture-based nanofiber membrane	27.7 kg/m^{2}h	> 99.5 %	NA	NA	(Ozbey-Unal et al., 2020a)
Synthetic seawater	VMD PGMD AGMD	PTFE	3.21 kg/m^{2}h 4.23 kg/m^{2}h 5.86 kg/m^{2}h	> 99.2 %	NA	NA	(Alkhudhiri et al., 2020)

Table 3.10 (continued) : Comparison of boron removal performances of various MD processes.

Feed water	Process	Membrane material	Flux	Boron rejection	GOR	SEC	Ref.
Geothermal water	AGMD	Reduced graphene oxide (rGO)/PVDF nanofibrous membrane	19.20 – 30 L/m^2h	96.89 – 98.16 %	NA	NA	(Eryildiz, Ozbey-Unal, et al., 2021a)
Synthetic NaCl and B solutions, real geothermal water	VAGMD	PVDF PP PTFE	4.5 – 2.6 $L/m^2.h$ (saline solution) 6.7 – 29 $L/m^2.h$ (boron solution) 4 – 28.2 $L/m^2.h$ (geothermal water)	> 99.2 %	0.18 – 1.16 (saline solution) 0.28 – 1.23 (boron solution) 0.16 – 1.16 (geothermal water)	80 - 520 kWh/m^3 (saline solution) 80 - 337 kWh/m^3 (boron solution) 80 - 553 kWh/m^3 (geothermal water)	This study

3.4 Conclusion

Boron is one of the most important elements. Besides its benefits, excessive amounts of boron can be harmful. In this study, MD was used to remove boron from aqueous solutions. The results showed that with the increasing pore sizes the permeate flux increased for all types of membranes due to the increasing penetration of vapor across membranes and decreasing mass transfer resistance. PP membranes reached the higher flux for saline water, synthetic boron solution, and real geothermal water, while PVDF membranes had lower flux values in general, because of its denser upper layer. Permeate water boron concentrations for both synthetic and geothermal water were lower than the limit value for drinking water accepted by WHO. Applied vacuum pressure to the AGMD enhanced the lower permeate flux, which addresses one of the main handicaps for the MD process by decreasing mass transfer resistance. Adding vacuum pressure also increased the GOR values. Although using the supplementary vacuum pump the specific energy consumption did not increase due to the increased permeate production amount. Also, with these promising results of the treatment of geothermal water successfully, it is possible to reduce energy consumption by taking advantage of hot geothermal water instead of heating the feed solution, which is another handicap for MD as well.

4. BIOMIMETIC HYDROPHOBIC MEMBRANE DEVELOPMENT FOR MEMBRANE DISTILLATION

4.1 Introduction

The membrane distillation (MD) process is being studied widely to meet the increasing water demand. MD is a thermally driven separation process which makes it different from other membrane processes such as reverse osmosis (RO), nanofiltration (NF), ultrafiltration (UF), or microfiltration (MF) (Alkhudhiri et al., 2012; W. Zhang et al., 2023). Since the vapor pressure difference is the driving force in MD, the water molecules are not allowed to pass through the membrane which acts like a selective barrier. So the non-volatile components are rejected by the membrane which means high- quality permeate water. For that purpose, hydrophobic membranes are utilized to let only vapor pass through the membrane pores while preventing water penetration.

Polyvinylidene fluoride (PVDF), polypropylene (PP) and polytetrafluoroethylene (PTFE) are the hydrophobic membranes used generally in MD (Mao, et al., 2022). However, MD application is limited due to the wetting problem (Li et al., 2022). The membranes used in MD are produced for other membrane processes as microfiltration. The special membranes for MD need to be designed to meet requirements such as hydrophobicity(Liao et al., 2013, 2014a; Phattaranawik, 2003).

The preparation of hydrophobic membranes can be done by several methods. Additives (Fontananova et al., 2006) and surface modification are the methods for preparing hydrophobic and superhydrophobic membranes. Different nanomaterials such as Al_2O_3, SiO_2, CNTs, ZnO, TiO_2, Fe_3O_4(Gethard et al., 2011; Hirota et al., 2016; Hu et al., 2020; Luo et al., 2020; Y. Zhang et al., 2023; H. Zhou et al., 2019) or fluorinated polymers (Islam et al., 2010; Khayet et al., 2019) are used for improving the performances of MD membranes.

Lotus leaf is the most known superhydrophobic natural plant that inspired researchers. Superhydrophobicity corresponds to a contact angle of 150° or more. The micropapillary structures give superhydrophobic properties. The superhydrophobicity,

water repellency and self-cleaning make the studies have grown on mimicking the lotus leaf surface (Darmanin & Guittard, 2014, 2015; AbdulKadir et al., 2020). Electrospinning is one of the successful and simple method for preparing lotus leaf-like membranes by improving the surface roughness with 3D micro and nano-scale fibers (Efome et al., 2016; Liao et al., 2013; Tijing et al., 2014). Spray coating is another method that is widely used for preparing superhydrophobic membranes (H.-K. Kim & Cho, 2015; F. Zhang et al., 2018)

In this study, we used different methods for preparing superhydrophobic membranes for MD. We used commercial membrane and modified it by coating and we also fabricated PVDF membranes by phase inversion and electrospinning methods. The fabricated membranes were also coated to make the hydrophobic membranes superhydrophobic. First, we tried to optimize the phase inversion method by changing the coagulation bath medium with different solutions. Ethanol bath enhanced the hydrophobicity while membranes became more fragile. We then applied the coating method to increase the hydrophobicities of both commercial and fabricated membranes for phase inversion and electrospun nanofiber membranes. The commercially available superhydrophobic coatings were also used for commercial and selected fabricated membranes and the results showed it was possible to reach up to 153° contact angle. After the characterization of membranes, VAGMD experiments were conducted with pure water and synthetic boron solutions. Flux and boron removal efficiencies were determined.

4.2 Material Methods

4.2.1 Materials

PVDF and PTFE were purchased from Sigma Aldrich. Ethanol, acetone and N,N-dimethyl acetamide (DMAc) were obtained from Merck. MWCNT and H_3BO_3 were purchased from Sigma Aldrich. PDMS was supplied from Dow, USA. SHBC and C solutions were purchased from Nasiol, Turkey. PN was supplied from Pearl Nano, USA. CS was supplied from Ritec, UK.

4.2.2 Membrane fabrication and modification

Membranes were fabricated through both phase inversion and electrospinning methods. The esired amount of PVDF polymer was dissolved in DMAc and stirred at

50 °C until obtaining a homogenous solution. Before using this dope solution it was waited at room temperature ca. 12 h to remove bubbles. The dope solutions were then cast on the glass plate with BYK Instruments automatic film applicator. Films immersed into the coagulation bath. Different coagulation bath mediums were tried as ethanol, water, water/ethanol, acetone/water. Electrospun membranes were fabricated by the lab-scale electrospinning method. The device has an energy source, polymer feeding syringe and collector. The polymer feeding rate was 1.6 mL/h, 15 cm syringe-collector distance, 29 kV of voltage and 2 hours working period during production experiments. The electrospinning device is given in Figure 4.1.

Different materials and solutions were used to modify the membranes. CNT ethanol solution was ultrasonicated for 30 min for dispersion of ethanol. Then magnetically stirred. The dip coating method was used to coat the CNT. PDMS was prepared by adding a curing agent to the elastomer base at a ratio of 1:10. And the solution was cast onto the membranes. Commercial hydrophobic coatings were applied with their spray application heads. Then dried at room temperature for 12 h.

4.2.3 Membrane characterization

Fabricated and modified membranes were characterized in terms of hydrophobicity and surface structure. Contact angle measurements were conducted for all membranes by using an Attension Tensiometer, Biolin Scientific. At least 5 measurements were done and mean values were calculated and used for determining the contact angle values of membranes. The surface structure of membranes was characterized by a Fei Quanta SEM device.

4.2.4 VAGMD performance

Characterized membranes were then tested with pure water and synthetic boron solution in lab scale VAGMD system at 70°C feed water temperature. The vacuum pressure was 0.08 bar and the cooling water temperature was adjusted to 20°C. The amount of collected permeate was recorded to calculate the flux values of membranes. The boron concentrations were analyzed via ICP-OES (Perkin Elmer Optima 7000 DV).

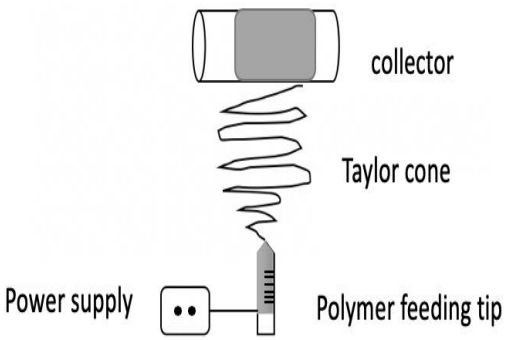

Figure 4.1 : Typical electrospinning device (Mutlu-Salmanli, 2018).

4.3 Results and Discussion

Fabricated membranes were characterized in terms of contact angle. PVDF-based phase inversion membranes were fabricated by using 3 different coagulation bath mediums to see the effect of the coagulation bath on the membrane hydrophobicity. Ethanol was used for that purpose. The contact angle was 87.27° for the water bath, 114.79° for the ethanol bath, and 92.15° for 1/1 ethanol/water bath for the pristine membrane as can be seen in Figure 4.2.

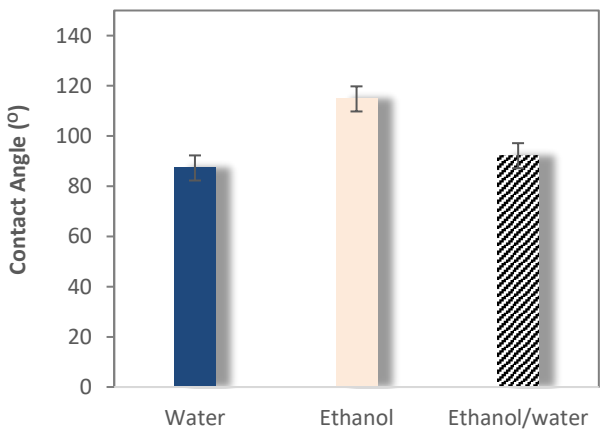

Figure 4.2 : Effect of coagulation bath medium on contact angle.

Another series of membranes were CNT added PVDF membranes. The contact angle for CNT-added PVDF membranes followed the same trend with pristine membranes. And also C60 added membranes had the same trend for contact angle values. Also addition of carbon nanomaterials to the PVDF membrane dope solution lowered the contact angles which means membranes became more hydrophilic (Figure 4.3). The results showed the positive effect of ethanol in a coagulation bath on hydrophobicity.

However, the membranes fabricated by using an ethanol bath and 1/1 ethanol/water bath were torn and couldn't be used for treatment experiments.

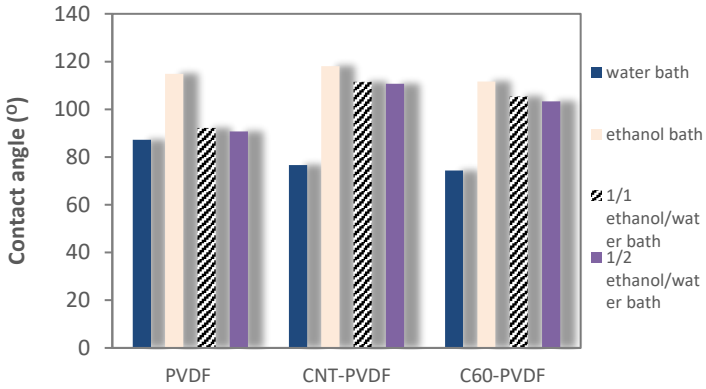

Figure 4.3 : Comparison of contact angles for different coagulation baths.

The pure water flux of membranes fabricated in a water bath medium is given in Figure 4.4. With the increasing contact angles, fluxes decreased as expected. Since the C60 added membrane is more hydrophilic the following experiments were conducted only with CNT added membrane. As an alternative to the ethanol addition, the acetone was used in a coagulation bath medium with water as a mixture of 1/2. According to the results, acetone in a coagulation bath was not found effective in terms of hydrophobicity.

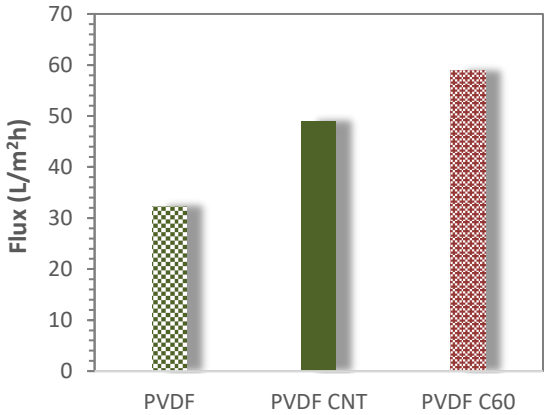

Figure 4.4 : Pure water flux of pristine and carbon nanomaterial added membranes.

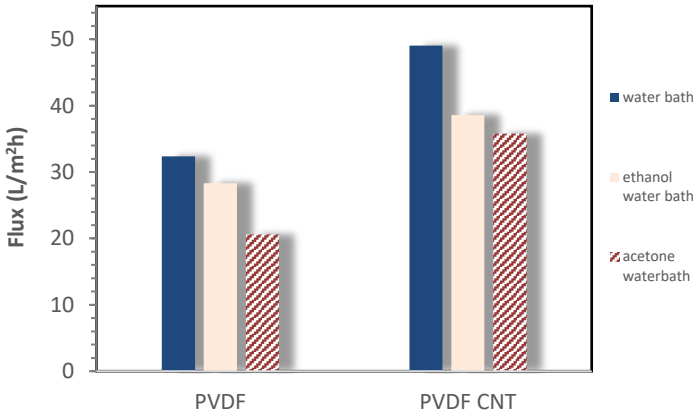

Figure 4.5 : Comparison of pristine and CNT-added membranes in different coagulation baths.

After phase inversion membrane fabrication studies, PVDF espun membrane was fabricated by using an electrospinning technique. Both phase inversion and electrospun membranes are modified by coated with nanomaterial. PVDF electrospun membrane was more hydrophobic than phase inversion membrane. However CNT coating decreased the contact angle values of membranes as can be seen in Figure 4.6. PTFE nanopowder addition to the PVDF membrane increased the contact angle up to 128.9°.

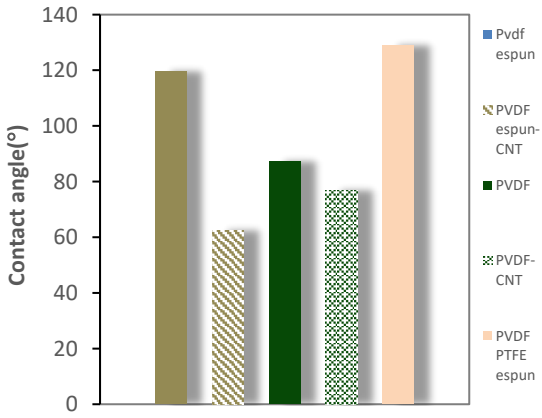

Figure 4.6 : Contact angle values of PVDF and PVDF CNT coated membranes fabricated with different methods.

Since the superhydrophobicity couldn't obtained with previous studies commercial hydrophobic coating solutions were used to modify both commercial and fabricated membranes. C, CS, GRM, PN, ZR53 and SHBC were used to coat the commercial GVSP membrane first. All coatings, except GRM, increased the hydrophobicity of commercial GVSP membrane. The contact angle of C-coated membrane was 141.5°, the PN coated was 141.6° and the SHBC coated was 143°. Then the electrospun PVDF

membrane was coated with the selected coating solutions which are SHBC, C, CS and PN. The results are given in Figure 4.7 a-b. According to the results, the superhydrophobicity was achieved with CS coating which exceeded 150° (Falde et al., 2016; F. Wang et al., 2021).

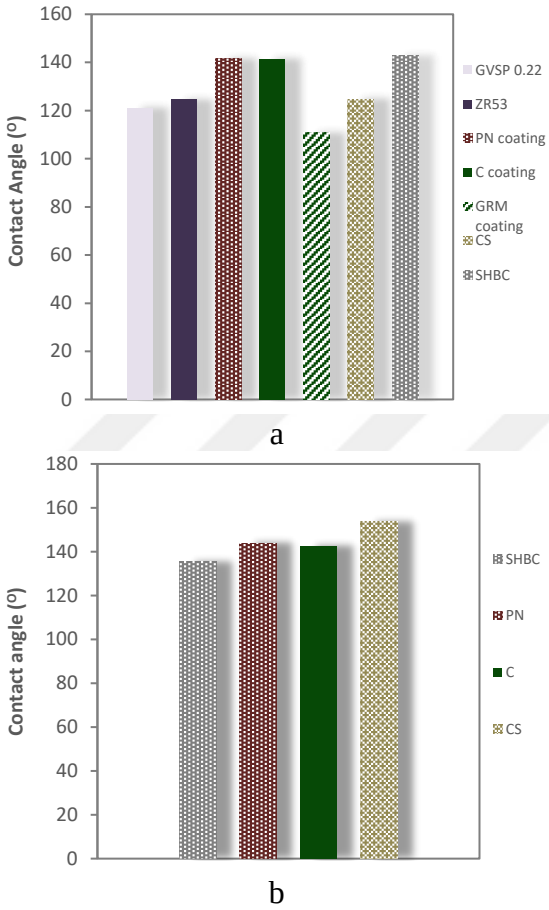

Figure 4.7 : Contact angle values of coated commercial (a) and electrospun (b) membranes.

SEM images of coated commercial and electrospun nanofiber membranes were as given in Figure 4.8 and Figure 4.9. Coating changes the surface morphology of membranes and causes the formation of structures like micropapillaes of lotus leaf which gives the superhydrophobic properties.

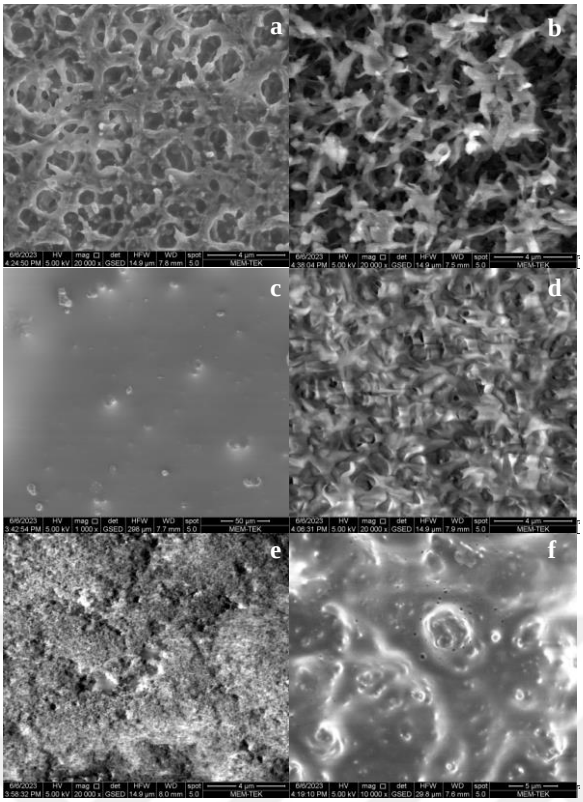

Figure 4.8 : SEM images of coated commercial membranes a)C b)CS c)GRM d)PN e)SHBC f)ZR53.

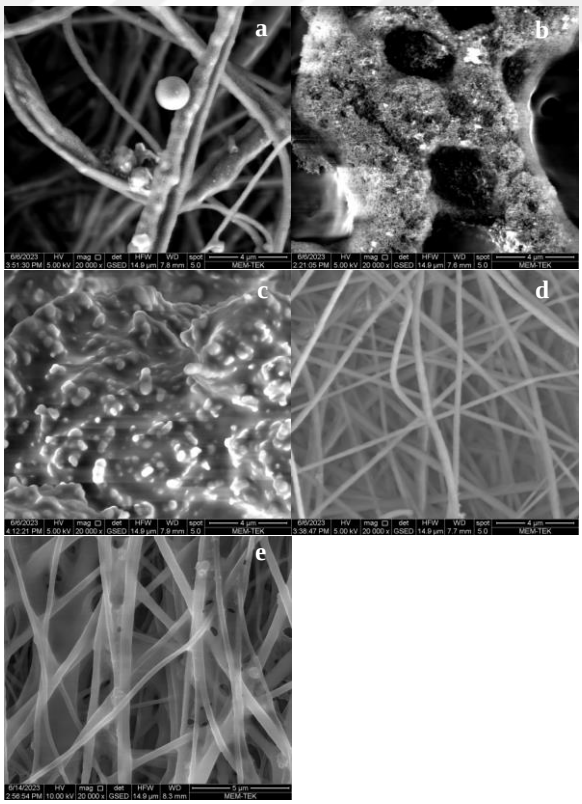

Figure 4.9 : SEM images of a)CS b)SHBC c)ZR53 d)PN e)C coated nanofiber membranes.

After characterization studies selected membranes were tested by using a VAGMD system with pure water and synthetic boron solution. Commercial GVSP membrane had higher fluxes than electrospun PVDF membrane. Boron rejections of membranes were higher than 90% which shows these coated membranes can be utilized in MD for boron removal effectively.

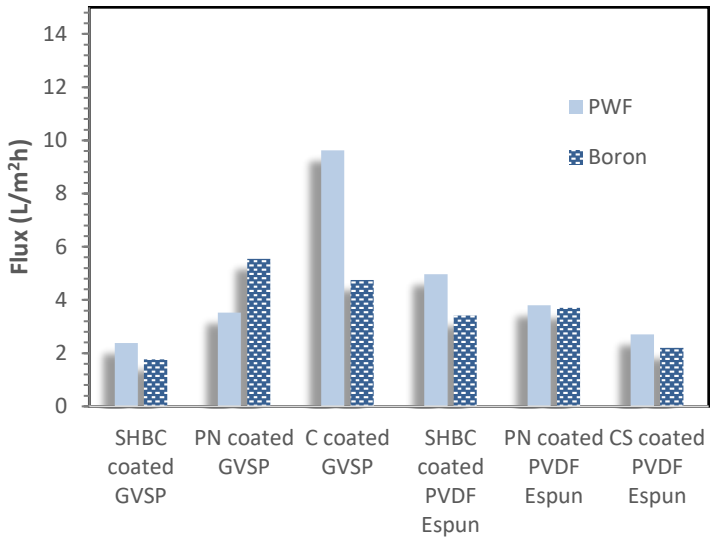

Figure 4.10 : Permeate water flux of coated membranes.

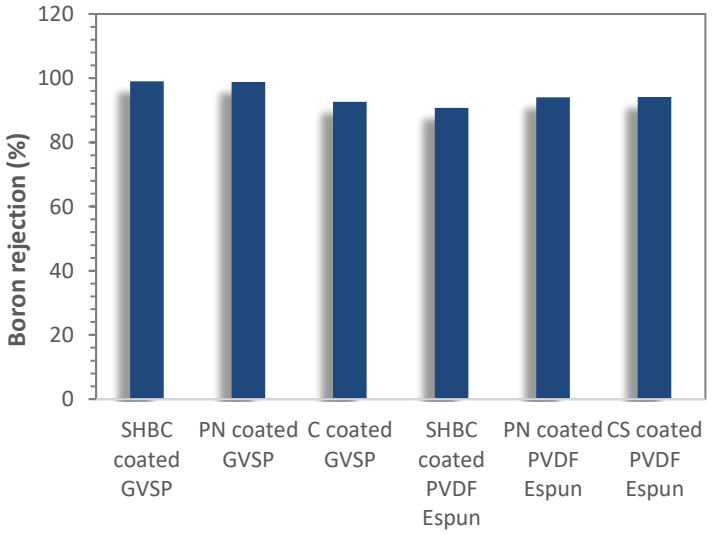

Figure 4.11 : Boron rejections of coated membranes.

4.4 Conclusion

The hydrophobic and superhydrophobic membranes were fabricated with different methods. Changing the coagulation bath medium for the phase inversion method affected the membrane hydrophobicity. Ethanol bath and ethanol/water bath increased the contact angles of membranes. However, it was not possible to use the membranes immersed in an ethanol bath since they were easily torn. Since the contact angles of those series of membranes were not higher than 118° electrospinning and coating of CNT were applied. Electrospun PVDF pristine membrane's contact angle was 119.6°. Using the commercially available different hydrophobic coatings increased the contact angles of commercial and fabricated/coated electrospun membranes. It was possible to reach a 153° contact angle by using CS coating for the PVDF electrospun membrane. And the boron removal efficiencies were higher than 90%.

5. FABRICATION OF NOVEL HYDROPHOBIC ELECTROSPUN NANOFIBER MEMBRANE USING POLYBENZOXAZINE FOR MEMBRANE DISTILLATION APPLICATION[3]

5.1 Introduction

Membrane distillation (MD) which is a thermal separation process is gaining attention in recent years especially for the removal of non-volatile components (H. Chang et al., 2021; J. G. Lee et al., 2018). It has lots of advantages compared to the conventional distillation and conventional desalination processes such as lower temperature and hydraulic pressure requirement, no need for pretreatment of feed water, less sensitivity to feed water quality and high-quality product (Eykens, De Sitter, et al., 2016; Safavi & Mohammadi, 2009b). MD is based on temperature difference across the membrane, which means the driving force is the vapor pressure difference. Since only the vapor can pass through the membrane, MD membranes should be hydrophobic to prevent the liquid passage through membrane pores while needs to have enough channels to transfer the vapor (Horseman et al., 2021; Ray et al., 2017). Different hydrophobic polymers such as polyvinylidene fluoride (PVDF), polytetrafluoroethylene and polypropylene and wide range of additives/nanomaterials were extensively studied by the researchers for fabricating MD membranes (Attia et al., 2017; Efome et al., 2020; J. Guo et al., 2019; Ju et al., 2020; Z. Liu et al., 2021; Ray et al., 2020). However, there is a need to develop novel materials to increase hydrophobicity and therefore, reduce the wetting of MD membranes.

There are several hydrophobic fabrication methods such as phase inversion (Pagliero et al., 2020), sol-gel method (X. Sun et al., 2009), electrospinning and electrospraying (Attia et al., 2018b), chemical vapor deposition (Tran et al., 2021) and layer by layer

[3] This chapter is based on 'Oyku Mutlu-Salmanli, Bahriye Eryildiz, Vahid Vatanpour, Zeynep Deliballi, Baris Kiskan, Ismail Koyuncu (2023), *Fabrication of novel hydrophobic electrospun nanofiber membrane using polybenzoxazine for membrane distillation application*, Desalination, 546, 116203 https://doi.org/10.1016/j.desal.2022.116203'

deposition (L. Zhang et al., 2022). Compared to other hydrophobic fabrication methods, electrospinning has gained a lot of attention as promising technique for membrane production. This technique which high voltage is used, offers several advantages such as high porosity, low thickness and high specific surface area compared to other membrane fabrication techniques (Kolesnik et al., 2021; K. Li et al., 2019; Pang et al., 2021) The electrospun membrane has been used in MD applications by many researchers due to excellent performance on permeate water flux and salt rejection, enhancement of hydrophobicity and prevention of wettability (Attia et al., 2017; K. Li et al., 2019; Y. T. Tsai et al., 2021).

One of the best strategies to address wetting problem is to enhance the hydrophobicity of the hydrophobic membrane surface by selecting a more hydrophobic copolymer compound with good mechanical strength and adequate thermal and chemical stability (Akbari et al., 2020). Polybenzoxazines (PBz) as an additive phenolic system has emerged as a feasible alternative for producing high-performance membranes in recent years due to the better thermal, chemical, and physical stability of the resultant membranes (Vatanpour et al., 2022). PBzs based surfaces can display significant hydrophobicity, and high post-curing water contact angles in contrast to their phenolic nature (Ghosh et al., 2007; Jiang et al., 2022). Phenolic hydroxyl groups in the PBz structure are expected to increase hydrophilicity as in classical phenol formaldehyde resins. In contrast, an opposite effect is observed from any PBz systems. The main reason for that the observed hydrophobicity is related to the phenolic –OH groups in PBz that form intramolecular hydrogen bonds with neighboring tertiary amine nitrogen, giving the structure a slightly helix geometry. Thus, water molecules cannot sufficiently interact with the phenolic –OH groups in the helix and interact with nitrogen, and the whole structure exhibits hydrophobic properties (L. Guo et al., 2008). Depending on the polymerization temperature, the hydrophobicity may increase further (H. Ishida, 2011).

PBz-based materials can be used in the production of both hydrophilic and hydrophobic nanofiber membranes. Nanofiber membranes containing PBz are used in high temperature filtration systems, solvent/chemical resistant membrane filtration, oil/water separation and proton exchange membrane filtration systems (H. Y. Li & Liu, 2013; Satilmis & Uyar, 2019; Shang et al., 2012). In nanofiber membrane production, PBz can be used in four different ways: (1) using PBz as the main polymer,

(2) mixing with other polymers, (3) mixing with carbon nanofibers, and (4) performing surface modification of the produced membranes with Bz (Vatanpour et al., 2022). Due to poor chain entanglement and overlapping during the electrospinning process, it is often difficult to create nanofibers from monomers, low molecular weight polymers as PBz precursors, or tiny compounds. Therefore, the fabrication of a high-quality nanofiber membrane has been accomplished by combining the PBz precursors with an appropriate polymer, such as CA, PAN and PVDF. Also, the degree of crosslinking, strength are increased, and cold flow is decreased with this method (Kiskan, 2018; Vatanpour et al., 2022).

In the literature, there are studies on the production of membranes using PBz (Vatanpour et al., 2022). Ma et al. obtained superhydrophobic, high-flux and high removal efficiency membranes by modifying the surface of nanofiber membranes with PBz (Ma et al., 2017). Yao et al. carried out proton exchange membrane production studies with PBz containing sulfonic acid. According to the obtained results, the selectivity of the produced membrane is considerably higher than the commercial Nafion 117 membrane (Yao et al., 2014). Periyasamy et al. developed an environment-friendly superhydrophobic/superoleophilic cotton sponge (CS) coated by PBz and stearic acid functionalized carbon balls for oil/water removal. By coating of PBz-carbon balls on the surface of cotton sponge, the hydrophilic CS is changed into superhydrophobic material with a water contact angle of 153° (Periyasamy et al., 2022). In a cellulose acetate nanofiber membrane produced for oil/water separation, membrane modification was performed with PBz containing fluorinated silica nanoparticles. It has been reported that the obtained membrane is not only superhydrophobic, but also highly stable and resistant to a wide pH range (Shang et al., 2012). Shirzad Kebria et al. (2020) fabricated new electrospun nanofiber membranes (ENMs) with better surface hydrophobicity by incorporating hyper-branched dendritic structures (HB-Den) for AGMD applications. They demonstrated that the addition of 0.0375 wt% (HB-Den) enhanced the surface contact angle, resulting in stable and preferable performance of the ENMs in air gap membrane distillation (Kebria et al., 2020). Essalhi et al. (2021) developed mixed matrix electrospun nanofibrous membranes (MM-ENMs) by combining nanofillers (MWCNs or GO) with polymeric solutions of various PVDF molecular weights. The best method for creating membranes with higher DCMD desalination performance was determined

to be incorporating MWCNs into the active surface of dual layer (DL)-MM- ENMs (Essalhi, Khayet, Tesfalidet, et al., 2021). Essalhi et al. (2021) investigated the optimum electrospinning fabrication conditions to enhance ENM perfirmance for DCMD. Results showed that among all fabricated membranes, the low thickness membrane fabricated with a polymer flow rate of 1.2 mL/h, an electric voltage of 24 kV and air gap distance of 27.5 cm presented excellent performance in DCMD (Essalhi, Khayet, Ismail, et al., 2021). However, the use of PBz based membranes in the MD process has not been reported in the literature. Therefore, it is essential study regarding production of containing PBz hydrophobic membrane in MD applications.

In this study, the fluorinated benzoxazine monomer was incorporated in the PVDF to improve membrane hydrophobicity and membrane stability in MD process. Fluoro-polymers have a wide range of applications in membrane technology, due to their excellent mechanical strength, chemical and thermal stability and low surface tension (Esmaeili et al., 2022). Among the entire fluoro-polymer family, PVDF is the most commonly used membrane material for a variety of applications, especially MD process due to good hydrophobicity and flexibility. The hydrophobic membrane was fabricated using electrospinning. The fabricated nanofibers were cured at high temperatures for different times to crosslink Bz, effectively. The membrane properties and morphologies of fabricated electrospun membranes were characterized. The treatment performance of electrospun nanofiber membranes were evaluated in VAGMD using salty water, boron solution and RO brine.

5.2 Material and Methods

5.2.1 Materials

4,4-Isopropylidenediphenol (bisphenol A) (Aldrich, 97%), 4-fluoroaniline (Aldrich, 99%), paraformaldehyde (Sigma-Aldrich, 95.0–100%) and xylene (Merck, extra pure) were used as received. Analytical grade sodium chloride and boric acid (H3BO3) was obtained from Merck. Distilled water was employed all over the research study. N, N-dimethyl acetamide (DMAc) and analytical grade acetone were supplied from Merck. Solef 6010 polyvinylidene fluoride (PVDF) was used to prepare electrospun membrane was supplied from Solvay.

5.2.2 Synthesis of bis-(4-fluorophenyl-bisphenol-benzoxazine) (BisF-Bz)

Paraformaldehyde (50.0 mmol, 1.5 g) and 4-fluoroaniline (25.0 mmol, 2.78 g) were dissolved in a 100 mL round bottomed flask with 8 mL of xylene. The reaction mixture was stirred at 120 °C for 12 h after the addition of bisphenol A (12.5 mmol, 2.85 g). Without additional purification, the solvent was evaporated under high vacuum, yielding a brown solid as a pure product. The product was vacuum dried for 24 h at 45 °C (yield ca. 95%). The product is abbreviated as BisF-Bz (Demir et al., 2013).

5.2.3 Characterization of BisF-Bz

Fourier-transform infrared spectroscopy (FT-IR) spectra were recorded on a PerkinElmer FT-IR Spectrum One spectrometer, having a resolution of 4 cm^{-1} and 16 scans. 1H NMR spectra were recorded on an Agilent NMR System VNMRS 500 spectrometer at room temperature in $CDCl_3$ with $Si(CH_3)_4$ as an internal standard. Differential scanning calorimetry (DSC) was performed on PerkinElmer Diamond DSC from 30 to 320 °C with a scanning rate of 10 °C/min under nitrogen flow (20 mL/min.). A typical DSC sample was between 1 and 5 mg in a 30 µL aluminum DSC pan.

5.2.4 Preparation of electrospun membranes

The membranes were fabricated by electrospinning method in a lab-scale (Eryildiz, Ozbey-Unal, et al., 2021b). The device has an energy source, a polymer feeding syringe and a collector. After homogenously dissolving of the PVDF and Bz in DMAC/acetone solution, the dope solution was fed to the spinning device. Polymer feeding rate was 1.2 m L/h, 15 cm syringe-collector distance, 24 kV of voltage and working period was 2 h for fabricating the nanofibrous membranes. PVDF was selected as a base polymer for each membrane (15 wt%) and PBz was selected as a second modifier polymer with 10 wt% ratio of the Bz precursor. Optimum PVDF concentration was determined in previous study (Ozbey-Unal et al., 2020b). More than 10 wt% Bz in PVDF doping solution reduced the viscisity of solution and suitable nanofibers were not obtained. Table 5.1 presented the dope solution compositions and curing times of the prepared MD membranes. The BisF-Bz added membranes, M3 membrane was also placed an oven for 1 h at 150 ºC to provide ring opening reaction and crosslinking of the oxazine ring to obtain PBz polymer mixed in the matrix of

PVDF nanofibers. This crosslinking procedure was performed for 2 h to the M4 membrane.

Table 5.1 : Dope solution compositions and heat treatment time.

Membrane	PVDF (wt%)	Bz (wt%)	DMAc/Acetone	Curing time (h)
M1	15	-	1/1	-
M2	15	10	1/1	-
M3	15	10	1/1	1
M4	15	10	1/1	2

5.2.5 Characterization of membranes

The prepared membranes were characterized in terms of contact angle, FT-IR, scanning electron microscopy (SEM) and tensile strength of membranes. The morphologies of prepared membranes were characterized by SEM branded FEI Quanta Feg 250 SEM. The membranes were coated with gold and palladium (Au/Pa). KSV Attension Theta branded contact angle meter was used to measure the contact angle of membranes. Distilled water was used to the contact angles determination. Ten measurements were conducted for each sample at least. The values were averaged and the results were given. Perkin Elmer Spektrum 100 ATR-FT-IR was used to analyze the structures of membranes. IR spectrum was accumulated in the range of 650–4000 cm^{-1}. Membrane mechanical properties of the tensile strength (kPa) and elongation at break (%) were obtained with an Exstar SII-DMS6100. Membranes were cut into a rectangle shape under 10 mN/min crosshead speed (50 ×10 mm) and tested.

The mean pore size and liquid entry pressure (LEP) values were measured using a capillary flow porometer (Quantachrome 3G Porometer). The gravimetric method was used to calculate the membrane porosity. Firstly, the membranes (2×2 cm) were submerged in isopropanol for 1 h. The weight of wetted samples was measured. Then, the samples were placed to dry in the oven at 90 ºC and weighed until the dry weight was kept constant throughout. The porosity (ε) was calculated using following equation:

$$\varepsilon = \frac{(m_w - m_{d)/} p_i}{(m_w - m_{d)/} p_i + m_d / p_p} \quad (5.1)$$

where m_w is the weight of the membrane and m_d is dry weight of the membrane. p_p is PVDF 6010 density (1.77 g/mL), p_i is isopropanol density (0.785 g/mL). Each membrane sample's porosity was determined using the average of three measurements.The design of the peel experiment is as follows. Stick half of the tape to the membrane surface, then peel 180° with tweezers. Then, examine the membrane's surface for damage.

5.2.6 MD studies

The experimental setup was given in Figure 5.1. Vacuum pressure was created by a vacuum pump. The temperature of feed water was arranged to 70 °C by using a heating bath and circulated via a peristaltic pump with 1.4 L/min flow rate (Re=6500). 20 °C cooling water flowed 480 mL/min rate from cooling bath was used to cool membrane module which has 7 mm air gap width. Active membrane area was a 44.18 cm^2 located in the middle of the module. The vacuum-assisted air gap membrane distillation experiments were carried out by applying 0.08 bar vacuum pressure. Three different water samples were tested which were salty water, synthetic boron solution (10 mg B/L) and real RO brine which had the highest boron concentration of 5231 mg/L. The removal efficiencies (R) were calculated by using conductivity measurements for both feed and permeate solutions. Both permeate flux (J) and R values were used for characterizing the membrane performance. J (L/m^2h) was calculated according to the following equation (M. A. E. R. Abu-Zeid et al., 2016);

$$J = \frac{\Delta m}{A.\Delta t} \tag{5.2}$$

Where Δm is the amount of the permeate water (L), A is the effective surface area of membrane used in the membrane module (m^2) and $\boldsymbol{\Delta t}$ is the operating time (h). The removal efficiency of both salt and boron solutions are calculated using the following equation;

$$R(\%) = \left(1 - \frac{C_p}{C_f}\right) x100 \tag{5.3}$$

Where the Cf is the concentration of feed solution and Cp is the concentration of permeate solution.

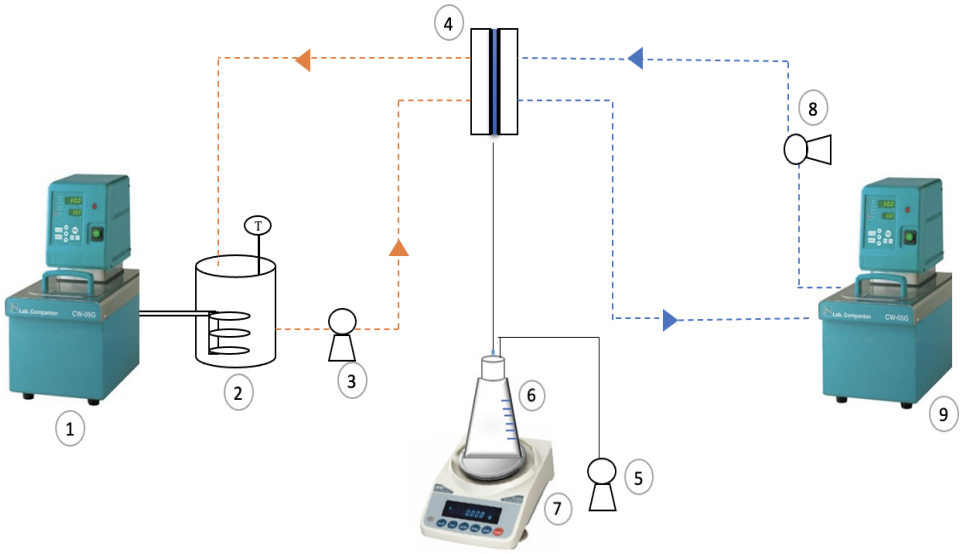

Figure 5.1: A schematic of the lab-scale VAGMD system. 1) Heating water bath, 2) feed tank, 3) pump, 4) membrane module, 5) vacuum pump, 6) distillate bottle, 7) scale, 8) pump, 9) Cooling water bath.

5.2.7 Analytical methods

The boron content of the samples was analyzed using the ICP-OES Optima 7000 device. At least five-points calibration done by using 3% HNO_3 and 1000 ppm boron solution. R^2 coefficient was higher than 0.999. Each sample was measured at least three times.

5.3 Results and Discussion

5.3.1 Characterization of PBz

Fluoro containing benzoxazine monomer (BisF-Bz) has been successful synthesized by a slightly modified benzoxazine synthesis reported previously (Demir et al., 2013). The synthesis of the BisF-Bz from bisphenol A, 4-fluoroaniline, and paraformaldehyde is depicted in Figure 5.2. During the synthesis, xylenes were selected as a solvent to reduce triazine side products, since syntheses trials with other solvents such as 1,4-dioxane, chloroform and toluene-ethanol binary system gave low yields with too much triazine formation (Gungor & Kiskan, 2018). Consequently, BisF-Bz could be obtained with high yield and without any purification step after synthesis. The chemical structure of the BisF-Bz monomer was confirmed by spectral and thermal analysis.

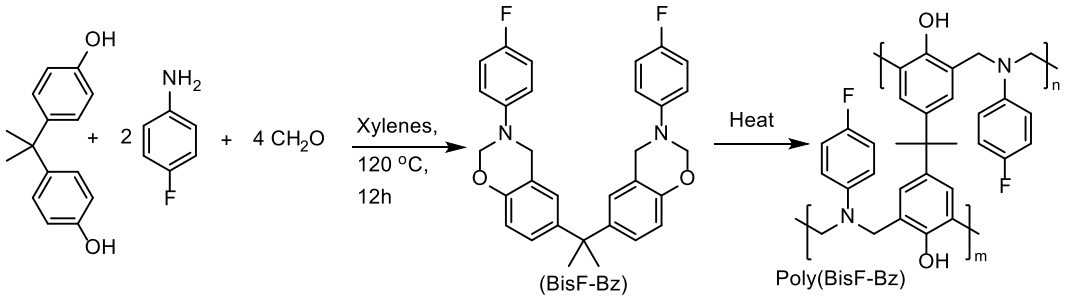

Figure 5.2: Synthesis of BisF-Bz monomer and its thermal polymerization to give poly(BisF-Bz).

The 1H NMR spectrum of BisF-Bz presented in Figure 5.3a, reveals the typical proton signals assigned to the oxazine ring structure at 5.3 (Ar–CH_2–N) and 4.6 ppm (O–CH_2–N), respectively. Aromatic protons were also detected between 7.1 and 6.77 ppm. Moreover, the methyl protons of isopropylidene bridge of bisphenol are apparent at 1.6 ppm.

The infrared absorption bands of the BisF-Bz (Figure 5.3) also verify the formation of oxazine ring. The out of plane infrared band of oxazine attached benzene and C–O–C oxazine-ring band mode emerge at 944 cm^{-1}, which is considered direct evidence of benzoxazine structure. Moreover, the aromatic ether of Bz ring could be detected as C–O symmetric stretching band at 1225 cm^{-1}. Additionally, the C=C and C–H aromatic stretching vibration bands could be also detectable at 1498 cm^{-1} and 3041 cm^{-1} (L. Han et al., 2017).

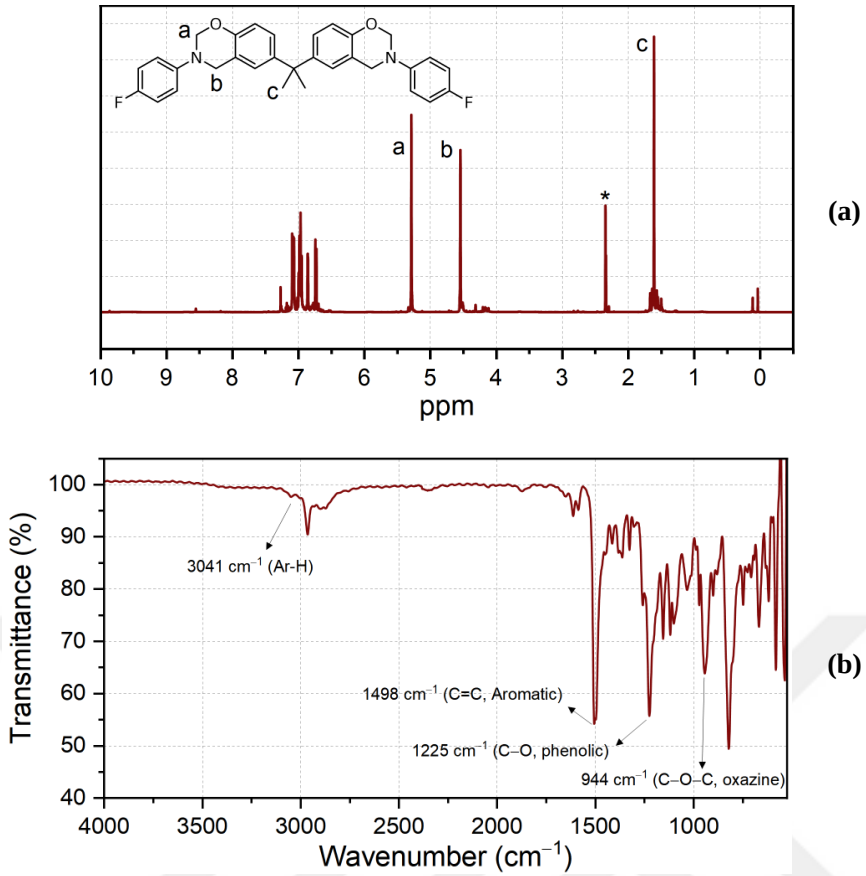

Figure 5.3: ^{1}H NMR (a) and FT-IR (b) spectra of BisF-Bz. (*Residual acetone).

It is well-known that the ring-opening polymerization (ROP) of benzoxazines is exothermic and can easily be monitored by dynamic scanning calorimetry (DSC). In general, the ROP temperature of benzoxazines is observed at between 150 and 240 °C depending on the functional groups of benzoxazines (Kiskan, 2018; Lochab et al., 2021). Figure 5.4 illustrates the DSC profile of the BisF-Bz under N_2 and with heating rate of 10 °C/min. The ROP of BisF-Bz initiates *ca.* at 176 ºC and exhibits a maximum peak at 238 °C with 166.8 J/g exotherm. Although the amount of curing exotherm is slightly higher than many of the previously reported benzoxazines, the onset and maximum curing temperatures are in accordance with typical benzoxazines (H. Ishida, 2011). In brief, the BisF-Bz can be cured below 200 °C to give the polybenzoxazine poly(BisF-Bz) (see Figure 5.2).

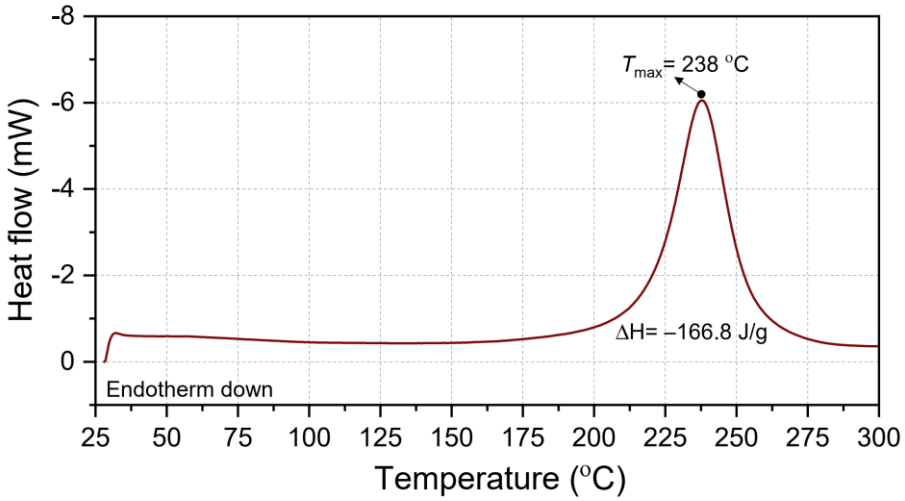

Figure 5.4: DSC thermogram of BisF-Bz.

5.3.2 Membrane characterization

When the SEM images are examined (Figure 5.5), the change in the fibers caused by the curing process can be clearly seen. The average fiber diameters were 605, 497, 357 and 346 nm for the M1, M2, M3 and M4 membranes, respectively. Due to the excessive solvent removal and PBz formation, the fiber diameters decreased after curing (Kao et al., 2013). By generating thin layers of crosslinked polymer, BisF-Bz addition might cement neighboring nanofibers and fill spaces between nanofibers (Ma et al., 2017; Shang et al., 2012). The addition and curing of BisF-Bz resulted in in-situ polymerization of monomers which giving rise to the Mannich bridge cross linking formation (Ma et al., 2019; Si et al., 2012). Besides, the BisF-Bz additive removed the filamentous structure in the electrospun membranes and provided the formation of more stable membrane layers with smoother membrane surface (Ertas & Uyar, 2017).

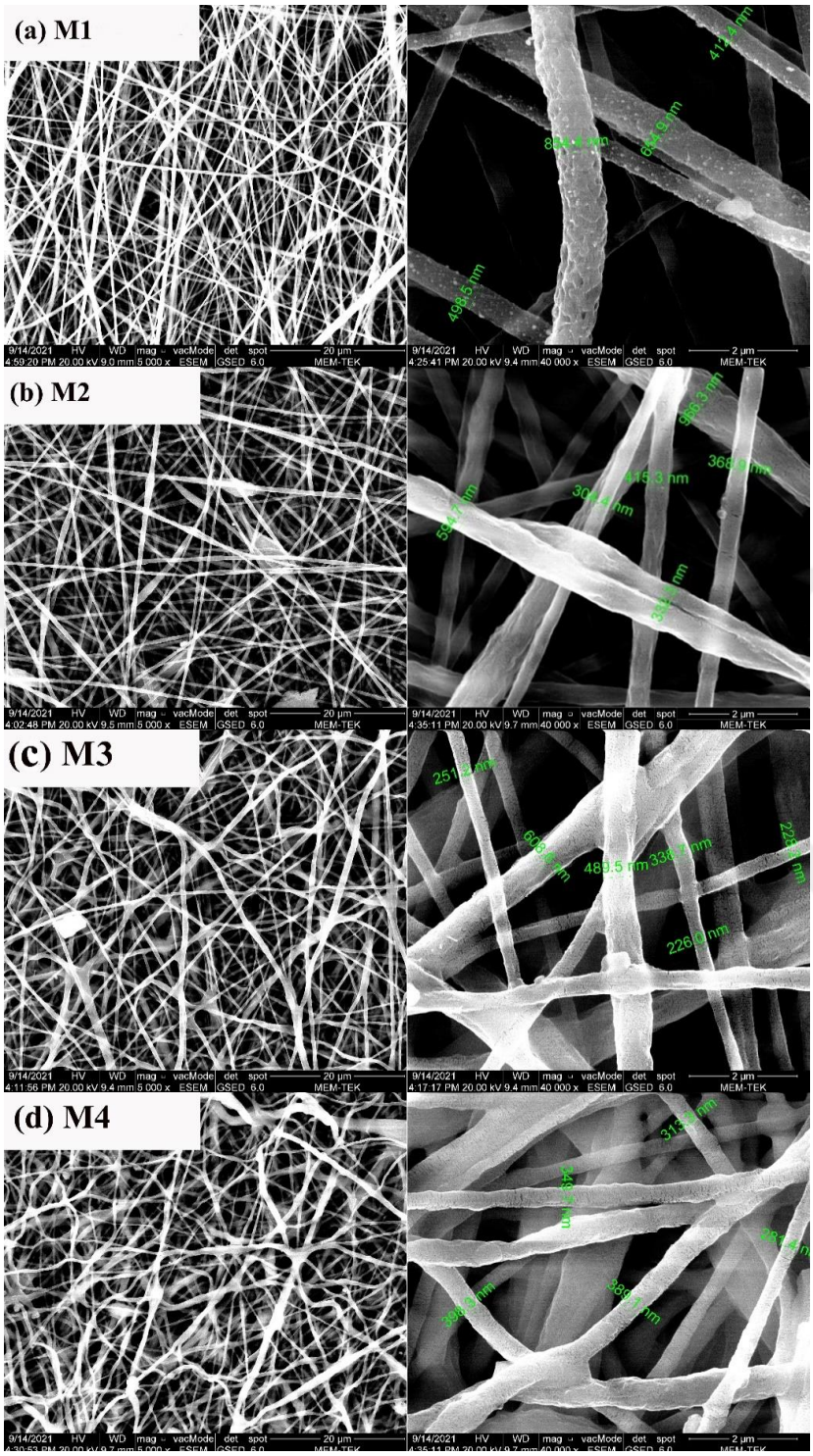

Figure 5.5: SEM images of (a) M1, (b) M2, (c) M3 and (d) M4 membranes.

Figure 5.6 shows the photographs of pristine PVDF and BisF-Bz blended PVDF crosslinked membranes. The uniform and stable nanofibrous PVDF membrane was obtained by addition of Bz in the PVDF matrix.

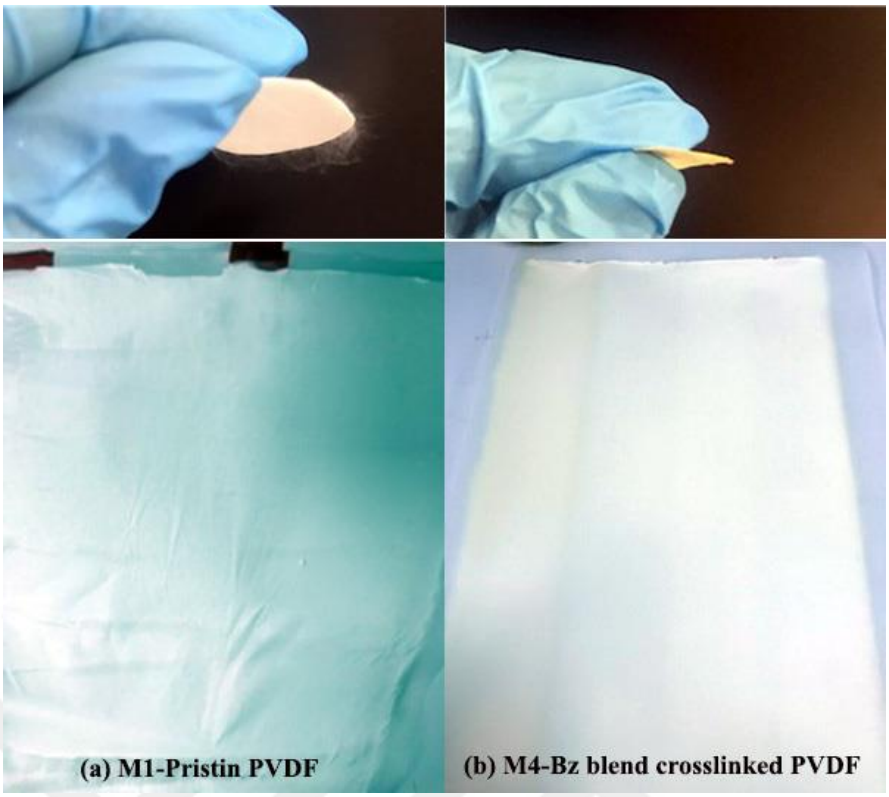

Figure 5.6: The images of pristine PVDF and PVDF/PBz crosslinked nanofiber membranes.

The differences in morphologies of the pure PVDF and PBz modified membranes were compared after peel experiments. Membrane photographs after peel tests are given in Figure 5.7 shows that pure PVDF membrane can be easily peeled away from the substrate, making the membrane susceptible to wetting by the feed solution during the MD operation while PBz modified membranes had more smooth and durable surface than PVDF membrane after peel tests.

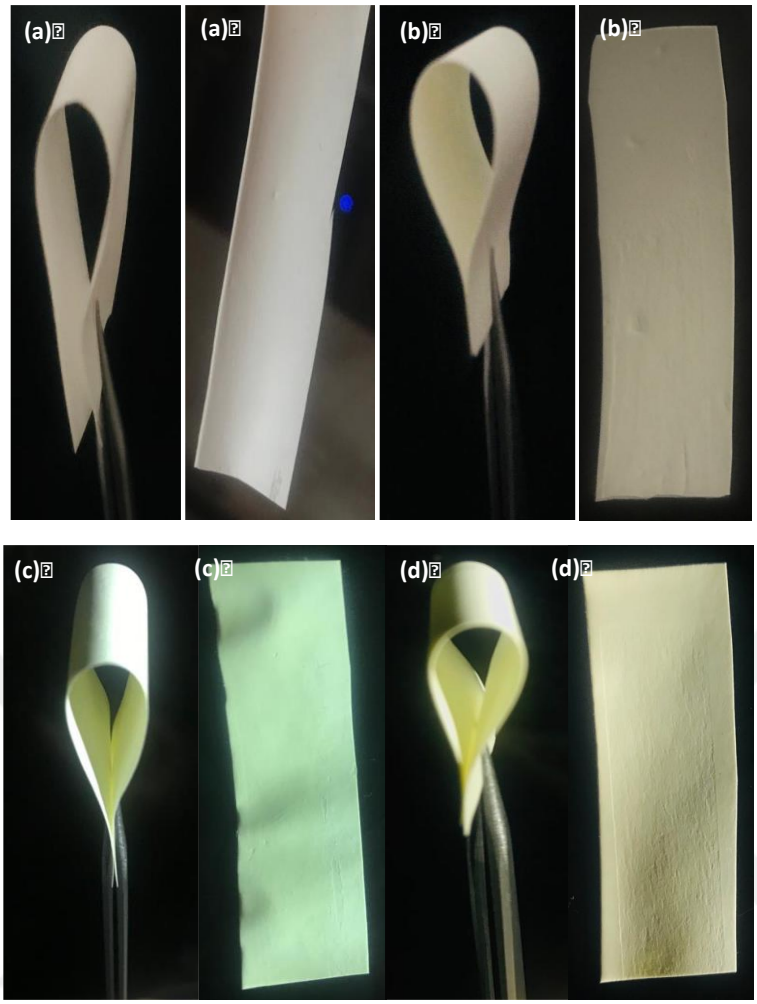

Figure 5.7: Photographs of a) M1, (b) M2, (c) M3 and (d) M4 membranes after peeling test.

Figure 5.8 represents the ATR-FT-IR spectra of the produced nanofibrous membranes. The band around 1510 cm^{-1} was assigned to the tri-substituted benzene ring stretching (Ertas & Uyar, 2017; Pakkethati et al., 2011). Asymmetric stretching mode of C–O (phenolic ether) in the polybenzoxazine was observed at 1223 cm^{-1}. The benzene ring's skeleton vibration was between 1622 and 1454 cm^{-1}, the band at about 975 cm^{-1} shows the characteristic absorption band of polybenzoxazine (Y. Zhu et al., 2021).

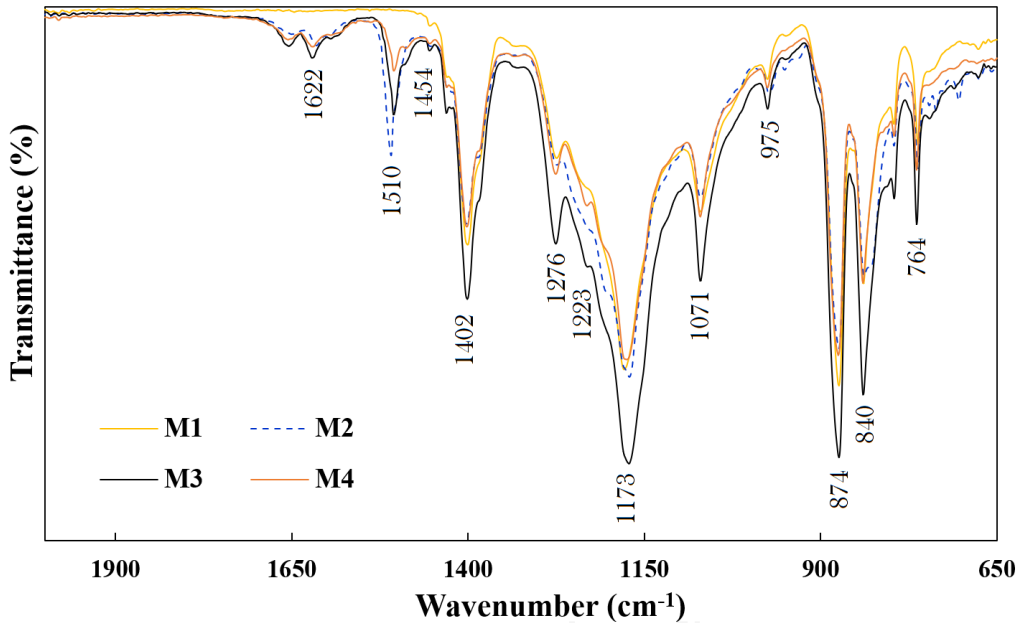

Figure 5.8: ATR-FT-IR spectra of the nanofibrous hydrophobic MD membranes.

The contact angle is one of the most important parameters in MD process to evaluate the hydrophobicity of the membranes (Figure 5.9 a). The pristine PVDF membrane exhibited a water contanct angle (WCA) value ca. 102.8º, whereas Bz addition increased the hydrophobicity and WCA to ca. 127.4º for the uncrosslinked membrane. This is due to the hydrophobic nature of the added Bz with fluorinated groups to the PVDF matrix. By applying heat to the BisF-Bz blended nanofibrous PVDF membranes, the WCA increased to 129.1º and 132.7º for one and double cured samples, respectively. It can be clearly seen that post-treatment affected the hydrophobicity. Which means the deep crosslinking of bonds makes the membranes more hydrophobic. PBz' s hydrophobicity has been attributed to its inter and intramolecular hydrogen bonding, which completely blocks the phenol and tertiary amine groups of PBz, preventing them from interacting with water molecules (Y. T. Chen et al., 2019; C. T. Liu & Liu, 2016; C. F. Wang et al., 2006). When the wetting properties of the PVDF nanofiber membrane and the PVDF/PBz modified membrane were compared as shown Figure 5.9(a), the pure PVDF membrane was resistant to wetting by high surface tension liquids but easily wetted by low surface tension liquids. The modified membranes with PBz display better antifouling performance than pure PVDF membrane. Figure 5.9 (b) shows the images of water droplets on the surface of M4 membranes after 10 min passing from dropping time. As shown, the contact angle of the water droplets and the membrane surface is high and the membrane has not wet. In order to assess the water resistance for durability, contact angles of evaporating

water droplets on the fabricated electrospun membranes were measured, as shown in Figure 5.9(c). When the evaporation period was extended to 30 minutes for the PVDF membrane, the WCAs rapidly dropped to 81.2, demonstrating the infiltration of water into the pores of the nanofibrous membranes. Water resistance was enhanced with addition of Bz. The Cassie-Baxter model was supported by the water contact angles of M4 membrane, which showed the hierarchical roughness surface can inhibit the pinning of the water droplet and showed minimal mark of sliding with evaporation (Zhu et al., 2018).

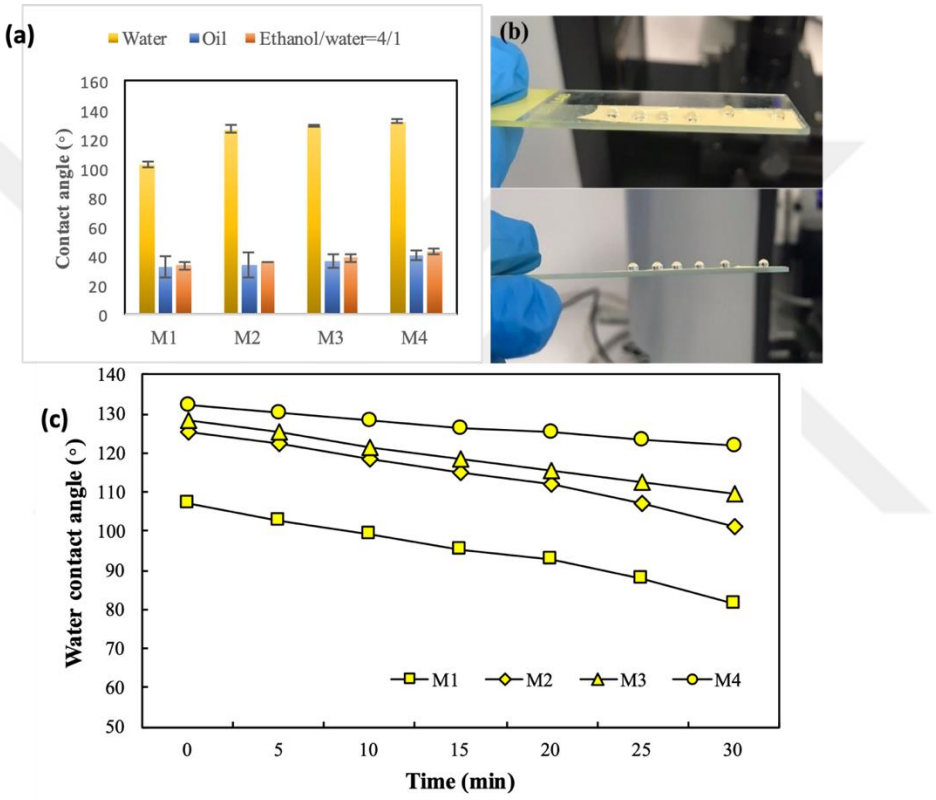

Figure 5.9: Contact angle results of the electrospun MD membranes for three different liquids, (b) image of water droplets on the surface of M4 membrane, (c) Water contact angles with increasing time of fabricated membranes.

The internal structure of the membrane, which was formed by the random accumulation of nanofibres as well as surface modification, may influence both pore size and liquid entry pressure. In general, membrane pore size must be large enough to allow high vapour flux while being small enough to retain a high LEP (Attia et al., 2018c). The fibre diameter determines the membrane pore size in electrospun membranes (Kolesnik et al., 2021). Larger fiber diameter correlates with higher pore size of electrospun nanofibers (Y. T. Tsai et al., 2021). The pore size of produced membranes are given in Table 5.2. The mean pore size were 0.412 μm, 0,408 μm,

0.406 μm and 0.403 μm for M1, M2, M3 and M4, respectively. This can be attributed to an increase of fiber density on the membrane surface caused by the addition of PBz, as seen in Figure 5.5, as well as a reduction in fiber size, as previously demonstrated. As shown in Table 5.2, the pure PVDF membrane had the lowest LEP (87 kPa) while the LEP values of modified membranes increased. According to the Young-Laplace equation, this difference is mostly due to membrane hydrophobicity, with WCAs of 102 and 132° for M1 and M4, respectively (Attia et al., 2018b). Also, LEP value can be increased by lowering average pore size or increasing membrane surface hydrophobicity (Song et al., 2022).

The porosity of electrospun membranes, a critical characteristic for increasing membrane permeate flux, may be controlled by changing fibre diameter (Attia et al., 2018a; X. Q. Wu et al., 2021). In Table 5.2, M1 membrane porosity was 75.24 ± 3.26%, while M4 membrane was 63.65± 2.70%. Compared to pure PVDF membrane, the porosity of modified membrane with PBz was decreased. This is due to the production of microspheres on the nanofibers, which fill part of the spaces between the crossing nanofibers (L. Zhou et al., 2022).

As can be seen in Table 5.2, Young's modulus of membranes was increased and elongation was decreased. The loose structure of pristine membrane makes membrane mechanically low strength. To compare pristine PVDF membrane the addition of PBz without curing enhanced the mechanical properties of electrospun membrane. But, after the crosslinking achieved by thermal curing, there was a significant improvement. The stiffening effect of the benzoxazine with polymerization and crosslinking of nanofibrous membranes are both responsible for this considerable improvement(Ertas & Uyar, 2017; Su et al., 2019). The higher elongation at break shows the higher flexibility which is also related with the stiffens effect of PBz (Pakkethati et al., 2011).

Table 5.2 : Mechanical properties of nanofibrous membranes.

Membrane Code	Membrane thickness (μm)	Porosity (%)	Pore size (μm)	LEP (kPa)	Young's Module (mPa)	Elongation at break (%)
M1	190 ± 0.2	75.24 ± 3.26	0.412± 1.36	87± 2.15	19.48±1.15	2.37±2.25
M2	143 ± 0.3	71.32 ± 1.72	0.408± 2.53	95± 1.28	23.19±2.32	1.03±1.77
M3	123 ± 0.3	63.68 ± 3.75	0.406± 1.49	97± 2.34	52.69±1.89	0.89±1.02
M4	75.0 ± 0.4	63.65± 2.70	0.403± 1.77	98± 2.06	73.49±3.12	0.62±1.87

5.3.3 VAGMD studies

After membrane characterization studies, PVDF and PVDF/PBz membranes were tested in lab-scale VAGMD system using NaCl solution (0.1 wt%). The results are depicted in Figure 5.10. Flux values increased with the Bz addition and also with the increasing curing application. The lowest permeate flux was 17.3 L/m^2.h for the pristine PVDF membrane while the highest flux was 21.2 L/m^2.h for the PVDF/PBz double crosslinked membrane. The permeate flux was increased to 20.4 L/m^2.h with Bz addition to the pristine membrane without crosslinking. Salt removal efficiencies were 96.7%, 98.8% and 99.5% for M1, M3 and M4, respectively. This rejection increase can be attributed to higher contact angle and smaller pore sizes (Hou et al., 2019; Yadav et al., 2022).

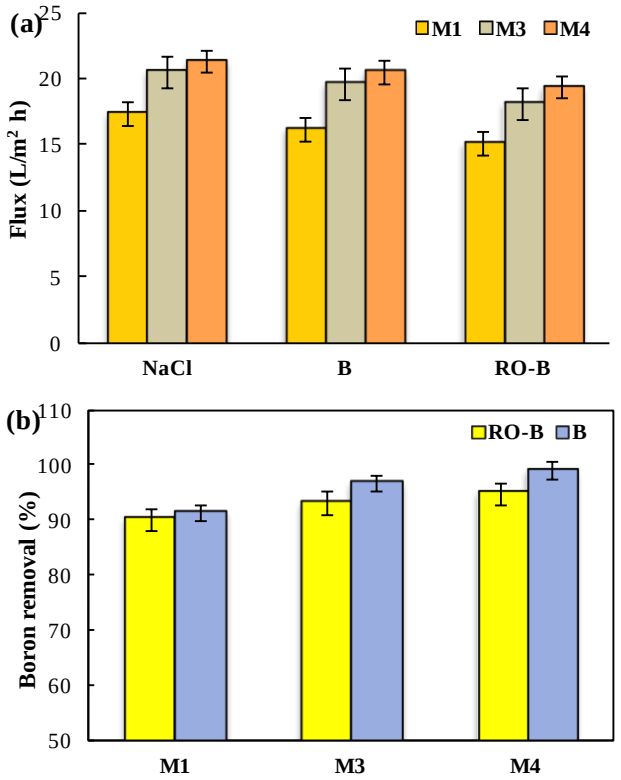

Figure 5.10: (a) Permeate flux and (b) removal efficiencies of nanofibrous membranes in the filtration of boron solutions and RO brine in VAGMD condition.

Same trend was also observed for the synthetic boron solution and for the RO brine (RO-B). The lowest permeate flux was 15 L/m^2 h for pristine membrane and RO-B feed. This increment can be attributed to increasing membrane hydrophobicity which is also lowers the membrane wetting (Dong et al., 2014a; Ren et al., 2017). Membrane thickness is the other parameter effect the permeate flux. The membrane thicknesses decreased to 75 from 190 µm for M4 and M1 membranes, respectively and the fluxes

increased. Higher thickness results in lower fluxes due to the decreasing heat and mass transfer (Swaminathan et al., 2018b; H. Yan et al., 2014). The permeate fluxes decreased compared the NaCl due to the increased concentration in feed solutions B and RO-B decreased the driving force (water vapor pressure) (Kurdian et al., 2013; Ren et al., 2017). The concentration polarization and temperature polarization are also responsible for decreasing of the driving force (Mutlu Salmanli et al., 2022a; Safavi & Mohammadi, 2009b)

Both permeate and feed water was analyzed with ICP-OES for determining the boron concentrations. The boron removal efficiencies are given in Figure 10b. According to the results, the boron rejection values are higher than 90%. Highest removal efficiency was 98.85% obtained for M4 membrane while the lowest was 90.06% for M1 membrane. Compared to the pristine PVDF membrane PBz addition and additional crosslinking was caused a considerable improvement on removal efficiency.

5.3.4 Comparison with literature

Table 5.3 shows brief comparison between our study with previous results. Since the contribution of Bz addition to PVDF membrane in membrane distillation is limited in the literature, the comparisons were made on the basis of PVDF and PVDF/various additives in this section. Some flux values are very different because of the difference of used systems with literature. The related studies are generally aimed to treat oil, solvent or organic pollutants but this study is the first study about boron removal with Bz added membranes. It should be noted that MD operating factors such as MD configuration, temperature difference and flow rate would have an impact on the MD performance. The PVDF/Bz membrane had a very competitive permeate flux. Also, the PVDF/Bz membrane had comparable membrane properties while exhibiting superior salt rejection and permeate flux, indicating its promising potential for MD applications.

Table 5.3 : Comparison of the results of PVDF/PBz membrane with literature.

Main polymer (wt%)	Additive (wt%)	Contact angle (°)	Pore size (μm)	LEP (kPa)	Porosity (%)	ΔT (ºC)	Flux	Rejection (%)	MD Configuration	Ref.
PVDF (15)	Mg/LBenzoxazine (10)	132.7			71.3	45	RO brine 19.28 L/m^2h Boron 20.44 L/m^2h	98% (RO brine) 95% (boron) 99.5% (0.1 wt%)	VAGMD	This study
PBz	Lignin	141	0.55	-	70	-	Water in toluene emulsion 278 L/m^2h	-	-	(Su et al., 2019)
Crosslinked PBz	-	106	-	-	-	-	357 g/m^2h	Isopropanol 100%	-	(Y. L. Liao et al., 2017)
PVDF	Tetrabutylammonium chloride/ fluorinated acrylate copolyme	135	0.26	210	71.34	40	54.39	>99.5	-	(Z. Li et al., 2019)
PVDF (15)	Reduced graphene oxide (0.039)	124.5	-	69.7	-	45	29.94	99.7 (0.1 wt% NaCl) 98.16 (60.84 mg B/L)	AGMD	(Eryildiz, Ozbey-Unal, et al., 2021b)
PVDF (8)	Silica	153.9	0.77	179	83	40	18.9	>99.9	DCMD	(Y. Liao et al., 2014b)
PVDF	Clay nanocomposite	154.2	0.64	200	81	65	~6	99.97 (3.5 wt% NaCl)	DCMD	(Prince et al., 2012)
PVDF (18)	-	130	-	-	-	45	~6.5	>99.5 (3.5 wt% NaCl)	AGMD	(Feng et al., 2008)
PVDF (13.5)	Fluoroalkyl silane-SiO_2	154.6	0.27	143	77	50	11.5	~99.9 (3.5 wt% NaCl)	VMD	(Yadav et al., 2022)
PVDF (15)-PTFE (12)	-	152.2	0.49	137	69	-	18.5	~99.9 (3.5 wt% NaCl)	VMD	(Dong et al., 2014b)

5.4 Conclusion

This work presents the first use of benzoxazine blended nanofiber membranes for MD application. The hydrophobic nanofiber membranes were fabricated by electrospinning of PVDF and PVDF/BisF-Bz blend solution. The effect of PBz and the effect of crosslinking on the properties of nanofibrous membranes were investigated. The contact angle of the membranes significantly increased from 102.8º for pristine membrane to 132.7º by BisF-Bz addition and crosslinking. The mechanical

properties of membranes enhanced while the thickness of membranes decreased and smoother membranes were obtained with addition of benzoxazine and crosslinking steps.

The nanofiber membranes were tested through VAGMD using three different feed water samples, NaCl, synthetic boron solution and RO brine. The lowest permeate flux was 15 $L/m^2.h$ for the pristine membrane with RO-B feed. Boron removal efficiencies of nanofiber membranes were determined and all results were higher than 90%. Compared to the pristine PVDF membrane, PVDF/PBz membrane had the higher flux, higher salt and boron rejection. All these results indicated that PBz blended PVDF nanofiber membranes could have a great potential to be a good candidate for membrane distillation.

6. EFFECT OF DIFFERENT PARAMETERS ON MEMBRANE CONCENTRATE TREATMENT BY USING VACUUM ASSISTED AIR GAP MEMBRANE DISTILLATION/CRYSTALLIZATION (VAGMD/C)[4]

6.1 Introduction

Membrane processes have great potential to fulfill the increasing demand for freshwater due to the increasing population (Balis et al., 2022; Salehi, 2022). Desalination plants can produce fresh water from saline water which makes it attractive especially for coastal regions. Although it is very efficient the high concentration brine formation is the main handicap that requires additional treatment so the brine management has received attention.

Boron is an element that has widespread application(Wolska & Bryjak, 2013). It is used in several industries as glass, detergent, and ceramic(Parks & Edwards, 2005) Although boron is an essential nutrient it can be harmful at higher concentrations. Boron exists as a pH-dependent borate salt of boric acid in the environment. Borate anion is found at higher pH while boric acid is dominant at lower pH (Mutlu-Salmanli & Koyuncu, 2022; Tagliabue et al., 2014b) The non-charged boric acid form can generally pass through membranes and so the removal efficiency of RO is only 40%-80% which means the acceptable boron limits by WHO are exceeded (Tang et al., 2017; S. Wang et al., 2022).

Cengeloglu et al. studied boron removal from water with 3 different RO membranes and they stated that 99% removal was achieved only the waters which have pH 11 (Cengeloglu et al., 2008) According to the study conducted by Oo and Song, boron

[4] This chapter is submitted to Desalination – Oyku Mutlu Salmanli and Ismail Koyuncu. "Effect of Different Parameters on Membrane Concentrate Treatment by Using Vacuum Assisted Air Gap Membrane Distillation/Crystallization (VAGMD/C)"

removal at pH 10 was 81% for 500mg/L boron concentration whereas 61% at pH 9 (Oo & Song, 2009).

Membrane distillation (MD) is one of the brine management technology. MD is known as an alternative to the desalination. MD is a thermally driven membrane process where the hydrophobic membranes are utilized. The vapor pressure difference is the driving force for MD (Pangarkar et al., n.d.; Srisurichan et al., 2006). Although MD is a thermally driven separation process it does not require as high temperature as conventional distillation (Choi, Naidu, et al., 2019; Yun et al., 2006). Although MD is quite effective method for boron removal, recovery needs to be carried out to ensure sustainability. Boron is one of the critical raw materials listed by the EU which means the recovery is also important for the circular economy approach (European Commission, 2023; Keersemaker, 2020). Membrane distillation-crystallisation (MDC) is a promising technique for water and resource recovery which is the combination of MD and crystallization. The addition of crystallization enhances the crystal growth and nucleation (Balis et al., 2022; Sparenberg et al., 2021)

In this study, vacuum-assisted airgap membrane distillation/crystallization (VAGMD/C) was investigated to remove and recover boron from RO concentrate. Synthetic boron solutions were used prior to the real RO concentrate. Different concentrations, different membranes and different pH were used to determine the effect of the process. Flux values and boron removal efficiencies were calculated. Boron removal from RO concentrate was conducted as long term. Obtained crystals were analyzed to examine the content of crystals.

6.2 Material Methods

6.2.1 Experimental setup

The lab-scale VAGMD/crystallization system was operated for the experimental investigations. The left side of the membrane module was the feeding side, the hydrophobic flat sheet membrane was placed in the middle of the module and thecooling part was the right side. Feeding tank capacity was 2L. Heating (Lab Companion-CW05G) and cooling tanks (Lab Companion-RW0525G) were used to adjust desired temperatures. Peristaltic pumps (Masterflex L/S) were used in both the feeding and cooling side to provide water flows. The vacuum pump was used to create

vacuum pressure on the permeate side of the membrane module. Permeate water was collected in the bottle and measured for water flux calculation. The effective area of the membrane was 44.18 cm^2. The conic heat-jacketed custom-made metallic crystallization tank was placed on the concentrate side which is the feeding side of VAGMD. The warm concentrate flowed back to the feeding tank from the membrane module and that concentrate was fed to the crystallization tank. The crystallization tank was cooled to 20 ±3 °C by using Lab Companion RW3-2025 bath circulator.

6.2.2 Experimental and operation procedure

In this study, different boron-contented synthetic feed waters and real RO brine were used. H_3BO_3 (Merck) was dissolved in ultra-pure water (<0.055 μS/cm, Sartorius, France) for preparing synthetic boron solutions. pH value of feed water was adjusted by using NaOH (Merck) and H_2SO_4 (Merck) solutions. Ion chromatography (IC) (Dionex ICS-3000) was used to measure the ionic content of feed and permeate waters. Analytical grade reagents were used and analysis was conducted at 30°C. 0.5M $NaCO_3$ was the anion eluent and 19 mM methanesulfonic acid was the cation eluent. The boron content of feed and permeate waters was measured by using Optima 7000 DV Inductively Coupled Plasma- Optical Emission Spectrophotometers (ICP-OES by Perkin Elmer). The five-point calibration was conducted by using a 1000 ppm B solution (inorganic ventures) and a 3% nitric acid solution prepared by using 65% HNO_3. All samples were measured three times.

Feedwater was heated to 70 °C by using a heating tank and circulated with a 1.4 L/min flow rate. The cooling water temperature was adjusted to a 20 °C flowing rate of 480 mL/min. The membrane module has a 7 mm air gap width. Vacuum pressure was 0.08 bar. Three different polymeric-type membranes were used in this study polyvinylidene fluoride (PVDF), polytetrafluoroethylene (PTFE), and polypropylene (PP). PP membranes were supplied from GE Water, PVDF and PTFE were purchased from Sterlitech. The properties of membranes were given in our previous study (Mutlu Salmanli et al., 2022b). PVDF and PVDF/Bz membranes were fabricated as reported in a previous study (Mutlu-Salmanli et al., 2023).

The cooling water at 20±3 °C was supplied by using a cooling tank to the crystallization tank. The content of the crystallization tank was mixed mechanically at

50 rpm for 72 h duration. The collected crystal samples were analyzed by a semi-quantitative X-ray fluorescence (XRF) device at METU Central Laboratory.

6.2.3 Performance evaluation of VAGMD/C system

The permeate water flux (J, L/m^2h) was calculated by using following equation(Abdelrazeq et al., 2020; M. A. E.-R. Abu-Zeid et al., 2015);

$$J = \frac{\Delta m}{A\,\Delta t} \tag{6.1}$$

Where Δm is the cumulative amount of the collected permeate water (kg), A is the effective membrane area (m^2) and Δt is the testing time (h).

The boron removal efficiency (R) was calculated by using the following equation;

$$R(\%) = \left(\frac{c_f - c_p}{c_f}\right) x100 \tag{6.2}$$

where c_f is the feed water boron concentration and c_p is the permeate water boron concentration.

Three main mechanisms control the mass transfer of the membrane distillation; molecular diffusion, Knudsen diffusion and Poiseuille flow. The proportion of the mean free path of the molecules being transported to the membrane pore diameter is known as the Knudsen number (Kn), which is the dominant mechanism in membrane distillation. Knudsen number can be calculated by following equation (Khayet, 2011; Sarbatly & Chiam, 2013);

$$\mathrm{K_n} = \frac{\lambda}{\mathrm{d}} \tag{6.3}$$

where λ is the mean free path of the vapor molecules and d is the membrane pore diameter.

6.3 Results and Discussion

6.3.1 VAGMD-C tests with synthetic boron solution

Before real RO brine tests the synthetic boron solution tests were conducted with vacuum-assisted air gap membrane distillation system. The concentration of synthetic

boron solutions was between 250-5000 mg/L. A commercial PVDF membrane was used. Permeate water flux and boron removal efficiencies were determined. Water flux and boron removal efficiency for all solutions at 70°C feed water temperature are presented in Figure 6.1. Flux values differed slightly thanks to the fact that MD is not much affected by inlet concentrations (Kabay & Bryjak, 2015; Mutlu-Salmanli et al., 2023; Najid et al., 2021). Regardless of the inlet boron concentration, the boron rejections were higher than 99% for all boron concentrations. However, after the crystallization process crystals were observed just for 5000 mgB/L so the following experiments continued with that concentration.

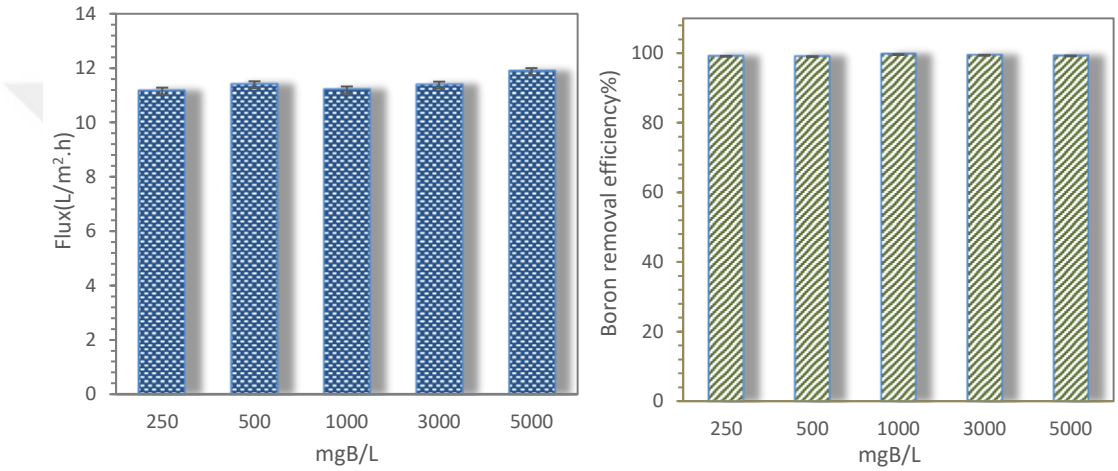

Figure 6.1 : Average permeate water flux and boron removal efficiency at different inlet concentrations.

After selecting the boron concentration experiments were conducted under different pH values of 5.5, 8 and 9.3. Boric acid (H_3BO_3) can be found as a borate ion form at higher pH. Since it is stated in the literature that the retention of borate ions in membranes is higher than in boric acid (Freger et al., 2015), the study was also tested by increasing the pH to see the effect of pH. The conversion between boric acid with a pKa of 9.1 and borate ion is expressed in the equation below (Guan et al., 2016; Mutlu-Salmanli & Koyuncu, 2022; Tagliabue et al., 2014b)

$$B(OH)_3 + H_2O \leftrightarrow B(OH)_4^- + H^+ \quad (6.4)$$

When the pH rises above the pKa value of 9.1, there are more borate ions in the water. Considering the boron removal efficiencies at these pH values (Figure 6.2), it was observed that the removal efficiency increased slightly with the increase in pH and higher than 99% for all pH values. In addition, crystal formation was higher at pH 9.3.

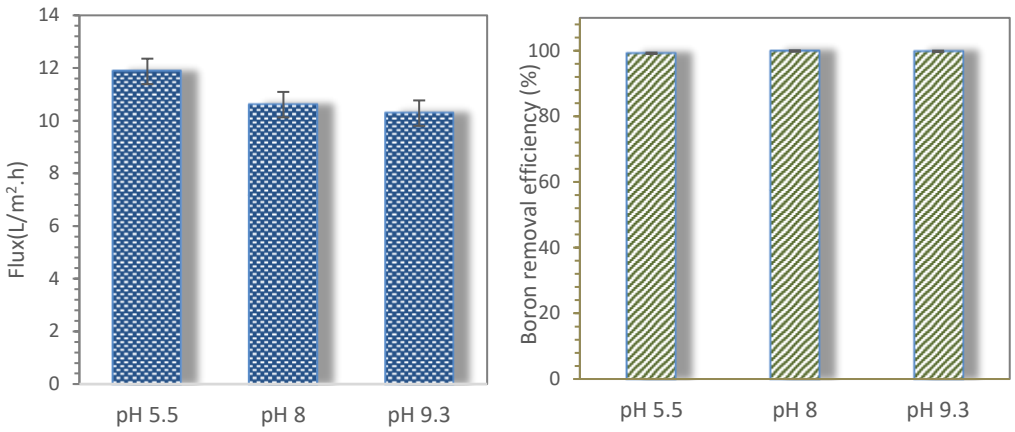

Figure 6.2 : Average permeate water flux and boron removal efficiency, at different pH.

Since crystallization was not very effective for pH 8 it was not selected for further studies. To evaluate the impact of membrane material on the permeate flux and removal efficiency was examined. The results are given in Figure 6.3.

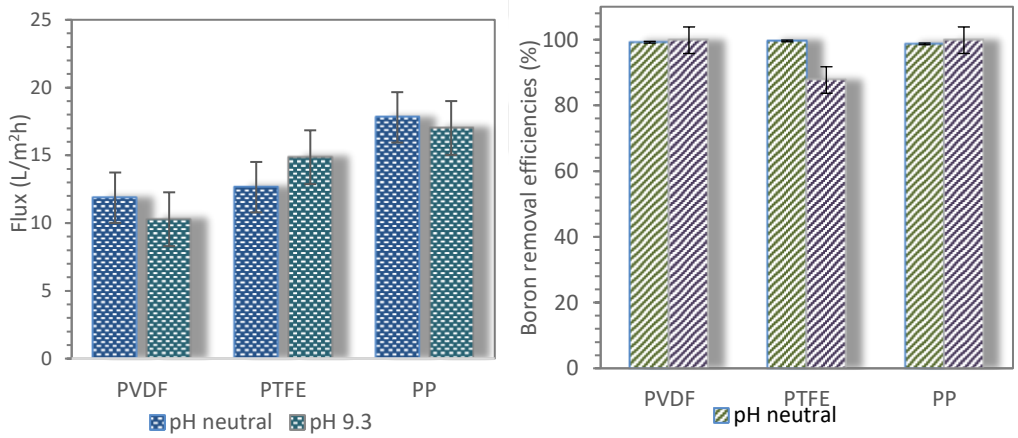

Figure 6.3 : Average permeate flux and boron removal efficiency at different pH and membrane types.

Figure 6.4 : PTFE membrane after experiment conducted at pH 9.3.

Due to the additional components for pH adjustment, the flux values at pH 9.3 were lower than the neutral pH of the solution except for PTFE. Membrane wetting occurred

for PTFE at higher pH so the flux increased (Figure 6.4). PP-type membrane showed higher flux values similar to the previous studies which is related to the membrane thickness. The heat conduction to the other side of the membrane decreases with the increasing thickness which means lower heat and mass transfer. Transmembrane flow is constrained by the membrane structure, which reduces the ease of penetration (Eykens, Hitsov, et al., 2016; Mutlu Salmanli et al., 2022b; Swaminathan et al., 2018a; H. Y. Wu et al., 2014). The concentrated feed water was transferred to the crystallization tank at 20±3 °C 50 rpm for 72 h after VAGMD experiments were done.Due to the increasing dissolution of boric acid with temperature, cooling crystallization was applied. The crystal structures can be seen from the SEM images (Figure 6.5)

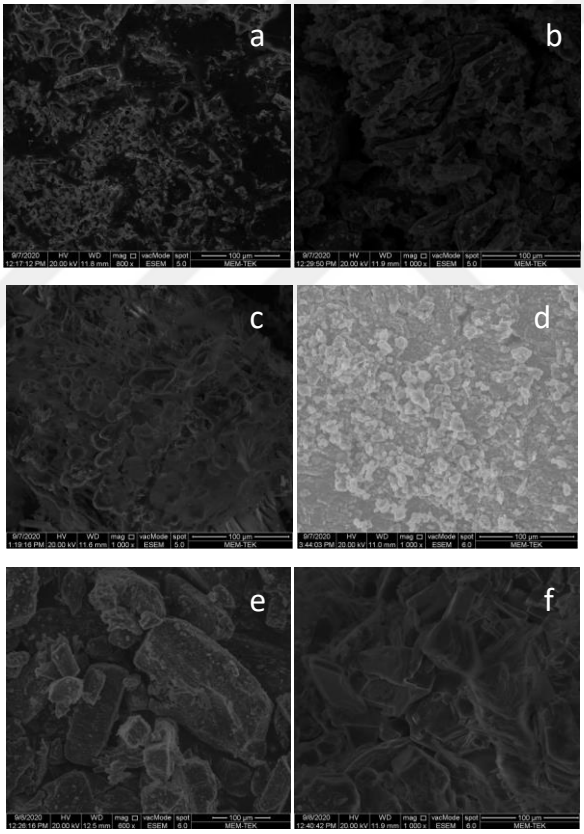

Figure 6.5 : SEM images of crystal from a) PVDF at neutral pH b)PVDF at pH 9.3 c) PTFE at neutral pH d) PTFE at pH 9.3 e)PP at neutral pH and f) PP at pH 9.3.

6.3.2 VAGMD/C tests with real RO concentrate

VAGMD/C process was operated to remove and recover boron from real RO concentrate. 3 different types of membranes were operated long-term at neutral pH of brine which is around 7. Permeate water flux of PP was the highest while PVDF was lowest similar to the synthetic boron solution studies. The permeate water flux

decreased when the bulk concentration increased with time according to Raoult's law since the mole fraction of water (Xi) decreases with the increasing solid fraction which is proportional to the partial pressure (Howard Devoe, 2001; S. Kim et al., 2018; Qtaishat et al., 2008) Due to the increasing feed concentration the viscosity of feed increase and this led to the thicken the concentration boundary layer which decreases the permeate flux (Han et al., 2022)

$$P^S = P^v(1 - X_i) \tag{6.5}$$

where x_i is the mole fraction of solid in the bulk liquid, P^s is the partial vapor pressure of water at Pa and P^v is the partial vapor pressure of pure water at Pa. To evaluate the system performance with real concentrate at pH 9.3 PP membrane was tested. After commercial membranes were fabricated electrospun nanofiber membranes were also tested in terms of concentrate treatment.

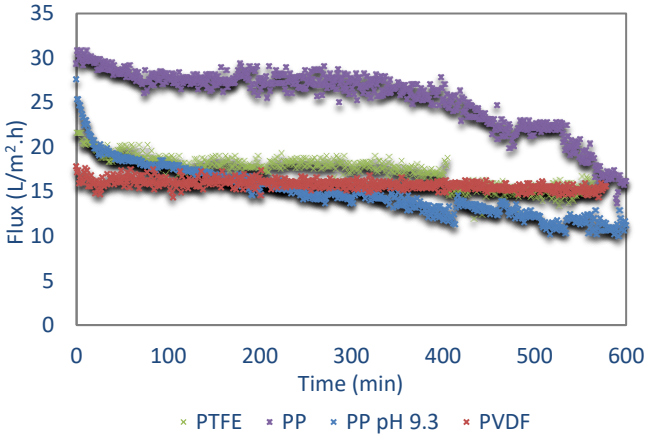

a

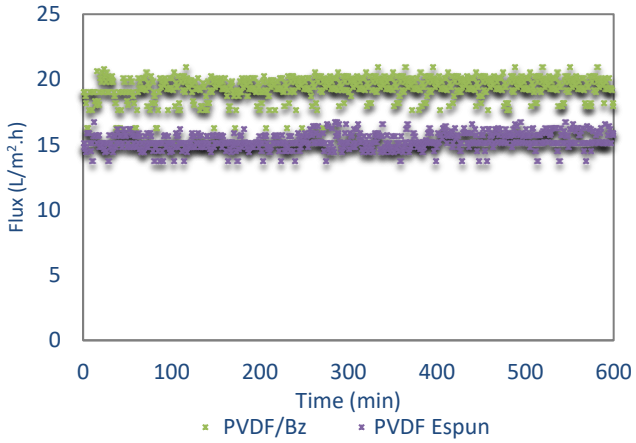

b (Mutlu-Salmanli, et al., 2023)

Figure 6.6 : Permeate water flux of a) commercial membranes, b)fabricated membranes in real concentrate.

Table 6.1 : Boron concentrations in feed, permeate and concentrate water for real RO concentrate.

Membrane	MD feed (mg/L)	MD permeate (mg/L)	MD concentrate (mg/L)	Boron Removal Efficiency (%)
PTFE	4953	41.56	19230	99.16
PVDF	5377	25.72	24920	99.52
PP	3633	35.08	26310	99.03
PP pH 9.3	4778	1.52	35220	99.96
PVDF Espun*	4823	478.98	17260	90.06
PVDF/Bz*	5231	60.24	17890	98.85

*(Mutlu-Salmanli, et al., 2023)

Flux decrease in time can be seen in Figure 6.6 a for commercial membranes. The precipitation and crystallization on the membrane surface can lead to a higher flux decrease in real concentrate. However permeate water flux is much more stable during experiment time for nanofiber membranes which showed it wasn't affected by scaling or fouling (Mericq et al., 2010). Boron removal efficiencies as can be seen in Table 6.1. And the feed boron concentrations were between 3633 and 5377 mg/L where concentrate water boron concentrations were increased up to 35220 mg/L which proves the efficiency of a system in terms of boron removal. The ion content of both feed water and permeate water for this study is given in Table A.1.

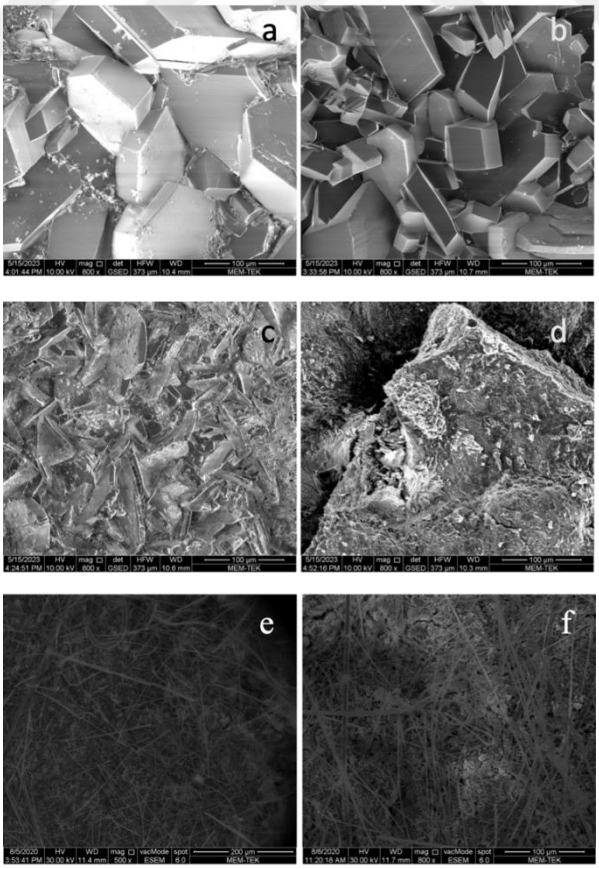

Figure 6.7 : SEM images of a) PTFE, b)PVDF, c)PP, d)PP at pH 9.3, e) PVDF/Bz and f) PVDF espun membranes at the end of long term VAGMD.

SEM images of membrane surfaces after long-term treatment are given in Figure 6.7. Crystal formation was obvious in the commercial membranes however fiber structure of developed membranes were not covered by crystals. This proves the nanofiber membranes didn't affected by scaling or fouling as stated above. And EDS images (Figure A 1-3). The XRF results as given in Table 6.2 which shows the B_2O_3 content of obtained crystals. Results showed that it was possible to reach the boron content up to 44.6%. The pH increment lowered the purity of crystals in terms of boron and the lowest B_2O_3 amount was obtained from the crystals of 0.45 PP membrane at pH 9.3. Fabricated nanofiber membranes gave higher results in terms of B_2O_3 content.

Table 6.2 : XRF analysis result of obtained crystals.

Compound (wt%)	**Membrane**					
	PVDF Espun	**PVDF/Bz**	**0.45 PVDF**	**0.45 PTFE**	**0.45 PP**	**0.45 PP pH 9.3**
Na_2O	4.69		8.34	3.37	7.18	37.0
MgO	14.7	2.52	17.4	14.9	14.0	11.7
K_2O	0.239	0.219	0.714	0.310	0.754	0.366
CaO	9.59	9.99	1.96	11.5	1.96	5.88
CO_2	16.7	23.1	17.5	13.8	17.4	11.6
Cl	1.59	0.935	5.36	2.05	4.38	3.95
MnO		0.0389	0.129		0.136	0.0591
Fe_2O_3	0.110	0.0661		0.219	0.0577	0.0230
NiO	0.0811	0.107	0.0502	0.0764	0.0508	0.0214
CuO	0.0157	0.0531		0.0245	0.0144	
						0.0082
ZnO	0.160	4.46	0.0823	0.537	0.337	0.0253
Al_2O_3	0.0665	0.0545	0.0412	0.0846	0.0770	0.0544
SiO_2	0.412	0.539	0.523	0.493	0.655	1.01
P_2O_5	0.0339	0.0137	0.0394	0.515	0.0427	0.0383
SO_3	18.7	13.0	23.5	21.5	22.4	16.3
As_2O_3	0.108	0.0452	0.267	0.198	0.297	0.130
SrO	0.904	0.232	0.157	0.414	0.172	0.144
Rb_2O			0.0065		0.0088	
Cr_2O3	0.0339			0.0535		
B_2O_3	**31.9**	**44.6**	**23.9**	**30.4**	**30.1**	**11.7**

6.4 Conclusion

VAGMD/C was evaluated for removal and recovery of boron from RO concentrate. Synthetic boron solution and real RO concentrate were fed to the VAGMD by using different membranes and different pH values. Concentrated brine with VAGMD was further concentrated with the crystallization process. Experiments showed the efficiency and capability of the VAGMD/C system in terms of boron removal and

recovery. According to the results discussed above, the following conclusions can be made:

- Since the increasing concentration permeate water flux decreased at higher pH for commercial membranes
- Compared to the commercial PVDF and PTFE membranes, permeate water flux values were higher for PP membranes.
- Permeate water flux was constant for fabricated nanofiber membranes during experiment time which shows fabricated membranes were more resistant to scaling and fouling compared to commercial membranes.
- Up to 44.6% B_2O_3 contented crystals were obtained successfully.
- The VAGMD/C process is effective for boron removal and recovery from high boron-contented waters.

7. BORON REMOVAL AND RECOVERY VIA VACUUM ASSISTED AIR GAP MEMBRANE DISTILLATION-CRYSTALLIZATION (VAGMD-C): A PILOT-SCALE STUDY[5]

7.1 Introduction

Boron is an essential element with a wide range of usage areas in industrial facilities. Glass, semi-conductor, leather, detergent, drug, and cosmetics are some of these industries. The procedures of these industries cause boron-contained wastewater formation(Özdemir & Kıpçak, 2010; Öztürk et al., 2008). Boron can also be found naturally in waters, depending on the properties of the region. Turkey has the most significant percentage (53%) of the world's natural reserves of boron ores (Boncukcuoğlu et al., 2003). The boron industry in the area results in highly concentrated water that needs to be treated; this water was used in this study. Aside from industrial requirements, humans and plants also need boron through dietary intake and as a micronutrient in a certain amount. Although boron is crucial for plant growth, it can be toxic when it exceeds the tolerance limit, which changes for every plant. Yellow leaf, detention of development, and even plant death occur when the limit values are exceeded (Guan et al., 2016; Hilal et al., 2011). An excessive amount of boron can also cause some diseases in human beings, i.e., diarrhea, anorexia, vomiting, and skin problems (Kot, 2015; Wolska & Bryjak, 2013). WHO has set the limit values for drinking water to be 2.4 mg/L in 2011. Due to this limit, the value is pretty high; many countries comply with their limitations. To preserve plants, the irrigation water boron limit value is lower than 0.3 mg/L (Freger et al., 2015; Guan et al., 2016; Tagliabue et al., 2014). Adsorption, ion exchange, precipitation, electrocoagulation, and membrane processes are some techniques for removing boron

[5] This chapter is based on' Oyku MUTLU SALMANLI, Anil KAZAK, Turker TURKEN, Mehmet Emin PASAOGLU, Bihter ZEYTUNCU and Ismail KOYUNCU (2023) *Boron removal and recovery via vacuum assisted air gap membrane distillation-crystallization (VAGMD-C): A pilot-scale study'*, Desalination, 547, 116229, https://doi.org/10.1016/j.desal.2022.116229

from waters that are found in the literature (da Silva Ribeiro et al., 2019; Köse & Öztürk, 2008; Ngwabebhoh et al., 2019; Shih et al., 2014). Due to some limitations of conventional methods, membrane processes have gained popularity in the last decades (Bártová et al., 2016; Boubakri et al., 2015; Bunani et al., 2017; Lan et al., 2021; Y. Li et al., 2020; Melnyk et al., 2005; Ozbey-Unal et al., 2018; Wang et al., 2018).

Reverse osmosis is a desalination technique that is used widely. The RO process is also used to remove boron from seawater in the literature (Güler et al., 2011; Taniguchi et al., 2004; Tu et al., 2010; Xu et al., 2010). However, pH is the main limitation of boron removal with RO. Under acidic conditions (pH<9), boron is generally found as boric acid, which can pass through membranes. Newly developed membranes (Lan et al., 2021; Y. Li et al., 2020; Wang et al., 2018) and different processes combined with RO (Ban et al., 2019; Farhat et al., 2013; Güler et al., 2011; La Cerva et al., 2019; Tomaszewska & Bodzek, 2013) are studied in the literature to enhance boron removal efficiency by using RO.

Membrane distillation is a thermally driven separation process that combines the distillation and membrane process. The main idea is to pass water vapor through membrane pores instead of water molecules. Hydrophobic membranes are used to achieve this goal. MD does not require temperatures as high as conventional distillation. Additionally, it has lower energy consumption than RO due to the lower pressure requirement. MD is also less susceptible to the highly concentrated feed waters [23,24]. Thus, it is advantageous, particularly for complex wastewaters which contain much more contaminants. In the literature, there are studies for boron removal which successfully use MD. Wen et al. achieved 99.97% boron removal efficiency for radioactive wastewater treatment, which contained 5000 ppm boron by using direct contact membrane distillation (DCMD) (Wen et al., 2016) Jia et al. investigated the vacuum membrane distillation for the treatment radioactive wastewater with contents of 10000 ppm boric acid and 550 ppm salt.. They reported that the boron rejection ratio was over 99.9% (F. Jia et al., 2017). In the seawater treatment via DCMD that was conducted by Boubakr et al., more than 90% removal efficiency of boron was achieved for the initial boron concentration of 5.37 ppm (Boubakri et al., 2015). A self prepared PVDF membrane was successfully tested in the DCMD system by Hou et al. Their feed water was natural seawater; the boron concentration was 4.65 ppm with a the salt concentration of 35000ppm. The boron removal efficiency was over 99.5%(Hou

et al., 2013). Air gap membrane distillation configuration was also a successful option for boron removal, according to the study conducted by Eryildiz et al. Higher than 90% boron removal efficiency was obtained for wastewaters with high boron content (Eryildiz et al., 2021). Geothermal waters, rich in boron and different anions and cations, were also tested using MD. 60 ppm boric acid in the feed solution was reduced to 0.145 ppm, which means that higher than 99.5% boron removal efficiency (Ozbey-Unal et al., 2018) and higher than 99.3% removal was achieved for fabricated electrospun nanofiber membranes (Ozbey-Unal et al., 2020). All these studies above are lab-scale tests. There are pilot scale studies of MD in the literature (Dow et al., 2016; Eykens et al., 2018; Gil et al., 2018; X. Jia et al., 2021; Lee et al., 2020; Palenzuela et al., 2018; Sun et al., 2015); however, none of them focus on boron removal. Removal is essential, but it is not sufficient alone. For a sustainable world, the recovery of sources is significant (Mutlu-Salmanli & Koyuncu, 2022). On the lab scale, there are a few studies about boron recovery [12,26], whereas there is no study on the pilot scale. For recovering salts from highly concentrated waters, the crystallization process combined with MD is a promising method (Choi et al., 2017, 2018; Edwie & Chung, 2013; Naidu et al., 2018; Tun et al., 2005). However, there is no study about pilot scale membrane distillation-crystallization for boron removal and recovery in the literature.

In this study, both the raw water, containing high boron concentrations, and the RO concentrate of this raw water were treated using pilot scale vacuum assisted air gap MD (VAGMD) and crystallization for the removal and recovery of boron. Different recovery rates were applied and the flux, conductivity, vacuum pressure, flow rate of MD system were observed. The removal efficiencies of boron, arsenic, conductivity, and hardness were analyzed for both feed, permeate, and concentrate waters. The obtained crystals following the crystallization process were analyzed in relation to boron content.

7.2 Materials & Methods

7.2.1 Experimental setup

The MD pilot scale setup used in this study was purchased from Aquastill (The Netherlands) and comprised of a spiral wound AGMD membrane module (Figure 7.1).

The pilot unit is made from modular aluminum building elements easily adapted to the required conditions. The technical data of the system is given in Table 7.1.

Figure 7.1 : Pilot scale MD unit.

The MD module had 6 hot and 6 cold parallel channels with a length of 1.5 m and was arranged in counter-current flow. Each hot channel has 2 membrane sides. The system had 2 heat exchangers for waste heat input and cooling and automatic feed and discharges of process streams. The membrane material is polyethylene (PE), with a 7.2 m^2 area in the module with a 4.2 bar liquid entry pressure value, a nominal pore size of 0.16 μm, a porosity of 80%, and a thickness of 10 μm. Mesh spacers inserted into hot and cold brine channels were made of PP with a thickness of 1.016 mm. Mesh spacers with a thickness of 0.34 mm were used between condenser and evaporator channels. By changing the connections, the pilot system can use multiple modules such as AGMD and V-AGMD. Generally, a membrane can produce 2-15 L/m^2h distillate based on the process conditions, and fluxes generated in normal practical conditions are between 2-5 L/m^2h. The setup has the main control screen that adjusts the feed water temperature, feed water, and condensate flow. The data obtained can be viewed instantly on the P&ID diagram on the control screen. The P&ID of MD unit is given in Figure 7.2.

Table 7.1 : Technical data of pilot MD.

Module		Cooling circuit	
Max. Brine temperature	80 °C	Max. cooling temperature	45 °C
Min. Brine temperature	2 °C	Min. Pressure.	3.5 bar
Max. Allowable pressure	0.6 bar	Max. Allowable pressure.	10 bar

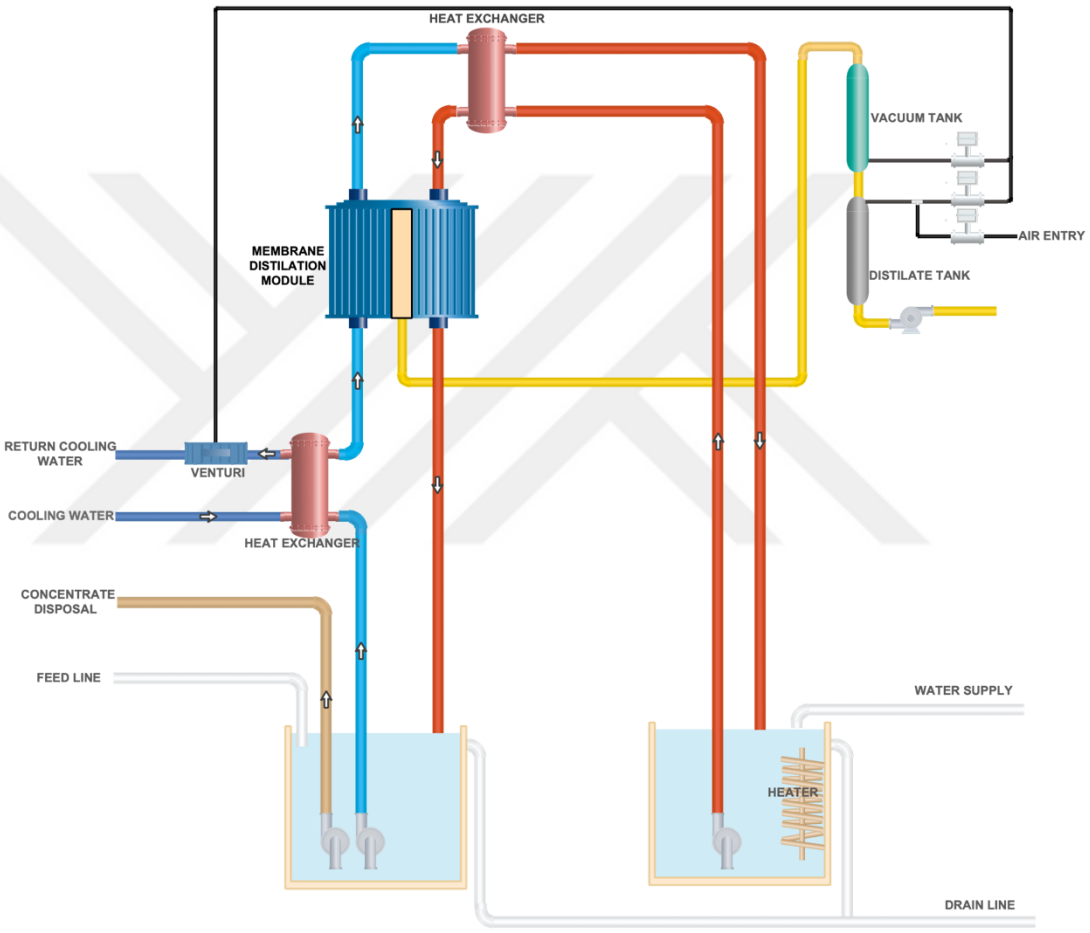

Figure 7.2 : P&ID of pilot scale MD unit.

7.2.2 Experimental method

The Aquastill branded pilot MD system was used to treat different water streams. In the first series of experiments, water with a conductivity value of 35 mS/cm was fed to the system. The obtained permeate has a 0.08 mS/cm conductivity value when feeding at 60°C. The feed water circulation rate was 800 L/h, and after optimizing the system settings, pilot scale membrane distillation was applied under the same operating conditions to the water stream obtained from the river.

Table 7.2 : Properties of River water.

Parameter	Value
B, ppm	2272
As, ppm	3.28
Hardness, ppm	2627
pH	7.11
Conductivity, µs/cm	4404

In the studies applied to the raw water, the MD system primarily operated in batch mode. The characteristics of raw water are given in Table 7.2. The system was operated at different recovery rates as; 50%, 70%, 75%, and 80%. The system was operated in batch mode by observing the operation parameters, and an 85% recovery rate was also reached. Flux, flow rate, conductivity, and vacuum pressures were observed for 3 hours of the experiment duration, and results were given as values vs. time graphs. The removal efficiencies of boron, arsenic, hardness, and conductivity were also calculated. After different recovery ratios were tested in batch mode, the MD system was operated in continuous mode. Two repeated studies were conducted for continuous mode for approximately 36 hours. Different recovery rates were tested, and a 90% recovery rate was obtained. 80% stable recovery rate was also tested. After raw water studies, the MD pilot system was tested using RO concentrate water from a river. The system was operated at 3 different recovery rates, which are 50%, 70%, and 75%. Flow rate, flux (J), vacuum pressure, and conductivity values were observed for the duration of the experiments, and the graphs were drawn as values vs. time. J ($Lm^{-2}h^{-1}$) depicts the production capacity of MD and was calculated by the following equation (Abu-Zeid et al., 2015);

$$J=\frac{\Delta m}{A.\Delta t} \tag{7.1}$$

Where Δm is the amount of permeate water (kg), A is the effective surface area of the membrane used in the membrane module (m^2), and Δt is the operating time (h). The link between the permeate flux and the vapor pressure difference across the membrane in the MD process is typically stated as follows according to the Darcy's Law (Attia et al., 2017; Liu et al., 2017):

$$J = Cm\Delta P \tag{7.2}$$

where Cm is the transmembrane mass transfer coefficient, ΔP is the mass transfer's driving force of the pressure difference. The Antoine equation can be used to determine the water vapor pressure(B. Li & Sirkar, 2005; Liu et al., 2017; Sun et al., 2015):

$$P = \exp\left[23.1964 - \frac{3816.44}{T - 46.13}\right] \tag{7.3}$$

The proportion of the mean free path of the molecules being transported to the membrane pore diameter is known as the Knudsen number (Kn), which is the controlling mechanism in membrane distillation (Khayet, 2011)

$$K_n = \frac{\lambda}{d} \tag{7.4}$$

where λ is the mean free path of the vapor molecules and d is the membrane pore diameter.

The Knudsen and molecular diffusion mechanisms take place together which the mass transfer is controlled by, when $0.01 < Kn < 1$. C_{kn}, the permeability coefficient of Knudsen diffusion, and Cmol, permeability coefficient of molecular diffusion and Cm, the total permeability coefficient, can be calculated by the following equations(Alkhudhiri et al., 2012; Khayet et al., 2004):

$$C_{Kn} = \frac{1}{3}\left(\frac{8m_w}{\pi R(T_m + 273.15)}\right)^{0.5} \frac{\varepsilon d}{d_m \tau} \tag{7.5}$$

$$C_{mol} = \frac{D_{w-a} P_{tm}}{P_m} \frac{\varepsilon}{d_m \tau} \frac{m_w}{R(T_m + 273.15)} \tag{7.6}$$

$$C_m = \left(\frac{1}{C_{Kn}} + \frac{1}{C_{mol}}\right)^{-1} \tag{7.7}$$

where mw is the molecular weight of water, ε is the membrane porosity, d is the membrane pore diameter, Tm is the average membrane temperature, R is the gas constant (8.134 J/mol°C), d_m is the thickness of membrane, τ is the membrane pore tortuosity, Ptm is the total pressure in the membrane pore, D_{w-a} is the diffusion

coefficient of the vapor molecules in air and Pm is the log-mean air pressure at membrane's both side.

Where the pore size is far less than the mean free path, the Knudsen mechanism is the controlling mechanism for mass transport (Kn>1). When the pore size is greater than the mean free path (Kn<0.01), the molecular diffusion mechanism is the dominant mechanism. In AGMD processes, since the partial pressure of the NCGs is nearly equal to atmospheric pressure, the Knudsen mechanism can be neglected. Therefore. the mass transfer occurs through the molecular diffusion mechanism (Cheng et al., 2009; Liu et al., 2017).

For the VAGMD process, there will be pressure gradients in the air gap; thus, the viscous flow can no longer be disregarded. Moleculer diffusion will finally stop once all of the NCGs have been eliminated (Fan & Peng, 2012; Liu et al., 2017).

Specific energy consumption (SEC) is the ratio of total energy consumption to the weight of distillate produced which can be calculated using the following equation (Abu-Zeid et al., 2016; Couto et al., 2020).

$$SEC = \frac{EC}{W} \tag{7.8}$$

The removal efficiencies of boron, arsenic, hardness, and conductivity were calculated according to Eq. 1, where the Cf is the concentration of feed solution, and Cp is the permeate solution.

$$R(\%) = \left(1 - \frac{C_p}{C_f}\right) x100 \tag{7.9}$$

Boron (B) and arsenic (As) in the solutions obtained during the studies were analyzed with an inductively coupled plasma optical emission spectrometer (ICP-OES, Perkin Elmer Optima 7000DV).

Concentrate waters obtained from the MD system had high pollutant content. The crystallization process was applied to these concentrates. Since boric acid dissolution decreases with decreasing temperatures, the crystallization process was conducted by cooling. 20±3 °C temperature was supplied with a cooling bath while the mechanical mixer applied a 50 rpm mixing rate. Semi-quantitative X-ray fluorescence (Rigaku ZSX Primus II) was used to characterize recovered precipitates. In these experiments, for the reuse of solids in the production process, the most critical parameter. B2O3,

was investigated. The MD system was used in two separate studies on raw water and RO concentrate treatment.

7.3 Results

7.3.1 Raw water experiments

The pilot scale membrane distillation tests were carried out in an Aquastill pilot scale V-AGMD system to treat river water with higher boron content, as seen in Table 7.2. The raw water from that river was first used as feed water directly to the MD system in batch mode experiments. For the 3 hour experiment duration, 50%, 70% 75%, 80% and 85% recovery rates were used. In the MD study, where raw water was fed directly, raw water was fed to the MD system continuously. In the graphs given in Figure 7.3, the results obtained in 180 minutes of all recovery rates are shared in order to show them as an equal time interval from the moment the recovery rates of 50%, 70%, 75%, 80% and 85% are reached in the MD system. The total time taken to reach each recovery rate within the scope of the study were found to be: 180 minutes for 0% to 50% recovery rate, 285 minutes for 50% to 70% recovery rate, 180 minutes for 70% to 75% recovery rate, 180 minutes for 75% to 80% recovery rate, 80% 405 minutes for a recovery rate of 80% to 85%. Permeate flux, permeate flow rate, vacuum pressure, and conductivity values change were observed during the operation period. According to the results, input conductivity values increased by 30-38% in each recovery at the end of the 3-hour operating time. In comparison, an approximately 17% permeate flow rate decrease was observed in each recovery rate (Table 7.3).

Table 7.3 : Recovery rates vs. average permeate fluxes.

Recovery Rate (%)	Average flux (L/ m^2h)
50	3.16
70	2.75
75	2.52
80	2.4
85	2.39

The flux difference is higher between 50% and 70% recovery rates than between 70% and 75% recovery rates since the distinction between ratios was higher. Due to

obtaining a more concentrated stream, the conductivity increment is higher when the recovery rate is higher. Vacuum pressures were between 0.15 bar and 0.20 bar with increasing recovery rates. Higher conductivity resulted in higher vacuum pressure. Although the input conductivity values differed widely, the permeate flow rate for different recovery rates did not change as much as the conductivity, which can be attributed to the fact that the MD is not largely affected by the inlet concentrations (Kabay & Bryjak, 2015; Najid et al., 2021). When the salt concentration exceeded 80 g/L, a decline in trend becomes more apparent (Xu et al., 2016).

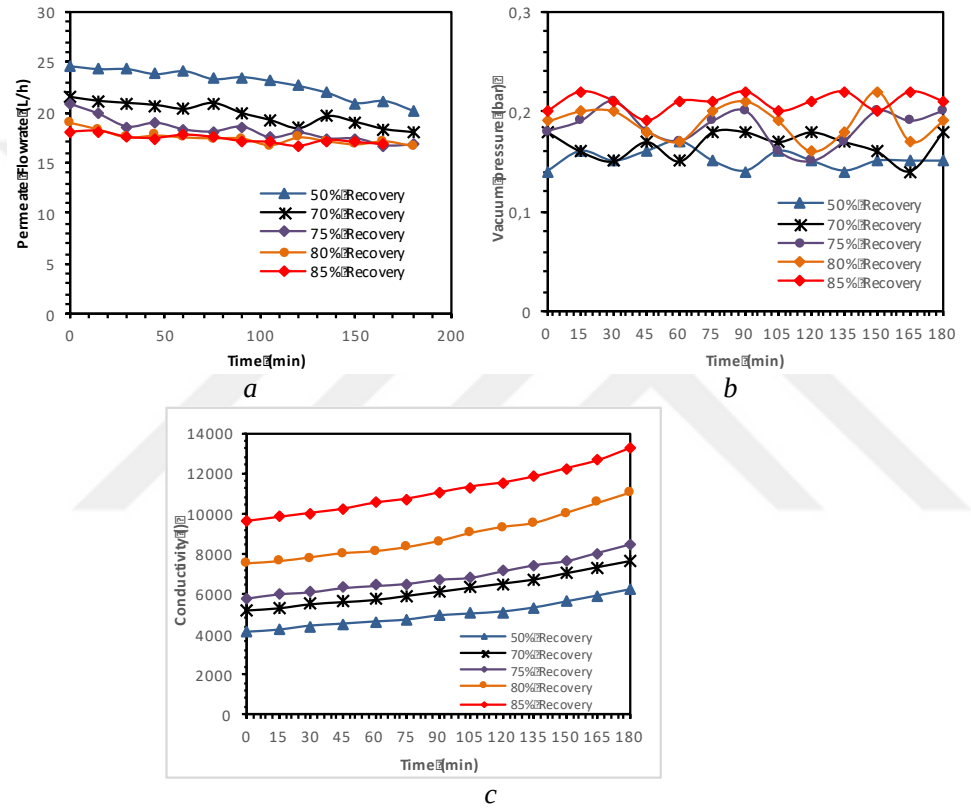

Figure 7.3 : a) Permeate flowrate, b) Vacuum pressure, c) feed conductivity, change during batch operation.

Water characteristics were given in Table 7.4 for feed, permeate and concentrate streams in terms of boron, arsenic, hardness, pH, and conductivity. According to the results, boron removal efficiencies were 98.66%, 97.4%, 98.1%, 97.5% and 96.6%, for the recovery rates of 50%, 70%, 75%, 80% and 85%, respectively. The arsenic removal efficiency was obtained as 100% for all recovery ratios (Figure 7.4). The system was operated in batch mode by observing the operation parameters, and an 85% recovery rate was reached at maximum.

Table 7.4 : Water characteristics for raw water batch operation.

Rec Rate (%)	Pilot MD Feed Water					Pilot MD Permeate Water					Pilot MD Concentrate Water				
	B (ppm)	As (ppm)	Hardness (ppm)	pH	Conductivity (µs/cm)	B (ppm)	As (ppm)	Hardness (ppm)	pH	Conductivity (µs/cm)	B (ppm)	As (ppm)	Hardness (ppm)	pH	Conductivity (µs/cm)
50	2164	3.2	3000	6.48	3440	29.1	ND	3	7.56	6.2	4376	4	6250	6.73	6240
70	2164	3.2	3000	6.48	3440	56.9	ND	77	6.92	47.9	5272	7.20	7600	6.59	7300
75	2164	3.2	3000	6.48	3440	41.0	ND	3	6.41	7.5	6408	4.80	9000	6.41	8340
80	2191	4	3100	7.27	4270	55.8	ND	3.7	5.27	9.5	10409	10	13575	5.93	14155
85	2191	4	3100	7.27	4270	75.5	ND	9.5	5.56	28.2	11924	20	14200	5.75	15080

ND: not detected

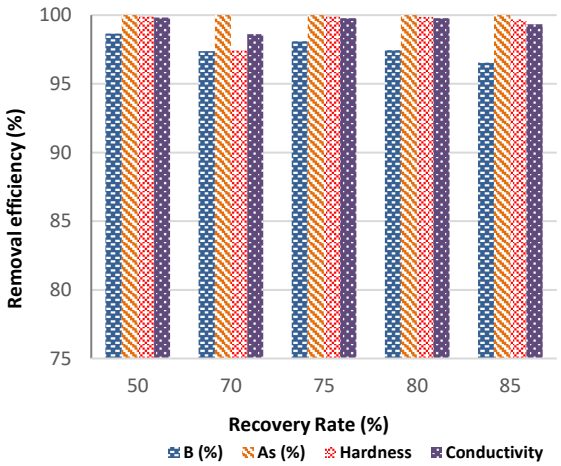

Figure 7.4 : Removal efficiencies of raw water batch operation.

After batch mode operations, raw water was fed to the MD system continuously, for approximately 36 hours. The results showed that it was possible to reach a 90% recovery rate. The permeate flow rate was an average of 30 L/h, and inlet conductivity value increased by 69% (Figure 7.5). The module entrance pressure increased exponentially for the 6 hour process period. As seen in Table 7.5, the inlet water comprises of 2086 ppm B, 4 ppm As, 3500 ppm hardness, 3790 (µs/cm) conductivity, and a pH of 7.13. The input conductivity values increased by approximately 69%, and the permeate flow rate was 30 L/h on average. The average vacuum pressure was 0.14 bar.

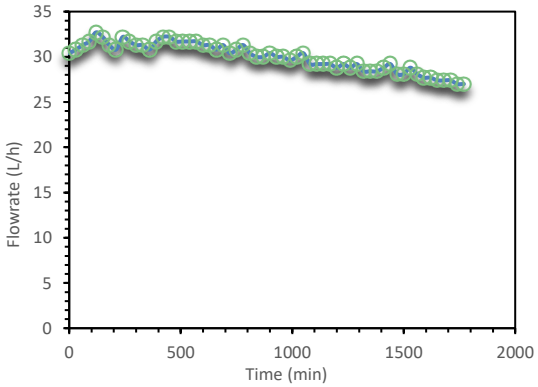

a

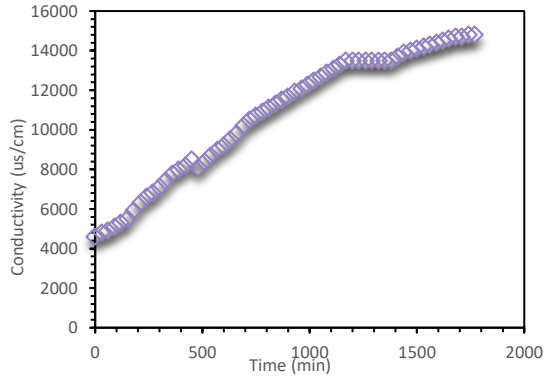

b

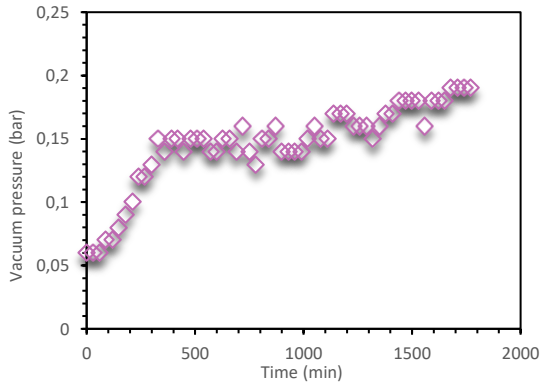

c

Figure 7.5 : a) Permeate flowrate, b) feed conductivity, c) Vacuum pressure, change during continuous feed raw water.

Table 7.5 : Water characteristics for raw water continuous operation.

Recovery Rate (%)	Pilot MD Feed Water					Pilot MD Permeate Water					Pilot MD Concentrate Water				
	B (ppm)	As (ppm)	Hardness (ppm)	pH	Conductivity (µs/cm)	B (ppm)	As (ppm)	Hardness (ppm)	pH	Conductivity (µs/cm)	B (ppm)	As (ppm)	Hardness (ppm)	pH	Conductivity (µs/cm)
70	2086	4	3100	7.13	3790	23	ND	3	6.24	10.3	5623	4.6	7600	6.55	9998
80	2086	4	3100	7.13	3790	47.2	ND	2.5	5.92	9.6	12579	4.8	13000	5.72	15670
90	2086	4	3100	7.13	3790	78	ND	4	6.34	11.4	12972	5.1	14400	5.68	17080

ND: not detected

According to the results, the B removal efficiency was 98.9% for the 70% recovery rate, while the removal efficiencies were 97.74% and 96.26% for a recovery rate of 80% and 90%, respectively (Figure 7.6) Duong et al. used the same pilot scale MD system for seawater desalination. The feed water has 55 ms/cm conductivity, and they achieved lower than 100 μs/cm permeate water conductivity which is higher than the results of this study (Duong et al., 2016).

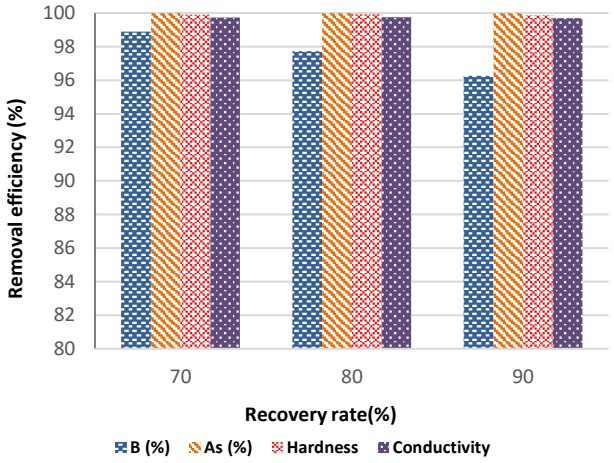

Figure 7.6 : Removal efficiencies for continuous operation.

7.3.2 RO concentrate experiments

After raw water experiments, RO concentrate treatment via MD was studied. In the MD study where RO Concentrate water was fed, the MD system was fed continuously. In the graphs given in Figure 7.7 , the results obtained in the 200-minute time frame of all recovery rates are shared in order to show them as an equal time interval from the moment the recovery rates of 50%, 70% and 75% are reached in the MD system. Since the higher recovery rates cause the formation of solid particles, which clogged the system lines, 80%, and 85% recovery rates could not be carried out for the concentrate stream. The total time taken to reach each recovery rate within the scope of the study is given as follows; It is 210 minutes for 0% to 50% recovery rate, 225 minutes for 50% to 70% recovery rate, and 255 minutes for 70% to 75% recovery rate.

Changes in conductivity in time affects the other operating parameters. Conductivity increment resulted in lower permeate flowrate, lower flux, and higher vacuum pressures. The average flux was 3.3 L/m^{2}h for 50% recovery rate while 2.98 L/m^{2}h and 2.81 L/m^{2}h for 70% and 75% recovery ratios, respectively. 20% increase in recovery rate decreased flux ca.10%. However, a 5% increase in recovery rate declined

flux approximately 6%. The permeate flow rate has the same trend with flux as expected. Average flow rates were 23.7 L/h, 21.5 L/h, and 20.2 L/h for the increasing recovery rates from 50% to 75%. Increasing feed salinity due to increasing recovery rates causes the partial pressure difference, the driving force of MD, to decline according to Raoult's law (Mutlu Salmanli et al., 2022b; Qtaishat et al., 2008). The decrease in vapor pressure is caused by decreased water activity caused by ion hydration and ionic association in salt solution (Guendouzi et al., 2001). So, as a result of the concentration of feed water, less water vapor is passing through the pores and water flux decreases slightly (Duong et al., 2016).

Additionally, the increasing feed concentration resulted in temperature polarization by increasing the feed solution's viscosity and also causes a concentration layer formation. These two layer together decrease the driving force. So, the fluxes and permeate flow rates decreased with increasing recovery rates (Duong et al., 2015; Mutlu Salmanli et al., 2022; Safavi & Mohammadi, 2009). The decrease in the permeate flowrate may also be a result of the release of carbon dioxide during the distillation process. Water vapor and carbon dioxide transfer through membrane pores might compete, lowering the production of permeate (Duong et al., 2015). With higher salinity, the vacuum pressures increased slightly. The average pressure was 0.066 bar for 50% recovery and 0.075 bar for the recovery rate of 75%.

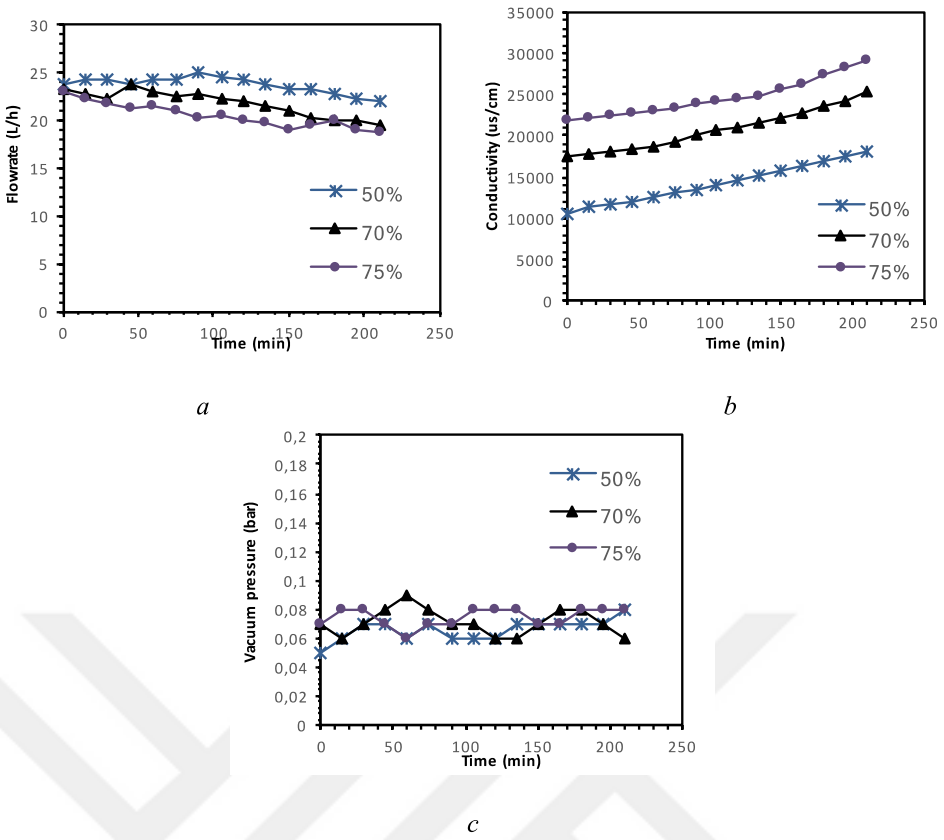

Figure 7.7 : a) Permeate flowrate, b) feed conductivity, c) Vacuum pressure, change during concentrate treatment.

Table 7.6 : Water characteristics for RO concentrate studies.

Recovery Rate (%)	Pilot MD Feed Water					Pilot MD Permeate Water					Pilot MD Concentrate Water				
	B (ppm)	As (ppm)	Hardness (ppm)	pH	Conductivity (µs/cm)	B (ppm)	As (ppm)	Hardness (ppm)	pH	Conductivity (µs/cm)	B (ppm)	As (ppm)	Hardness (ppm)	pH	Conductivity (µs/cm)
50	5000	1.6	430	8.92	8840	76.8	ND	12.5	8.94	205	10011	2	1350	8.64	19460
70	9803	1	830	8.82	22200	102	ND	7.0	9.10	228	17123	1.6	1400	8.88	32100
75	16512	0.8	1600	8.39	60100	134	ND	9.8	8.97	345	27640	2	7100	8.22	47700

ND: not detected

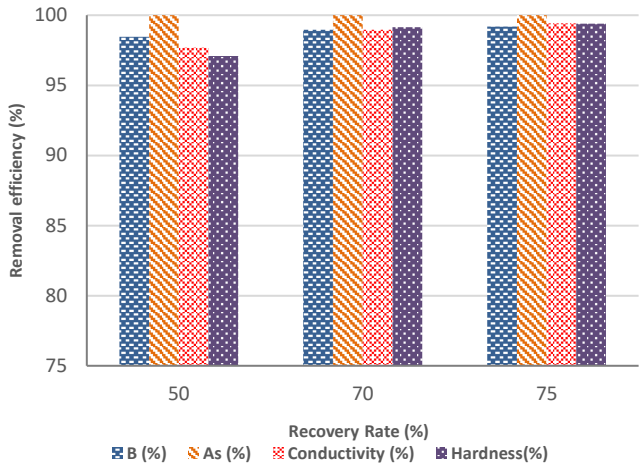

Figure 7.8 : Removal efficiencies for RO concentrate studies.

RO concentrate treatment using MD for River water was conducted at 3 different recovery rates, 50%,70%, and 75%, on batch mode. As can be seen in Table 7.6 boron concentrations of permeate waters are 76.8, 102, and 134 ppm for 50%, 70%, and 75% recovery rates, respectively. Boron removal efficiencies were approximately 99% for all recovery rates. At the same time, arsenic removal efficiencies were 100% (Figure 7.8). Eykens et al. used pilot scale Aquastill MD for recovery of cheese-making brine, and they obtained ca. 200µs/cm conductivity for permeate water, similar to the results of this study (Eykens et al., 2018).

According to the results obtained, while the MD process is applied directly to raw water with 2086 ppm B, 4 ppm As, 3500 ppm hardness, and 3790 µs/cm conductivity, boron removal efficiencies were 98.9% for the 70% recovery rate, and for the 80% and 90% recovery rates the efficiencies were 97.74% and 96.26%, respectively. In addition, vacuum pressures were observed to be 0.14 bar. RO concentrate, in which the reverse osmosis system is used as a pre-treatment, has B varying between 5000-16512 ppm, As varying between 0.8-1.6 ppm, hardness varying between 430-1600 ppm, and conductivity values varying between 8840-60100 µs/cm. When the MD process was applied to the RO concentrate, boron removal efficiencies were approximately 99% for all recovery rates. In addition, the vacuum pressures vary between 0.066 bar and 0.075 bar. In this case, boron removal efficiencies of the MD system are higher in reverse osmosis concentrates. The reason for this situation can be shown as the negative effect of raw water having more hardness ions (calcium and magnesium) on B removal since it can cause scaling and wetting of MD membrane (Hsieh et al., 2021). This explanation is also supported by the fact that the measured

vacuum pressures were lower and fluxes are higher when the MD system was applied to the RO concentrate, which had removed the ions causing hardness in the water.

MD requires less energy than RO which makes it an attractive option. As seen in the, Table 7.7, for this study, the specific energy consumption of the two-stage RO system is 164 kWh/m^3, and the specific energy consumption of the MD system is 121.1 kWh/m^3, of which 87.8 kWh/m^3 is the thermal energy consumption. In this case, it can be seen that the energy consumption of the MD system was lower.

Table 7.7 : Energy consumption of RO and MD system.

Method	Permeate flow rate (L/ h)	Thermal Energy Consumption (kWh/ m^3)	SEC (kWh/ m^3)	Max. Recovery Rate (%)
2 Stage Reverse Osmosis (BWRO + SWRO)	1000	0	164	80
MD System	800	87.8	121.1	85

7.3.3 Crystallization experiments

In addition to the RO and MD studies carried out with the flows of the River Stream, the concentrated liquids with high pollutant content obtained from the MD system were subjected to the crystallization process. Following filtration the obtained solids were dried in an oven at 104 ° C for dry weight determination. Then, semi-quantitative XRF analyzes were performed on the obtained dry solids. In these analyses, the B_2O_3 ratio, the most critical parameter for the obtained solid to participate in the regeneration process, was examined.

Two MD studies were carried out by feeding raw water directly and feeding the concentrate obtained through the RO process within the scope of the river stream. Concentrates obtained from MD in both types of studies were subjected to the aforementioned processes.

Raw water from the river before the liming unit, fed to the MD system intermittently and continuously, it was characterized by a boron content of 2500-3000 ppm, which was then concentrated to 12000 ppm boron in the water with these studies.

The obtained concentrate from MD contains approximately 85-95 gr solid per liter, which means ca. 10% wt of concentrate. The solid part contains approximately 40-45% B_2O_3, which is essential for boron recovery for boric acid production. The obtained crystals as given in Figure 7.9. The XRF results of the crystals are shown in

Table 7.8. The % B_2O_3 of this solid is similar to colemanite and ulexite substances. Colemanite can contain 13.67% to 44.5% B_2O_3, according to different studies (Aksoğan et al., 2016; Erdogmus, 2014; Okuno et al., 2009; Oto et al., 2013; Sevim, 2011; Sevinç et al., 2017) and ulexite can contain 43% B_2O_3 (Aghajanian et al., 2022). Colemanite has a wide spectrum of usage in different areas such as; textile, glass, glass fiber, cosmetics, detergents, fertilizers, photography, antiseptics, nuclear applications, concrete, and metallurgy applications, which makes it an important and valuable mineral, along and with ulexite, it is the predominant mineral to used in boron steel production instead of fluorite (Aghajanian et al., 2022; Poslu & Arslan, 1995; Rap, A., 2013; Arslan, 2021a; Yildiz, 2004; Yunlu, 2016).

Figure 7.9 : Crystals obtained from River raw water treatment.

The raw river water was passed through the BWRO membrane, the first stage of the RO system, at a pH of 7 (the pH of the raw water itself). Then the pH of the water was increased to 9 using NaOH before passing through the SWRO membrane, the second stage of the system. The concentrate of SWRO, which has 90% recovery, has a boron concentration of approximately 10000 ppm. This concentrate was fed to the MD system, and a 75% water recovery rate was achieved in the MD system studies. The concentrate taken from the MD system operated at a 75% recovery rate has approximately 25000 ppm boron content.

A study was carried out with the solid substance of the MD concentrate with the recovery rate of 75%. 1 Liter of MD concentrate contained approximately 100 grams solid. The amount of sodium in the fed water was observed to be high due to the pH

adjustment in the previous RO study. This situation showed that the obtained solid matter is different from the solid obtained in the raw water supply of the river.

In the concentrate obtained in the river RO-MD study, the B_2O_3 solid constitutes 35% of the total solid and the amount of Na_2O is approximately 60%. The image of the crystal solid material obtained and the XRF analysis results of the solid obtained at a 75% recovery rate are given in Figure 7.10 and Table 7.8. The B_2O_3 ratio increased with the increasing recovery rates, which are consistent with the study of Jia et al. (F. Jia et al., 2017a). They also used VMDC for boric acid recovery, and according to their results, they were able to obtain boric acid crystals with the highest recovery rate.

Figure 7.10 : Crystals obtained from RO concentrate treatment.

In the solid, due to the high sodium content of the MD concentrate, unlike the raw water concentrate, the formation of an ore called "tincal" holds the Na_2O component, which is where the 36.5% B_2O_3 component is thought to be obtained (Aghajanian et al., 2022). This ore is the source of the substance "Borax", which is a form of boron mineral. This solid material, which shows crystalline deposits structurally, is not readily soluble in water. The crystal structure of the solid material, which can only be dissolved at high temperatures (90^{o}C and above), causes the particles to become more compact and difficult to break down and physically looks like granulated sugar. Tincal and colemanite are used to produce boric acid and refined boron products such as borax decahydrate and pentahydrate (Güyagüler, 2001; Arslan, 2021b). The effect of crystallization process parameters such as temperature and the mixing rate on the crystal quality needs to be further explored for future research.

Table 7.8 : XRF Results of crystals obtained from MD Concentrate of raw water and RO concentrate.

Compound	Raw water			RO Concentrate
	Recovery Rate (%)			
	80%	85%	90%	75%
Na_2O	32.0	29.6	34.8	59.5
MgO	12.5	12.9	11.5	0.926
K_2O	0.067	0.0849	0.0570	0.202
CaO	2.00	3.27	1.31	0.877
Sc_2O_3	0.0077	0.0217	0.0070	0.0005
TiO_2	0.0060	0.0515	0.0015	0.0038
V_2O_5	0.0020	0.0048	0.0019	-
MnO	0.0179	0.0188	0.0174	0.0001
Fe_2O_3	0.0028	0.0049	0.0015	0.0026
NiO	0.0016	0.0017	0.0014	-
CuO	0.0006	0.0006	0.0005	0.0006
ZnO	0.0022	0.0025	0.0005	0.0006
Al_2O_3	0.319	0.417	0.419	0.385
SiO_2	0.792	1.25	1.17	0.471
P_2O_5	0.0037	0.0092	0.0005	0.0001
SO_3	9.41	11.1	6.47	2.75
SeO_2	0.0004	0.0003	-	0.0002
As_2O_3	0.139	0.146	0.138	0.0115
SnO_2	0.0019	0.0018	0.0021	0.0018
ZrO_2	0.143	0.152	0.157	0.151
SrO	0.0525	0.0665	0.0468	0.085
B_2O_3	**42.4**	**40.8**	**43.9**	**34.7**

7.4 Conclusion

Since the higher amounts of boron can be harmful to living creatures, it needs to be removed from water sources. However, it is an essential element, so the removal alone is not enough alone and needs to be completed with a recovery step. Membrane distillation is a good alternative for treating different contaminants in concentrated waters. This paper shows the promising potential of membrane distillation for treating water with high boron content water. MD was investigated for the treatment of raw water obtained from the mine drainage area directly and also for RO concentrate. 100% As removal and higher than 96% B removal were achieved for all VAGMD experiments. The operational parameters changed with changing recovery rates. Different recovery rates were applied between 50% and 85% for raw water batch experiments. After the batch operation, VAGMD operated for 36 hours as a continuous

system, and a max 90% recovery rate was achieved. Since the RO concentrate is a highly concentrated water stream, only 50%, 70%, and 75% recovery rates were able to be tested. Conductivity values increased over time, and flow rates decreased as expected. Due to the NaOH addition in the RO step, the crystals obtained from concentrate treatment experiments have a high Na_2O compound fraction. It was possible to obtain up to ca. 44% B_2O_3 contented boron crystals, which have a wide range of industrial usage areas. The results proved that the VAGMDC is a promising method for the removal and recovery of boron.

8. CONCLUSIONS AND RECOMMENDATIONS

Increasing demand for clean water due to the increasing industrial activities and growing population makes the recovery of water and resources much more important. Reverse osmosis usage has increased to fulfill this water demand in recent years. Due to the increasing usage of reverse osmosis (RO), the concentrate treatment gained importance. Thus the preparation of hydrophobic membranes and boron removal and recovery from RO concentrate was studied by using membrane distillation crystallization (MDC). The most important conclusions with a holistic approach are as follows:

- In the first experimental section VAGMD method was found as optimal MD configuration due to the higher fluxes and GOR while lower SEC values than AGMD. Higher than 99.2% boron removal efficiencies were obtained with VAGMD.
- After the selection of VAGMD configuration hydrophobic membrane preparation studies were conducted by modification of commercial and fabricated membranes. Membranes coated with PN, C, and SHBC coatings were found quite hydrophobic. Moreover, a superhydrophobic membrane was prepared with CS coating on PVDF nanofiber membrane which has a contact angle of 153° and boron rejection of 94.1%.
- Following the membrane modification studies effect of BisF-Bz monomer on the hydrophobicity of PVDF membrane was investigated. Two times thermal curing application of BisF-Bz blended PVDF membrane represented the highest hydrophobicity. 19.28 L/m^2h permeate water flux was obtained for real RO brine with 98% boron rejection.
- Crystallization process integration to the MD was investigated for boron recovery. According to the lab scale VAGMDC studies increase of pH negatively affected the permeate water flux.

- Fabricated nanofiber membranes were more resistant to scaling and fouling compared to commercial membranes.
- Obtained crystals had up to 44.6% B_2O_3 content by using fabricated nanofiber membranes.
- Pilot scale VAGMDC was operated successfully following to the lab scale VAGMDC studies. At least 40% B_2O_3 contented crystals were obtained. Hence results showed that pilot scale VAGMDC could be applied for the removal and recovery of boron.

To conclude, the VAGMDC system was used successfully for RO concentrate treatment. Results showed that boron could be separated from concentrate stream with very good purity. The following recommendations could be given for further studies;

- Renewable energy sources such as solar energy should be used for MD to heat the feed water.
- Membrane preparation studies could be investigated to reduce membrane wetting and scaling challenges in pilot and real scale of MD.
- The performance of developed novel MD membranes investigation should be carried to pilot scale from lab scale.
- Novel hydrophobic membranes could be used in pilot-scale MD process.
- The crystals obtained from VAGMDC studies should be investigated for further usage as raw material.

REFERENCES

Abdelgaied, M., Kabeel, A. E., & Sathyamurthy, R. (2020). Improving the performance of solar powered membrane distillation systems using the thermal energy storage mediums and the evaporative cooler. *Renewable Energy*, 157, 1046–1052. https://doi.org/10.1016/j.renene.2020.05.123

Abdelrazeq, H., Khraisheh, M., Al Momani, F., McLeskey, J. T., Hassan, M. K., Gad-el-Hak, M., & Tafreshi, H. V. (2020). Performance of electrospun polystyrene membranes in synthetic produced industrial water using direct-contact membrane distillation. *Desalination*, 493, 114663. https://doi.org/10.1016/j.desal.2020.114663

Abu-Zeid, M. A. E. R., Zhang, L., Jin, W. Y., Feng, T., Wu, Y., Chen, H. L., & Hou, L. (2016). Improving the performance of the air gap membrane distillation process by using a supplementary vacuum pump. *Desalination*, 384, 31–42. https://doi.org/10.1016/j.desal.2016.01.020

Abu-Zeid, M. A. E.-R., Zhang, Y., Dong, H., Zhang, L., Chen, H.-L., & Hou, L. (2015). A comprehensive review of vacuum membrane distillation technique. *Desalination*, 356, 1–14. https://doi.org/10.1016/j.desal.2014.10.033

Aghajanian, A., Thomas, C., Sainz-Aja, J., & Cimentada, A. (2022). Colemanite filler from wastes in recycled concrete. In The Structural Integrity of Recycled Aggregate Concrete Produced with Fillers and Pozzolans (pp. 79–103). Elsevier. https://doi.org/10.1016/B978-0-12-824105-9.00007-X

Ahmad, A. Y., Al-Ghouti, M. A., Khraisheh, M., & Zouari, N. (2022). Development and application of bio-waste-derived adsorbents for the removal of boron from groundwater. *Groundwater for Sustainable Development*, 18, 100793. https://doi.org/10.1016/j.gsd.2022.100793

Ahmed, F. E., Lalia, B. S., & Hashaikeh, R. (2017). Membrane-based detection of wetting phenomenon in direct contact membrane distillation. *Journal of Membrane Science*, 535, 89–93. https://doi.org/10.1016/j.memsci.2017.04.035

Akbari, B., Lashanizadegan, A., Darvishi, P., & Pouranfard, A. (2020). Chinese Journal of Chemical Engineering Preparation of hydrophobic fl at sheet membranes from PVDF-HFP copolymer for enhancing the oxygen permeance in nitrogen / oxygen gas mixture. *Chinese Journal of Chemical Engineering*, 28(6), 1566–1581. https://doi.org/10.1016/j.cjche.2020.02.018

Aksoğan, O., Binici, H., & Ortlek, E. (2016). Durability of concrete made by partial replacement of fine aggregate by colemanite and barite and cement by ashes of corn stalk, wheat straw and sunflower stalk ashes. *Construction and Building Materials*, 106, 253–263. https://doi.org/10.1016/j.conbuildmat.2015.12.102

Al-Ithari, A. J., Sathasivan, A., Ahmed, R., Vuthaluru, H. B., Zhan, W., & Ahmed, M. (2011). Superiority of date seed ash as an adsorbent over other ashes and ferric chloride in removing boron from seawater. *Desalination and Water Treatment*, 32(1–3), 324–328. https://doi.org/10.5004/dwt.2011.2717

Alkhudhiri, A., Bin Darwish, N., Hakami, M. W., Abdullah, A., Alsadun, A., & Abu Homod, H. (2020). Boron Removal by Membrane Distillation: A Comparison Study. *Membranes*, 10(10), 263. https://doi.org/10.3390/membranes10100263

Alkhudhiri, A., Darwish, N., & Hilal, N. (2012). Membrane distillation: A comprehensive review. *Desalination*, 287, 2–18. https://doi.org/10.1016/j.desal.2011.08.027

Alkhudhiri, A., & Hilal, N. (2017). Air gap membrane distillation: A detailed study of high saline solution. *Desalination*, 403, 179–186. https://doi.org/10.1016/j.desal.2016.07.046

Alsaadi, A. S., Francis, L., Maab, H., Amy, G. L., & Ghaffour, N. (2015). Evaluation of air gap membrane distillation process running under sub-atmospheric conditions: Experimental and simulation studies. *Journal of Membrane Science*, 489, 73–80. https://doi.org/10.1016/j.memsci.2015.04.008

Andrés-Mañas, J. A., Ruiz-Aguirre, A., Acién, F. G., & Zaragoza, G. (2020). Performance increase of membrane distillation pilot scale modules operating in vacuum-enhanced air-gap configuration. *Desalination*, 475, 114202. https://doi.org/10.1016/j.desal.2019.114202

Arjmandi, M., Pourafshari Chenar, M., Altaee, A., Arjmandi, A., Peyravi, M., Jahanshahi, M., & Binaeian, E. (2020). Caspian seawater desalination and whey concentration through forward osmosis (FO)-reverse osmosis (RO) and FO-FO-RO hybrid systems: Experimental and theoretical study. *Journal of Water Process Engineering*, 37, 101492. https://doi.org/10.1016/j.jwpe.2020.101492

Asghari, M., Harandizadeh, A., Dehghani, M., & Harami, H. R. (2015). Persian Gulf desalination using air gap membrane distillation: Numerical simulation and theoretical study. *Desalination*, 374, 92–100. https://doi.org/10.1016/j.desal.2015.07.019

Atherton Seidell & William F Linke. (1958). *Solubilities*. Inorganic and Metalorganic Compounds. A Compilation of Solubility Data from the Periodical Literature (4th ed., Vol. 1). Van Nostrand Company.

Attia, H., Alexander, S., Wright, C. J., & Hilal, N. (2017). Superhydrophobic electrospun membrane for heavy metals removal by air gap membrane distillation (AGMD). *Desalination*, 420(June), 318–329. https://doi.org/10.1016/j.desal.2017.07.022

Attia, H., Johnson, D. J., Wright, C. J., & Hilal, N. (2018a). Comparison between dual-layer (superhydrophobic–hydrophobic) and single superhydrophobic layer electrospun membranes for heavy metal recovery by air-gap membrane distillation. *Desalination*, 439(April), 31–45. https://doi.org/10.1016/j.desal.2018.04.003

Attia, H., Johnson, D. J., Wright, C. J., & Hilal, N. (2018b). Robust superhydrophobic electrospun membrane fabricated by combination of electrospinning and electrospraying techniques for air gap membrane distillation. *Desalination*, 446(August), 70–82. https://doi.org/10.1016/j.desal.2018.09.001

Attia, H., Johnson, D. J., Wright, C. J., & Hilal, N. (2018c). Robust superhydrophobic electrospun membrane fabricated by combination of electrospinning and electrospraying techniques for air gap membrane distillation. *Desalination*, 446(June), 70–82. https://doi.org/10.1016/j.desal.2018.09.001

Ayyildiz, H. F., & Kara, H. (2005). Boron removal by ion exchange membranes. *Desalination*, 180(1–3), 99–108. https://doi.org/10.1016/j.desal.2004.12.031

Bachelier, N., Chappey, C., Langevin, D., Métayer, M., & Verchère, J.-F. (1996). Facilitated transport of boric acid by 1,3-diols through supported liquid membranes. *Journal of Membrane Science*, 119(2), 285–294. https://doi.org/10.1016/0376-7388(96)00134-2

Balasubramanian, R., Lakshmi Narasimhan, T. S., Viswanathan, R., & Nalini, S. (2008). Investigation of the Vaporization of Boric Acid by Transpiration Thermogravimetry and Knudsen Effusion Mass Spectrometry. *The Journal of Physical Chemistry B*, 112(44), 13873–13884. https://doi.org/10.1021/jp8058883

Balis, E., Griffin, J. C., & Hiibel, S. R. (2022). Membrane Distillation-Crystallization for inland desalination brine treatment. *Separation and Purification Technology*, 290, 120788. https://doi.org/10.1016/j.seppur.2022.120788

Ban, S.-H., Im, S.-J., Cho, J., & Jang, A. (2019). Comparative performance of FO-RO hybrid and two-pass SWRO desalination processes: Boron removal. *Desalination*, 471, 114114. https://doi.org/10.1016/j.desal.2019.114114

Banasiak, L. J., & Schäfer, A. I. (2009). Removal of boron, fluoride and nitrate by electrodialysis in the presence of organic matter. *Journal of Membrane Science*, 334(1–2), 101–109. https://doi.org/10.1016/j.memsci.2009.02.020

Bártová, Š., Kůs, P., Skala, M., & Vonková, K. (2016). Reverse osmosis for the recovery of boric acid from the primary coolant at nuclear power plants. *Nuclear Engineering and Design*, 300, 107–116. https://doi.org/10.1016/j.nucengdes.2016.01.018

Bick, A., & Oron, G. (2015). Seawater Reverse Osmosis Permeate. In *Boron Separation Processes* (pp. 325–338). Elsevier. https://doi.org/10.1016/B978-0-444-63454-2.00015-0

Boncukcuoğlu, R., Kocakerim, M. M., Kocadağistan, E., & Yilmaz, M. T. (2003). Recovery of boron of the sieve reject in the production of borax. Resources, *Conservation and Recycling*, 37(2), 147–157. https://doi.org/10.1016/S0921-3449(02)00072-1

Boubakri, A., Bouguecha, S. A.-T., Dhaouadi, I., & Hafiane, A. (2015a). Effect of operating parameters on boron removal from seawater using membrane distillation process. *Desalination*, 373, 86–93. https://doi.org/10.1016/j.desal.2015.06.025

Boubakri, A., Bouguecha, S. A.-T., Dhaouadi, I., & Hafiane, A. (2015b). Effect of operating parameters on boron removal from seawater using membrane distillation process. *Desalination*, 373, 86–93. https://doi.org/10.1016/j.desal.2015.06.025

Bryjak, M., Poźniak, G., & Kabay, N. (2007). Donnan dialysis of borate anions through anion exchange membranes: A new method for regeneration of boron selective resins. *Reactive and Functional Polymers*, 67(12), 1635–1642. https://doi.org/10.1016/j.reactfunctpolym.2007.07.028

Bunani, S., Arda, M., Kabay, N., Yoshizuka, K., & Nishihama, S. (2017a). Effect of process conditions on recovery of lithium and boron from water using bipolar membrane electrodialysis (BMED). *Desalination*, 416, 10–15. https://doi.org/10.1016/j.desal.2017.04.017

Bunani, S., Arda, M., Kabay, N., Yoshizuka, K., & Nishihama, S. (2017b). Effect of process conditions on recovery of lithium and boron from water using bipolar membrane electrodialysis (BMED). *Desalination*, 416, 10–15. https://doi.org/10.1016/j.desal.2017.04.017

Butterwick L, de Oude N, Raymond K. (1989). Safety assessment of boron in aquatic and terrestrial environments *Ecotoxicology and Environmental Safety*, 416, 10–15. https://doi.org/10.1016/0147-6513(89)90055-9.

Cath, T., Childress, A., & Elimelech, M. (2006). Forward osmosis: Principles, applications, and recent developments. *Journal of Membrane Science*, 281(1–2), 70–87. https://doi.org/10.1016/j.memsci.2006.05.048

Cengeloglu, Y., Arslan, G., Tor, A., Kocak, I., & Dursun, N. (2008). Removal of boron from water by using reverse osmosis. *Separation and Purification Technology*, 64(2), 141–146. https://doi.org/10.1016/j.seppur.2008.09.006

Çermikli, E., Şen, F., Altıok, E., Wolska, J., Cyganowski, P., Kabay, N., Bryjak, M., Arda, M., & Yüksel, M. (2020). Performances of novel chelating ion exchange resins for boron and arsenic removal from saline geothermal water using adsorption-membrane filtration hybrid process. *Desalination*, 491, 114504. https://doi.org/10.1016/j.desal.2020.114504

Chafidz, A., Kerme, E. D., Wazeer, I., Khalid, Y., Ajbar, A., & Al-Zahrani, S. M. (2016). Design and fabrication of a portable and hybrid solar-powered membrane distillation system. *Journal of Cleaner Production*, 133, 631–647. https://doi.org/10.1016/j.jclepro.2016.05.127

Chamani, H., Woloszyn, J., Matsuura, T., Rana, D., & Lan, C. Q. (2021). Pore wetting in membrane distillation: A comprehensive review. *Progress in Materials Science*, 122, 100843. https://doi.org/10.1016/j.pmatsci.2021.100843

Chang, H., Liu, B., Zhang, Z., Pawar, R., Yan, Z., Crittenden, J. C., & Vidic, R. D. (2021). A Critical Review of Membrane Wettability in Membrane Distillation from the Perspective of Interfacial Interactions. *Environmental Science and Technology*, 55(3), 1395–1418. https://doi.org/10.1021/acs.est.0c05454

Chang, H.-M., Chen, S.-S., Cai, Z.-S., Chang, W.-S., Ray, S. S., Nguyen, N. C., Li, C.-W., & Paswan, M. (2020). Iodide recovery and boron removal from thin-film transistor liquid crystal display wastewater through forward osmosis. *Journal of Cleaner Production*, 258, 120587. https://doi.org/10.1016/j.jclepro.2020.120587

Chen, F., Guo, L., Zhang, X., Leong, Z. Y., Yang, S., & Yang, H. Y. (2017). Nitrogen-doped graphene oxide for effectively removing boron ions from seawater. *Nanoscale*, 9(1), 326–333. https://doi.org/10.1039/C6NR07448K

Chen, X., Chen, T., Li, J., Qiu, M., Fu, K., Cui, Z., Fan, Y., & Drioli, E. (2019). Ceramic nanofiltration and membrane distillation hybrid membrane processes for the purification and recycling of boric acid from simulative radioactive waste water. *Journal of Membrane Science*, 579, 294–301. https://doi.org/10.1016/j.memsci.2019.02.044

Chen, X., Gao, X., Fu, K., Qiu, M., Xiong, F., Ding, D., Cui, Z., Wang, Z., Fan, Y., & Drioli, E. (2018). Tubular hydrophobic ceramic membrane with asymmetric structure for water desalination via vacuum membrane distillation process. *Desalination*, 443, 212–220. https://doi.org/10.1016/j.desal.2018.05.027

Chen, Y., Lyu, J., Wang, Y., Chen, T., Tian, Y., Bai, P., & Guo, X. (2019). Synthesis, Characterization, Adsorption, and Isotopic Separation Studies of Pyrocatechol-Modified MCM-41 for Efficient Boron Removal. *Industrial & Engineering Chemistry Research*, 58(8), 3282–3292. https://doi.org/10.1021/acs.iecr.8b04748

Chen, Y. T., Liao, Y. L., Sun, Y. M., Hu, C. C., Lai, J. Y., & Liu, Y. L. (2019). Lignin as an effective agent for increasing the separation performance of crosslinked polybenzoxazine based membranes in pervaporation dehydration application. *Journal of Membrane Science*, 578(February), 156–162. https://doi.org/10.1016/j.memsci.2019.02.036

Cheng, L.-H., Wu, P.-C., & Chen, J. (2009). Numerical Simulation and Optimal Design of AGMD-Based Hollow Fiber Modules for Desalination. *Industrial & Engineering Chemistry Research*, 48(10), 4948–4959. https://doi.org/10.1021/ie800832z

Chieng, H. J., & Chong, M. F. (2013). Boron Adsorption on Palm Oil Mill Boiler (POMB) Ash Impregnated with Chemical Compounds. *Industrial & Engineering Chemistry Research*, 52(41), 14658–14670. https://doi.org/10.1021/ie401215n

Choi, Y., Naidu, G., Jeong, S., Lee, S., & Vigneswaran, S. (2018). Fractional-submerged membrane distillation crystallizer (F-SMDC) for treatment of high salinity solution. *Desalination*, 440, 59–67. https://doi.org/10.1016/j.desal.2018.01.027

Choi, Y., Naidu, G., Jeong, S., Vigneswaran, S., Lee, S., Wang, R., & Fane, A. G. (2017). Experimental comparison of submerged membrane distillation configurations for concentrated brine treatment. *Desalination*, 420, 54–62. https://doi.org/10.1016/j.desal.2017.06.024

Choi, Y., Naidu, G., Nghiem, L. D., Lee, S., & Vigneswaran, S. (2019). Membrane distillation crystallization for brine mining and zero liquid discharge: Opportunities, challenges, and recent progress. *Environmental Science: Water Research & Technology*, 5(7), 1202–1221. https://doi.org/10.1039/C9EW00157C

Choi, Y., Ryu, S., Naidu, G., Lee, S., & Vigneswaran, S. (2019). Integrated submerged membrane distillation-adsorption system for rubidium recovery. *Separation and Purification Technology*, 218, 146–155. https://doi.org/10.1016/j.seppur.2019.02.050

Chorghe, D., Sari, M. A., & Chellam, S. (2017). Boron removal from hydraulic fracturing wastewater by aluminum and iron coagulation: Mechanisms and limitations. *Water Research*, 126, 481–487. https://doi.org/10.1016/j.watres.2017.09.057

Coll, M. T., Fortuny, A., & Sastre, A. M. (2014). Boron reduction by supported liquid membranes using ALiCY and ALiDEC ionic liquids as carriers. *Chemical Engineering Research and Design*, 92(4), 758–763. https://doi.org/10.1016/j.cherd.2013.11.010

Comesaña, A., Rodriguez-Monsalve, J., Cerpa, A., & Alguacil, F. J. (2011). Non-dispersive solvent extraction with strip dispersion (NDSXSD) pertraction of Cd(II) in HCl medium using ionic liquid CYPHOS IL101. *Chemical Engineering Journal*, 175, 228–232. https://doi.org/10.1016/j.cej.2011.09.099

Couto, C. F., Santos, A. V., Amaral, M. C. S., Lange, L. C., de Andrade, L. H., Foureaux, A. F. S., & Fernandes, B. S. (2020). Assessing potential of nanofiltration, reverse osmosis and membrane distillation drinking water treatment for pharmaceutically active compounds (PhACs) removal. *Journal of Water Process Engineerin*g, 33, 101029. https://doi.org/10.1016/j.jwpe.2019.101029

da Silva Ribeiro, T., Grossi, C. D., Merma, A. G., dos Santos, B. F., & Torem, M. L. (2019). Removal of boron from mining wastewaters by electrocoagulation method: Modelling experimental data using artificial neural networks. *Minerals Engineering*, 131, 8–13. https://doi.org/10.1016/j.mineng.2018.10.016

Darmanin, T., & Guittard, F. (2014). Wettability of conducting polymers: From superhydrophilicity to superoleophobicity. *Progress in Polymer Science*, 39(4), 656–682. https://doi.org/10.1016/j.progpolymsci.2013.10.003

Darmanin, T., & Guittard, F. (2015). Superhydrophobic and superoleophobic properties in nature. *Materials Today*, 18(5), 273–285. https://doi.org/10.1016/j.mattod.2015.01.001

Darwish, N. B., Alkhudhiri, A., AlAlawi, A., AlRomaih, H., & Hilal, N. (2020). Experimental investigation of forward osmosis process for boron removal from water. *Journal of Water Process Engineering*, 38, 101570. https://doi.org/10.1016/j.jwpe.2020.101570

Debasish Mohapatra, Gautam Roy Chaudhury, & KyungHo Park. (2008). Recovery of boron from wastewater using 2, 2, 4-trimethyl-1, 3-pentanediol in carbon tetrachloride. *Indian Journal of Chemical Technology*, 15(5), 483–487.

del Mar de la Fuente García-Soto, M., & Camacho, E. M. (2006). Boron removal by means of adsorption with magnesium oxide. *Separation and Purification Technology*, 48(1), 36–44. https://doi.org/10.1016/j.seppur.2005.07.023

del Mar de la Fuente García-Soto, M., & Muñoz Camacho, E. (2005). Boron removal from industrial wastewaters by ion exchange: An analytical control parameter. *Desalination*, 181(1–3), 207–216. https://doi.org/10.1016/j.desal.2005.01.015

Demey, H., Vincent, T., Ruiz, M., Nogueras, M., Sastre, A. M., & Guibal, E. (2014). Boron recovery from seawater with a new low-cost adsorbent material. *Chemical Engineering Journal*, 254, 463–471. https://doi.org/10.1016/j.cej.2014.05.057

Demey, H., Vincent, T., Ruiz, M., Sastre, A. M., & Guibal, E. (2014). Development of a new chitosan/Ni(OH)2-based sorbent for boron removal. *Chemical Engineering Journal*, 244, 576–586. https://doi.org/10.1016/j.cej.2014.01.052

Demir, K. D., Kiskan, B., Latthe, S. S., Demirel, A. L., & Yagci, Y. (2013). Thermally curable fluorinated main chain benzoxazine polyethers via Ullmann coupling. *Polymer Chemistry*, 4(6), 2106–2114. https://doi.org/10.1039/c2py21029k

Dolati, M., Aghapour, A. A., Khorsandi, H., & Karimzade, S. (2017). Boron removal from aqueous solutions by electrocoagulation at low concentrations. *Journal of Environmental Chemical Engineering*, 5(5), 5150–5156. https://doi.org/10.1016/j.jece.2017.09.055

Dong, Z. Q., Ma, X. Hua, Xu, Z. L., You, W. T., & Li, F. B. (2014a). Superhydrophobic PVDF-PTFE electrospun nanofibrous membranes for desalination by vacuum membrane distillation. *Desalination*, 347, 175–183. https://doi.org/10.1016/j.desal.2014.05.015

Dow, N., Gray, S., Li, J., Zhang, J., Ostarcevic, E., Liubinas, A., Atherton, P., Roeszler, G., Gibbs, A., & Duke, M. (2016). Pilot trial of membrane distillation driven by low grade waste heat: Membrane fouling and energy assessment. *Desalination*, 391, 30–42. https://doi.org/10.1016/j.desal.2016.01.023

Duong, H. C., Chivas, A. R., Nelemans, B., Duke, M., Gray, S., Cath, T. Y., & Nghiem, L. D. (2015). Treatment of RO brine from CSG produced water by spiral-wound air gap membrane distillation—A pilot study. *Desalination*, 366, 121–129. https://doi.org/10.1016/j.desal.2014.10.026

Duong, H. C., Cooper, P., Nelemans, B., Cath, T. Y., & Nghiem, L. D. (2016). Evaluating energy consumption of air gap membrane distillation for seawater desalination at pilot scale level. *Separation and Purification Technology*, 166, 55–62. https://doi.org/10.1016/j.seppur.2016.04.014

Dydo, P. (2012). The mechanism of boric acid transport during an electrodialytic desalination process. *Journal of Membrane Science*, 407–408, 202–210. https://doi.org/10.1016/j.memsci.2012.03.045

Dydo, P. (2013). The effect of process parameters on boric acid transport during the electrodialytic desalination of aqueous solutions containing selected salts. *Desalination*, 310, 43–49. https://doi.org/10.1016/j.desal.2012.04.007

Dydo, P., Nemś, I., & Turek, M. (2012). Boron removal and its concentration by reverse osmosis in the presence of polyol compounds. *Separation and Purification Technology*, 89, 171–180. https://doi.org/10.1016/j.seppur.2012.01.018

Dydo, P., & Turek, M. (2013). Boron transport and removal using ion-exchange membranes: A critical review. *Desalination*, 310, 2–8. https://doi.org/10.1016/j.desal.2012.08.024

Dydo, P., & Turek, M. (2014). The concept for an ED–RO integrated system for boron removal with simultaneous boron recovery in the form of boric acid. *Desalination*, 342, 35–42. https://doi.org/10.1016/j.desal.2013.09.020

Edwie, F., & Chung, T.-S. (2013). Development of simultaneous membrane distillation–crystallization (SMDC) technology for treatment of saturated brine. *Chemical Engineering Science*, 98, 160–172. https://doi.org/10.1016/j.ces.2013.05.008

Efome, J. E., Rana, D., Matsuura, T., & Lan, C. Q. (2016). Enhanced performance of PVDF nanocomposite membrane by nanofiber coating: A membrane for sustainable desalination through MD. *Water Research*, 89, 39–49. https://doi.org/10.1016/j.watres.2015.11.040

Efome, J. E., Rana, D., Matsuura, T., Yang, F., Cong, Y., & Lan, C. Q. (2020). Triple-Layered Nanofibrous Metal-Organic Framework-Based Membranes for Desalination by Direct Contact Membrane Distillation. *ACS Sustainable Chemistry and Engineering*, 8(17), 6601–6610. https://doi.org/10.1021/acssuschemeng.9b06791

El Amali, A., Bouguecha, S., & Maalej, M. (2004). Experimental study of air gap and direct contact membrane distillation configurations: Application to geothermal and seawater desalination. *Desalination*, 168, 357. https://doi.org/10.1016/j.desal.2004.07.020

El-Bourawi, M. S., Ding, Z., Ma, R., & Khayet, M. (2006). A framework for better understanding membrane distillation separation process. *Journal of Membrane Science*, 285(1–2), 4–29. https://doi.org/10.1016/j.memsci.2006.08.002

Erdogmus, E. (2014). Combined effect of waste colemanite and silica fume on properties of cement mortar. *Science and Engineering of Composite Materials*, 21(3). https://doi.org/10.1515/secm-2013-0041

Ertas, Y., & Uyar, T. (2017). Fabrication of cellulose acetate/polybenzoxazine cross-linked electrospun nanofibrous membrane for water treatment. *Carbohydrate Polymers*, 177(September), 378–387. https://doi.org/10.1016/j.carbpol.2017.08.127

Eryildiz, B., Ozbey-Unal, B., Gezmis-Yavuz, E., Koseoglu-Imer, D. Y., Keskinler, B., & Koyuncu, I. (2021a). Flux-enhanced reduced graphene oxide (rGO)/PVDF nanofibrous membrane distillation membranes for the removal of boron from geothermal water. *Separation and Purification Technology*, 274, 119058. https://doi.org/10.1016/j.seppur.2021.119058

Eryildiz, B., Yuksekdag, A., Korkut, S., & Koyuncu, İ. (2021). Performance evaluation of boron removal from wastewater containing high boron content according to operating parameters by air gap membrane distillation. *Environmental Technology & Innovation*, 22, 101493. https://doi.org/10.1016/j.eti.2021.101493

Esmaeili, M., Khorshidi, S., & Vatanpour, V. (2022). Stabilize thin nanoparticle layer of zeolitic imidazole framework-8 (ZIF-8) on different PVDF substrates by contra-diffusion method for high-efficiency ultrafiltration application. *Journal of Industrial and Engineering Chemistry*, 8(xxxx). https://doi.org/10.1016/j.jiec.2022.02.002

Essalhi, M., Khayet, M., Ismail, N., Sundman, O., & Tavajohi, N. (2021). Improvement of nanostructured electrospun membranes for desalination by membrane distillation technology. *Desalination*, 510(April), 115086. https://doi.org/10.1016/j.desal.2021.115086

Essalhi, M., Khayet, M., Tesfalidet, S., Alsultan, M., & Tavajohi, N. (2021). Desalination by direct contact membrane distillation using mixed matrix electrospun nanofibrous membranes with carbon-based nanofillers: A strategic improvement. *Chemical Engineering Journal*, 426(April), 131316. https://doi.org/10.1016/j.cej.2021.131316

Eykens, L., De Sitter, K., Boeckaert, C., Boeckx, J., & Borgmans, G. (2018). Recovery of brines from cheese making using membrane distillation at lab and pilot scale. *Journal of Food Engineering*, 219, 52–61. https://doi.org/10.1016/j.jfoodeng.2017.09.016

Eykens, L., De Sitter, K., Dotremont, C., Pinoy, L., & Van der Bruggen, B. (2016). How To Optimize the Membrane Properties for Membrane Distillation: A Review. *Industrial and Engineering Chemistry Research*, 55(35), 9333–9343. https://doi.org/10.1021/acs.iecr.6b02226

Eykens, L., Hitsov, I., De Sitter, K., Dotremont, C., Pinoy, L., Nopens, I., & Van der Bruggen, B. (2016). Influence of membrane thickness and process conditions on direct contact membrane distillation at different salinities. *Journal of Membrane Science*, 498, 353–364. https://doi.org/10.1016/j.memsci.2015.07.037

Faigon, M., & Hefer, D. (2008). Boron rejection in SWRO at high pH conditions versus cascade design. *Desalination*, 223(1–3), 10–16. https://doi.org/10.1016/j.desal.2007.02.070

Falde, E. J., Yohe, S. T., Colson, Y. L., & Grinstaff, M. W. (2016). Superhydrophobic materials for biomedical applications. *Biomaterials*, 104, 87–103. https://doi.org/10.1016/j.biomaterials.2016.06.050

Fam, W., Phuntsho, S., Lee, J. H., Cho, J., & Shon, H. K. (2014). Boron transport through polyamide-based thin film composite forward osmosis membranes. *Desalination*, 340, 11–17. https://doi.org/10.1016/j.desal.2014.02.010

Farhat, A., Ahmad, F., Hilal, N., & Arafat, H. A. (2013). Boron removal in new generation reverse osmosis (RO) membranes using two-pass RO without pH adjustment. *Desalination*, 310, 50–59. https://doi.org/10.1016/j.desal.2012.10.003

Feng, C., Khulbe, K. C., Matsuura, T., Gopal, R., Kaur, S., Ramakrishna, S., & Khayet, M. (2008). Production of drinking water from saline water by air-gap membrane distillation using polyvinylidene fluoride nanofiber membrane. *Journal of Membrane Science*, 311(1–2), 1–6. https://doi.org/10.1016/j.memsci.2007.12.026

Figueira, M., Reig, M., Fernández de Labastida, M., Cortina, J. L., & Valderrama, C. (2022). Boron recovery from desalination seawater brines by selective ion exchange resins. *Journal of Environmental Management*, 314, 114984. https://doi.org/10.1016/j.jenvman.2022.114984

Fontananova, E., Jansen, J. C., Cristiano, A., Curcio, E., & Drioli, E. (2006). Effect of additives in the casting solution on the formation of PVDF membranes. *Desalination*, 192(1–3), 190–197. https://doi.org/10.1016/j.desal.2005.09.021

Fortuny, A., Coll, M. T., & Sastre, A. M. (2012a). Boron Removal from Seawater by Supported Liquid Membranes Using Cyphos IL 104 as a Carrier. *Procedia Engineering*, 44, 807–808. https://doi.org/10.1016/j.proeng.2012.08.579

Fortuny, A., Coll, M. T., & Sastre, A. M. (2012b). Use of methyltrioctyl/decylammonium bis 2,4,4-(trimethylpentyl)phosphinate ionic liquid (ALiCY IL) on the boron extraction in chloride media. *Separation and Purification Technology*, 97, 137–141. https://doi.org/10.1016/j.seppur.2012.02.037

Freger, V. (Slava), Shemer, H., Sagiv, A. (Avi), & Semiat, R. (Rafi). (2015). Boron Removal Using Membranes. *In Boron Separation Processes* (pp. 199–217). Elsevier. https://doi.org/10.1016/B978-0-444-63454-2.00008-3

Fujioka, T., Tu, K. L., Khan, S. J., McDonald, J. A., Roux, A., Poussade, Y., Drewes, J. E., & Nghiem, L. D. (2014). Rejection of small solutes by reverse osmosis membranes for water reuse applications: A pilot-scale study. *Desalination*, 350, 28–34. https://doi.org/10.1016/j.desal.2014.07.002

Fukuda, H., Tsuchiya, K., Toba, Y., Eguchi, M., & Tokoro, C. (2020). Rapid boron removal from wastewater using low-crystalline magnesium oxide. *Journal of Environmental Chemical Engineering*, 8(5), 104171. https://doi.org/10.1016/j.jece.2020.104171

Gethard, K., Sae-Khow, O., & Mitra, S. (2011). Water Desalination Using Carbon-Nanotube-Enhanced Membrane Distillation. *ACS Applied Materials & Interfaces*, 3(2), 110–114. https://doi.org/10.1021/am100981s

Ghasemian, S., Sahari, M. A., Barzegar, M., & Ahmadi Gavlighi, H. (2017). Omega-3 PUFA concentration by a novel PVDF nano-composite membrane filled with nano-porous silica particles. *Food Chemistry*, 230, 454–462. https://doi.org/10.1016/j.foodchem.2017.02.135

Ghosh, N. N., Kiskan, B., & Yagci, Y. (2007). Polybenzoxazines-New high performance thermosetting resins: Synthesis and properties. *Progress in Polymer Science* (Oxford), 32(11), 1344–1391. https://doi.org/10.1016/j.progpolymsci.2007.07.002

Gil, J. D., Roca, L., Zaragoza, G., & Berenguel, M. (2018). A feedback control system with reference governor for a solar membrane distillation pilot facility. *Renewable Energy*, 120, 536–549. https://doi.org/10.1016/j.renene.2017.12.107

Glueckstern, P., & Priel, M. (2003). Optimization of boron removal in old and new SWRO systems. *Desalination*, 156(1–3), 219–228. https://doi.org/10.1016/S0011-9164(03)00344-8

Goli, E., Hiemstra, T., Van Riemsdijk, W. H., Rahnemaie, R., & Malakouti, M. J. (2010). Diffusion of Neutral and Ionic Species in Charged Membranes: Boric Acid, Arsenite, and Water. *Analytical Chemistry*, 82(20), 8438–8445. https://doi.org/10.1021/ac1009436

González, D., Amigo, J., & Suárez, F. (2017). Membrane distillation: Perspectives for sustainable and improved desalination. *Renewable and Sustainable Energy Reviews*, 80, 238–259. https://doi.org/10.1016/j.rser.2017.05.078

Greenwood, N. N., & Earnshaw, A. (1997). *Chemistry of the elements* (2nd ed). Butterworth-Heinemann.

Guan, Z., Lv, J., Bai, P., & Guo, X. (2016). Boron removal from aqueous solutions by adsorption—A review. *Desalination*, 383, 29–37. https://doi.org/10.1016/j.desal.2015.12.026

Güell, R., Fontàs, C., Anticó, E., Salvadó, V., Crespo, J. G., & Velizarov, S. (2011). Transport and separation of arsenate and arsenite from aqueous media by supported liquid and anion-exchange membranes. *Separation and Purification Technology*, 80(3), 428–434. https://doi.org/10.1016/j.seppur.2011.05.015

Guijt, C., Meindersma, G., Reith, T., & Haan, A. (2005). Air gap membrane distillation2. Model validation and hollow fibre module performance analysis. *Separation and Purification Technology*, 43(3), 245–255. https://doi.org/10.1016/j.seppur.2004.09.016

Guillén-Burrieza, E., Zaragoza, G., Miralles-Cuevas, S., & Blanco, J. (2012). Experimental evaluation of two pilot-scale membrane distillation modules used for solar desalination. *Journal of Membrane Science,* 409–410, 264–275. https://doi.org/10.1016/j.memsci.2012.03.063

Güler, E., Kabay, N., Yüksel, M., Yavuz, E., & Yüksel, Ü. (2011). A comparative study for boron removal from seawater by two types of polyamide thin film composite SWRO membranes. *Desalination*, 273(1), 81–84. https://doi.org/10.1016/j.desal.2010.10.045

Güler, E., Kabay, N., Yüksel, M., Yiğit, N. Ö., Kitiş, M., & Bryjak, M. (2011). Integrated solution for boron removal from seawater using RO process and sorption-membrane filtration hybrid method. *Journal of Membrane Science*, 375(1–2), 249–257. https://doi.org/10.1016/j.memsci.2011.03.050

Güler, E., Kaya, C., Kabay, N., & Arda, M. (2015). Boron removal from seawater: State-of-the-art review. *Desalination*, 356, 85–93. https://doi.org/10.1016/j.desal.2014.10.009

Gungor, F. S., & Kiskan, B. (2018). Tailoring polyvinyl alcohol with triazinanes and formaldehyde. *Reactive and Functional Polymers*, 124, 115–120. https://doi.org/10.1016/j.reactfunctpolym.2018.01.014

Guo, J., Deka, B. J., Kim, K. J., & An, A. K. (2019). Regeneration of superhydrophobic TiO2 electrospun membranes in seawater desalination by water flushing in membrane distillation. *Desalination*, 468(January). https://doi.org/10.1016/j.desal.2019.06.020

Guo, L., Yuan, W., Li, J., Zhang, Z., & Xie, Z. (2008). Stable superhydrophobic surfaces over a wide pH range. *Applied Surface Science*, 254(7), 2158–2161. https://doi.org/10.1016/j.apsusc.2007.08.089

Guo, W. S., Shim, W. G., Vigneswaran, S., & Ngo, H. H. (2005). Effect of operating parameters in a submerged membrane adsorption hybrid system: Experiments and mathematical modeling. *Journal of Membrane Science*, 247(1–2), 65–74. https://doi.org/10.1016/j.memsci.2004.09.009

Güyagüler, T. (2001). *Türkiye Bor Potansiyeli*. 4, 18–27.

H. Ishida, T. A. (2011). *Handbook of benzoxazine resins*. Elsevier.

H. Polat, A.Vengosh, I. Pankratov, & M.Polat. (2004). A new methodology for removal of boron from water by coal and fly ash. *Desalination*, 164, 173–188.

Han, D., Hwang, M., & Kim, I. S. (2017). Effect of boron rejection and recovery rate on a single-pass design of SWRO using hybrid membrane inter-stage design (HID) concept. *Desalination*, 404, 215–223. https://doi.org/10.1016/j.desal.2016.11.007

Han, F., Bian, Y., & Zhang, C. (2022). Conductive heating vacuum membrane distillation for brine desalination: Study on operational conditions, temperature polarization and energy consumption. *Desalination*, 531, 115726. https://doi.org/10.1016/j.desal.2022.115726

Han, F., Mao, J., & Liu, S. (2022). Preparation of reduced graphene oxide-carbon nanotubes membranes for conductive heating membrane distillation treatment of humic acid. *Separation and Purification Technology*, 302, 122181. https://doi.org/10.1016/j.seppur.2022.122181

Han, L., Iguchi, D., Gil, P., Heyl, T. R., Sedwick, V. M., Arza, C. R., Ohashi, S., Lacks, D. J., & Ishida, H. (2017). Oxazine Ring-Related Vibrational Modes of Benzoxazine Monomers Using Fully Aromatically Substituted, Deuterated, 15N Isotope Exchanged, and Oxazine-Ring-Substituted Compounds and Theoretical Calculations. *Journal of Physical Chemistry A*, 121, 6269–6282. https://doi.org/10.1021/acs.jpca.7b05249

Hanay, A., Boncukcuoğlu, R., Kocakerim, M. M., & Yilmaz, A. E. (2003). Boron removal from geothermal waters by ion exchange in a batch reactor. 12(10)(10), 1190–1194.

Henry Ezechi, E., Hasnain Isa, M., Kutty, S. R. bin M., & Ahmed, Z. (2015). Electrochemical removal of boron from produced water and recovery. *Journal of Environmental Chemical Engineering*, 3(3), 1962–1973. https://doi.org/10.1016/j.jece.2015.05.015

Hilal, N., Kim, G. J., & Somerfield, C. (2011). Boron removal from saline water: A comprehensive review. *Desalination*, 273(1), 23–35. https://doi.org/10.1016/j.desal.2010.05.012

Hirota, Y., Kayama, M., Kamiya, T., & Ito, A. (2016). Hydrophobic Al2O3 Membrane for Sucrose Concentration via Vacuum Membrane Distillation System. *Journal of Chemical Engineering of Japan*, 49(10), 915–919. https://doi.org/10.1252/jcej.16we067

Horseman, T., Yin, Y., Christie, K. S., Wang, Z., Tong, T., & Lin, S. (2021). Wetting, Scaling, and Fouling in Membrane Distillation: State-of-the-Art Insights on Fundamental Mechanisms and Mitigation Strategies. *ACS ES&T Engineering*, 1(1), 117–140. https://doi.org/10.1021/acsestengg.0c00025

Hou, D., Dai, G., Wang, J., Fan, H., Luan, Z., & Fu, C. (2013a). Boron removal and desalination from seawater by PVDF flat-sheet membrane through direct contact membrane distillation. *Desalination*, 326, 115–124. https://doi.org/10.1016/j.desal.2013.07.023

Hou, D., Dai, G., Wang, J., Fan, H., Luan, Z., & Fu, C. (2013b). Boron removal and desalination from seawater by PVDF flat-sheet membrane through direct contact membrane distillation. *Desalination*, 326, 115–124. https://doi.org/10.1016/j.desal.2013.07.023

Hou, D., Ding, C., Fu, C., Wang, D., Zhao, C., & Wang, J. (2019). Electrospun nanofibrous omniphobic membrane for anti-surfactant-wetting membrane distillation desalination. *Desalination*, 468(August 2018), 114068. https://doi.org/10.1016/j.desal.2019.07.008

Hou, D., Wang, J., Sun, X., Luan, Z., Zhao, C., & Ren, X. (2010a). Boron removal from aqueous solution by direct contact membrane distillation. *Journal of Hazardous Materials*, 177(1–3), 613–619. https://doi.org/10.1016/j.jhazmat.2009.12.076

Hou, D., Wang, J., Sun, X., Luan, Z., Zhao, C., & Ren, X. (2010b). Boron removal from aqueous solution by direct contact membrane distillation. *Journal of Hazardous Materials*, 177(1–3), 613–619. https://doi.org/10.1016/j.jhazmat.2009.12.076

Howard Devoe. (2001). Thermodymanics and Chemistry (2nd ed.). Prentice Hall.

Hsieh, I.-M., Thakur, A. K., & Malmali, M. (2021). Comparative analysis of various pretreatments to mitigate fouling and scaling in membrane distillation. *Desalination*, 509, 115046. https://doi.org/10.1016/j.desal.2021.115046

Hu, W., Huang, J., Zhang, X., Zhao, S., Pei, L., Zhang, C., Liu, Y., & Wang, Z. (2020). A mechanically robust and reversibly wettable benzoxazine/epoxy/mesoporous TiO2 coating for oil/water separation. *Applied Surface Science*, 507, 145168. https://doi.org/10.1016/j.apsusc.2019.145168

Hung, W.-C., Horng, R. S., & Tsai, C.-H. (2022). Effects of process conditions on simultaneous removal and recovery of boron from boron-laden wastewater using improved bipolar membrane electrodialysis (BMED). *Journal of Water Process Engineering*, 47, 102650. https://doi.org/10.1016/j.jwpe.2022.102650

Hussain, A., Sharma, R., Minier-Matar, J., Hirani, Z., & Adham, S. (2019). Application of emerging ion exchange resin for boron removal from saline groundwater. *Journal of Water Process Engineering*, 32, 100906. https://doi.org/10.1016/j.jwpe.2019.100906

Hyung, H., & Kim, J.-H. (2006). A mechanistic study on boron rejection by sea water reverse osmosis membranes. *Journal of Membrane Science*, 286(1–2), 269–278. https://doi.org/10.1016/j.memsci.2006.09.043

İpekçi, D., Altıok, E., Bunani, S., Yoshizuka, K., Nishihama, S., Arda, M., & Kabay, N. (2018). Effect of acid-base solutions used in acid-base compartments for simultaneous recovery of lithium and boron from aqueous solution using bipolar membrane electrodialysis (BMED). *Desalination*, 448, 69–75. https://doi.org/10.1016/j.desal.2018.10.001

İpekçi, D., Kabay, N., Bunani, S., Altıok, E., Arda, M., Yoshizuka, K., & Nishihama, S. (2020). Application of heterogeneous ion exchange membranes for simultaneous separation and recovery of lithium and boron from aqueous solution with bipolar membrane electrodialysis (EDBM). *Desalination*, 479, 114313. https://doi.org/10.1016/j.desal.2020.114313

Irawan, C., Kuo, Y.-L., & Liu, J. C. (2011). Treatment of boron-containing optoelectronic wastewater by precipitation process. *Desalination*, 280(1–3), 146–151. https://doi.org/10.1016/j.desal.2011.06.064

Islam, Md. S., Akter, N., & Karim, M. R. (2010). Preparation of superhydrophobic membranes by electrospinning of fluorinated silane functionalized pullulan. *Colloids and Surfaces A: Physicochemical and Engineering Aspects*, 362(1–3), 117–120. https://doi.org/10.1016/j.colsurfa.2010.04.004

Itakura, T., Sasai, R., & Itoh, H. (2005). Precipitation recovery of boron from wastewater by hydrothermal mineralization. *Water Research*, 39(12), 2543–2548. https://doi.org/10.1016/j.watres.2005.04.035

Jacob, C. (2007). Seawater desalination: Boron removal by ion exchange technology. *Desalination*, 205(1–3), 47–52. https://doi.org/10.1016/j.desal.2006.06.007

Jia, F., Li, J., & Wang, J. (2017a). Recovery of boric acid from the simulated radioactive wastewater by vacuum membrane distillation crystallization. *Annals of Nuclear Energy*, 110, 1148–1155. https://doi.org/10.1016/j.anucene.2017.07.024

Jia, F., Li, J., & Wang, J. (2017b). Recovery of boric acid from the simulated radioactive wastewater by vacuum membrane distillation crystallization. *Annals of Nuclear Energy*, 110, 1148–1155. https://doi.org/10.1016/j.anucene.2017.07.024

Jia, X., Lan, L., Zhang, X., Wang, T., Wang, Y., Ye, C., & Lin, J. (2021). Pilot-scale vacuum membrane distillation for decontamination of simulated radioactive wastewater: System design and performance evaluation. *Separation and Purification Technology*, 275, 119129. https://doi.org/10.1016/j.seppur.2021.119129

Jiang, G., Zhang, C., Xie, S., Wang, X., Li, W., Cai, J., Lu, F., Han, Y., Ye, X., & Xue, L. (2022). Facile Fabrication of Electrospun Nanofibrous Aerogels for Efficient Oil Absorption and Emulsified Oil–Water Separation. *ACS Omega*, 7(8), 6674–6681. https://doi.org/10.1021/acsomega.1c06080

Jin, X., She, Q., Ang, X., & Tang, C. Y. (2012). Removal of boron and arsenic by forward osmosis membrane: Influence of membrane orientation and organic fouling. *Journal of Membrane Science*, 389, 182–187. https://doi.org/10.1016/j.memsci.2011.10.028

Jin, X., Tang, C. Y., Gu, Y., She, Q., & Qi, S. (2011). Boric Acid Permeation in Forward Osmosis Membrane Processes: Modeling, Experiments, and Implications. *Environmental Science & Technology*, 45(6), 2323–2330. https://doi.org/10.1021/es103771a

Ju, J., Li, Z., Lv, Y., Liu, M., Fejjari, K., Kang, W., & Liao, Y. (2020). Electrospun PTFE/PI bi-component membranes with robust 3D superhydrophobicity and high water permeability for membrane distillation. *Journal of Membrane Science*, 611, 118420. https://doi.org/10.1016/j.memsci.2020.118420

Jung, S., & Kim, M.-J. (2016). Optimal conditions for recovering boron from seawater using boron selective resins. *Korean Journal of Chemical Engineering*, 33(8), 2411–2417. https://doi.org/10.1007/s11814-016-0096-4

Kabay, N., & Bryjak, M. (2015). Boron Removal From Seawater Using Reverse Osmosis Integrated Processes. *In Boron Separation Processes* (pp. 219–235). Elsevier. https://doi.org/10.1016/B978-0-444-63454-2.00009-5

Kabay, N., Köseoğlu, P., Yapıcı, D., Yüksel, Ü., & Yüksel, M. (2013). Coupling ion exchange with ultrafiltration for boron removal from geothermal water-investigation of process parameters and recycle tests. *Desalination*, 316, 17–22. https://doi.org/10.1016/j.desal.2013.01.027

Kabay, N., Sarp, S., Yuksel, M., Arar, Ö., & Bryjak, M. (2007). Removal of boron from seawater by selective ion exchange resins. *Reactive and Functional Polymers*, 67(12), 1643–1650. https://doi.org/10.1016/j.reactfunctpolym.2007.07.033

Kabay, N., Sarp, S., Yuksel, M., Kitis, M., Koseoğlu, H., Arar, Ö., Bryjak, M., & Semiat, R. (2008). Removal of boron from SWRO permeate by boron selective ion exchange resins containing N-methyl glucamine groups. *Desalination*, 223(1–3), 49–56. https://doi.org/10.1016/j.desal.2007.01.199

Kabay, N., Yilmaz, İ., Bryjak, M., & Yüksel, M. (2006). Removal of boron from aqueous solutions by a hybrid ion exchange–membrane process. *Desalination*, 198(1–3), 158–165. https://doi.org/10.1016/j.desal.2006.09.011

Kabay, N., Yilmaz-Ipek, I., Soroko, I., Makowski, M., Kirmizisakal, O., Yag, S., Bryjak, M., & Yuksel, M. (2009). Removal of boron from Balcova geothermal water by ion exchange–microfiltration hybrid process. *Desalination*, 241(1–3), 167–173. https://doi.org/10.1016/j.desal.2007.10.100

Kabay, N., Yılmaz, I., Yamac, S., Samatya, S., Yuksel, M., Yuksel, U., Arda, M., Sağlam, M., Iwanaga, T., & Hirowatari, K. (2004). Removal and recovery of boron from geothermal wastewater by selective ion exchange resins. I. Laboratory tests. *Reactive and Functional Polymers*, 60, 163–170. https://doi.org/10.1016/j.reactfunctpolym.2004.02.020

Kabeel, A. E., Abdelgaied, M., & El-Said, E. M. S. (2017). Study of a solar-driven membrane distillation system: Evaporative cooling effect on performance enhancement. *Renewable Energy*, 106, 192–200. https://doi.org/10.1016/j.renene.2017.01.030

Kao, T. H., Chen, J. K., Cheng, C. C., Su, C. I., & Chang, F. C. (2013). Low-surface-free-energy polybenzoxazine/polyacrylonitrile fibers for biononfouling membrane. *Polymer*, 54(1), 258–268. https://doi.org/10.1016/j.polymer.2012.11.020

Karakaplan, M., Tural, S., Tural, B., Turgut, Y., & Hoşgören, H. (2004). The Solvent Extraction of Boron with Synthesized Aliphatic 1,3-Diols: Stripping and Extraction Behavior of Boron by 2,2,5-Trimethyl-1,3-hexanediol. *Solvent Extraction and Ion Exchange*, 22(6), 897–911. https://doi.org/10.1081/SEI-200037400

Kavak, D. (2009). Removal of boron from aqueous solutions by batch adsorption on calcined alunite using experimental design. *Journal of Hazardous Materials*, 163(1), 308–314. https://doi.org/10.1016/j.jhazmat.2008.06.093

Kebria, M. R. S., Rahimpour, A., Salestan, S. K., Seyedpour, S. F., Jafari, A., Banisheykholeslami, F., & Tavajohi Hassan Kiadeh, N. (2020). Hyper-branched dendritic structure modified PVDF electrospun membranes for air gap membrane distillation. *Desalination*, 479(November 2019), 114307. https://doi.org/10.1016/j.desal.2019.114307

Kezia, K., Lee, J., Hill, A. J., & Kentish, S. E. (2013). Convective transport of boron through a brackish water reverse osmosis membrane. *Journal of Membrane Science*, 445, 160–169. https://doi.org/10.1016/j.memsci.2013.05.041

Khayet, M. (2011). Membranes and theoretical modeling of membrane distillation: A review. *Advances in Colloid and Interface Science*, 164(1–2), 56–88. https://doi.org/10.1016/j.cis.2010.09.005

Khayet, M., García-Payo, C., & Matsuura, T. (2019). Superhydrophobic nanofibers electrospun by surface segregating fluorinated amphiphilic additive for membrane distillation. *Journal of Membrane Science*, 588, 117215. https://doi.org/10.1016/j.memsci.2019.117215

Khayet, M., & Matsuura, T. (2011a). Air Gap Membrane Distillation. *In Membrane Distillation* (pp. 361–398). Elsevier. https://doi.org/10.1016/B978-0-444-53126-1.10013-2

Khayet, M., & Matsuura, T. (2011b). Membranes Used in MD and Design. *In Membrane Distillation* (pp. 17–40). Elsevier. https://doi.org/10.1016/B978-0-444-53126-1.10002-8

Kim, C., Lee, S., Shon, H. K., Elimelech, M., & Hong, S. (2012). Boron transport in forward osmosis: Measurements, mechanisms, and comparison with reverse osmosis. *Journal of Membrane Science*, 419–420, 42–48. https://doi.org/10.1016/j.memsci.2012.06.042

Kim, D. H., Moon, S.-H., & Cho, J. (2003). Investigation of the adsorption and transport of natural organic matter (NOM) in ion-exchange membranes. *Desalination*, 151(1), 11–20. https://doi.org/10.1016/S0011-9164(02)00968-2

Kim, H.-K., & Cho, Y.-S. (2015). Fabrication of a superhydrophobic surface via spraying with polystyrene and multi-walled carbon nanotubes. *Colloids and Surfaces A: Physicochemical and Engineering Aspects*, 465, 77–86. https://doi.org/10.1016/j.colsurfa.2014.10.029

Kim, J. E., Phuntsho, S., Chekli, L., Choi, J. Y., & Shon, H. K. (2018). Environmental and economic assessment of hybrid FO-RO/NF system with selected inorganic draw solutes for the treatment of mine impaired water. *Desalination*, 429, 96–104. https://doi.org/10.1016/j.desal.2017.12.016

Kim, S., Kim, S., Ahmed, Z., Cha, D. K., & Cho, J. (2018). Flux model for the membrane distillation process to treat wastewater: Effect of solids concentration. *Journal of Membrane Science*, 566, 396–405. https://doi.org/10.1016/j.memsci.2018.09.018

Kim, Y., Choi, Y., Choi, J., & Lee, S. (2020). Powdered activated carbon (PAC) – vacuum-assisted air gap membrane distillation (V-AGMD) hybrid system to treat wastewater containing surfactants: Effect of operating conditions. *Environmental Engineering Research*, 26(5), 200377–0. https://doi.org/10.4491/eer.2020.377

Kir, E., Gurler, B., & Gulec, A. (2011). Boron removal from aqueous solution by using plasma-modified and unmodified anion-exchange membranes. *Desalination*, 267(1), 114–117. https://doi.org/10.1016/j.desal.2010.08.037

Kiskan, B. (2018). Adapting benzoxazine chemistry for unconventional applications. *Reactive and Functional Polymers*, 129(May 2017), 76–88. https://doi.org/10.1016/j.reactfunctpolym.2017.06.009

Kluczka, J., Trojanowska, J., & Zołotajkin, M. (2015). Utilization of fly ash zeolite for boron removal from aqueous solution. *Desalination and Water Treatment*, 54(7), 1839–1849. https://doi.org/10.1080/19443994.2014.892033

Kocherginsky, N. M., Yang, Q., & Seelam, L. (2007). Recent advances in supported liquid membrane technology. *Separation and Purification Technology*, 53(2), 171–177. https://doi.org/10.1016/j.seppur.2006.06.022

Kochkodan, V., Darwish, N. B., & Hilal, N. (2015). The Chemistry of Boron in Water. *In Boron Separation Processes* (pp. 35–63). Elsevier. https://doi.org/10.1016/B978-0-444-63454-2.00002-2

Kolesnik, I., Tverdokhlebova, T., Danilenko, N., Plotnikov, E., Kulbakin, D., Zheravin, A., Bouznik, V., & Bolbasov, E. (2021). Characterization and Determination of the Biocompatibility of Porous Polytetrafluoroethylene Membranes Fabricated via Electrospinning. *Journal of Fluorine Chemistry*, 246(October 2020), 109798. https://doi.org/10.1016/j.jfluchem.2021.109798

Koltuniewicz, A. B., Witek, A., & Bezak, K. (2004). Efficiency of membrane-sorption integrated processes. *Journal of Membrane Science*, 239(1), 129–141. https://doi.org/10.1016/j.memsci.2004.02.037

Köse, T. E., & Öztürk, N. (2008). Boron removal from aqueous solutions by ion-exchange resin: Column sorption–elution studies. *Journal of Hazardous Materials*, 152(2), 744–749. https://doi.org/10.1016/j.jhazmat.2007.07.041

Koseoglu, H., Harman, B. I., Yigit, N. O., Guler, E., Kabay, N., & Kitis, M. (2010). The effects of operating conditions on boron removal from geothermal waters by membrane processes. *Desalination*, 258(1–3), 72–78. https://doi.org/10.1016/j.desal.2010.03.043

Koseoglu, H., Kabay, N., Yüksel, M., & Kitis, M. (2008). The removal of boron from model solutions and seawater using reverse osmosis membranes. *Desalination*, 223(1–3), 126–133. https://doi.org/10.1016/j.desal.2007.01.189

Kot, F. S. (2015). Boron in the Environment. *In Boron Separation Processes* (pp. 1–33). Elsevier. https://doi.org/10.1016/B978-0-444-63454-2.00001-0

Kurdian, A. R., Bahreini, M., Montazeri, G. H., & Sadeghi, S. (2013). Modeling of direct contact membrane distillation process: Flux prediction of sodium sulfate and sodium chloride solutions. *Desalination*, 323, 75–82. https://doi.org/10.1016/j.desal.2013.05.002

Kwon, T., Hirata, M., Sakuma, S., Hano, T., & Yamagishi, T. (2005). Continuous Recovery of Boron from Wastewater with a Diol. *Solvent Extraction and Ion Exchange*, 23(3), 391–400. https://doi.org/10.1081/SEI-200056524

La Cerva, M., Gurreri, L., Cipollina, A., Tamburini, A., Ciofalo, M., & Micale, G. (2019). Modelling and cost analysis of hybrid systems for seawater desalination: Electromembrane pre-treatments for Reverse Osmosis. *Desalination*, 467, 175–195. https://doi.org/10.1016/j.desal.2019.06.010

Lan, N., Wang, K. Y., Weber, M., Maletzko, C., & Chung, T.-S. (2021). Investigation of novel molecularly tunable thin-film nanocomposite nanofiltration hollow fiber membranes for boron removal. *Journal of Membrane Science*, 620, 118887. https://doi.org/10.1016/j.memsci.2020.118887

Landsman, M. R., Lawler, D. F., & Katz, L. E. (2020). Application of electrodialysis pretreatment to enhance boron removal and reduce fouling during desalination by nanofiltration/reverse osmosis. *Desalination*, 491, 114563. https://doi.org/10.1016/j.desal.2020.114563

Lawson, K. W., & Lloyd, D. R. (1997). Membrane distillation. *Journal of Membrane Science*, 124(1), 1–25. https://doi.org/10.1016/S0376-7388(96)00236-0

Lee, C., Nguyen, T.-T., Adha, R. S., Shon, H. K., & Kim, I. S. (2020). Influence of hydrodynamic operating conditions on organic fouling of spiral-wound forward osmosis membranes: Fouling-induced performance deterioration in FO-RO hybrid system. *Water Research*, 185, 116154. https://doi.org/10.1016/j.watres.2020.116154

Lee, C.-K., Park, C., Woo, Y. C., Choi, J.-S., & Kim, J.-O. (2020). A pilot study of spiral-wound air gap membrane distillation process and its energy efficiency analysis. *Chemosphere*, 239, 124696. https://doi.org/10.1016/j.chemosphere.2019.124696

Lee, H. (2002). Characterization of anion exchange membranes fouled with humate during electrodialysis. *Journal of Membrane Science*, 203(1–2), 115–126. https://doi.org/10.1016/S0376-7388(01)00792-X

Lee, H.-J., Kim, D. H., Cho, J., & Moon, S.-H. (2003). Characterization of anion exchange membranes with natural organic matter (NOM) during electrodialysis. *Desalination*, 151(1), 43–52. https://doi.org/10.1016/S0011-9164(02)00971-2

Lee, J. G., Kim, W. S., Choi, J. S., Ghaffour, N., & Kim, Y. D. (2018). Dynamic solar-powered multi-stage direct contact membrane distillation system: Concept design, modeling and simulation. *Desalination*, 435, 278–292. https://doi.org/10.1016/j.desal.2017.04.008

Lee, S., Kim, Y., & Hong, S. (2018). Treatment of industrial wastewater produced by desulfurization process in a coal-fired power plant via FO-MD hybrid process. *Chemosphere*, 210, 44–51. https://doi.org/10.1016/j.chemosphere.2018.06.180

Li, B., Hou, D., Li, C., & Yun, Y. (2022). Mussels-inspired design a carbon nanotube based underwater superoleophobic/hydrophobic Janus membrane with robust anti-oil-fouling for direct contact membrane distillation. *Separation and Purification Technology*, 294, 121163. https://doi.org/10.1016/j.seppur.2022.121163

Li, H. Y., & Liu, Y. L. (2013). Polyelectrolyte composite membranes of polybenzimidazole and crosslinked polybenzimidazole-polybenzoxazine electrospun nanofibers for proton exchange membrane fuel cells. *Journal of Materials Chemistry A*, 1(4), 1171–1178. https://doi.org/10.1039/c2ta00270a

Li, K., Hou, D., Fu, C., Wang, K., & Wang, J. (2019). Fabrication of PVDF nanofibrous hydrophobic composite membranes reinforced with fabric substrates via electrospinning for membrane distillation desalination. *Journal of Environmental Sciences* (China), 75, 277–288. https://doi.org/10.1016/j.jes.2018.04.002

Li, L., & Sirkar, K. K. (2017). Studies in vacuum membrane distillation with flat membranes. *Journal of Membrane Science*, 523, 225–234. https://doi.org/10.1016/j.memsci.2016.09.028

Li, L., Zi, F. T., & Zheng, Y. F. (2008). The characterization of fluorocarbon films on NiTi alloy by magnetron sputtering. *Applied Surface Science*, 255(2), 432–434. https://doi.org/10.1016/j.apsusc.2008.06.174

Li, M., Li, K., Wang, L., & Zhang, X. (2020). Feasibility of concentrating textile wastewater using a hybrid forward osmosis-membrane distillation (FO-MD) process: Performance and economic evaluation. *Water Researc*h, 172, 115488. https://doi.org/10.1016/j.watres.2020.115488

Li, X., Wang, Z., Han, X., & Wang, J. (2022). Facile fabrication of hydroxyl-rich polyamide TFC RO membranes for enhanced boron removal performance. *Desalination*, 531, 115723. https://doi.org/10.1016/j.desal.2022.115723

Li, Y., Wang, S., Song, X., Zhou, Y., Shen, H., Cao, X., Zhang, P., & Gao, C. (2020). High boron removal polyamide reverse osmosis membranes by swelling induced embedding of a sulfonyl molecular plug. *Journal of Membrane Science*, 597, 117716. https://doi.org/10.1016/j.memsci.2019.117716

Li, Z., Liu, Y., Yan, J., Wang, K., Xie, B., Hu, Y., Kang, W., & Cheng, B. (2019). Electrospun polyvinylidene fluoride/fluorinated acrylate copolymer tree-like nanofiber membrane with high flux and salt rejection ratio for direct contact membrane distillation. *Desalination*, 466(May), 68–76. https://doi.org/10.1016/j.desal.2019.05.005

Liang, C. H. (2005). Separation properties of high temperature reverse osmosis membranes for silica removal and boric acid recovery. *Journal of Membrane Science*, 246(2), 127–135. https://doi.org/10.1016/j.memsci.2004.07.006

Liang, H., Gong, W., & Li, G. (2008). Performance evaluation of water treatment ultrafiltration pilot plants treating algae-rich reservoir water. *Desalination*, 221(1–3), 345–350. https://doi.org/10.1016/j.desal.2007.01.093

Liao, Y. L., Hu, C. C., Lai, J. Y., & Liu, Y. L. (2017). Crosslinked polybenzoxazine based membrane exhibiting in-situ self-promoted separation performance for pervaporation dehydration on isopropanol aqueous solutions. *Journal of Membrane Science*, 531(February), 10–15. https://doi.org/10.1016/j.memsci.2017.02.039

Liao, Y., Wang, R., & Fane, A. G. (2013). Engineering superhydrophobic surface on poly(vinylidene fluoride) nanofiber membranes for direct contact membrane distillation. *Journal of Membrane Science*, 440, 77–87. https://doi.org/10.1016/j.memsci.2013.04.006

Liao, Y., Wang, R., & Fane, A. G. (2014a). Fabrication of Bioinspired Composite Nanofiber Membranes with Robust Superhydrophobicity for Direct Contact Membrane Distillation. *Environmental Science & Technology*, 48(11), 6335–6341. https://doi.org/10.1021/es405795s

Liao, Y., Wang, R., & Fane, A. G. (2014b). Fabrication of bioinspired composite nanofiber membranes with robust superhydrophobicity for direct contact membrane distillation. *Environmental Science and Technology*, 48(11), 6335–6341. https://doi.org/10.1021/es405795s

Lim, Y. J., Goh, K., Kurihara, M., & Wang, R. (2021). Seawater desalination by reverse osmosis: Current development and future challenges in membrane fabrication – A review. *Journal of Membrane Science*, 629, 119292. https://doi.org/10.1016/j.memsci.2021.119292

Lin, J.-Y., Shih, Y.-J., Chen, P.-Y., & Huang, Y.-H. (2016). Precipitation recovery of boron from aqueous solution by chemical oxo-precipitation at room temperature. *Applied Energy*, 164, 1052–1058. https://doi.org/10.1016/j.apenergy.2014.12.058

Liu, C. T., & Liu, Y. L. (2016). PH-Induced switches of the oil- and water-selectivity of crosslinked polymeric membranes for gravity-driven oil-water separation. *Journal of Materials Chemistry A*, 4(35), 13543–13548. https://doi.org/10.1039/c6ta05968f

Liu, X., Wu, J., & Wang, J. (2019). Removal of nuclides and boric acid from simulated radioactive wastewater by forward osmosis. *Progress in Nuclear Energy*, 114, 155–163. https://doi.org/10.1016/j.pnucene.2019.03.014

Liu, Z., Gao, J., & Xiao, C. (2021). Preparation and vacuum membrane distillation performance of a superhydrophobic polypropylene hollow fiber membrane modified via ATRP. *Desalination*, 512, 115130. https://doi.org/10.1016/j.desal.2021.115130

Liu, Z., Gao, Q., Lu, X., Ma, Z., Zhang, H., & Wu, C. (2017). Experimental study of the optimal vacuum pressure in vacuum assisted air gap membrane distillation process. *Desalination*, 414, 63–72. https://doi.org/10.1016/j.desal.2017.03.031

Lochab, B., Monisha, M., Amarnath, N., Sharma, P., Mukherjee, S., & Ishida, H. (2021). Review on the accelerated and low-temperature polymerization of benzoxazine resins: Addition polymerizable sustainable polymers. *Polymers*, 13(8). https://doi.org/10.3390/polym13081260

Luo, J., Huo, L., Wang, L., Huang, X., Li, J., Guo, Z., Gao, Q., Hu, M., Xue, H., & Gao, J. (2020). Superhydrophobic and multi-responsive fabric composite with excellent electro-photo-thermal effect and electromagnetic interference shielding performance. *Chemical Engineering Journal*, 391, 123537. https://doi.org/10.1016/j.cej.2019.123537

Lyu, J., Zeng, Z., Zhang, N., Liu, H., Bai, P., & Guo, X. (2017). Pyrocatechol-modified resins for boron recovery from water: Synthesis, adsorption and isotopic separation studies. *Reactive and Functional Polymers*, 112, 1–8. https://doi.org/10.1016/j.reactfunctpolym.2016.12.016

Ma, W., Guo, Z., Zhao, J., Yu, Q., Wang, F., Han, J., Pan, H., Yao, J., Zhang, Q., Samal, S. K., De Smedt, S. C., & Huang, C. (2017). Polyimide/cellulose acetate core/shell electrospun fibrous membranes for oil-water separation. *Separation and Purification Technology*, 177, 71–85. https://doi.org/10.1016/j.seppur.2016.12.032

Ma, W., Zhang, M., Liu, Z., Kang, M., Huang, C., & Fu, G. (2019). Fabrication of highly durable and robust superhydrophobic-superoleophilic nanofibrous membranes based on a fluorine-free system for efficient oil/water separation. *Journal of Membrane Science*, 570–571(August 2018), 303–313. https://doi.org/10.1016/j.memsci.2018.10.035

Mani, K. N. (1991). Electrodialysis water splitting technology. *Journal of Membrane Science*, 58(2), 117–138. https://doi.org/10.1016/S0376-7388(00)82450-3

Matsumoto, M., Kondo, K., Hirata, M., Kokubu, S., Hano, T., & Takada, T. (1997). Recovery of Boric Acid from Wastewater by Solvent Extraction. *Separation Science and Technology*, 32(5), 983–991. https://doi.org/10.1080/01496399708000940

Melnyk, L., Goncharuk, V., Butnyk, I., & Tsapiuk, E. (2005). Boron removal from natural and wastewaters using combined sorption/membrane process. *Desalination*, 185(1–3), 147–157. https://doi.org/10.1016/j.desal.2005.02.076

Mericq, J.-P., Laborie, S., & Cabassud, C. (2010). Vacuum membrane distillation of seawater reverse osmosis brines. *Water Research*, 44(18), 5260–5273. https://doi.org/10.1016/j.watres.2010.06.052

Mezher, T., Fath, H., Abbas, Z., & Khaled, A. (2011). Techno-economic assessment and environmental impacts of desalination technologies. *Desalination*, 266(1–3), 263–273. https://doi.org/10.1016/j.desal.2010.08.035

Mollah, M. Y. A., Schennach, R., Parga, J. R., & Cocke, D. L. (2001). Electrocoagulation (EC)—Science and applications. *Journal of Hazardous Materials*, 84(1), 29–41. https://doi.org/10.1016/S0304-3894(01)00176-5

Munirasu, S., Banat, F., Durrani, A. A., & Haija, M. A. (2017). Intrinsically superhydrophobic PVDF membrane by phase inversion for membrane distillation. *Desalination*, 417, 77–86. https://doi.org/10.1016/j.desal.2017.05.019

Mutlu Salmanli, O., Yuksekdag, A., & Koyuncu, I. (2022a). Boron removal by using vacuum assisted air gap membrane distillation (VAGMD). *Environmental Technology and Innovation*, 26, 102395. https://doi.org/10.1016/j.eti.2022.102395

Mutlu-Salmanli, O., Eryildiz, B., Vatanpour, V., Deliballi, Z., Kiskan, B., & Koyuncu, I. (2023). Fabrication of novel hydrophobic electrospun nanofiber membrane using polybenzoxazine for membrane distillation application. *Desalination*, 546, 116203. https://doi.org/10.1016/j.desal.2022.116203

Mutlu-Salmanli, O., Kazak, A., Turken, T., Pasaoglu, M. E., Zeytuncu, B., & Koyuncu, I. (2023). Boron removal and recovery via vacuum assisted air gap membrane distillation-crystallization (VAGMD-C): A pilot-scale study. *Desalination*, 547, 116229. https://doi.org/10.1016/j.desal.2022.116229

Mutlu-Salmanli, O., & Koyuncu, I. (2022). Boron removal and recovery from water and wastewater. *Reviews in Environmental Science and Bio/Technology*, 21(3), 635–664. https://doi.org/10.1007/s11157-022-09629-w

Nagasawa, H., Iizuka, A., Yamasaki, A., & Yanagisawa, Y. (2011). Utilization of Bipolar Membrane Electrodialysis for the Removal of Boron from Aqueous Solution. *Industrial & Engineering Chemistry Research*, 50(10), 6325–6330. https://doi.org/10.1021/ie1014684

Naidu, G., Shim, W. G., Jeong, S., Choi, Y., Ghaffour, N., & Vigneswaran, S. (2017). Transport phenomena and fouling in vacuum enhanced direct contact membrane distillation: Experimental and modelling. *Separation and Purification Technology*, 172, 285–295. https://doi.org/10.1016/j.seppur.2016.08.024

Naidu, G., Zhong, X., & Vigneswaran, S. (2018). Comparison of membrane distillation and freeze crystallizer as alternatives for reverse osmosis concentrate treatment. *Desalination*, 427, 10–18. https://doi.org/10.1016/j.desal.2017.10.043

Najid, N., Kouzbour, S., Ruiz-García, A., Fellaou, S., Gourich, B., & Stiriba, Y. (2021). Comparison analysis of different technologies for the removal of boron from seawater: A review. *Journal of Environmental Chemical Engineering*, 9(2), 105133. https://doi.org/10.1016/j.jece.2021.105133

Ngwabebhoh, F. A., Mammadli, N., & Yildiz, U. (2019). Bioinspired modified nanocellulose adsorbent for enhanced boron recovery from aqueous media: Optimization, kinetics, thermodynamics and reusability study. *Journal of Environmental Chemical Engineering*, 7(5), 103281. https://doi.org/10.1016/j.jece.2019.103281

Noguchi, M., Nakamura, Y., Shoji, T., Iizuka, A., & Yamasaki, A. (2018). Simultaneous removal and recovery of boron from waste water by multi-step bipolar membrane electrodialysis. *Journal of Water Process Engineering*, 23, 299–305. https://doi.org/10.1016/j.jwpe.2018.04.010

Ofir, E., Brenner, A., Muuler, K., & Gitis, V. (2011). Boron removal from seawater by electro-chemical treatment as part of water desalination. *Desalination and Water Treatment*, 31(1–3), 102–106. https://doi.org/10.5004/dwt.2011.2334

Okuno, K., Kawai, M., & Yamada, H. (2009). Development of Novel Neutron Shielding Concrete. *Nuclear Technology*, 168(2), 545–552. https://doi.org/10.13182/NT09-A9241

Oladipo, A. A., & Gazi, M. (2017). Targeted boron removal from highly-saline and boron-spiked seawater using magnetic nanobeads: Chemometric optimisation and modelling studies. *Chemical Engineering Research and Design*, 121, 329–338. https://doi.org/10.1016/j.cherd.2017.03.024

Oo, M. H., & Ong, S. L. (2010). Implication of zeta potential at different salinities on boron removal by RO membranes. *Journal of Membrane Science*, 352(1–2), 1–6. https://doi.org/10.1016/j.memsci.2010.01.030

Oo, M. H., & Song, L. (2009). Effect of pH and ionic strength on boron removal by RO membranes. *Desalination*, 246(1–3), 605–612. https://doi.org/10.1016/j.desal.2008.06.025

Oto, B., Gür, A., Kaçal, M. R., Doğan, B., & Arasoğlu, A. (2013). Photon attenuation properties of some concretes containing barite and colemanite in different rates. *Annals of Nuclear Energy*, 51, 120–124. https://doi.org/10.1016/j.anucene.2012.06.033

Ozbey-Unal, B., Gezmis-Yavuz, E., Eryildiz, B., Koseoglu-Imer, D. Y., Keskinler, B., & Koyuncu, I. (2020a). Boron removal from geothermal water by nanofiber-based membrane distillation membranes with significantly improved surface hydrophobicity. *Journal of Environmental Chemical Engineering*, 8(5), 104113. https://doi.org/10.1016/j.jece.2020.104113

Ozbey-Unal, B., Gezmis-Yavuz, E., Eryildiz, B., Koseoglu-Imer, D. Y., Keskinler, B., & Koyuncu, I. (2020b). Boron removal from geothermal water by nanofiber-based membrane distillation membranes with significantly improved surface hydrophobicity. *Journal of Environmental Chemical Engineering*, 8(5). https://doi.org/10.1016/j.jece.2020.104113

Ozbey-Unal, B., Imer, D. Y., Keskinler, B., & Koyuncu, I. (2018). Boron removal from geothermal water by air gap membrane distillation. *Desalination*, 433, 141–150. https://doi.org/10.1016/j.desal.2018.01.033

Özdemir, M., & Kıpçak, İ. (2010). Recovery of boron from borax sludge of boron industry. *Minerals Engineering*, 23(9), 685–690. https://doi.org/10.1016/j.mineng.2010.04.003

Ozturk, N., & Kavak, D. (2005). Adsorption of boron from aqueous solutions using fly ash: Batch and column studies. *Journal of Hazardous Materials*, 127(1–3), 81–88. https://doi.org/10.1016/j.jhazmat.2005.06.026

Öztürk, N., Kavak, D., & Köse, T. E. (2008). Boron removal from aqueous solution by reverse osmosis. *Desalination*, 223(1–3), 1–9. https://doi.org/10.1016/j.desal.2007.01.178

Pagliero, M., Bottino, A., Comite, A., & Costa, C. (2020). Novel hydrophobic PVDF membranes prepared by nonsolvent induced phase separation for membrane distillation. *Journal of Membrane Science*, 596(September 2019), 117575. https://doi.org/10.1016/j.memsci.2019.117575

Pakkethati, K., Boonmalert, A., Chaisuwan, T., & Wongkasemjit, S. (2011). Development of polybenzoxazine membranes for ethanol-water separation via pervaporation. *Desalination*, 267(1), 73–81. https://doi.org/10.1016/j.desal.2010.09.008

Palenzuela, P., Miralles-Cuevas, S., Cabrera-Reina, A., & Cornejo-Ponce, L. (2018). Techno-economic assessment of a multi-effect distillation plant installed for the production of irrigation water in Arica (Chile). *Science of The Total Environment*, 643, 423–434. https://doi.org/10.1016/j.scitotenv.2018.06.183

Pang, H., Tian, K., Li, Y., Su, C., Duan, F., & Xu, Y. (2021). Super-hydrophobic PTFE hollow fiber membrane fabricated by electrospinning of Pullulan/PTFE emulsion for membrane deamination. *Separation and Purification Technology*, 274(August 2020), 118186. https://doi.org/10.1016/j.seppur.2020.118186

Pangarkar, B. L., Sane, M. G., & Parjane, S. B. (2011). Flux enhancement of air gap membrane distillation for desalination of groundwater by surface modification of membrane. *International Journal of ChemTech Research*, 3(4), 1816-1820.

Park, J.-S., Choi, J.-H., Yeon, K.-H., & Moon, S.-H. (2006). An approach to fouling characterization of an ion-exchange membrane using current–voltage relation and electrical impedance spectroscopy. *Journal of Colloid and Interface Science*, 294(1), 129–138. https://doi.org/10.1016/j.jcis.2005.07.016

Park, S. H., Kim, J. H., Moon, S. J., Jung, J. T., Wang, H. H., Ali, A., Quist-Jensen, C. A., Macedonio, F., Drioli, E., & Lee, Y. M. (2020). Lithium recovery from artificial brine using energy-efficient membrane distillation and nanofiltration. *Journal of Membrane Science*, 598, 117683. https://doi.org/10.1016/j.memsci.2019.117683

Parks, J. L., & Edwards, M. (2005). Boron in the Environment. *Critical Reviews in Environmental Science and Technology*, 35(2), 81–114. https://doi.org/10.1080/10643380590900200

Pearce, E. M. (1978). Kirk-Othmer encyclopedia of chemical technology, 3rd ed., Vol. I, Wiley-Interscience, New York, 1978. *Journal of Polymer Science: Polymer Letters Edition*, 16(5), 248–248. https://doi.org/10.1002/pol.1978.130160508

Peng, X., Li, L., Shi, D., Zhang, L., Li, H., Nie, F., & Song, F. (2018). Recovery of boric acid from salt lake brines by solvent extraction with 2-butyl-1- n -octanol. *Hydrometallurgy*, 177, 161–167. https://doi.org/10.1016/j.hydromet.2018.03.013

Periyasamy, T., Asrafali, S. P., Haldhar, R., Madhappan, S., Vanaraj, R., Raorane, C. J., & Kim, S. C. (2022). Modified Cotton Sponge with Bio-Based Polybenzoxazine for Plasticizer Absorption and Oil-Water Separation. *ACS Applied Polymer Materials*, 4(2), 950–959. https://doi.org/10.1021/acsapm.1c01408

Phattaranawik, J. (2003). Effect of pore size distribution and air flux on mass transport in direct contact membrane distillation. *Journal of Membrane Science*, 215(1–2), 75–85. https://doi.org/10.1016/S0376-7388(02)00603-8

Ping, Q., Abu-Reesh, I. M., & He, Z. (2015). Boron removal from saline water by a microbial desalination cell integrated with donnan dialysis. *Desalination*, 376, 55–61. https://doi.org/10.1016/j.desal.2015.08.019

Ping, Q., Abu-Reesh, I. M., & He, Z. (2016). Enhanced boron removal by electricity generation in a microbial fuel cell. *Desalination*, 398, 165–170. https://doi.org/10.1016/j.desal.2016.07.031

Pinotti, C. N., de Souza, L. M., Marques, W. P., Proveti, J. R. C., Jesus, H. C., Freitas, J. C. C., Porto, P. S. S., Muniz, E. P., & Passamani, E. C. (2022). A new magnetic composite with potential application in boron adsorption: *Development, characterization, and removal tests. Materials Chemistry and Physics*, 277, 125368. https://doi.org/10.1016/j.matchemphys.2021.125368

Poslu, K., & Arslan, İ. (1995). *Dünya bor mineralleri ve bileşikleri üretiminde Türkiye'nin yeri*. 33–34.

Prince, J. A., Singh, G., Rana, D., Matsuura, T., Anbharasi, V., & Shanmugasundaram, T. S. (2012). Preparation and characterization of highly hydrophobic poly (vinylidene fluoride) – Clay nanocomposite nanofiber membranes (PVDF – clay NNMs) for desalination using direct contact membrane distillation. *Journal of Membrane Science* 398, 80–86. https://doi.org/10.1016/j.memsci.2012.01.012

Puranik, A. A., Rodrigues, L. N., Chau, J., Li, L., & Sirkar, K. K. (2019). Porous hydrophobic-hydrophilic composite membranes for direct contact membrane distillation. *Journal of Membrane Science*, 591, 117225. https://doi.org/10.1016/j.memsci.2019.117225

Qtaishat, M., Matsuura, T., Kruczek, B., & Khayet, M. (2008). Heat and mass transfer analysis in direct contact membrane distillation. *Desalination*, 219(1–3), 272–292. https://doi.org/10.1016/j.desal.2007.05.019

Quist-Jensen, C. A., Ali, A., Mondal, S., Macedonio, F., & Drioli, E. (2016). A study of membrane distillation and crystallization for lithium recovery from high-concentrated aqueous solutions. *Journal of Membrane Science*, 505, 167–173. https://doi.org/10.1016/j.memsci.2016.01.033

Rap, A. (2013). Areas of usage of boron (p. 35) [Annual]. Eti Mining Operations General Directorate.

Ray, S. S., Bakshi, H. S., Dangayach, R., Singh, R., Deb, C. K., Ganesapillai, M., Chen, S. S., & Purkait, M. K. (2020). Recent developments in nanomaterials-modified membranes for improved membrane distillation performance. *Membranes*, 10(7), 1–29. https://doi.org/10.3390/membranes10070140

Ray, S. S., Chen, S. S., Nguyen, N. C., Hsu, H. Te, Nguyen, H. T., & Chang, C. T. (2017). Poly(vinyl alcohol) incorporated with surfactant based electrospun nanofibrous layer onto polypropylene mat for improved desalination by using membrane distillation. *Desalination*, 414, 18–27. https://doi.org/10.1016/j.desal.2017.03.032

Recepoğlu, Y. K., Kabay, N., Ipek, I. Y., Arda, M., Yüksel, M., Yoshizuka, K., & Nishihama, S. (2018). Packed bed column dynamic study for boron removal from geothermal brine by a chelating fiber and breakthrough curve analysis by using mathematical models. *Desalination*, 437, 1–6. https://doi.org/10.1016/j.desal.2018.02.022

Remy, P., Muhr, H., Plasari, E., & Ouerdiane, I. (2005). Removal of boron from wastewater by precipitation of a sparingly soluble salt. *Environmental Progress*, 24(1), 105–110. https://doi.org/10.1002/ep.10058

Ren, L. F., Xia, F., Chen, V., Shao, J., Chen, R., & He, Y. (2017). TiO2-FTCS modified superhydrophobic PVDF electrospun nanofibrous membrane for desalination by direct contact membrane distillation. *Desalination*, 423, 1–11. https://doi.org/10.1016/j.desal.2017.09.004

Safavi, M., & Mohammadi, T. (2009a). High-salinity water desalination using VMD. *Chemical Engineering Journal*, 149(1–3), 191–195. https://doi.org/10.1016/j.cej.2008.10.021

Sagiv, A., & Semiat, R. (2004). Analysis of parameters affecting boron permeation through reverse osmosis membranes. *Journal of Membrane Science*, 243(1–2), 79–87. https://doi.org/10.1016/j.memsci.2004.05.029

Salehi, M. (2022). Global water shortage and potable water safety; Today's concern and tomorrow's crisis. *Environment International*, 158, 106936. https://doi.org/10.1016/j.envint.2021.106936

Samatya, S., Köseoğlu, P., Kabay, N., Tuncel, A., & Yüksel, M. (2015). Utilization of geothermal water as irrigation water after boron removal by monodisperse nanoporous polymers containing NMDG in sorption–ultrafiltration hybrid process. *Desalination*, 364, 62–67. https://doi.org/10.1016/j.desal.2015.02.030

Samatya, S., Tuncel, A., & Kabay, N. (2012). Boron Removal from Geothermal Water by a Novel Monodisperse Porous Poly(GMA- co -EDM) Resin Containing N -Methyl-D-Glucamine Functional Group. *Solvent Extraction and Ion Exchange*, 30(4), 341–349. https://doi.org/10.1080/07366299.2012.686857

Sánchez, J., Rivas, B. L., Nazar, E., Bryjak, M., & Kabay, N. (2013). Boron removal by liquid-phase polymer-based retention technique using poly(glycidyl methacrylate N -methyl D -glucamine). *Journal of Applied Polymer Science*, 129(3), 1541–1545. https://doi.org/10.1002/app.38851

Sánchez, J., Wolska, J., Yörükoğlu, E., Rivas, B. L., Bryjak, M., & Kabay, N. (2016). Removal of boron from water through soluble polymer based on N-methyl-D-glucamine and regenerated-cellulose membrane. *Desalination and Water Treatment*, 57(2), 861–869. https://doi.org/10.1080/19443994.2014.979369

Sarbatly, R., & Chiam, C.-K. (2013). Evaluation of geothermal energy in desalination by vacuum membrane distillation. *Applied Energy*, 112, 737–746. https://doi.org/10.1016/j.apenergy.2012.12.028

Satilmis, B., & Uyar, T. (2019). Fabrication of Thermally Crosslinked Hydrolyzed Polymers of Intrinsic Microporosity (HPIM)/Polybenzoxazine Electrospun Nanofibrous Membranes. *Macromolecular Chemistry and Physics*, 220(1), 1–11. https://doi.org/10.1002/macp.201800326

Şenol Arslan, D. (2021a). Türkiye'de farklı yörelerde bulunan kolemanit minerallerinin fiziksel, kimyasal ve termal özelliklerinin tayini. *Gümüşhane Üniversitesi Fen Bilimleri Enstitüsü Dergisi*. https://doi.org/10.17714/gumusfenbil.931377

Sevim, U. K. (2011). Colemanite ore waste concrete with low shrinkage and high split tensile strength. *Materials and Structures*, 44(1), 187–193. https://doi.org/10.1617/s11527-010-9618-4

Sevinç, A. H., Durgun, M. Y., & Eken, M. (2017). A Taguchi approach for investigating the engineering properties of concretes incorporating barite, colemanite, basaltic pumice and ground blast furnace slag. *Construction and Building Materials*, 135, 343–351. https://doi.org/10.1016/j.conbuildmat.2016.12.209

Shang, Y., Si, Y., Raza, A., Yang, L., Mao, X., Ding, B., & Yu, J. (2012). An in situ polymerization approach for the synthesis of superhydrophobic and superoleophilic nanofibrous membranes for oil-water separation. *Nanoscale*, 4(24), 7847–7854. https://doi.org/10.1039/c2nr33063f

Shih, Y.-J., Liu, C.-H., Lan, W.-C., & Huang, Y.-H. (2014). A novel chemical oxo-precipitation (COP) process for efficient remediation of boron wastewater at room temperature. *Chemosphere*, 111, 232–237. https://doi.org/10.1016/j.chemosphere.2014.03.121

Shim, W. G., He, K., Gray, S., & Moon, I. S. (2015). Solar energy assisted direct contact membrane distillation (DCMD) process for seawater desalination. *Separation and Purification Technology*, 143, 94–104. https://doi.org/10.1016/j.seppur.2015.01.028

Si, Y., Ren, T., Li, Y., Ding, B., & Yu, J. (2012). Fabrication of magnetic polybenzoxazine-based carbon nanofibers with Fe 3O 4 inclusions with a hierarchical porous structure for water treatment. *Carbon*, 50(14), 5176–5185. https://doi.org/10.1016/j.carbon.2012.06.059

Song, J., Deng, Q., Huang, M., & Kong, Z. (2022). Carbon nanotube enhanced membrane distillation for salty and dyeing wastewater treatment by electrospinning technology. *Environmental Research*, 204(PA), 111892. https://doi.org/10.1016/j.envres.2021.111892

Sparenberg, M.-C., Chergaoui, S., Sang Sefidi, V., & Luis, P. (2021). Crystallization control via membrane distillation-crystallization: A review. *Desalination*, 519, 115315. https://doi.org/10.1016/j.desal.2021.115315

Srisurichan, S., Jiraratananon, R., & Fane, A. (2006). Mass transfer mechanisms and transport resistances in direct contact membrane distillation process. *Journal of Membrane Science*, 277(1–2), 186–194. https://doi.org/10.1016/j.memsci.2005.10.028

Su, P. K., Chang, C. H., Sun, Y. M., Hu, C. C., Lai, J. Y., & Liu, Y. L. (2019). Porous membranes of thermosetting polybenzoxazine resins with interconnected-pores for organic solvent microfiltration. *Journal of Membrane Science*, 586(May), 267–273. https://doi.org/10.1016/j.memsci.2019.05.061

Suárez, F., Ruskowitz, J. A., Tyler, S. W., & Childress, A. E. (2015). Renewable water: Direct contact membrane distillation coupled with solar ponds. *Applied Energy*, 158, 532–539. https://doi.org/10.1016/j.apenergy.2015.08.110

Sun, L., Wang, L., Wang, Z., Li, B., & Wang, S. (2015). Characteristics analysis of cross flow vacuum membrane distillation process. *Journal of Membrane Science*, 488, 30–39. https://doi.org/10.1016/j.memsci.2015.03.071

Sun, M., Li, M., Zhang, X., Wu, C., & Wu, Y. (2020). Graphene oxide modified porous P84 co-polyimide membranes for boron recovery by bipolar membrane electrodialysis process. *Separation and Purification Technology*, 232, 115963. https://doi.org/10.1016/j.seppur.2019.115963

Sun, X., Li, G., Zhang, Y., Li, Y., & Li, H. (2009). Preparation of Super-hydrophobic Polyethersulphone Membrane by Sol-gel Method. *Advanced Materials Research*, 82, 839–842. https://doi.org/10.4028/www.scientific.net/AMR.79-82.839

Swaminathan, J., Chung, H. W., Warsinger, D. M., & Lienhard V, J. H. (2018a). Energy efficiency of membrane distillation up to high salinity: Evaluating critical system size and optimal membrane thickness. *Applied Energy*, 211, 715–734. https://doi.org/10.1016/j.apenergy.2017.11.043

Tagliabue, M., Reverberi, A. P., & Bagatin, R. (2014a). Boron removal from water: Needs, challenges and perspectives. *Journal of Cleaner Production*, 77, 56–64. https://doi.org/10.1016/j.jclepro.2013.11.040

Tang, Y. P., Luo, L., Thong, Z., & Chung, T. S. (2017). Recent advances in membrane materials and technologies for boron removal. *Journal of Membrane Science*, 541, 434–446. https://doi.org/10.1016/j.memsci.2017.07.015

Tang, Y. P., Yuwen, S., Chung, T. S., Weber, M., Staudt, C., & Maletzko, C. (2016). Synthesis of hyperbranched polymers towards efficient boron reclamation via a hybrid ultrafiltration process. Journal of Membrane Science, 510, 112–121. https://doi.org/10.1016/j.memsci.2016.03.024

Taniguchi, M., Fusaoka, Y., Nishikawa, T., & Kurihara, M. (2004). Boron removal in RO seawater desalination. *Desalination*, 167, 419–426. https://doi.org/10.1016/j.desal.2004.06.157

Tapiero, Y., Sánchez, J., & Rivas, B. L. (2017). Interpenetrating polymers supported on microporous polypropylene membranes for the transport of chromium ions. *Chinese Journal of Chemical Engineering*, 25(7), 938–946. https://doi.org/10.1016/j.cjche.2016.12.011

Tijing, L. D., Choi, J.-S., Lee, S., Kim, S.-H., & Shon, H. K. (2014). Recent progress of membrane distillation using electrospun nanofibrous membrane. *Journal of Membrane Science*, 453, 435–462. https://doi.org/10.1016/j.memsci.2013.11.022

Tomaszewska, B., & Bodzek, M. (2013). Desalination of geothermal waters using a hybrid UF-RO process. Part I: Boron removal in pilot-scale tests. *Desalination*, 319, 99–106. https://doi.org/10.1016/j.desal.2012.05.029

Tran, T. T. Van, Nguyen, C. H., Lin, W. C., & Juang, R. S. (2021). Improved stability of a supported liquid membrane process via hydrophobic modification of PVDF support by plasma activation and chemical vapor deposition. *Separation and Purification Technology*, 277(August), 119615. https://doi.org/10.1016/j.seppur.2021.119615

Tsai, H.-C., & Lo, S.-L. (2011). Boron removal and recovery from concentrated wastewater using a microwave hydrothermal method. *Journal of Hazardous Materials*, 186(2–3), 1431–1437. https://doi.org/10.1016/j.jhazmat.2010.12.010

Tsai, H.-C., Lo, S.-L., & Kuo, J. (2011). Using pretreated waste oyster and clam shells and microwave hydrothermal treatment to recover boron from concentrated wastewater. *Bioresource Technology*, 102(17), 7802–7806. https://doi.org/10.1016/j.biortech.2011.06.036

Tsai, Y. T., Maggay, I. V., Venault, A., & Lin, Y. F. (2021). Fluorine-free and hydrophobic/oleophilic PMMA/PDMS electrospun nanofibrous membranes for gravity-driven removal of water from oil-rich emulsions. *Separation and Purification Technology*, 279(May), 119720. https://doi.org/10.1016/j.seppur.2021.119720

Tu, K. L., Chivas, A. R., & Nghiem, L. D. (2013). Enhanced boron rejection by NF/RO membranes by complexation with polyols: Measurement and mechanisms. *Desalination*, 310, 115–121. https://doi.org/10.1016/j.desal.2012.08.017

Tu, K. L., Nghiem, L. D., & Chivas, A. R. (2010). Boron removal by reverse osmosis membranes in seawater desalination applications. *Separation and Purification Technology*, 75(2), 87–101. https://doi.org/10.1016/j.seppur.2010.07.021

Tu, K. L., Nghiem, L. D., & Chivas, A. R. (2011). Coupling effects of feed solution pH and ionic strength on the rejection of boron by NF/RO membranes. *Chemical Engineering Journal*, 168(2), 700–706. https://doi.org/10.1016/j.cej.2011.01.101

Tun, C. M., Fane, A. G., Matheickal, J. T., & Sheikholeslami, R. (2005). Membrane distillation crystallization of concentrated salts—Flux and crystal formation. *Journal of Membrane Science*, 257(1–2), 144–155. https://doi.org/10.1016/j.memsci.2004.09.051

Turek, M., Dydo, P., Trojanowska, J., & Campen, A. (2007). Adsorption/co-precipitation—Reverse osmosis system for boron removal. *Desalination*, 205(1–3), 192–199. https://doi.org/10.1016/j.desal.2006.02.056

Vanoppen, M., Stoffels, G., Demuytere, C., Bleyaert, W., & Verliefde, A. R. D. (2015). Increasing RO efficiency by chemical-free ion-exchange and Donnan dialysis: Principles and practical implications. *Water Research*, 80, 59–70. https://doi.org/10.1016/j.watres.2015.04.030

Vatanpour, V., Kiskan, B., Zeytuncu, B., & Koyuncu, I. (2022). Polybenzoxazines in fabrication of separation membranes: A review. *Separation and Purification Technology*, 278, 119562.

Wae AbdulKadir, W. A. F., Ahmad, A. L., Seng, O. B., & Che Lah, N. F. (2020). Biomimetic hydrophobic membrane: A review of anti-wetting properties as a potential factor in membrane development for membrane distillation (MD). *Journal of Industrial and Engineering Chemistry*, 91, 15–36. https://doi.org/10.1016/j.jiec.2020.08.005

Wang, C. F., Su, Y. C., Kuo, S. W., Huang, C. F., Sheen, Y. C., & Chang, F. C. (2006). Low-surface-free-energy materials based on polybenzoxazines. *Angewandte Chemie - International Edition*, 45(14), 2248–2251. https://doi.org/10.1002/anie.200503957

Wang, F., Zhao, X., Wahid, F., Zhao, X., Qin, X., Bai, H., Xie, Y., Zhong, C., & Jia, S. (2021). Sustainable, superhydrophobic membranes based on bacterial cellulose for gravity-driven oil/water separation. *Carbohydrate Polymers*, 253, 117220. https://doi.org/10.1016/j.carbpol.2020.117220

Wang, Q.-Z., Xiao, Y.-K., Wang, Y.-H., Zhang, C.-G., & Wei, H.-Z. (2010). Boron Separation by the Two-step Ion-Exchange for the Isotopic Measurement of Boron. *Chinese Journal of Chemistry*, 20(1), 45–50. https://doi.org/10.1002/cjoc.20020200110

Wang, S., Bing, S., Zhang, H., Zhou, Y., Zhang, L., & Gao, C. (2022). Surface engineering design of polyamide membranes for enhanced boron removal in seawater desalination. *Journal of Membrane Science*, 651, 120425. https://doi.org/10.1016/j.memsci.2022.120425

Wang, S., Zhou, Y., & Gao, C. (2018). Novel high boron removal polyamide reverse osmosis membranes. *Journal of Membrane Science*, 554, 244–252. https://doi.org/10.1016/j.memsci.2018.03.014

Wang, Z., Chen, Z., Zhang, Z., Li, J., Chen, K., Liang, H., Lv, L., Chang, Y., Liu, S., Yang, W., Yang, Z., Yuan, H., Meng, X., Liu, T., Wang, F., Li, J., & Xing, G. (2022). Multifunctional high boron content MOFs nano-co-crystals for precise boron neutron capture therapy for brain glioma in situ. *Nano Today*, 45, 101558. https://doi.org/10.1016/j.nantod.2022.101558

Wen, X., Li, F., & Zhao, X. (2016). Removal of nuclides and boron from highly saline radioactive wastewater by direct contact membrane distillation. *Desalination*, 394, 101–107. https://doi.org/10.1016/j.desal.2016.05.001

Wolska, J., & Bryjak, M. (2013). Methods for boron removal from aqueous solutions—A review. *Desalination*, 310, 18–24. https://doi.org/10.1016/j.desal.2012.08.003

Wu, H. Y., Wang, R., & Field, R. W. (2014). Direct contact membrane distillation: An experimental and analytical investigation of the effect of membrane thickness upon transmembrane flux. *Journal of Membrane Science*, 470, 257–265. https://doi.org/10.1016/j.memsci.2014.06.002

Wu, X. Q., Mirza, N. R., Huang, Z., Zhang, J., Zheng, Y. M., Xiang, J., & Xie, Z. (2021). Enhanced desalination performance of aluminium fumarate MOF-incorporated electrospun nanofiber membrane with bead-on-string structure for membrane distillation. *Desalination*, 520(March), 115338. https://doi.org/10.1016/j.desal.2021.115338

Xu, J., Gao, X., Chen, G., Zou, L., & Gao, C. (2010a). High performance boron removal from seawater by two-pass SWRO system with different membranes. *Water Supply*, 10(3), 327–336. https://doi.org/10.2166/ws.2010.397

Xu, J., Gao, X., Chen, G., Zou, L., & Gao, C. (2010b). High performance boron removal from seawater by two-pass SWRO system with different membranes. *Water Supply*, 10(3), 327–336. https://doi.org/10.2166/ws.2010.397

Yadav, P., Farnood, R., & Kumar, V. (2022). Superhydrophobic modification of electrospun nanofibrous Si@PVDF membranes for desalination application in vacuum membrane distillation. *Chemosphere*, 287, 132092. https://doi.org/10.1016/j.chemosphere.2021.132092

Yan, C., Yi, W., Ma, P., Deng, X., & Li, F. (2008). Removal of boron from refined brine by using selective ion exchange resins. *Journal of Hazardous Materials*, 154(1–3), 564–571. https://doi.org/10.1016/j.jhazmat.2007.10.067

Yan, H., Wang, R., & Field, R. W. (2014). Direct contact membrane distillation: An experimental and analytical investigation of the effect of membrane thickness upon transmembrane flux. *Journal of Membrane Science* , 470, 257–265.

Y**ang, Y., Liu, Q., Wang, H., Ding, F., Jin, G., Li, C., & Meng, H.** (2017). Superhydrophobic modification of ceramic membranes for vacuum membrane distillation. *Chinese Journal of Chemical Engineering*, 25(10), 1395–1401. https://doi.org/10.1016/j.cjche.2017.05.003

Yang, Z., Ma, X.-H., & Tang, C. Y. (2018). Recent development of novel membranes for desalination. *Desalination*, 434, 37–59. https://doi.org/10.1016/j.desal.2017.11.046

Yao, B., Yan, X., Ding, Y., Lu, Z., Dong, D., Ishida, H., Litt, M., & Zhu, L. (2014). Synthesis of sulfonic acid-containing polybenzoxazine for proton exchange membrane in direct methanol fuel cells. *Macromolecules*, 47(3), 1039–1045. https://doi.org/10.1021/ma4020214

Yildiz, Ö. (2004). The effect of heat treatment on colemanite processing: A ceramics application. *Powder Technology*, 142, 7–12.

Yilmaz, A. E., Boncukcuoğlu, R., & Kocakerim, M. M. (2007). A quantitative comparison between electrocoagulation and chemical coagulation for boron removal from boron-containing solution. *Journal of Hazardous Materials*, 149(2), 475–481. https://doi.org/10.1016/j.jhazmat.2007.04.018

Yilmaz, İ., Kabay, N., Brjyak, M., Yüksel, M., Wolska, J., & Koltuniewicz, A. (2006). A submerged membrane–ion-exchange hybrid process for boron removal. *Desalination*, 198(1–3), 310–315. https://doi.org/10.1016/j.desal.2006.01.031

Yoshikawa, E., Sasaki, A., & Endo, M. (2012). Removal of boron from wastewater by the hydroxyapatite formation reaction using acceleration effect of ammonia. *Journal of Hazardous Materials*, 237–238, 277–282. https://doi.org/10.1016/j.jhazmat.2012.08.045

Yun, Y., Ma, R., Zhang, W., Fane, A. G., & Li, J. (2006). Direct contact membrane distillation mechanism for high concentration NaCl solutions. *Desalination*, 188(1–3), 251–262. https://doi.org/10.1016/j.desal.2005.04.123

Yunlu K. (2016). *Bor bilesikleri, sentez yontemleri, ozellikleri, uygulamalari* (1st ed.).

Yürüm, A., Taralp, A., Bıçak, N., Özbelge, H. Ö., & Yılmaz, L. (2013). High performance ligands for the removal of aqueous boron species by continuous polymer enhanced ultrafiltration. *Desalination*, 320, 33–39. https://doi.org/10.1016/j.desal.2013.04.020

Zarzoum, K., Zhani, K., Ben Bacha, H., & Koschikowski, J. (2019). Experimental parametric study of membrane distillation unit using solar energy. *Solar Energy*, 188, 1274–1282. https://doi.org/10.1016/j.solener.2019.07.025

Zelmanov, G., & Semiat, R. (2014). Boron removal from water and its recovery using iron (Fe+3) oxide/hydroxide-based nanoparticles (NanoFe) and NanoFe-impregnated granular activated carbon as adsorbent. *Desalination*, 333(1), 107–117. https://doi.org/10.1016/j.desal.2013.11.027

Zerze, H., Karagoz, B., Ozbelge, H. O., Bicak, N., Aydogan, N., & Yilmaz, L. (2013). Imino-bis-propane diol functional polymer for efficient boron removal from aqueous solutions via continuous PEUF process. *Desalination*, 310, 158–168. https://doi.org/10.1016/j.desal.2012.07.013

Zhang, F., Qian, H., Wang, L., Wang, Z., Du, C., Li, X., & Zhang, D. (2018). Superhydrophobic carbon nanotubes/epoxy nanocomposite coating by facile one-step spraying. *Surface and Coatings Technology*, 341, 15–23. https://doi.org/10.1016/j.surfcoat.2018.01.045

Zhang, H., Liu, M., Sun, D., Li, B., & Li, P. (2016). Evaluation of commercial PTFE membranes for desalination of brine water through vacuum membrane distillation. *Chemical Engineering and Processing: Process Intensification*, 110, 52–63. https://doi.org/10.1016/j.cep.2016.09.023

Zhang, L., Feng, Y., Li, Y., Jiang, Y., Wang, S., Xiang, J., Zhang, J., Cheng, P., & Tang, N. (2022). Stable construction of superhydrophobic surface on polypropylene membrane via atomic layer deposition for high salt solution desalination. *Journal of Membrane Science*, 647(January), 120289. https://doi.org/10.1016/j.memsci.2022.120289

Zhang, W., Yu, S., Ning, R., Li, P., Ji, X., & Xu, Y. (2023). Treatment of high-salinity brine containing dissolved organic matters by vacuum membrane distillation: A fouling mitigation approach via microbubble aeration. *Journal of Environmental Management*, 342, 118142. https://doi.org/10.1016/j.jenvman.2023.118142

Zhang, Y., Chong, J. Y., Zhao, Y., Xu, R., Asakawa, A., & Wang, R. (2023). Facile hydrophobic modification of hydrophilic membranes by fluoropolymer coating for direct contact membrane distillation. *Journal of Membrane Science*, 672, 121432. https://doi.org/10.1016/j.memsci.2023.121432

Zhang, Y., Liang, X., Jiang, T., Chen, Z., & Ji, X. (2022). Removal of boron from aqueous solutions by N-methyl-D-glucamine@γ-glycidoxypropyl-trimethoxysilane with nonwoven basalt fibers support. *Materials Today Communications*, 31, 103611. https://doi.org/10.1016/j.mtcomm.2022.103611

Zhao, Q., Zhao, D. L., Feng, F., Chung, T.-S., & Chen, S. B. (2022). Thin-film nanocomposite reverse osmosis membranes incorporated with citrate-modified layered double hydroxides (LDHs) for brackish water desalination and boron removal. *Desalination*, 527, 115583. https://doi.org/10.1016/j.desal.2022.115583

Zhou, H., Chen, R., Liu, Q., Liu, J., Yu, J., Wang, C., Zhang, M., Liu, P., & Wang, J. (2019). Fabrication of ZnO/epoxy resin superhydrophobic coating on AZ31 magnesium alloy. *Chemical Engineering Journal*, 368, 261–272. https://doi.org/10.1016/j.cej.2019.02.032

Zhou, L., Li, C. L., Chang, P. T., Tan, S. H., Ahmad, A. L., & Low, S. C. (2022). Intrinsic microspheres structure of electrospun nanofibrous membrane with rational superhydrophobicity for desalination via membrane distillation. *Desalination*, 527(December 2021), 115594. https://doi.org/10.1016/j.desal.2022.115594

Zhu, Y., Du, Y., Su, J., Mo, Y., Yu, S., & Wang, Z. (2021). Durable superhydrophobic melamine sponge based on polybenzoxazine and Fe_3O_4 for oil/water separation. *Separation and Purification Technology*, 275, 119130. https://doi.org/10.1016/j.seppur.2021.119130

Zhu, Z., Liu, Y., Hou, H., Shi, W., Qu, F., Cui, F., & Wang, W. (2018). Dual-Bioinspired Design for Constructing Membranes with Superhydrophobicity for Direct Contact Membrane Distillation. *Environmental Science and Technology*, 52(5), 3027–3036. https://doi.org/10.1021/acs.est.7b06227

Zohdi, N., Mahdavi, F., Abdullah, L. C., & Choong, T. S. (2014). Removal of boron from aqueous solution using magnetic carbon nanotube improved with tartaric acid. *Journal of Environmental Health Science and Engineering*, 12(1), 3. https://doi.org/10.1186/2052-336X-12-3

APPENDICES

APPENDIX A: Supplementary information for Chapter 6

APPENDIX A: Supplementary Information for Chapter 6

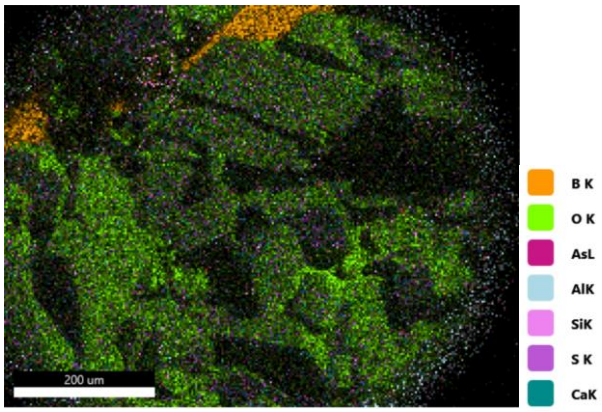

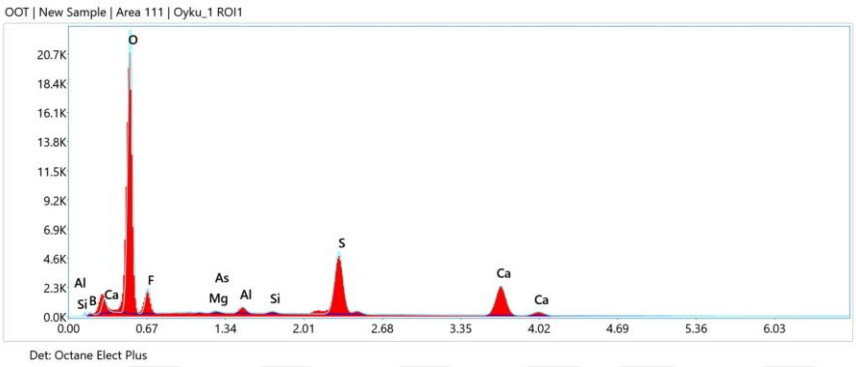

Figure A.1 : SEM-EDX results of PTFE.

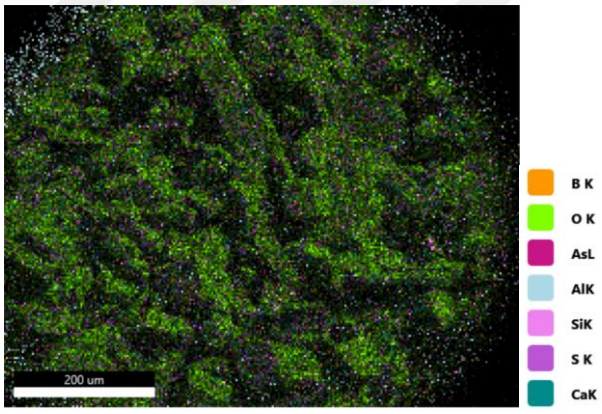

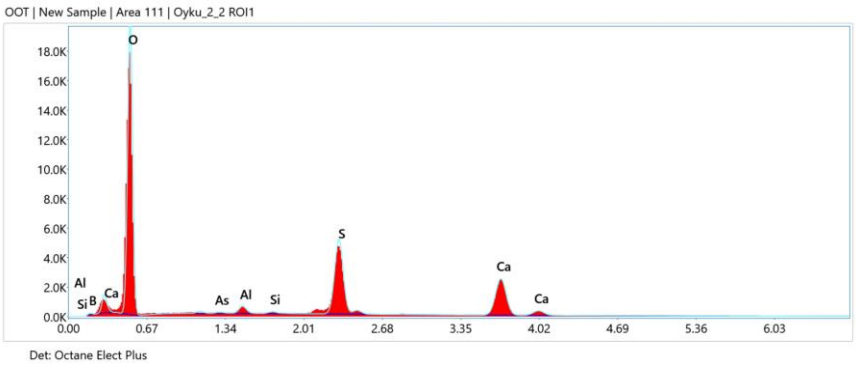

Figure A.2 : SEM EDX of PVDF.

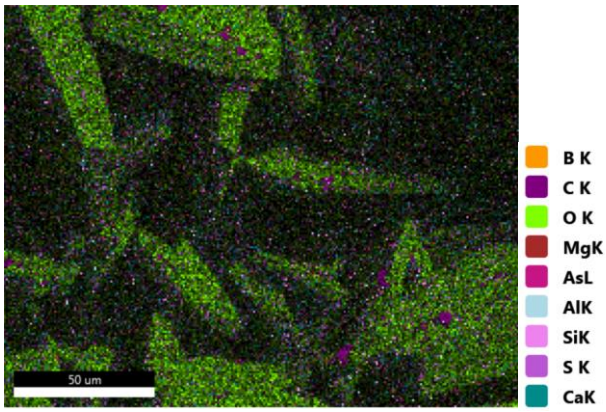

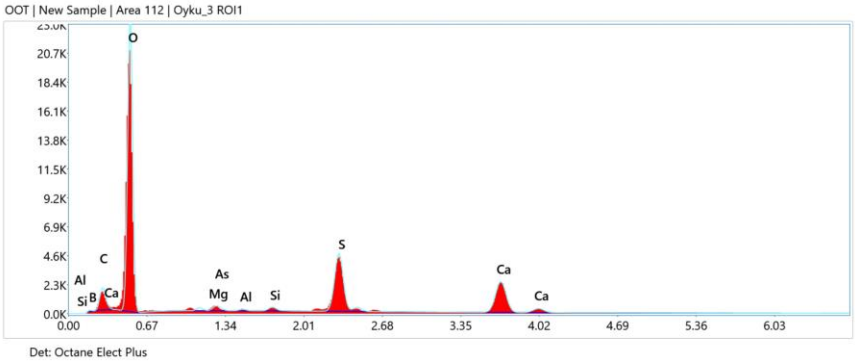

Figure A.3 : SEM-EDX of PP.

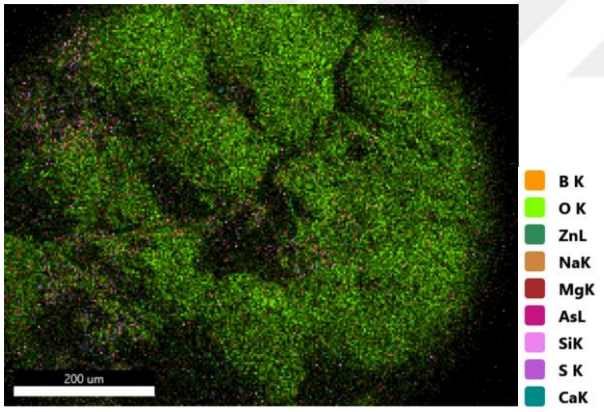

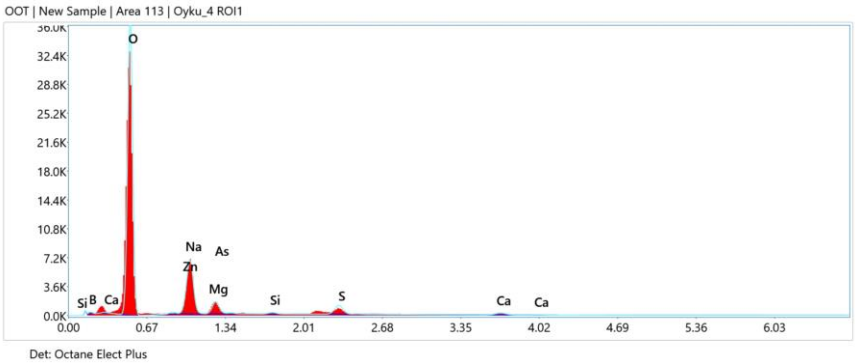

Figure A.4 : SEM-EDX of PP at pH 9.3.

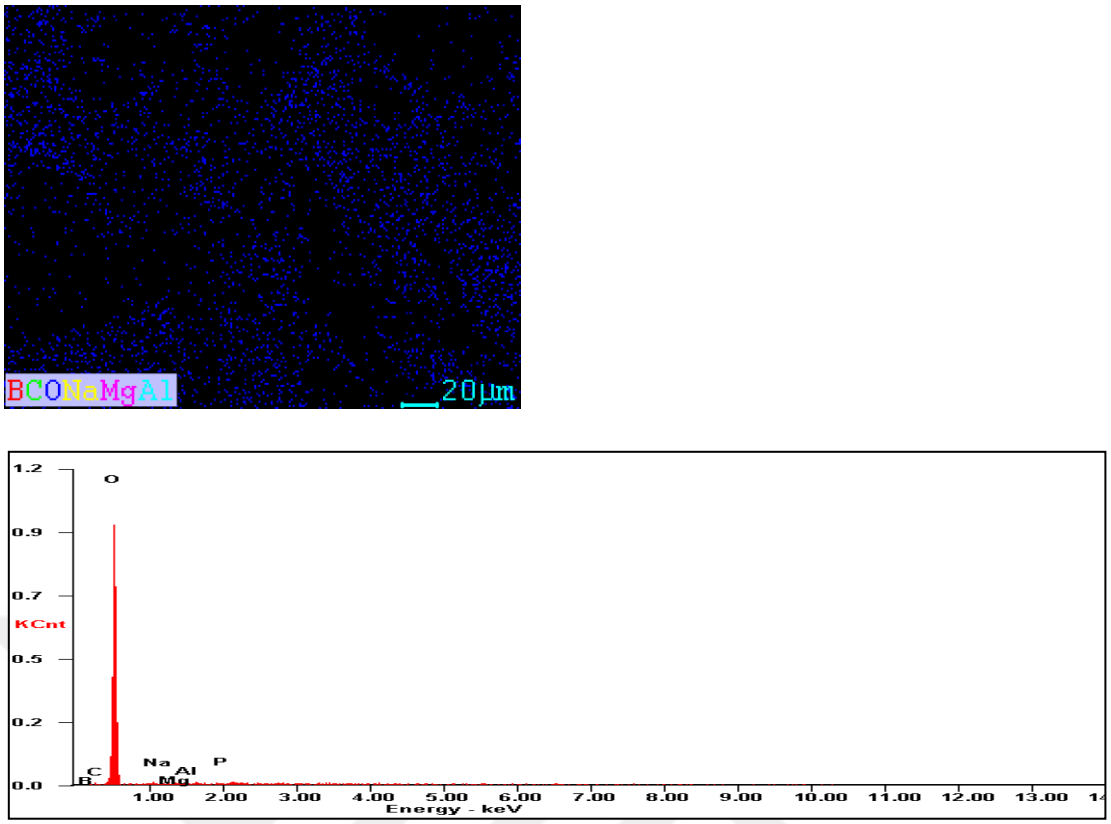

Figure A.5 : SEM-EDX of PVDF espun.

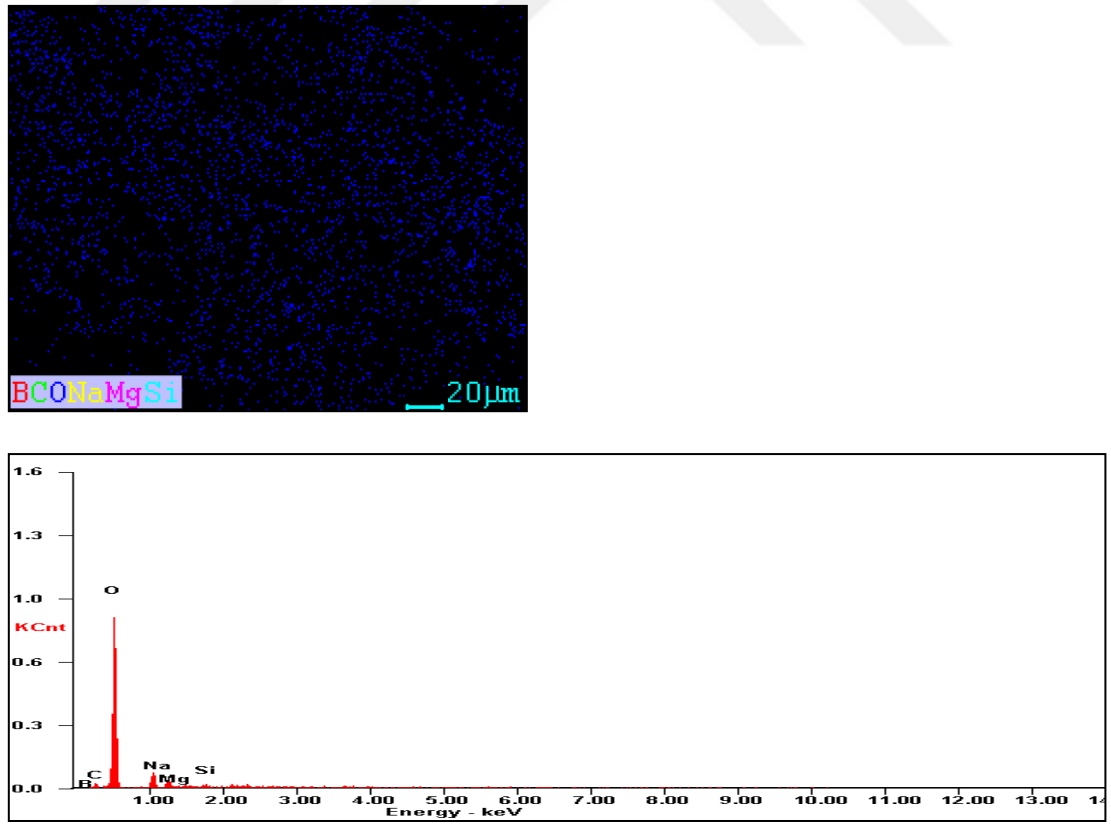

Figure A.6 : SEM-EDX of PVDF/Bz.

Table A.1 : Ion content of feed and permeate waters.

Parameters (mg/L)	Feed	PVDF	PTFE	PP	Feed pH 9.3	PP pH 9.3	PVDF Espun	PVDF /Bz
F^-	<0.04	<0.04	1.39	<0.04	<0.04	<0.04	<0.04	<0.04
Cl^-	928.16	6.77	57.99	1.97	828.38	17.83	55.38	2.18
NO_2^-	<0.10	<0.10	<0.10	<0.10	<0.10	<0.10	<0.10	<0.10
Br^-	<0.10	<0.10	<0.10	<0.10	<0.10	<0.10	<0.10	<0.10
NO_3^-	4.94	0.90	1.69	0.36	26.90	2.04	9.27	0.24
PO_4^{-3}	<0.20	<0.20	<0.20	<0.20	<0.20	<0.20	<0.20	<0.20
SO_4^{-2}	8397.96	28.91	559.91	2.04	8325.73	12.78	65.72	9.81
Li^+	11.92	0.05	0.77	<0.02	16.54	<0.02	<0.02	0.04
Na^+	1382.55	8.55	81.52	1.36	11088.78	8.47	28.30	4.4
NH_4^+	46.52	<0.10	<0.10	<0.10	<0.10	1.38	2.65	5.02
K^+	50.91	0.55	3.20	0.19	109.01	0.91	3.54	1.93
Mg^{+2}	847.87	6.84	74.79	0.49	1595.75	2.45	11.79	14.19
Ca^{+2}	895.19	7.29	51.60	2.64	1089.65	13.12	45.77	10.60

CURRICULUM VITAE

Name Surname **:** Öykü MUTLU SALMANLI

EDUCATION

- **B.Sc.** **:** 2012, Istanbul University, Faculty of Engineering, Environmental Engineering Department
- **M.Sc.** **:** 2015, Istanbul University, Faculty of Engineering, Environmental Engineering Department

PROFESSIONAL EXPERIENCE:

- 2015 – present, Researcher at Prof. Dr. Dincer Topacik National Research and Application Center on Membrane Technologies in Istanbul Technical University
- 2014-2015 Research and Teaching Assistant, Duzce University
- 2015-2016 Research and Teaching Assistant, Istanbul University
- 2016-2022 Research and Teaching Assistant, Istanbul Technical University
- 2021-2023 Visiting research scholar, Duke University

REWARDS:

- 2012 – Istanbul University, Environmental Engineering Department, graduated with 2nd grade
- International Doctoral Research Fellowship, The Scientific and Research Council of Turkey (TUBITAK)
- PhD Scholarship Program Intended for Priority Areas, The Scientific and Research Council of Turkey (TUBITAK)

PUBLICATIONS, PRESENTATIONS AND PATENTS ON THE THESIS:

- **Mutlu-Salmanli, O.,** Kazak A., Turken T., Pasaoglu M.E., Zeytuncu B., Koyuncu I. 2023. Boron removal and recovery via vacuum assisted air gap membrane distillation-crystallization (VAGMD-C): A pilot-scale study, Desalination, 547, 116229 http://dx.doi.org/10.1016/j.desal.2022.116229
- **Mutlu-Salmanli, O.,** Eryildiz B., Vatanpour V., Deliballi Z., Kiskan B., Koyuncu, I. 2023. Fabrication of novel hydrophobic electrospun nanofiber membrane using polybenzoxazine for membrane distillation application, *Desalination*, 546, 116203 https://doi.org/10.1016/j.desal.2022.116203

- **Mutlu-Salmanli, O**., Koyuncu, I. 2022. Boron removal and recovery from water and wastewater, *Rev Environ Sci Biotechnol*, 21, 635–664 https://doi.org/10.1007/s11157- 022-09629-w
- **Mutlu Salmanli O.,** Yuksekdag A., Koyuncu I. 2022. Boron removal by using vacuum assisted air gap membrane distillation (VAGMD), *Environmental Technology&Innovation*, http://dx.doi.org/10.1016/j.eti.2022.102395
- **Mutlu-Salmanli Ö.,** Koyuncu I**.** 2021: The effect of pH on the removal and recovery of boron from water. 4th IWA Resource Recovery Conference 2021,(oral presentation) 5-8 September, Turkey.
- **Mutlu-Salmanli O.,** Eryildiz B., Yuksekdag A., Koyuncu I**.,** Boron Removal From Geothermal Waters By Vacuum Assisted Air Gap Membrane Distillation Process Using PTFE Added PVDF Membranes, 9th Geochemistry Symposium with International Participation, (oral presentation) 17-20 October 2022, Turkey.

OTHER PUBLICATIONS, PRESENTATIONS AND PATENTS:

- Vatanpour V., Kose-Mutlu B., **Mutlu-Salmanli O**., Ilyasoglu G., Asadzadeh-Khaneghah S., Habibi-Yangjeh A., Koyuncu I. (2022), *$Bi_4O_5I_2$ nanosheets as a novel nanofiller for fabrication of antifouling polyethersulfone nanocomposite membranes,* Journal of Industrial and Engineering Chemistry, https://doi.org/10.1016/j.jiec.2022.10.035
- Ormancı-Acar T., Korkut S., Keskin B., Ağtaş M., Erdinç Taş C., **Mutlu-Salmanlı O.**, Türken T., Menceloğlu Y.Z., Ünal S., Koyuncu I (2022), *Combining S-DADPS monomer and halloysite nanotube for fabrication superior nanofiltration membrane*, Polymer, 255, 125174, https://doi.org/10.1016/j.polymer.2022.125174
- Ilyasoglu G., Kose Mutlu B., **Mutlu Salmanli O**., Koyuncu I. (2022), *Removal of organic micropollutans by adsorptive membrane,* Chemosphere, http://dx.doi.org/10.1016/j.chemosphere.2022.134775
- Ormanci-Acar T., Keskin B., Korku S, **Mutlu-Salmanlı O**., Turken T., Koseoglu-Imer D.Y., Demir T.U., Menceloglu Y.Z., Unal S, Koyuncu I. (2021), *Fabrication of halloysite nanotubes embedded thin film nanocomposite membranes for dye removal,* Journal of Applied Polymer Science, https://doi.org/10.1002/app.50986
- **Mutlu Salmanlı Ö.**, Güneş Durak S., Türkoğlu Demirkol G., Tüfekci N. (2019), *Effect of PVP concentration on prepared PEI membranes for potential use on water treatment: effect of additive on membranes prepared for water treatment*, Water Supply, 19 (7), 2072-2078, Doi: 10.2166/ws.2019.084
- Ormanci-Acar T., Celebi F., Keskin B., **Mutlu-Salmanlı Ö**., Türken T., Tufani A., Imer D.Y., Ince G.O., Demir Tugba U, Menceloglu Y.Z., Ünal S., Koyuncu I., Agtas M. (2018), *Fabrication and characterization of temperature and pH resistant thin film nanocomposite membranes embedded with halloysite nanotubes for dye rejection*, Desalination, 429, 20-32., Doi: 10.1016/j.desal.2017.12.005.
- Güneş Durak S., Özçoban M.Ş., Balcıoğlu E.B., **Mutlu Ö**., Türkoğlu Demirkol G., Tüfekci N. (2017), *The Effect of Leachate on the Compacted and Consolidated Clay Soils*, Eurasian Journal of Environmental Research,(1), 36-47.

- Çelik S.Ö., Güneş Durak S., Ormancı Acar T., Türkoğlu Demirkol G., **Mutlu Ö**., Tüfekci N., (2017), *Influence of Pyrogallol on the Catalytic Effects of Fe3 During Fe2 Oxidation with Atmospheric Oxygen*, Journal of Advances in Technology and Engineering Studies, 3 (5), 170-175.
- Türkoglu Demirkol G., Dizge N., Ormancı Acar T., **Mutlu Ö**., Tüfekci N. (2017), *Influence Of Nanoparticles On Filterability Of Fruit-Juice Industry Wastewater Using Submerged Membrane Bioreactor*, Water Science and Technology, 76(3), 705-711., Doi:10.2166/wst.2017.255
- **Mutlu Ö**., Türkoglu Demirkol G., Çetin E. (2017), *Removal Of Natural Organic Matter From Drinking Water By Hybrid Coagulation Adsorption Membrane Filtration*, Fresenius Environmental Bulletin, 26(1), 499-509.
- **Mutlu-Salmanli Oyku**, Eryildiz Bahriye, Yuksekdag Ayse, Koyuncu Ismail, Boron Removal From Geothermal Waters By Vacuum Assisted Air Gap Membrane Distillation Process Using PTFE Added PVDF Membranes, 9th Geochemistry Symposium with International Participation, 17-20 October, Turkey.
- **Mutlu-Salmanli Öykü**, Koyuncu Ismail, The effect of pH on the removal and recovery of boron from water, 4th IWA Resource Recovery Conference 2021, 5-8 September, Turkey.
- **Mutlu Salmanli Öykü**, Tüfekci Neşe, Üretilen Polimerik Düz Plaka Membranlarda PVP Konsantrasyonunun Etkisi, 5th International Symposium On Environment and Morals, 25-25 September 2020, Turkey.
- Ormancı Acar Türkan, Ağtaş Meltem, **Mutlu Öykü**, Çelebi Ferda, Türken Türker,İmer Derya Yüksel,Altaş Adnan,Menceloğlu Yusuf Ziya,Ünal Serkan,Koyuncu İsmail, *Flux-enhanced TFN NF membranes containing halloysite nanotubes for dye rejection*, 8th IWA Membrane Technology Conference Exhibition for Water and Wastewater Treatment and Reuse,5-9 September 2017, Singapore.
- Ormancı Acar Türkan, Çelebi Ferda, Türken Türker, **Mutlu Öykü**, İmer Derya Yüksel, Altaş Adnan, Menceloğlu Yusuf Ziya, Ünal Serkan, Demir I, Koyuncu İsmail, Ağtaş Meltem, *Fabrication and characterization of temperature and pH resistant TFN membranes embedded with halloysite nanotubes for dye rejection*, 3rd International Conference on Desalination using Membrane Technology, 2-5 April 2017, Canary Island, Spain.
- **Mutlu Öykü**, Çelik Suna Özden, Tüfekci Neşe, *Effect of PVP Concentration on Prepared PEI Membranes for Potential Use on Water Treatment*, 19th International Symposium on Environmental Pollution and its Impact on Life in the Mediterranean Region, 4-6 October 2017, Rome, Italy.
- **Mutlu Öykü**, Türkoğlu Demirkol Güler,Tüfekci Neşe, *Preparation, Characterization and Properties of Psf / Nanoclay Membranes: Effect of Nanoclay*, 19th International Symposium on Environmental Pollution and its Impact on Life in the Mediterranean Region, 4-6 October 2017, Rome, Italy.

- Türkoğlu Demirkol Güler, Balcıoğlu Gökhan, Çelik Suna Özden, **Mutlu Öykü**, Güneş Durak Sevgi, Tüfekci Neşe, *Determination of the clay soil adsorption capacity ofmetal ions in landfill leachate,* 19th International Symposium on Environmental Pollution and its Impact on Life in the Mediterranean Region, 4-6 October 2017, Rome, Italy.
- Güneş Durak Sevgi, Özçoban Mehmet Şükrü, Balcıoğlu Esra Billur, **Mutlu Öykü,** Türkoğlu Demirkol Güler,Tüfekci Neşe, The Effect of Leachate on the Compacted and Consolidated Clay Soils, 2nd International Conference On Civil And Environmental Engineering, 8-10 May 2017, Cappadocia, Nevşehir, Turkey.
- Ormancı Acar Türkan, Keskin Başak, Korkut Sevde, ,**Mutlu-Salmanlı Öykü**, Ağtaş Meltem, Türken Türker, İmer Derya Yüksel, Altaş Adnan,Menceloğlu Yusuf Ziya,Ünal Serkan, ,Koyuncu İsmail, Investigation of Nanofiltration Membrane Production and Performance by Interfacial Polymerization with Halloysite Nanotube Additive*, Workshop on Desalination Technologies, 21 Kasım 2017, Istanbul, Turkey.*
- Ormancı Acar Türkan, Taş C. Erdinç, Korkut Sevde, Türken Türker, **Mutlu-Salmanlı Öykü,** İmer Derya Yüksel, Menceloğlu Yusuf Ziya, Ünal Serkan, ,Koyuncu İsmail, Sulfonated Diamine Monomer and Halloysite Nanotube Additive NF Membrane Production and Performance Values*, MEM-TEK 2017 5. National Membrane Technologies and Applications* Symposium *,21-23 September 2017, , Istanbul, Turkey.*
- **Mutlu Öykü**, Türkoglu Demırkol Güler, Çetin Ender (2015). *Removal of Natural Organic Matter from Drinking Water by Coagulation Adsorption and Membrane Filtration.* (MESAEP)18th International Symposium on Environmental Pollution and its Impact on Life in the Mediterranean Region, 26-30 October 2015.
- Özçoban Mehmet Sükrü, Sevgi Günes Durak, **Mutlu Öykü**, Tüfekcı Nese (2015). *Evaluation Of Metal Ions Of Permeability Removal Rate Relatıons In The Natural Compacted And Consolidated Clay Soils.* ICOEST International Conference on Environmental Science and Technology, 104-104.
- Turkan Ormanci Acar, Türkoglu Demırkol Güler, Sevgi Gunes Durak, **Mutlu Öykü,**Tüfekcı Nese (2013). *Removing Of Fe II And Humic Acid Together By Adsorption And Coagulation Process.* International Conference on Environmental Science and Technology, 280-281.
- Türkoglu Demırkol Güler, **Mutlu Öykü**, Sevgi Durak Gunes, Turkan Ormanci Acar (2015). *Assessment of Ecological Balance Water Fault in Terms of Fish Passages*. 11th National Environmental Engineering Congress, 778-778.
- **Mutlu Öykü**, Turkan Ormanci Acar, Türkoglu Demırkol Güler, Sevgi Günes Durak (2015). *Removal of Natural Organic Compounds in Drinking Waters by Coagulation Method.* 11th National Environmental Engineering Congress, 777-777.
- **Mutlu Öykü**, Türkoglu Demirkol Güler, Çelik Suna Özden, Tüfekci Nese (2015). E Waste Management apllication problems and proposed solutions in Turkey, 7th National Solid Waste Management Congress, 123-123.

- **Mutlu Öykü**, Tüfekcı Nese (2015). The Effects of Polymer Concentration and the Production of PVDF Membranes on the Characterization of Membranes, Healthy Water Management Congress, 60-60.
- Çelık Suna Özden, Tüfekcı Nese**, Mutlu Öykü**, Türkoglu Demırkol Güler (2015). Production and Characterization of Flat Plate Membranes with Chitosan Additives on Different Surfaces. Healthy Water Management Congress, 100-100